Supporting Information

Facile Selective Synthesis of 2-Methyl-5-amino-1,2,4-oxadiazolium Bromides as Further Targets for Nucleophilic Additions

Mikhail V. Il'in,[a] Dmitrii S. Bolotin, [a,*] Vitalii V. Suslonov,[b] and Vadim Yu. Kukushkin[a]

[a] Institute of Chemistry, Saint Petersburg State University, Universitetskaya Nab. 7/9, Saint Petersburg, Russian Federation. E-mail: d.s.bolotin@spbu.ru

[b] Center for X-ray Diffraction Studies, Saint Petersburg State University, Universitetskii Pr., 26, Saint Petersburg, Russian Federation

Table of Contents

Experimental Section

Materials and instrumentation. Solvents, nitriles, *N*-methylhydroxylamine hydrochloride, isocyanides, bromine, and tribenzylamine were obtained from commercial sources and used as received. All syntheses were conducted in air. Chromatographic separation was carried out on Macherey-Nagel silica gel 60 M (0.063–0.2 mm). Analytical TLC was performed on unmodified Merck ready-to-use plates (TLC silica gel 60 F254) with UV detection. Melting points were measured on a Stuart SMP30 apparatus in capillaries and are not corrected. Electrospray ionization mass-spectra were obtained on a Bruker maXis spectrometer equipped with an electrospray ionization (ESI) source. The instrument was operated in positive ion mode using an *m/z* range 50–1200. The nebulizer gas flow was 1.0 bar and the drying gas flow 4.0 L/min. For HRESI$^+$, the studied compounds were dissolved in MeOH. Infrared spectra (4000–400 cm^{-1}) were recorded on a Shimadzu IR Prestige-21 instrument in KBr pellets. ^{1}H, ^{13}C{^{1}H} DEPT 135° NMR spectra were measured on a Bruker Avance 400 in $CDCl_3$ and $(CD_3)_2SO$ at ambient temperature; the residual solvent signal was used as the internal standard.

X-ray structure determinations. A single-crystal X-ray diffraction experiments were carried out using Agilent Technologies «SuperNova» and «Xcalibur» diffractometers with monochromated CuKα and MoKα radiation, respectively. The crystals were kept at 100(2) K during all data collection. The structures had been solved by the Superflip[1] and ShelXS/ShelXT[2] structure solution programs using Charge Flipping, Direct Methods and Intrinsic Phasing, respectively, and refined by means of the ShelXL[3] program, incorporated in the OLEX2 program package.[4] Structure **6** contains infinite channels along the inversion axis, in which the diffuse electron density was determined. That density has been treated as a diffuse contribution to the overall scattering without specific atom positions by SQUEEZE/PLATON.[5] CCDC numbers 1834203–1834208 contains the supplementary crystallographic data for this paper. These data can be obtained free of charge from the Cambridge Crystallographic Data Centre via www.ccdc.cam.ac.uk/data_request/cif.

Analytical and spectroscopy data. Aminonitrones and compounds **1–20** were characterized by HRESI$^+$-MS, IR, ^{1}H and ^{13}C{^{1}H} NMR spectroscopies. In addition, **4**, **6**, **17**, **18**, **19,** and **20** were studied by single-crystal X-ray diffraction.

The HRESI$^+$ mass-spectra of aminonitrones exhibit a set of peaks corresponding to the quasi-ions $[M + H]^+$, $[M + Na]^+$, $[2M + H]^+$, and $[2M + Na]^+$. The IR spectra of aminonitrones display from one to three weak-to-strong bands in the range of 3433–3141 cm^{-1}, which were attributed to the N–H stretches. Medium-to-strong intensity bands at 3051–2857 cm^{-1} were assigned to the ν(C–H) vibrations. The spectra exhibit a very strong band at 1641–1610 cm^{-1} from ν(C=N). The ^{1}H NMR spectra of aminonitrones recorded in $CDCl_3$ display one broad signal at δ 6.72–5.69 from the amide H atoms and one signal at δ 4.16–3.19 from the nitrone methyl group. The ^{13}C{^{1}H} NMR spectra of aminonitrones exhibited signals at δ 149.26–146.29, which are characteristic of the *C*(=N)NH resonances. In the high-field region, the spectra of aminonitrones display one signal of the N*C*H$_3$ resonances at δ 46.90–41.65.

The HRESI$^+$ mass-spectra of **1–16** exhibit peaks corresponding to the quasi-ions $[M]^+$. The IR spectra of **1–16** display from one to three weak-to-medium bands in the range of 3481–3186 cm^{-1}, which were attributed to the N–H stretches. Weak-to-strong bands at 3086–2718 cm^{-1} were assigned to the ν(C–H). The IR spectra of **1–16** display one or two medium-to-very-strong bands in the range of 1685–1590 cm^{-1}, which were attributed to the C=N stretches.

The ^{1}H NMR spectra of **1–13** and **15–16** display a broad signal of NH in the region of δ 13.02–10.37 (no signal of the NH was observed for **14**, which could be explained in terms of fast exchange with water). Another characteristic feature of the spectra of **1–16** is availability of one singlet at δ 4.44–3.99 from NCH$_3$. The ^{1}H NMR spectra of **1–8** measured in $(CD_3)_2SO$ display two sets of signals of the C*H*NH (δ 3.79–3.62 and 3.58–3.44, respectively) of the cyclohexyl moiety with total integral intensity to 1H, whereas the spectrum of **10** displays two signals of the CH$_2$ moiety at δ 4.74 and 4.64, which indicates the availability of two tautomeric forms of these compounds around the C–N$_{amino}$ bond in the solutions. The ^{13}C{^{1}H} NMR spectra of **3–10** recorded

in $(CD_3)_2SO$ exhibit two set of signals of the C atoms of the 1,2,4-oxadiazolium ring in the region of δ 167.42–160.64, whereas the spectra of **1**–**2** and **11**–**16** display one set of signals. The spectra of **1**–**10** exhibit two set of signals of the NCH_3 (δ 54.32–43.67 and 53.52–43.04), whereas in the spectrum of **14** two set of signals of the CH_2 moiety (δ 63.86 and 61.13) were observed. This is coherent with the ^{1}H NMR data indicating the availability of the two tautomers in solutions.

Syntheses and characterization of the aminonitrones. A suspension of 2 g (24.0 mmol) of MeNHOH•HCl, 1.2 g (30.0 mmol) of NaOH, and 20 mmol of RCN in 10 mL of MeOH was stirred for 3 h at 65 °C, and then the mixture was filtered off. The solvent was evaporated *in vacuo* at 50 °C. The residue was dissolved in a mixture of 25 mL CH_2Cl_2 with 1 mL of MeOH; the solution was filtered off, and the solvent was evaporated at a reduced pressure at 40 °C. The product was crystallized under Me_2CO, and the precipitate which formed, was filtered off, washed with diethyl ether (10 mL), and dried at 50 °C for 2 h in air and then at RT in air.

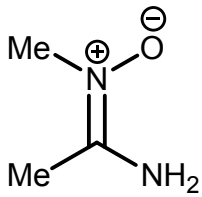

Yeld: 57% (1.003 g). Mp: 98–100 °C. R_f = 0.3 ($CHCl_3$/MeOH, 3:1). High resolution ESI$^+$-MS (MeOH, *m/z*): 89.0703 ([M + H]$^+$, calcd 89.0709), 111.0531 ([M + Na]$^+$, calcd 111.0529), 177.1339 ([2M + H]$^+$, calcd 177.1346), 199.1169 ([2M + Na]$^+$, calcd 199.1165). IR (KBr, selected bands, cm^{-1}): 3361 (s), 3228 (s), 3141 (s) *ν*(N–H); 1669 (s) *ν*(C=N). ^{1}H NMR ($CDCl_3$, *δ*): 6.72 (s, br, 2H, N*H*$_2$), 3.38 (s, 3H, NC*H*$_3$), 2.07 (s, 3H, CC*H*$_3$). ^{13}C{^{1}H} NMR ($CDCl_3$, *δ*): 146.29 (*C*=N); 130.53, 130.04, 128.86, 128.14 (Ar); 41.65 (N*C*H$_3$); 15.35 (C*C*H$_3$).

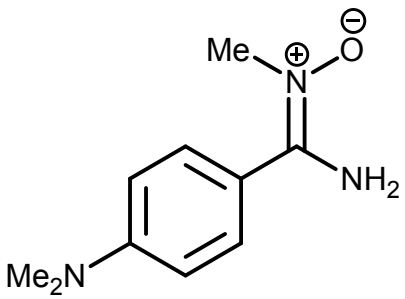

Yeld: 58% (2.239 g). Mp: 121–123 °C. R_f = 0.5 ($CHCl_3$/MeOH, 3:1) High resolution ESI$^+$-MS (MeOH, *m/z*): 194.1290 ([M + H]$^+$, calcd 194.1288), 216.1112 ([M + Na]$^+$, calcd 216.1107), 387.2512 ([2M + H]$^+$, calcd 387.2503), 49.2331 ([2M + Na]$^+$, calcd 409.2322 IR (KBr, selected bands, cm^{-1}): 3379 (s), 3220 (w-m) *ν*(N–H); 2978 (m), 2929 (m), 2900 (m) *ν*(C–H); 1610 (vs) *ν*(C=N).^{1}H NMR ($CDCl_3$, *δ*): 7.28 (d, J_{HH}^3 = 8.9 Hz, 2H, C*H*), 6.73 (d, J_{HH}^3 = 8.9 Hz, 2H, C*H*), 5.69 (s, br, 2H, NH_2), 3.53 (s, 3H, ONCH_3), 3.04 (s, 6H, CN(CH_3)$_2$). ^{13}C{^{1}H} NMR ($CDCl_3$, *δ*): 149.20 (*C*=N); 151.43, 129.06, 116.68, 111.55 (Ar); 43.31 (ON*C*H_3); 40.08 (CN(*C*H_3)$_2$).

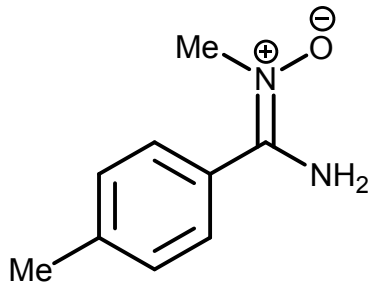

Yeld: 62% (2.022 g). Mp: 116–117 °C. R_f = 0.5 ($CHCl_3$/MeOH, 3:1). High resolution ESI$^+$-MS (MeOH, *m/z*): 165.1027 ([M + H]$^+$, calcd 165.1022), 187.0847 ([M + Na]$^+$, calcd 187.0842), 329.1982 ([2M + H]$^+$, calcd 329.1972), 351.1802 ([2M + Na]$^+$, calcd 351.1791). IR (KBr, selected bands, cm^{-1}): 3400 (m), 3319 (m), 3273 (m) *ν*(N–H); 3051 (m), 3024 (m), 2941 (m), *ν*(C–H); 1638 (vs) *ν*(C=N). ^{1}H NMR ($CDCl_3$, *δ*): 7.21 (d, J_{HH}^3 = 8.3 Hz, 2H, C*H*), 7.18 (d, J_{HH}^3 = 8.3 Hz, 2H, C*H*), 6.31 (s, br, 2H, NH_2), 3.24 (s, 3H, NCH_3), 2.32 (s, 3H, CCH_3). ^{13}C{^{1}H} NMR ($CDCl_3$, *δ*): 149.07 (*C*=N); 140.80, 129.50, 127.99, 127.12 (Ar); 43.08 (N*C*H_3); 21.33 (C*C*H_3).

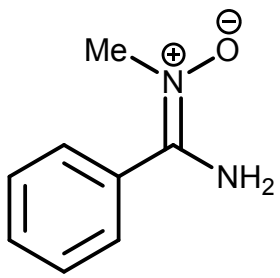

Yeld: 68% (2.04 g). Mp: 92–94 °C. R_f = 0.4 ($CHCl_3$/MeOH, 3:1). High resolution ESI$^+$-MS (MeOH, *m/z*): 151.0860 ([M + H]$^+$, calcd 151.0866). IR (KBr, selected bands, cm^{-1}): 3325 (s) *ν*(N–H); 3057 (m-s), 2936 (m-s), 2857 (m-s) *ν*(C–H); 1641 (vs) *ν*(C=N). ^{1}H NMR ($CDCl_3$, *δ*): 7.42–7.37

(m, 3H, C*H*), 7.33–7.31 (m, 2H, C*H*), 6.45 (s, br, 2H, NH_2), 3.19 (s, 3H, CH_3). $^{13}C\{^1H\}$ NMR ($CDCl_3$, δ): 149.26 (*C*=N); 130.53, 130.04, 128.86, 128.14 (Ar); 43.00 (*C*H_3).

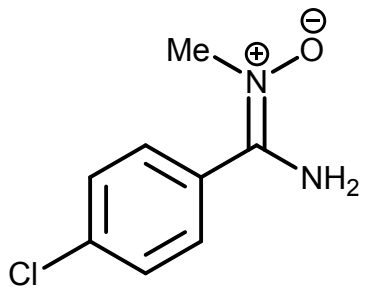

Yeld: 90% (3.312 g). Mp: 144–146 °C. R_f = 0.4 ($CHCl_3$/MeOH, 3:1). High resolution ESI$^+$-MS (MeOH, *m/z*): 185.0478 ([M + H]$^+$, calcd 185.0476), 369.0887 ([M + Na]$^+$, calcd 369.0880), 391.0706 ([2M + H]$^+$, calcd 391.0699), 207.0298 ([2M + Na]$^+$, calcd 207.0296 IR (KBr, selected bands, cm^{-1}): 3407 (w-m), 3283 (s), 3216 (sh) *v*(N–H); 2975 (s), 2934 (s) *v*(C–H); 1647 (vs) *v*(C=N). ^1H NMR ($CDCl_3$, δ): 7.47 (d, J_{HH}^3 = 8.4 Hz, 2H, C*H*), 7.37 (d, J_{HH}^3 = 8.4 Hz, 2H, C*H*), 5.99 (s, br, 2H, NH_2), 3.41 (s, 3H, CH_3). $^{13}C\{^1H\}$ NMR ($CDCl_3$, δ): 147.85 (*C*=N); 136.75, 129.57, 129.26, 128.43 (Ar); 43.25 (*C*H_3).

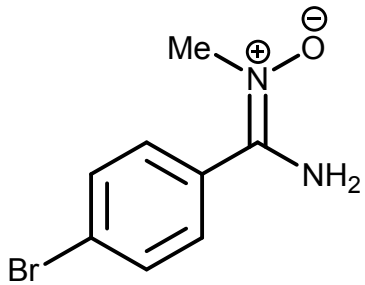

Yeld: 72% (3.283 g). Mp: 134–136 °C. R_f = 0.4 ($CHCl_3$/MeOH, 3:1). High resolution ESI$^+$-MS (MeOH, *m/z*): 228.9981 ([M + H]$^+$, calcd 228.9971), 458.9871 ([2M + H]$^+$, calcd 458.9850), 480.9691 ([2M + Na]$^+$, calcd 480.9669). IR (KBr, selected bands, cm^{-1}): 3404 (m-s), 3233 (m-s) *v*(N–H); 3021 (m-s), 2937 (m) *v*(C–H); 1641 (vs) *v*(C=N).^1H NMR ($CDCl_3$, δ): 7.64 (d, J_{HH}^3 = 8.4 Hz, 2H, C*H*), 7.32 (d, J_{HH}^3 = 8.4 Hz, 2H, C*H*), 5.82 (s, br, 2H, NH_2), 3.46 (s, 3H, CH_3). $^{13}C\{^1H\}$ NMR ($CDCl_3$, δ): 147.24 (*C*=N); 132.47, 129.66, 128.79, 125.28 (Ar); 43.59 (*C*H_3).

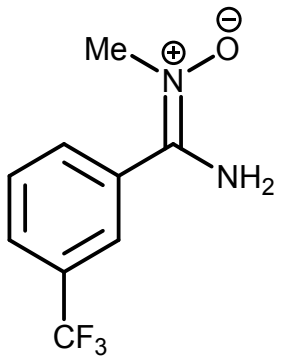

Yeld: 71% (3.096 g). Mp: 115–116 °C. R_f = 0.4 ($CHCl_3$/MeOH, 3:1). High resolution ESI$^+$-MS (MeOH, *m/z*): 219.0746 ([M + H]$^+$, calcd 219.0740), 241.0567 ([M + Na]$^+$, calcd 241.0559), 437.1422 ([2M + H]$^+$, calcd 437.1407), 459.1243 ([2M + Na]$^+$, calcd 459.1226). IR (KBr, selected bands, cm^{-1}): 3359 (s), 3321 (s) ν(N–H); 2983 (s), 2940 (s) ν(C–H); 1647 (vs) ν(C=N). ^{1}H NMR ($CDCl_3$, δ): 7.74-7.73 (m, 1H, C*H*), 7.65-7.60 (m, 3H, C*H*), 6.46 (s, br, 2H, NH_2), 3.30 (s, 3H, CH_3). ^{13}C{^{1}H} NMR ($CDCl_3$, δ): 147.51 (*C*=N); 131.74, 131.41 (q, J_{CF}^2 = 33.1 Hz),131.66 (s), 130.89 (s), 129.71 (s), 127.34, 127.31 (q, J_{CF}^3 = 3.6 Hz), 125.11, 125.07 (q, J_{CF}^3 = 3.7 Hz) (Ar); 124.68, 121.97 (q, CF_3, J_{CF}^1 = 272.7 Hz), 43.28 (CH_3).

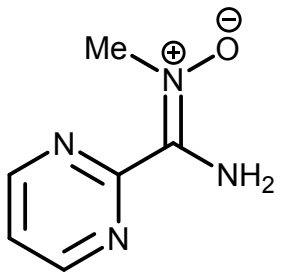

Yeld: 71% (2.158 g). Mp: 133–135 °C. R_f = 0.5 ($CHCl_3$/MeOH, 3:1). High resolution ESI$^+$-MS (MeOH, *m/z*): 153.0776 ([M + H]$^+$, calcd 153.0771), 305.1483 ([M + Na]$^+$, calcd 305.1467), 175.0597 ([2M + H]$^+$, calcd 175.0590), 327.1304 ([2M + Na]$^+$, calcd 327.1288). IR (KBr, selected bands, cm^{-1}): 3433 (s), 3224 (m), ν(N–H); 3051 (m), 2976 (m), 2932 (m) ν(C–H); 1621 (vs) ν(C=N). ^{1}H NMR ($CDCl_3$, δ): 8.78 (d, J_{HH}^3 = 4.9 Hz, 2H, C*H*), 7.25 (t, J_{HH}^3 = 4.9 Hz, 1H, C*H*), 6.44 (s, br, 2H, NH_2), 4.16 (s, 3H, CH_3). ^{13}C{^{1}H} NMR ($CDCl_3$, δ): 156.88, 155.79, 144.71, 119.82 (*C*=N and Ar); 46.90 (CH_3).

Syntheses and Characterization of 2-Methyl-5-amino-1,2,4-oxadiazolium Bromides (1–16). A solution of bromine (62 mL, 1.2 mmol) in chloroform (1 mL) was added in small portions to a stirred solution of R'NC (1.2 mmol) in chloroform (2 mL). After 1 min, powders of $RC(NH_2)=N^+(Me)O^-$ (1 mmol) and tribenzylamine (287 mg, 1 mmol) were added in one portion to the formed solution and the resulted mixture was stirred at RT for 5 min. The solvent was evaporated *in vacuo* at 40 °C. Crude product was subjected to column chromatography on silica gel ($CHCl_3$/MeOH, gradient from 85 to 95%) to give the target oxadiazolium salts.

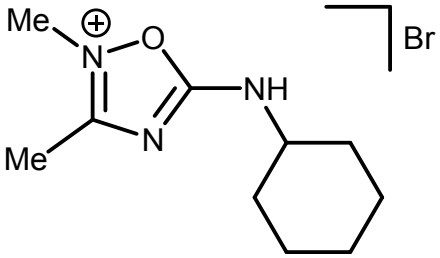

1. Yeld: 72% (199 mg). Mp: 141–143 °C (dec.). R_f = 0.2 ($CHCl_3$/MeOH, 3:1). High resolution ESI$^+$-MS (MeOH, *m/z*) 196.1450 ([M]$^+$, calcd 196.1444). IR (KBr, selected bands, cm^{-1}): 3393 (m), 3203 (w) *v*(N–H); 3078 (w-m), 3005 (w-m), 2934 (m), 2856 (m) *v*(C–H); 1669 (vs) *v*(C=N). ^{1}H NMR ($(CD_3)_2SO$, *δ*): 10.39 (s, br, 1H, N*H*), 3.99 (s, 3H, NCH_3), 3.62 + 3.44 (m, br, 1H, C*H*NH), 2.53 (s, 3H, CCH_3), 1.91–1.14 (m, 10H, $(CH_2)_5$). ^{13}C{^{1}H} NMR ($(CD_3)_2SO$, *δ*): 167.05, 166.44 (CH_3–*C*(=N)N and NH–*C*(=N)O); 53.96 + 53.23 (N*C*H_3); 37.01 (NH*C*H); 32.13, 25.09, 24.50 ($(CH_2)_5$); 12.75 (C*C*H_3).

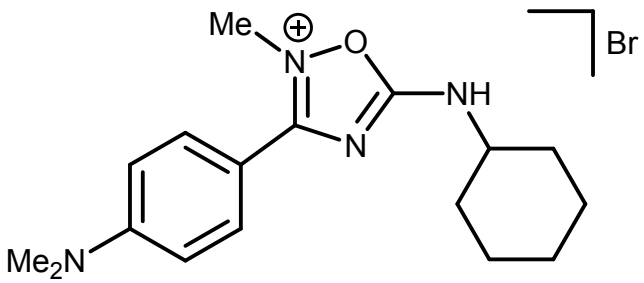

2. Yeld: 88% (335 mg). Mp: 136–138 °C (dec.). R_f = 0.1 ($CHCl_3$/MeOH, 9:1). High resolution ESI$^+$-MS (MeOH, *m/z*): 301.2017 ([M]$^+$, calcd 301.2023). IR (KBr, selected bands, cm^{-1}): 3423 (w-m), 3204 (w) *v*(N–H); 3061 (w-m), 2926 (m-s), 2854 (m-s), 2744 (m) *v*(C–H); 1674 (vs), 1607 (vs) *v*(C=N). ^{1}H NMR ($(CD_3)_2SO$, *δ*): 10.59 + 10.37 (s, br, 1H, N*H*), 7.83 (d, J_{HH}^3 = 8.1 Hz, 2H, C*H*),

6.89 (d, J_{HH}^3 = 8.1 Hz, 2H, C*H*), 4.09 (s, 3H, ONCH_3), 3.73 + 3.50 (m, br, 1H, C*H*NH), 3.09 (s, 6H, CN(CH_3)$_2$), 1.96–1.16 (m, 10H, (CH_2)$_5$). ^{13}C{^{1}H} NMR ((CD$_3$)$_2$SO, δ): 166.55, 165.84 ((CH$_3$)$_2$NC$_6$H$_4$–*C*(=N)N and NH–*C*(=N)O) 154.50, 132.22, 112.07, 106.76 (Ar); 53.90 + 53.21 (ON*C*H$_3$); 40.10 (CN(*C*H$_3$)$_2$); 32.23, 25.18, 24.54 ((*C*H$_2$)$_5$). The *C*HNH signal overlaps with the residual signal of the solvent.

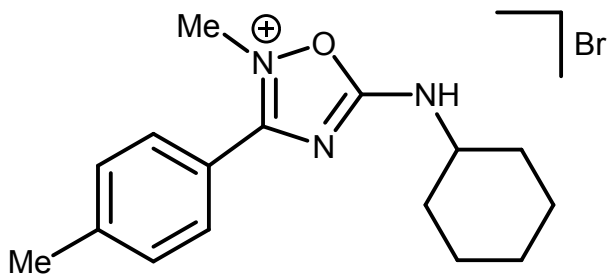

3. Yeld: 93% (327 mg). Mp: 157–158 °C (dec.). R_f = 0.2 (CHCl$_3$/MeOH, 9:1). High resolution ESI$^+$-MS (MeOH, *m/z*): 272.1750 ([M]$^+$, calcd 272.1757). IR (KBr, selected bands, cm^{-1}): 3437 (w), 3192 (w) ν(N–H); 3054 (w-m), 2930 (s), 2853 (s), 2732 (m-s) ν(C–H); 1668 (vs), 1610 (s) ν(C=N). ^{1}H NMR ((CD$_3$)$_2$SO, δ): 10.77 + 10.57 (s, br, 1H, N*H*), 7.89 (d, J_{HH}^3 = 7.8 Hz, 2H, C*H*), 7.53 (d, J_{HH}^3 = 7.8 Hz, 2H, C*H*), 4.14 (s, 3H, NCH_3), 3.76 + 3.54 (m, br, 1H, C*H*NH), 2.46 (s, 3H, CCH_3), 1.98–1.17 (m, 10H, (CH_2)$_5$). ^{13}C{^{1}H} NMR ((CD$_3$)$_2$SO, δ): 166.33, 166.23, 165.60 (CH$_3$C$_6$H$_4$–*C*(=N)N, (*E*)–NH–*C*(=N)O, and (*Z*)–NH–*C*(=N)O); 145.71, 130.56, 130.31, 119.38 (Ar); 54.08 + 53.35 (N*C*H$_3$); 39.71 (*C*HNH); 32.15, 25.14, 24.51 ((*C*H$_2$)$_5$); 21.78 (C*C*H$_3$).

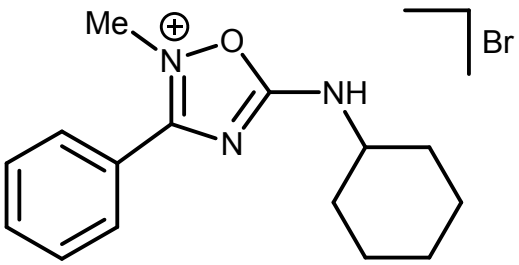

4. Yeld: 92% (311 mg). Mp: 98–100 °C (dec.). R_f = 0.2 (CHCl$_3$/MeOH, 9:1). High resolution ESI$^+$-MS (MeOH, *m/z*): 258.1605 ([M]$^+$, calcd 258.1601). IR (KBr, selected bands, cm^{-1}): 3438 (w), 3357 (w), 3209 (w) ν(N–H); 3064 (w-m), 2930 (m-s), 2854 (s), 2742 (m-s) ν(C–H); 1680 (vs), 1600(m-s) ν(C=N). ^{1}H NMR ((CD$_3$)$_2$SO, δ): 10.76 (s, br, 1H, N*H*), 7.98 (d, J_{HH}^3 = 7.4 Hz, 2H, C*H*), 7.83 (t, J_{HH}^3 = 7.4 Hz, 1H, C*H*), 7.72 (t, J_{HH}^3 = 7.4 Hz, 2H, C*H*), 4.14 (s, 3H, CH_3), 3.76 + 3.55 (m,

br, 1H, C*H*NH), 1.98–1.17 (m, 10H, (CH_2)$_5$). ^{13}C{^{1}H} NMR ((CD$_3$)$_2$SO, δ): 166.40, 166.24, 165.52 (C$_6$H$_5$–*C*(=N)N, (*E*)–NH–*C*(=N)O, and (*Z*)–NH–*C*(=N)O); 134.81, 130.28, 129.99, 122.30 (Ar); 54.15 + 53.40 (*C*H$_3$); 32.13, 25.14, 24.52 ((*C*H$_2$)$_5$).The *C*HNH signal overlaps with the residual signal of the solvent.

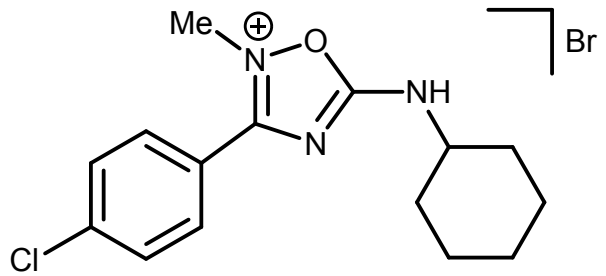

5. Yeld: 85% (316 mg). Mp: 173–174 °C (dec.). R_f = 0.3 (CHCl$_3$/MeOH, 9:1). High resolution ESI$^+$-MS (MeOH, *m/z*): 292.1213 ([M]$^+$, calcd 292.1211). IR (KBr, selected bands, cm^{-1}): 3423 (w), 3186 (w) *v*(N–H); 3024 (w-m), 2931 (m-s), 2855 (m-s), 2741 (m) *v*(C–H); 1667 (vs), 1596 (m-s) *v*(C=N). ^{1}H NMR ((CD$_3$)$_2$SO, δ): 10.74 (s, br, 1H, N*H*), 8.00 (d, J_{HH}^3 = 8.4 Hz, 2H, C*H*), 7.80 (d, J_{HH}^3 = 8.4 Hz, 2H, C*H*), 4.14 (s, 3H, C*H*$_3$), 3.75 + 3.55 (m, br, 1H, C*H*NH), 1.98–1.17 (m, 10H, (C*H*$_2$)$_5$). ^{13}C{^{1}H} NMR ((CD$_3$)$_2$SO, δ): 166.37, 166.21, 165.36, 164.67 ((*E*)–ClC$_6$H$_4$–*C*(=N)N, (*Z*)–ClC$_6$H$_4$–*C*(=N)N, (*E*)–NH–*C*(=N)O, and (*Z*)–NH–*C*(=N)O); 139.78, 132.21, 130.20, 121.17 (Ar); 54.17 + 53.44 (*C*H$_3$); 32.13, 25.12, 24.50 ((C*H*$_2$)$_5$). The *C*HNH signal overlaps with the residual signal of the solvent.

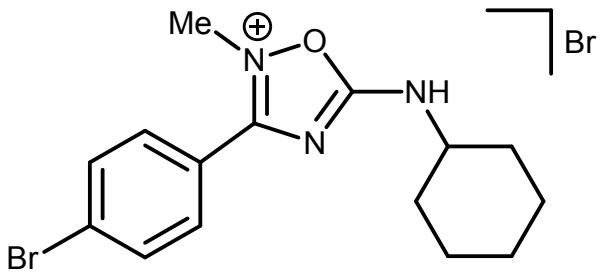

6. Yeld: 92% (383 mg). Mp: 169–170 °C (dec.). R_f = 0.3 (CHCl$_3$/MeOH, 9:1). High resolution ESI$^+$-MS (MeOH, *m/z*): 336.0699 ([M]$^+$, calcd 336.0706). IR (KBr, selected bands, cm^{-1}): 3418 (w), 3186 (w) *v*(N–H); 3051 (m), 2933 (s), 2854 (s), 2742 (m) *v*(C–H); 1667 (vs), 1590 (vs) *v*(C=N). ^{1}H NMR ((CD$_3$)$_2$SO, δ): 10.66 (s, br, 1H, N*H*), 7.95–7.83 (m, 4H, C*H*), 4.13 (s, 3H, C*H*$_3$), 3.75 + 3.55 (m, br, 1H, C*H*NH), 1.98–1.20 (m, 10H, (C*H*$_2$)$_5$). ^{13}C{^{1}H} NMR ((CD$_3$)$_2$SO, δ): 166.38,

166.22, 164.81 (BrC_6H_4–*C*(=N)N, (*E*)–NH–*C*(=N)O, and (*Z*)–NH–*C*(=N)O); 133.13, 132.21, 128.95, 121.50 (Ar); 54.17 + 53.43 (CH_3); 39.55 (*C*HNH); 32.13, 25.13, 24.50 ($(CH_2)_5$).

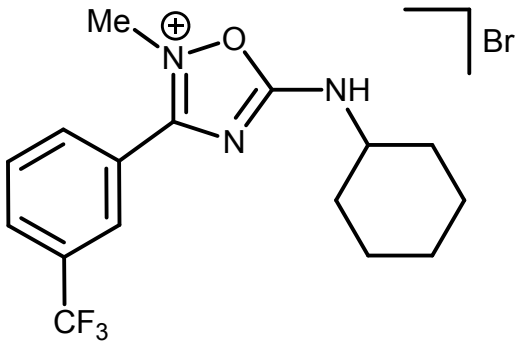

7. Yeld: 90% (365 mg). Mp: 127–129 °C (dec.). R_f = 0.4 ($CHCl_3$/MeOH, 9:1). High resolution ESI^+-MS (MeOH, *m/z*): 326.1460 ($[M]^+$, calcd 326.1475). IR (KBr, selected bands, cm^{-1}): 3375 (m), 3194 (w) *v*(N–H); 3067 (m), 2940 (m-s), 2858 (m), 2760 (w-m) *v*(C–H); 1679 (vs), 1618 (m) *v*(C=N). ^1H NMR ($(CD_3)_2SO$, *δ*): 10.81 (s, br, 1H, N*H*), 8.28 (d, J_{HH}^3 = 7.5 Hz, 1H, C*H*), 8.21 (d, J_{HH}^3 = 7.5 Hz, 2H, C*H*), 7.98 (t, J_{HH}^3 = 7.5 Hz, 1H, C*H*), 4.15 (s, 3H, CH_3), 3.79 + 3.58 (m, br, 1H, C*H*NH), 1.99–1.18 (m, 10H, $(CH_2)_5$). $^{13}C\{^1H\}$ NMR ($(CD_3)_2SO$, *δ*): 166.47, 166.27, 164.34 ($CF_3C_6H_4$–*C*(=N)N, (*E*)–NH–*C*(=N)O, and (*Z*)–NH–*C*(=N)O); 134.31, 134.16, 131.57, 131.46, 131.15, 131.12, 130.98, 130.65, 130.32, 130.00 (Ar); 125.22, 122.51 (q, CF_3, = 272.7 Hz); 54.18 + 53.50 (CH_3); 39.35 (*C*HNH); 32.13, 25.11, 24.45 ($(CH_2)_5$).

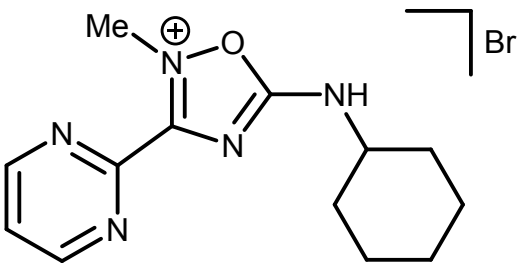

8. Yeld: 88% (299 mg). Mp: 146–148°C (dec.). R_f = 0.1 ($CHCl_3$/MeOH, 9:1). High resolution ESI^+-MS (MeOH, *m/z*): 260.1510 ($[M]^+$, calcd 260.1506). IR (KBr, selected bands, cm^{-1}): 3423 (w-m) *v*(N–H); 2991 (m-s), 2936 (s), 2856 (s) *v*(C–H); 1685 (vs) *v*(C=N). ^1H NMR ($(CD_3)_2SO$, *δ*): 10.84 (s, br, 1H, N*H*), 9.21 (d, J_{HH}^3 = 4.8 Hz, 2H, C*H*), 7.94 (t, J_{HH}^3 = 4.8 Hz, 1H, C*H*), 4.44 (s, 3H, CH_3), 3.79 + 3.58 (m, br, 1H, C*H*NH), 1.99–1.15 (m, 10H, $(CH_2)_5$). $^{13}C\{^1H\}$ NMR ($(CD_3)_2SO$, *δ*): 166.76,

166.55, 160.64 ($C_4H_3N_2$–*C*(=N)N, (*E*)–NH–*C*(=N)O, and (*Z*)–NH–*C*(=N)O); 159.12, 152.39, 125.02 (Ar); 54.32 + 53.52 (*C*H_3); 32.18, 25.12, 24.52 ((*C*H_2)$_5$). The *C*HNH signal overlaps with the residual signal of the solvent.

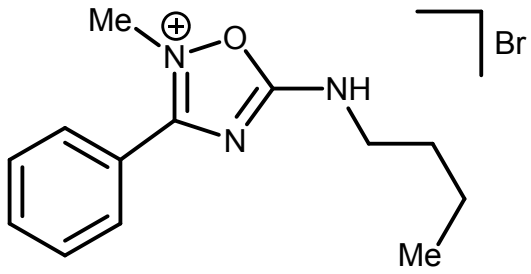

9. Yeld: 91% (284 mg). Mp: 98–100 °C (dec.). R_f = 0.2 ($CHCl_3$/MeOH, 9:1). High resolution ESI$^+$-MS (MeOH, *m/z*): 232.1440 ([M]$^+$, calcd 232.1444). IR (KBr, selected bands, cm^{-1}): 3413 (w-m), 3199 (w) *v*(N–H); 3061 (w-m), 2987 (w-m), 2940 (m), 2868 (m), 2760 (w-m) *v*(C–H); 1672 (vs), 1602 (m-s) *v*(C=N). ^{1}H NMR ((CD$_3$)$_2$SO, *δ*): 10.72 (s, br, 1H, N*H*), 7.98 (d, J_{HH}^3 = 7.2 Hz, 2H, C*H*), 7.83 (t, J_{HH}^3 = 7.2 Hz, 1H, C*H*), 7.72 (t, J_{HH}^3 = 7.2 Hz, 2H, C*H*), 4.15 (s, 3H, C*H*$_3$), 3.50 (t, J_{HH}^3 = 6.1 Hz, 2H, NH–C*H*$_2$), 1.66–1.59 (m, 2H, C*H*$_2$), 1.41–1.34 (m, 2H, C*H*$_2$), 0.92 (t, J_{HH}^3 = 7.1 Hz, 3H, C*H*$_3$). ^{13}C{^{1}H} NMR ((CD$_3$)$_2$SO, *δ*): 167.13, 167.00, 166.33, 165.52 ((*E*)–C$_6$H$_5$–*C*(=N)N, (*Z*)–C$_6$H$_5$–*C*(=N)N, (*E*)–NH–*C*(=N)O, and (*Z*)–NH–*C*(=N)O); 134.85, 130.27, 130.02, 122.28 (Ar); 43.67 + 43.04 (*C*H_3); 39.61 (NH−*C*H_2); 30.80 + 30.56 (*C*H_2); 19.72 + 19.60 (*C*H_2); 13.92 (*C*H_3).

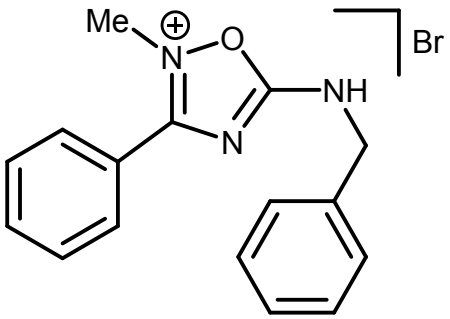

10. Yeld: 86% (298 mg). Mp: 120 °C (dec.). R_f = 0.5 ($CHCl_3$/MeOH, 9:1). High resolution ESI$^+$-MS (MeOH, *m/z*): 266.1286 ([M]$^+$, calcd 266.1288). IR (KBr, selected bands, cm^{-1}): 3422 (w), 3202 (w) *v*(N–H); 3053 (w-m), 2994 (w-m), 2933 (m), 2837 (m), 2745 (m) *v*(C–H); 1676 (vs), 1598 (m-s) *v*(C=N). ^{1}H NMR ((CD$_3$)$_2$SO, *δ*): 11.23 (s, br, 1H, N*H*), 8.00 (d, J_{HH}^3 = 7.4 Hz, 2H, C*H*), 7.84

(t, J_{HH}^3 = 7.4 Hz,1H, C*H*), 7.72 (t, J_{HH}^3 = 7.4 Hz, 2H, C*H*), 7.48–7.35 (m, 5H, C*H*), 4.74 + 4.64 (s, 2H, CH_2), 4.18 (s, 3H, CH_3). $^{13}C\{^1H\}$ NMR ($(CD_3)_2SO$, δ): 167.42, 167.05, 166.36, 165.46 ((*E*)–C_6H_5–*C*(=N)N, (*Z*)–C_6H_5–*C*(=N)N, (*E*)–NH–*C*(=N)O, and (*Z*)–NH–*C*(=N)O); 136.69, 134.91, 130.33, 130.04, 129.13, 128.41, 128.32, 122.22 (Ar); 47.23 + 46.54 (*C*H_3); 39.74 (*C*H_2).

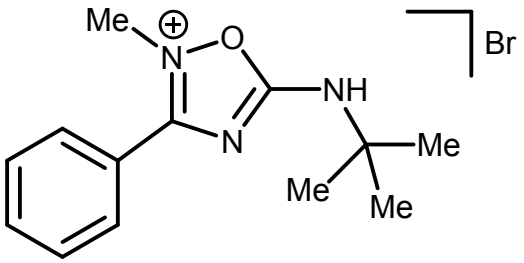

11. Yeld: 70% (218 mg). Mp: 147–148 °C (dec.). R_f = 0.1 ($CHCl_3$/MeOH, 9:1). High resolution ESI^+-MS (MeOH, *m/z*): 232.1447 ($[M]^+$, calcd 232.1444). IR (KBr, selected bands, cm^{-1}): 3481 (w-m), 3408 (w-m), 3193 (w) *ν*(N–H); 3076 (w-m), 2978 (m), 2853 (m), 2806 (m), 2733 (m) *ν*(C–H); 1659 (vs), 1602 (m) *ν*(C=N). ^1H NMR ($(CD_3)_2SO$, δ): 10.46 (s, br, 1H, N*H*), 7.99 (d, J_{HH}^3 = 7.4 Hz, 2H, C*H*), 7.84 (t, J_{HH}^3 = 7.4 Hz, 1H, C*H*), 7.73 (t, J_{HH}^3 = 7.4 Hz, 2H, C*H*), 4.16 (s, 3H, NCH_3), 1.47 (s, 9H, C(CH_3)$_3$). $^{13}C\{^1H\}$ NMR ($(CD_3)_2SO$, δ): 165.97, 165.08 (C_6H_5–*C*(=N)N and NH–*C*(=N)O); 134.83, 130.25, 130.05, 122.35 (Ar); 54.75 (N*C*H_3); 39.83 (*C*(CH$_3$)$_3$); 28.53 (C(*C*H$_3$)$_3$).

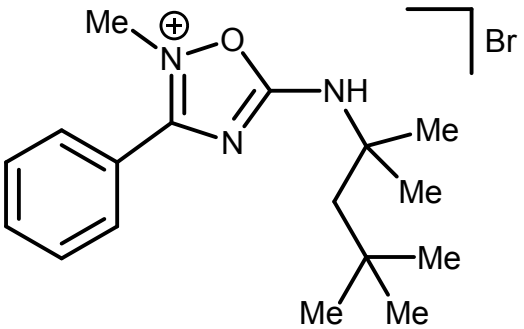

12. Yeld: 65% (239 mg). Mp: 124–126 °C (dec.). R_f = 0.2 ($CHCl_3$/MeOH, 9:1). High resolution ESI^+-MS (MeOH, *m/z*): 288.2064 ($[M]^+$, calcd 288.2070). IR (KBr, selected bands, cm^{-1}): 3476 (m), 3412 (m), 3194 (w) *ν*(N–H); 3080 (m), 2954 (s), 2905 (s), 2867 (s), 2738 (m-s) *ν*(C–H); 1659 (vs), 1603 (s) *ν*(C=N). ^1H NMR ($(CD_3)_2SO$, δ): 10.43 (s, br, 1H, N*H*), 7.99 (d, J_{HH}^3 = 7.4 Hz, 2H, C*H*), 7.84 (t, J_{HH}^3 = 7.4 Hz, 1H, C*H*), 7.73 (t, J_{HH}^3 = 7.4 Hz, 2H, C*H*), 4.17 (s, 3H, NCH_3), 1.85 (s, 2H, CH_2), 1.51 (s, 6H, C(CH_3)$_2$), 0.99 (s, 9H, C(CH_3)$_3$). $^{13}C\{^1H\}$ NMR ($(CD_3)_2SO$, δ): 165.42,

164.83 (C_6H_5–*C*(=N)N, NH–*C*(=N)O); 134.81, 130.29, 129.99, 122.30 (Ar); 58.35 (N*C*H_3); 50.42 (NH–*C*); 31.72, 31.47, 29.13 (C(*C*H_3)$_2$*C*H_2*C*(*C*H_3)$_3$).

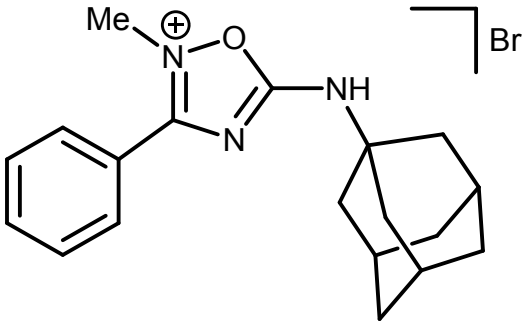

13. Yeld: 92% (359 mg). Mp: 141–142 °C (dec.). R_f = 0.1 ($CHCl_3$/MeOH, 9:1). High resolution ESI$^+$-MS (MeOH, *m/z*): 310.1903 ([M]$^+$, calcd 310.1914). IR (KBr, selected bands, cm^{-1}): 3394 (m), 3191 (m) *ν*(N–H); 3062 (m), 2909 (vs), 2852 (vs) *ν*(C–H); 1657 (vs), 1603(vs) *ν*(C=N). ^{1}H NMR ($(CD_3)_2SO$, *δ*): 10.38 (s, br, 1H, N*H*), 7.98 (d, J_{HH}^3 = 7.6 Hz, 2H, C*H*), 7.84 (t, J_{HH}^3 = 7.6 Hz, 1H, C*H*), 7.72 (t, J_{HH}^3 = 7.6 Hz, 2H, C*H*), 4.15 (s, 3H, CH_3), 2.13 (s, 3H, C*H*), 2.07 (s, 6H, CH_2), 1.68 (s, 6H, CH_2). ^{13}C{^{1}H} NMR ($(CD_3)_2SO$, *δ*): 165.62, 164.92 (C_6H_5–*C*(=N)N and NH–*C*(=N)O); 134.81, 130.24, 130.04, 122.33 (Ar); 55.06 (N*C*H_3); 40.84, 35.76, 29.24 (*C*H and *C*H_2).

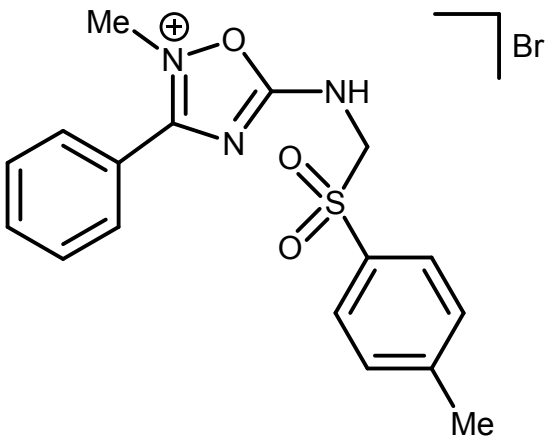

14. Yeld: 95% (403 mg). Mp: 134–136 °C (dec.). R_f = 0.5 ($CHCl_3$/MeOH, 9:1). High resolution ESI$^+$-MS (MeOH, *m/z*): 344.1060 ([M]$^+$, calcd 344.1063). IR (KBr, selected bands, cm^{-1}): 3434 (w-m) *ν*(N–H); 2928 (w-m), 2730 (m) *ν*(C–H); 1669 (vs), 1605 (m) *ν*(C=N). ^{1}H NMR ($(CD_3)_2SO$, *δ*): 7.86–7.82 (m, 5H, C*H*), 7.73–7.69 (m, 2H, C*H*), 7.48–7.47 (m, 2H, C*H*), 5.16 (s, 2H, CH_2), 4.17 (s, 3H, N−CH_3), 2.31 (s, 3H, C−CH_3). ^{13}C{^{1}H} NMR ($(CD_3)_2SO$, *δ*): 168.77, 167.65 (C_6H_5–*C*(=N)N

and NH–*C*(=N)O); 145.98, 145.23, 134.44, 130.62, 130.30, 130.03, 129.26, 129.03, 128.93, 128.72 (Ar); 63.86 + 61.13 (CH_2); 40.09 (NCH_3); 21.53 (CCH_3).

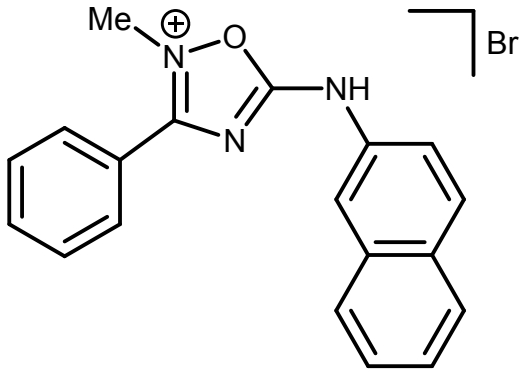

15. Yeld: 70% (267 mg). Mp: 147–148 °C (dec.). R_f = 0.7 ($CHCl_3$/MeOH, 9:1). High resolution ESI^+-MS (MeOH, *m/z*): 302.1291 ($[M]^+$, calcd 302.1288). IR (KBr, selected bands, cm^{-1}): 3432 (w-m), 3213 (w) *v*(N–H); 3052 (w-m), 2986 (w-m), 2925 (w-m), 2860 (w-m), 2735 (m) *v*(C–H); 1657 (vs), 1625 (vs) *v*(C=N). ^1H NMR ($(CD_3)_2SO$, *δ*): 13.02 (s, br, 1H, N*H*), 8.20–7.56 (m, 12H, C*H*), 4.33 (s, 3H, CH_3). $^{13}C\{^1H\}$ NMR ($(CD_3)_2SO$, *δ*): 165.23, 164.95 (C_6H_5–*C*(=N)N and NH–*C*(=N)O); 135.13, 133.52, 131.31, 130.50, 130.16, 130.04, 128.20, 127.61, 126.59, 122.05, 120.32, 117.93 (Ar), 39.99 (CH_3).

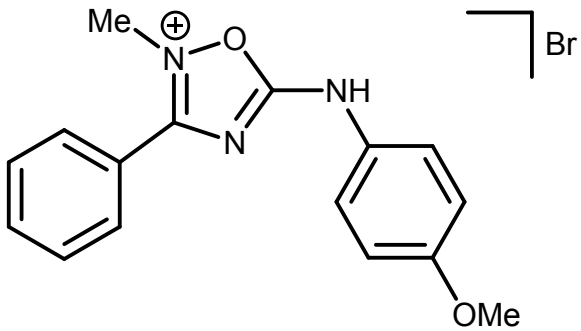

16. Yeld: 90% (326 mg). Mp: 131–133 °C (dec.). R_f = 0.6 ($CHCl_3$/MeOH, 9:1). High resolution ESI^+-MS (MeOH, *m/z*): 282.1242 ($[M]^+$, calcd 282.1237). IR (KBr, selected bands, cm^{-1}): 3443 (w), 3201 (w) *v*(N–H); 3086 (w), 2989 (w-m), 2836 (m), 2718 (m-s) *v*(C–H); 1658 (vs), 1593 (m) *v*(C=N). ^1H NMR ($(CD_3)_2SO$, *δ*): 12.75 (s, br, 1H, N*H*), 8.03 (d, J_{HH}^3 = 7.6 Hz, 2H, C*H*), 7.86 (t, J_{HH}^3 = 7.6 Hz, 1H, C*H*), 7.75 (t, J_{HH}^3 = 7.6 Hz, 2H, C*H*), 7.69–7.40 (m, 2H, C*H*), 7.08 (d, J_{HH}^3 = 9.0 Hz, 2H, C*H*), 4.24 (s, 3H, NCH_3), 3.79 (s, 3H, OCH_3). $^{13}C\{^1H\}$ NMR ($(CD_3)_2SO$, *δ*):

165.44, 164.96 (C_6H_5–*C*(=N)N and NH–*C*(=N)O); 135.05, 133.35, 130.13, 122.13, 115.27 (Ar); 55.94 (N*C*H_3); 39.78 (O*C*H_3).

Synthesis and characterization of 5-amino-1,2,4-oxadiazole (17). Powders of NH_2OH•HCl (209 mg, 3 mmol) and NaOH (120 mg, 3 mmol) were added in one portion to a solution of **4** (338 mg, 1 mmol) in ethanol (5 mL). The resulted mixture was stirred upon reflux for 3 h. The solvent was evaporated *in vacuo* at 40 °C. Crude product was subjected to column chromatography on silica gel (hexane/EtOAc, 9 : 1) to give the target oxadiazole in good yields.

17. Yield: 88% (213 mg). Mp: 121–123 °C. R_f = 0.3 (Hexane/EtOAc, 9:1). High resolution ESI^+-MS (MeOH, *m/z*): 244.1451 ($[M + H]^+$, calcd 244.1444), 266.1269 ($[M + Na]^+$, calcd 266.1264), 509.2659 ($[2M + Na]^+$, calcd 509.2635). $HRESI^-$-MS (*m/z*): 242.1278 ($[M – H]^-$, calcd 242.1288). IR (KBr, selected bands, cm^{-1}): 3289 (s) 3243 (s) *ν*(N–H); 3092 (m-s), 2928 (s), 2855 (s) *ν*(C–H); 1643 (vs) *ν*(C=N). ^1H NMR ($(CD_3)_2SO$, *δ*): 8.39 (d, J_{HH}^3 = 7.6 Hz, 1H, C*H*), 7.89 (d, J_{HH}^3 = 7.6 Hz, 2H, C*H*), 7.52–7.50 (m, 3H, C*H* + N*H*), 3.52 (m, br, 1H, NH–C*H*), 1.96–1.17 (m, 10H, $(CH_2)_5$). $^{13}C\{^1H\}$ NMR ($(CD_3)_2SO$, *δ*): 171.22, 167.84 (C_6H_5–*C*(=N)N and NH–*C*(=N)O); 131.24, 129.31, 128.07, 127.12 (Ar); 52.83 (NH–C*H)*, 32.84, 25.52, 24.80 ($(CH_2)_5$).

Synthesis and characterization of 2-Amino-1,2,4-triazole (18). N_2H_2•H_2O (146 mL, 3 mmol) was added in one portion to a solution of **4** (338 mg, 1 mmol) in ethanol (5 mL). The resulted mixture was stirred upon reflux for 3 h. The solvent was evaporated *in vacuo* at 40 °C. Crude product was subjected to column chromatography on silica gel (Hexane/EtOAc, 1 : 1) to give the target triazole in good yields.

18. Yield: 95% (230 mg). Mp: 177–178 °C. R_f = 0.4 (Hexane/EtOAc, 1:1). High resolution ESI^+-MS (MeOH, *m/z*): 243.1592 ($[M + H]^+$, calcd 243.1604). $HRESI^-$-MS (*m/z*): 241.1446 ($[M – H]^-$, calcd 241.1448). IR (KBr, selected bands, cm^{-1}): 3304 (s) *ν*(N–H); 3061 (m), 2930 (s), 2855 (s) *ν*(C–H); 1594 (s), 1559 (vs), 1530 (s) *ν*(C=N). ^1H NMR ($(CD_3)_2SO$, *δ*): 12.09 (s, br, 1H, N–N*H*), 7.90 (d, J_{HH}^3 = 7.3 Hz, 2H, C*H*), 7.40–7.35 (m, 3H, C*H*), 6.51 (s, br, 1H, CH–N*H*), 3.35 (m, br, 1H, NH–C*H* and H_2O), 1.91–1.16 (m, 10H, $(CH_2)_5$). $^{13}C\{^1H\}$ NMR ($(CD_3)_2SO$, *δ*): 158.92, 157.70 (C_6H_5–*C*(=N)N and NH–*C*(=N)NH); 132.82, 128.82, 128.65, 125.88 (Ar); 51.86 (NH–C*H)*, 33.36, 25.80, 25.08 ($(CH_2)_5$).

Synthesis and characterization of 2-Amino-1,3,5-triazine (19). Powder of $PhC(NH_2)=NH$ (211 mg, 3 mmol) was added in one portion to a solution of **4** (338 mg, 1 mmol) in ethanol (5 mL). The resulted mixture was stirred upon reflux for 48 h. The solvent was evaporated *in vacuo* at 40 °C. Crude product was subjected to column chromatography on silica gel (Hexane/EtOAc, 9 : 1) to give the target triazine in good yields.

19. Yield: 64% (211 mg). Mp: 137–139 °C. R_f = 0.6 (Hexane/EtOAc, 9:1). High resolution ESI^+-MS (MeOH, *m/z*): 331.1922 ($[M + H]^+$, calcd 331.1917). $HRESI^-$-MS (*m/z*): 329.1724 ($[M – H]^-$, calcd 329.1761), 365.1491 ($[M + Cl]^-$, calcd 365.1491). IR (KBr, selected bands, cm^{-1}): 3262 (m) *ν*(N–H); 2930 (m-s), 2856 (m) *ν*(C–H); 1567 (s), 1535 (s), 1517 (sh) *ν*(C=N). ^1H NMR ($(CD_3)_2SO$, *δ*): 8.52–8.47 (m, 4H, C*H*), 8.07–8.05 (d, J_{HH}^3 = 7.9 Hz, br, 1H, N*H*), 7.62–7.54 (m, 6H, C*H*), 4.02 (m, br, 1H, NH–C*H*), 1.99–1.07 (m, 10H, $(CH_2)_5$). $^{13}C\{^1H\}$ NMR ($(CD_3)_2SO$, *δ*): 170.75, 170.54, 165.56 (C_6H_5–*C*(=N)N and NH–*C*(=N)N); 136.90, 136.81, 132.46, 132.33, 129.00, 128.96, 128.60, 128.50 (Ar); 49.87 (NH–C*H)*, 32.62, 25.75, 25.24 ($(CH_2)_5$).

Syntheses and Characterization of ureide (20). A solution of **7c** (338 mg, 1 mmol) in a mixture of ethanol (4 mL) and water (1 mL) was stirred upon reflux for 48 h. The solvent was evaporated *in vacuo* at 40 °C. Crude product was subjected to column chromatography on silica gel (Hexane/EtOAc, 9 : 1) to give the target acylurea in good yields.

20. Yield: 95% (234 mg). Mp: 160–161 °C. R_f = 0.2 (Hexane/EtOAc, 9:1). High resolution ESI^+-MS (MeOH, *m/z*): 247.1444 ($[M + H]^+$, calcd 247.1441), 269.1263 ($[M + Na]^+$, calcd 269.1260). $HRESI^-$-MS (*m/z*): 245.1251 ($[M – H]^-$, calcd 245.1285), 513.2389 ($[2M + Na – 2H]^-$, calcd 513.2472). IR (KBr, selected bands, cm^{-1}): 3381 (w-m), 3282 (w) *ν*(N–H); 3136 (w), 3070 (w), 2941 (m-s), 2922 (m-s), 2855 (m) *ν*(C–H); 1691 (vs) *ν*(C=O). ^1H NMR ($(CD_3)_2SO$, *δ*): 10.66 (s, 1H, (CO)N*H*(CO)), 8.67 (d, J_{HH}^3 = 7.6 Hz, 1H, CH–N*H*), 7.97 (d, J_{HH}^3 = 7.6 Hz, 2H, C*H*), 7.62 (t, J_{HH}^3 = 7.6 Hz, 1H, C*H*), 7.50 (t, J_{HH}^3 = 7.6 Hz, 2H, C*H*), 3.65 (m, br, 1H, NH–C*H* and H_2O), 1.88–1.25 (m, 10H, $(CH_2)_5$). $^{13}C\{^1H\}$ NMR ($(CD_3)_2SO$, *δ*): 168.91, 153.07 (C_6H_5–*C*(=O)NH and NH–*C*(=O)NH); 133.17, 133.06, 128.93, 128.55 (Ar); 48.26 (NH–C*H)*, 32.79, 25.55, 24.63 ($(CH_2)_5$).

Spectra of the aminonitrones

Acquisition Parameter

Source Type	ESI	Ion Polarity	Positive	Set Nebulizer	0.3 Bar
Focus	Not active	Set Capillary	3200 V	Set Dry Heater	180 °C
Scan Begin	50 m/z	Set End Plate Offset	-500 V	Set Dry Gas	4.0 l/min
Scan End	3000 m/z	Set Collision Cell RF	300.0 Vpp	Set Divert Valve	Source

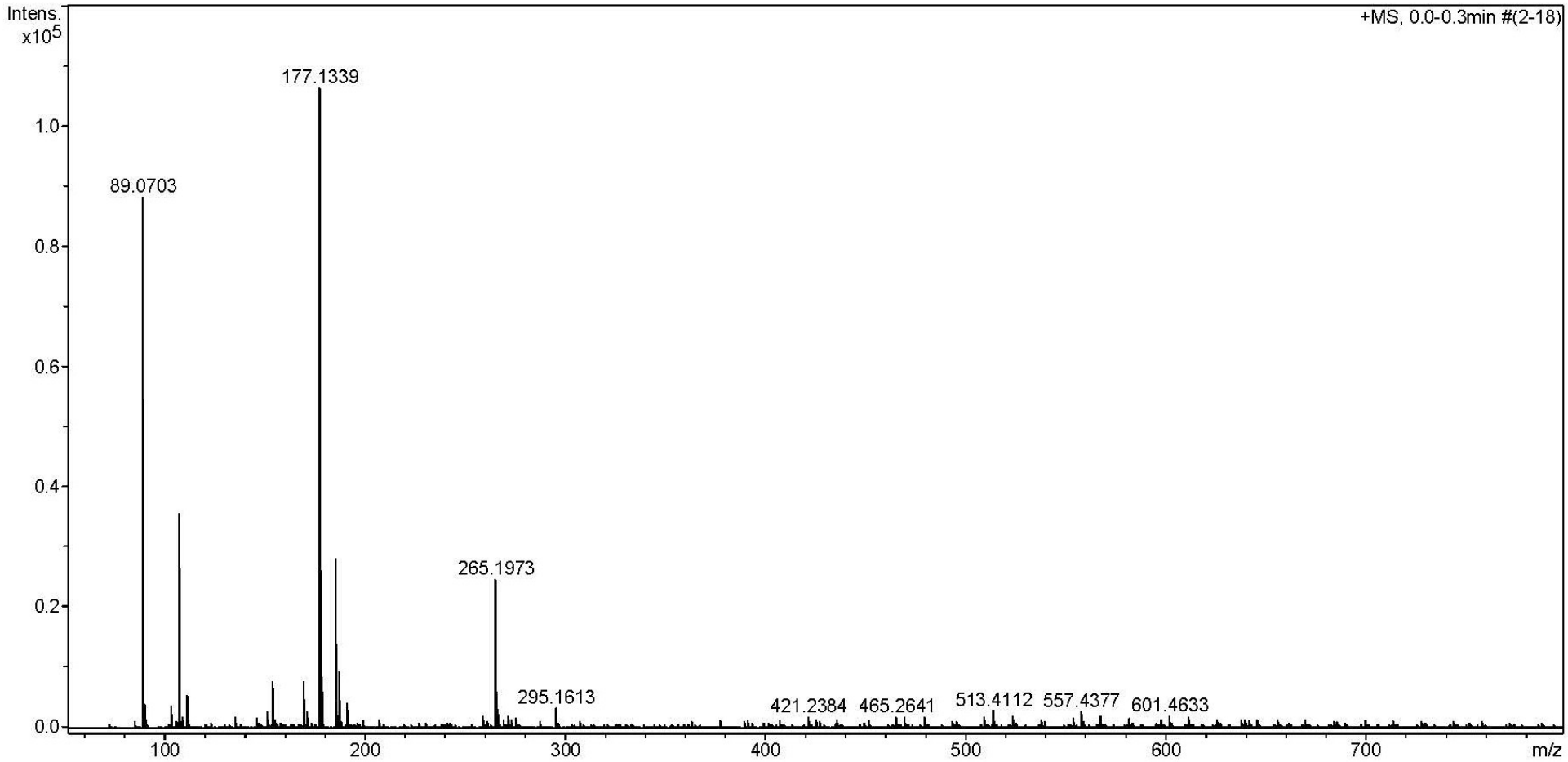

Figure 1S. HRESI$^+$-MS of $MeC(NH_2)=N^+(Me)O^-$.

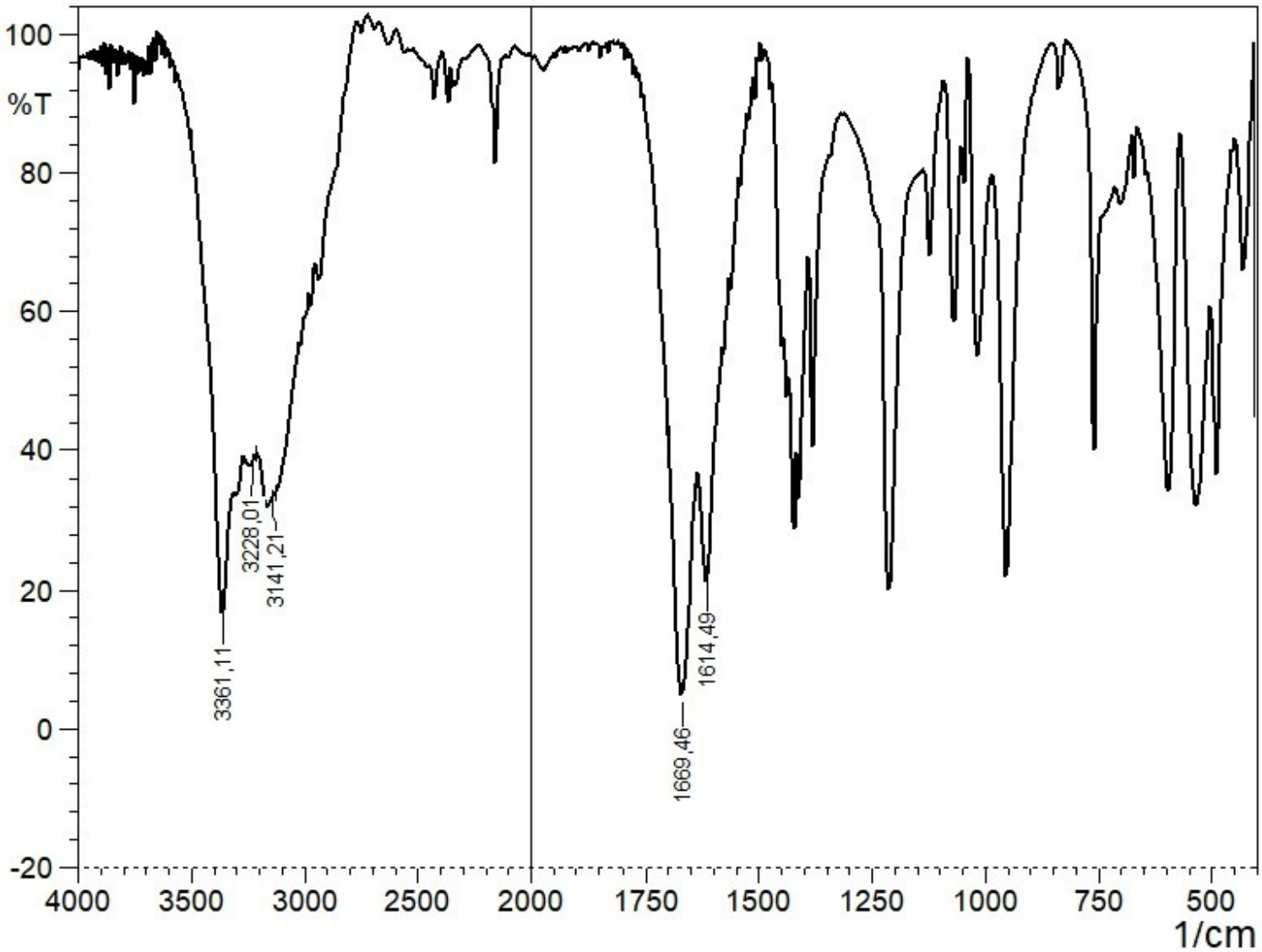

Figure 2S. IR spectrum of $MeC(NH_2)=N^+(Me)O^-$.

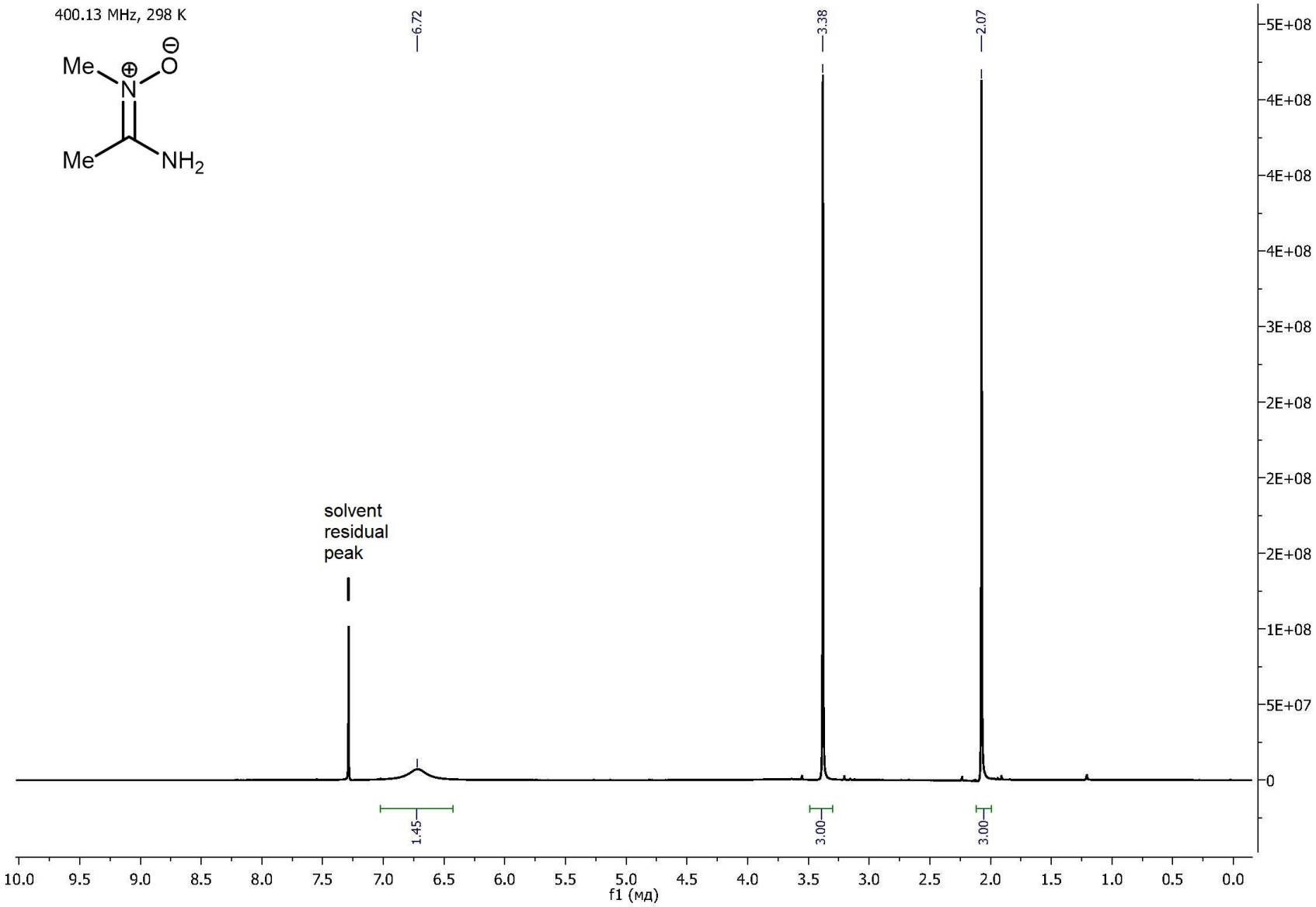

Figure 3S. ^{1}H NMR spectrum of $MeC(NH_2)=N^{+}(Me)O^{-}$.

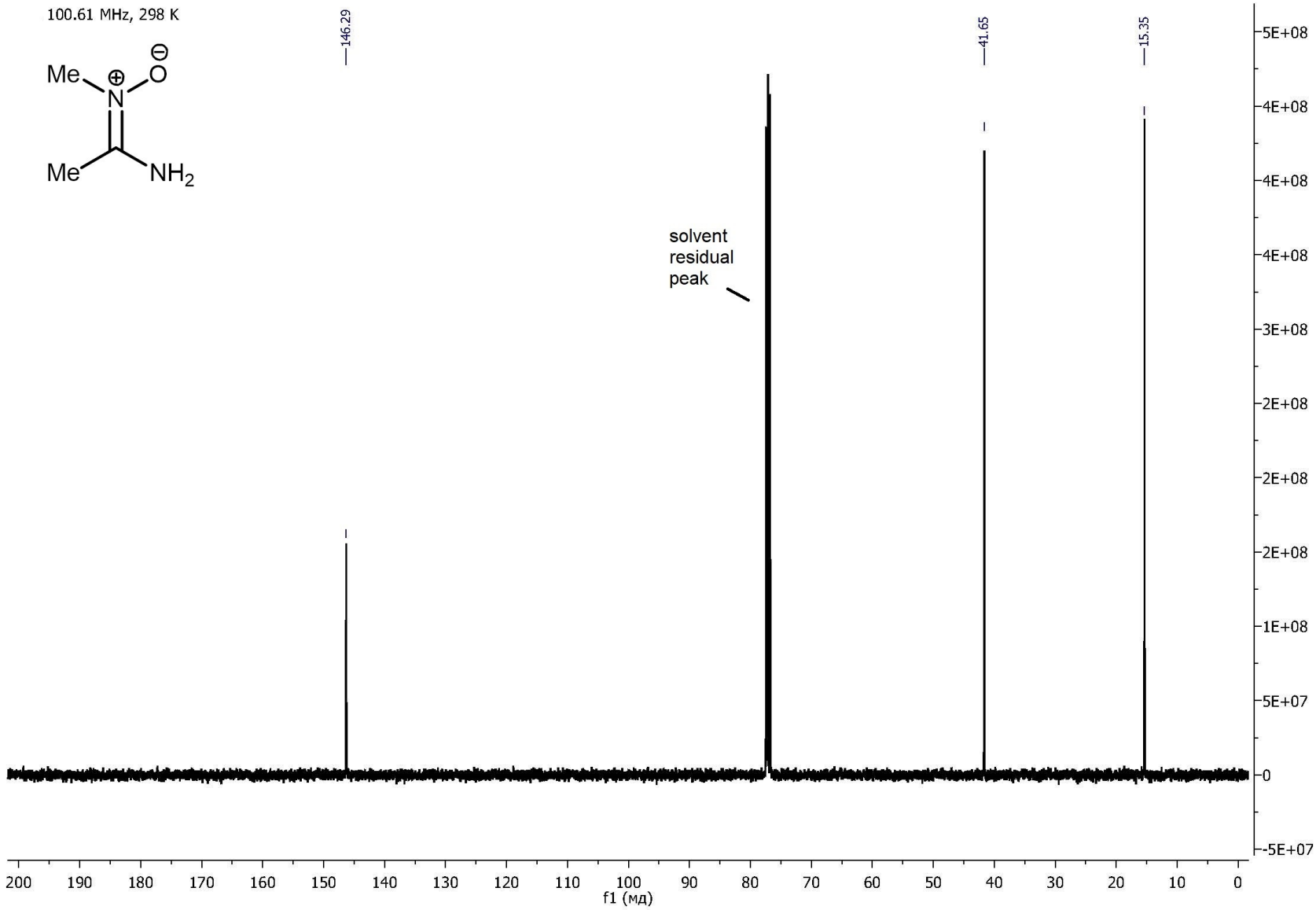

Figure 4S. $^{13}C\{^{1}H\}$ NMR spectrum of $MeC(NH_2)=N^{+}(Me)O^{-}$.

Acquisition Parameter

Source Type	ESI	Ion Polarity	Positive	Set Nebulizer	1.0 Bar
Focus	Active	Set Capillary	4500 V	Set Dry Heater	180 °C
Scan Begin	50 m/z	Set End Plate Offset	-500 V	Set Dry Gas	4.0 l/min
Scan End	1200 m/z	Set Collision Cell RF	300.0 Vpp	Set Divert Valve	Source

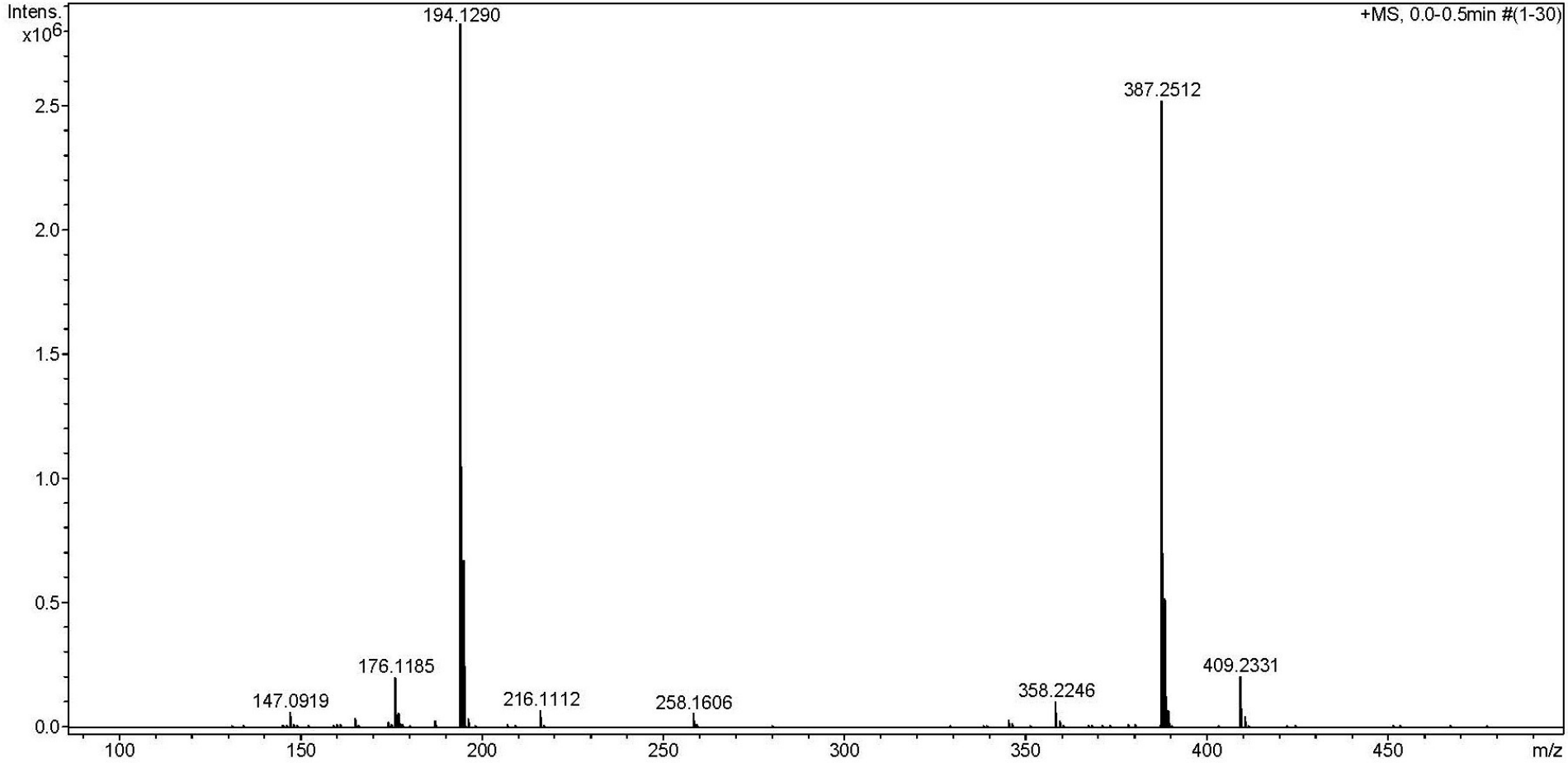

Figure 5S. HRESI$^+$-MS of *p*-$Me_2NC_6H_4C(NH_2)=N^+(Me)O^-$.

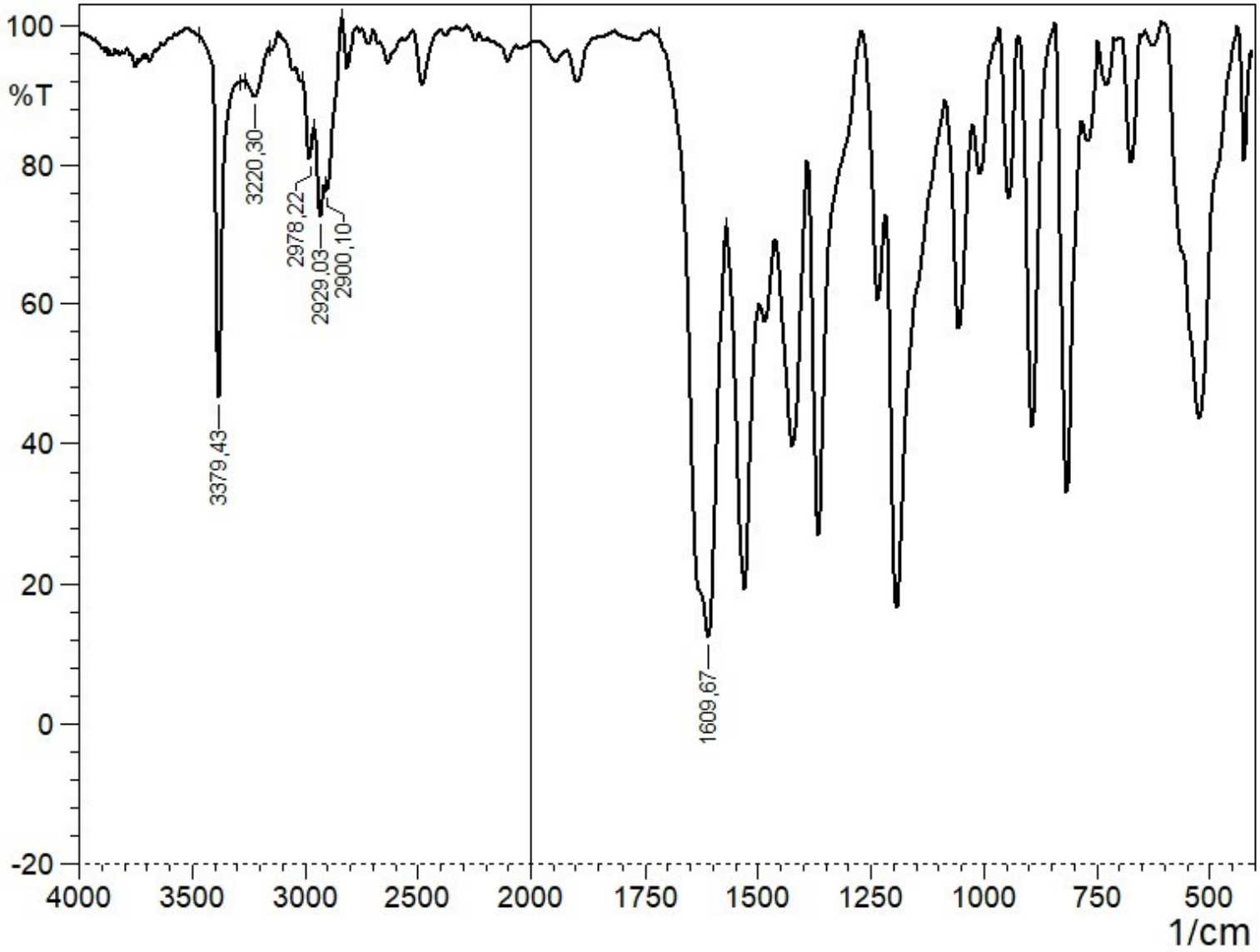

Figure 6S. IR spectrum of *p*-$Me_2NC_6H_4C(NH_2)=N^+(Me)O^-$.

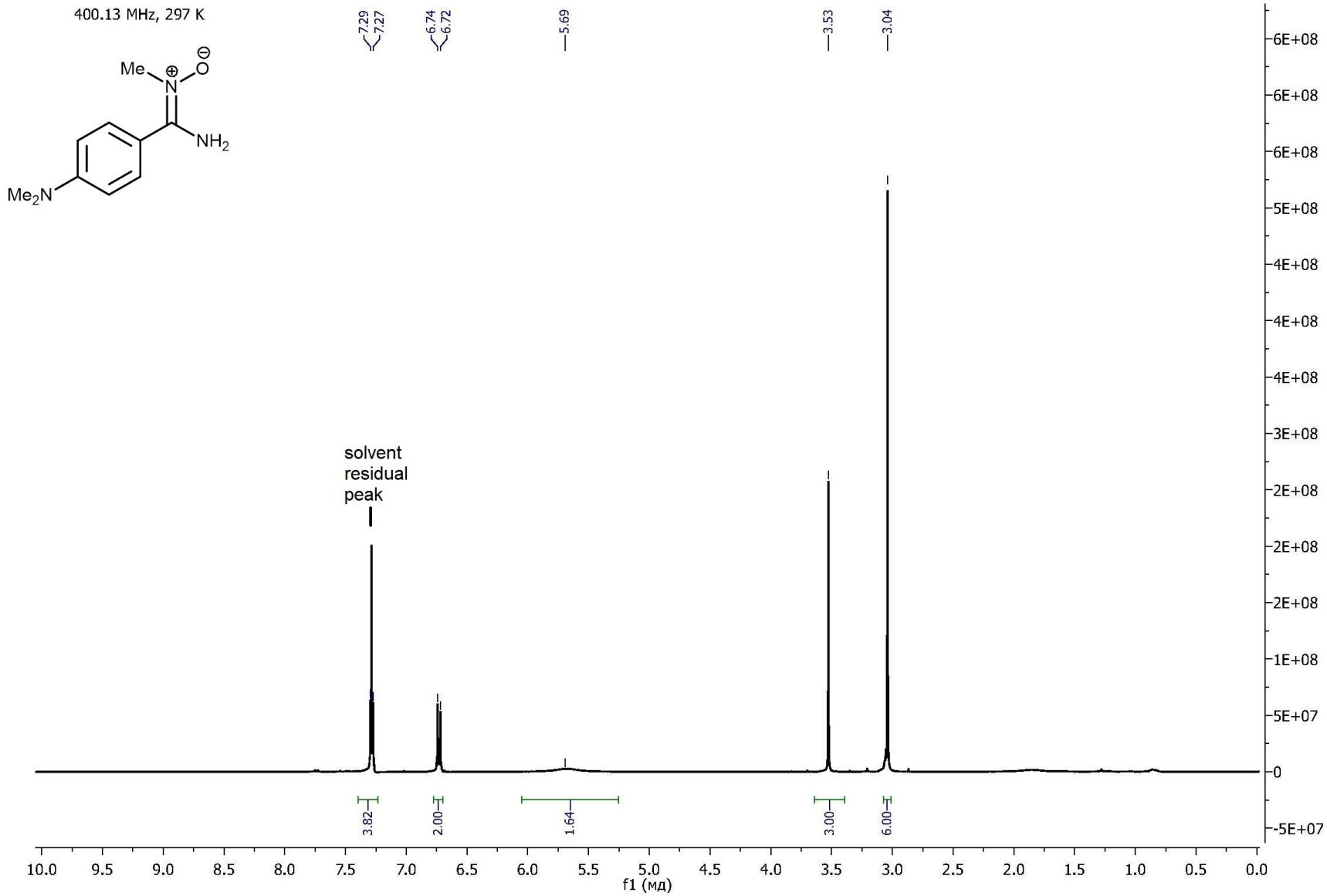

Figure 7S. ^{1}H NMR spectrum of *p*-$Me_2NC_6H_4C(NH_2)=N^+(Me)O^-$.

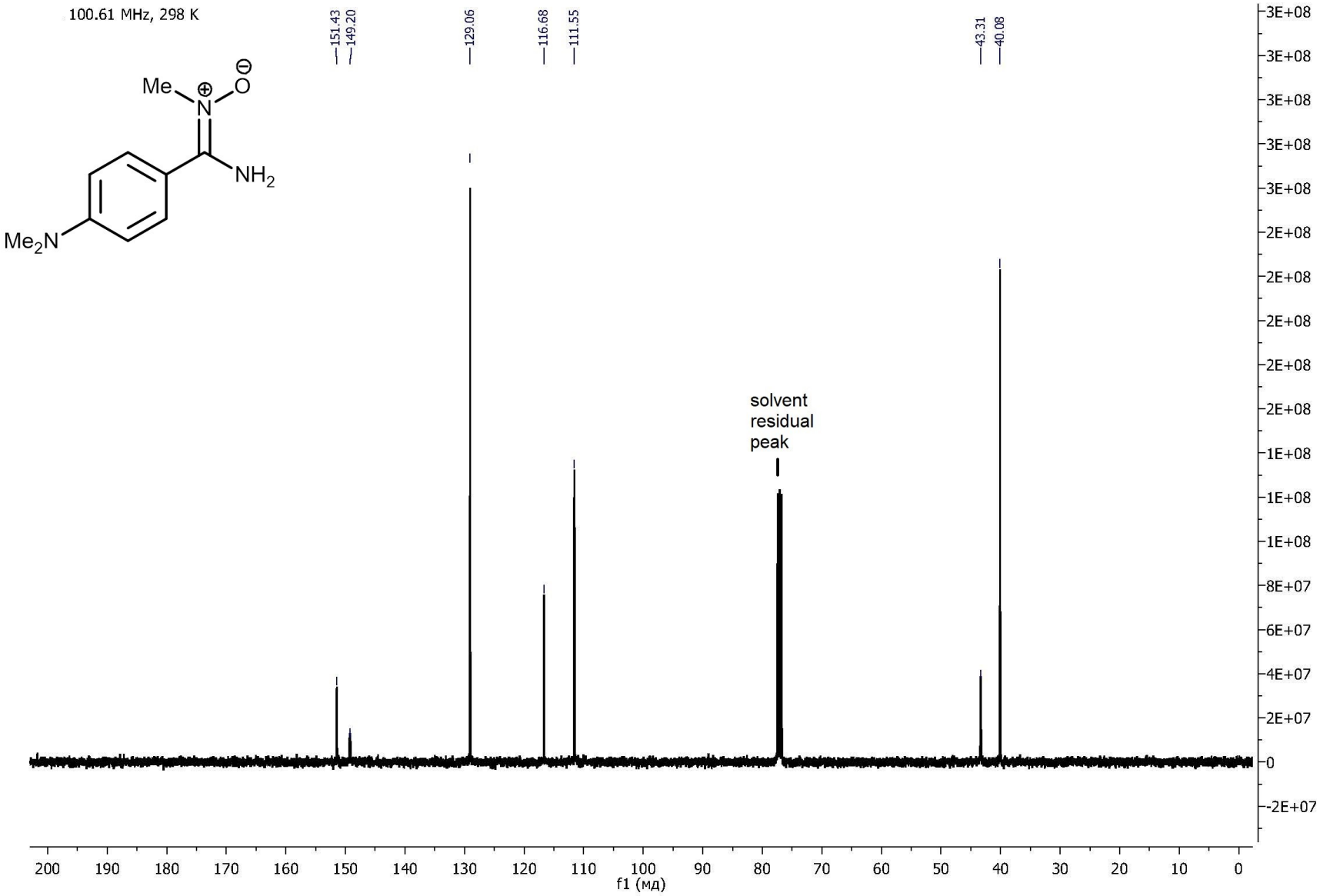

Figure 8S. $^{13}C\{^{1}H\}$ NMR spectrum of *p*-$Me_2NC_6H_4C(NH_2)=N^+(Me)O^-$.

Acquisition Parameter

Source Type	ESI	Ion Polarity	Positive	Set Nebulizer	1.0 Bar
Focus	Active	Set Capillary	4500 V	Set Dry Heater	180 °C
Scan Begin	50 m/z	Set End Plate Offset	-500 V	Set Dry Gas	4.0 l/min
Scan End	1200 m/z	Set Collision Cell RF	300.0 Vpp	Set Divert Valve	Source

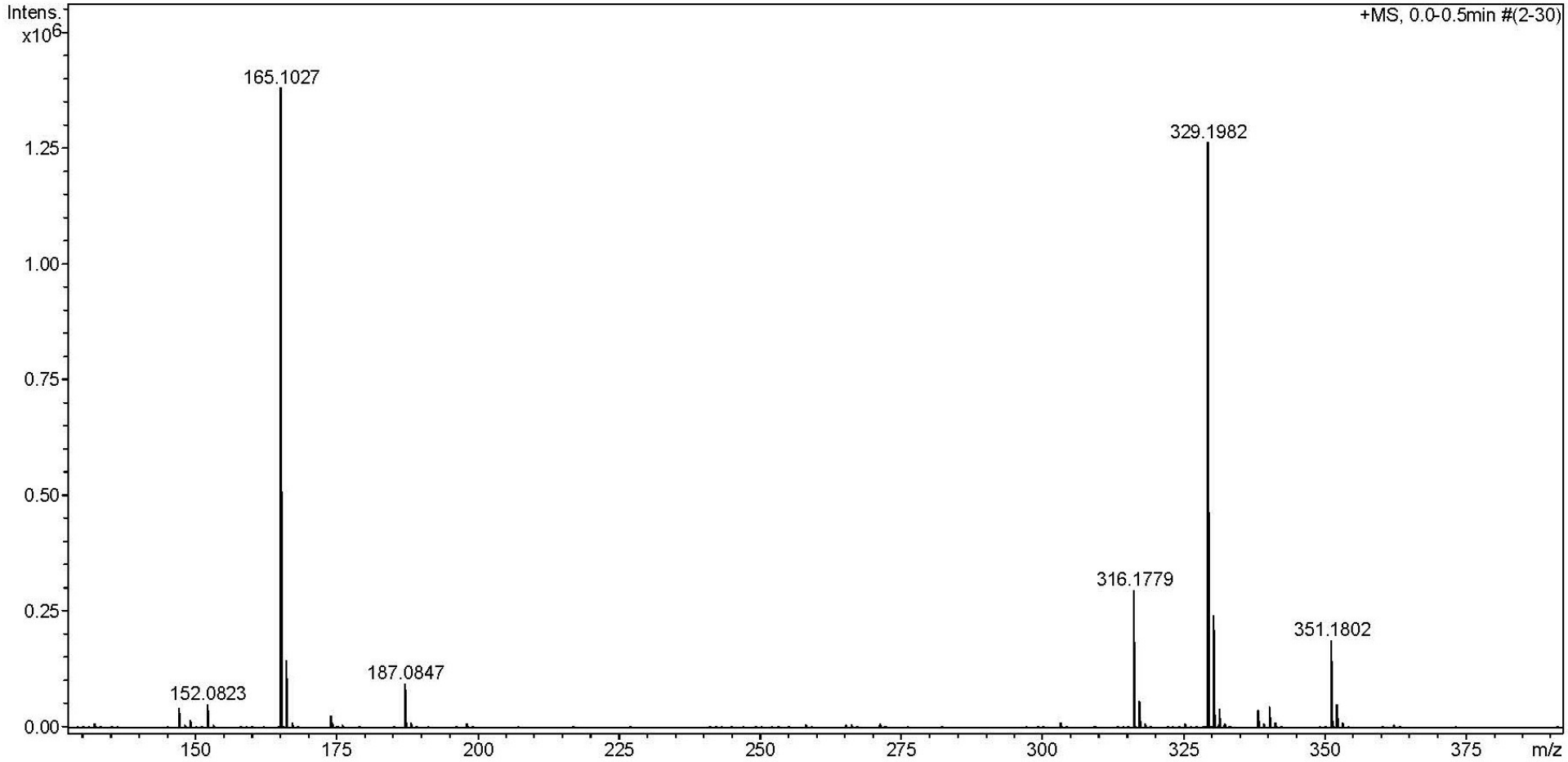

Figure 9S. HRESI$^+$-MS of *p*-$MeC_6H_4C(NH_2)=N^+(Me)O^-$.

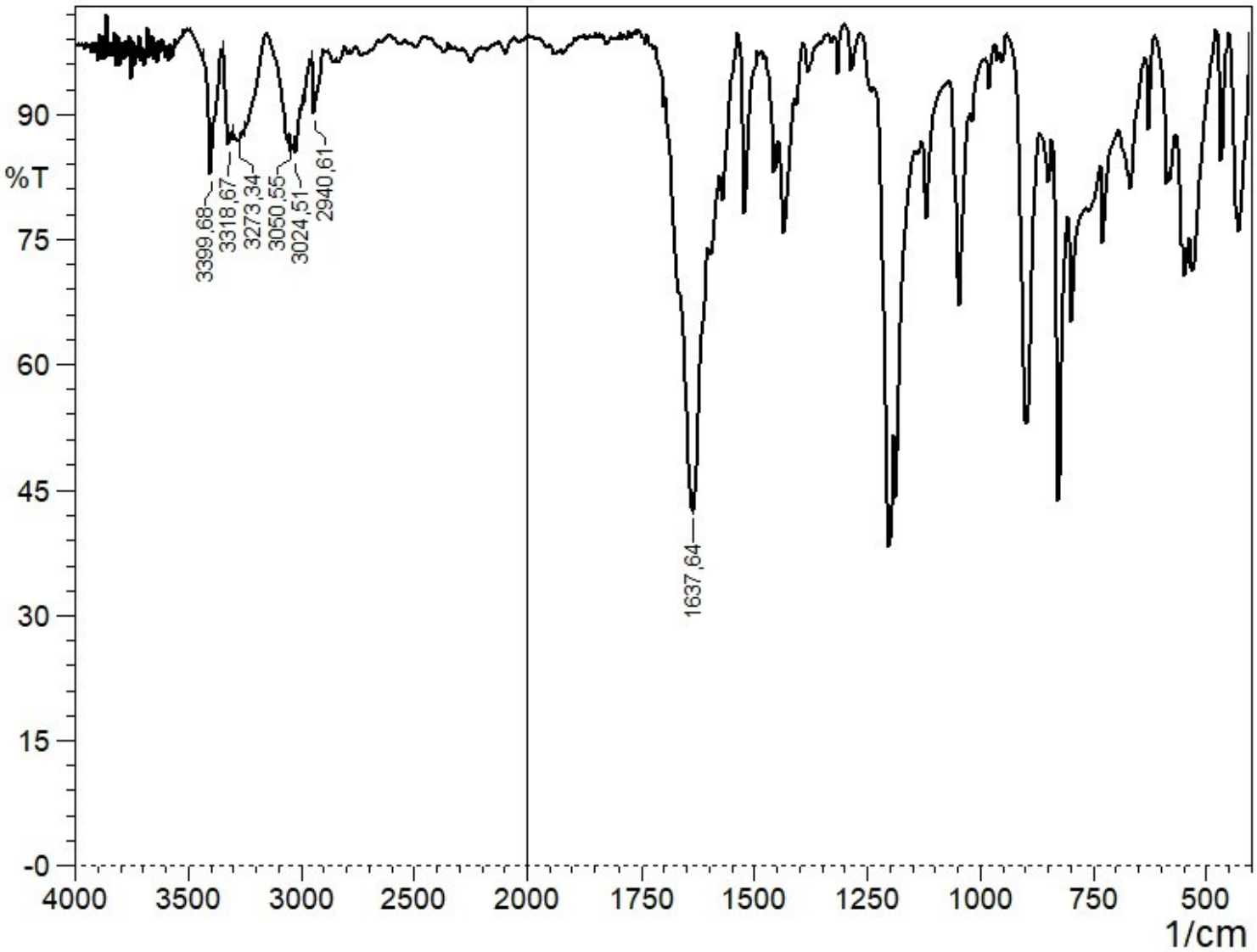

Figure 10S. IR spectrum of *p*-$MeC_6H_4C(NH_2)=N^+(Me)O^-$.

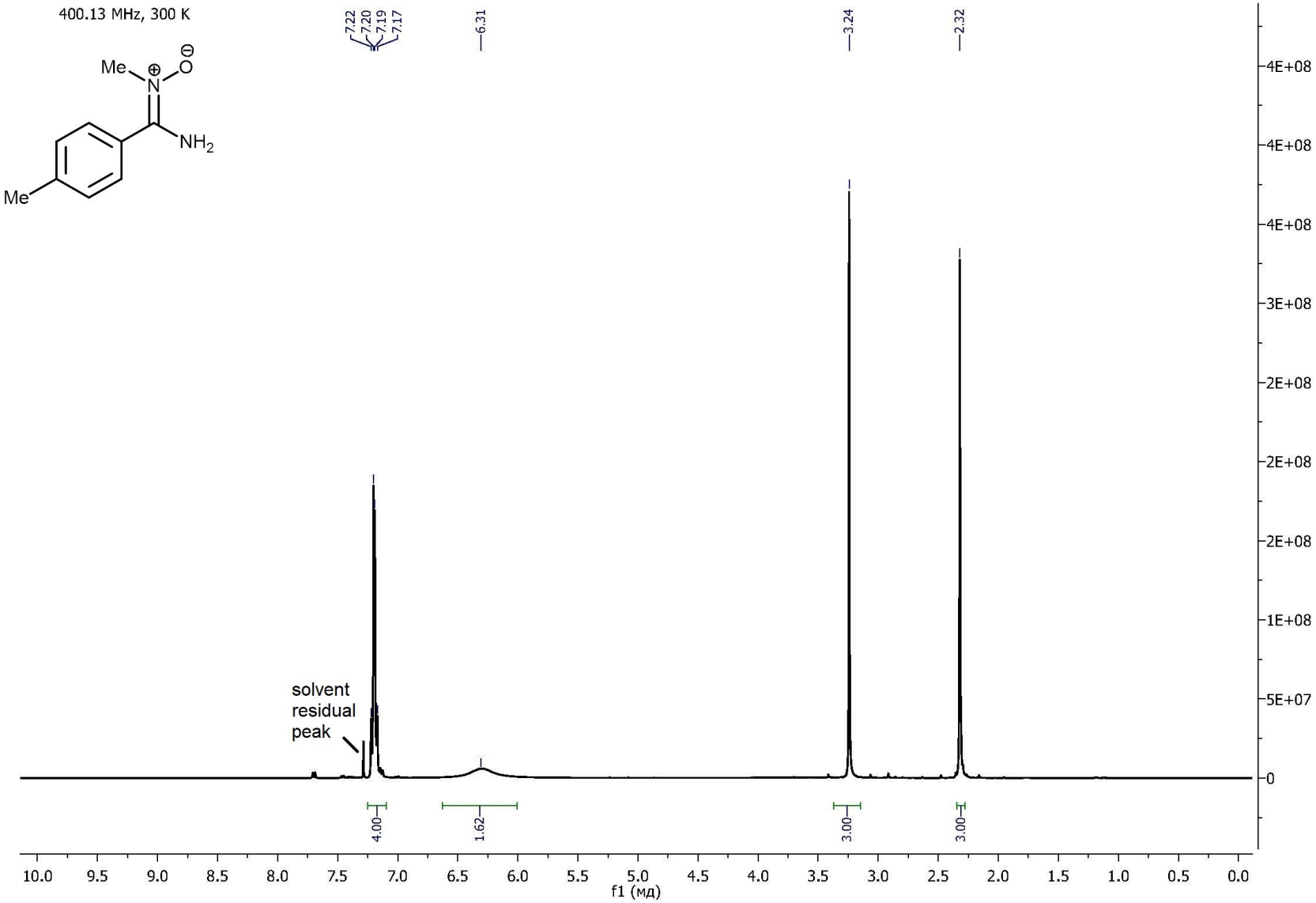

Figure 11S. ^{1}H NMR spectrum of *p*-$Me_2NC_6H_4C(NH_2)=N^+(Me)O^-$.

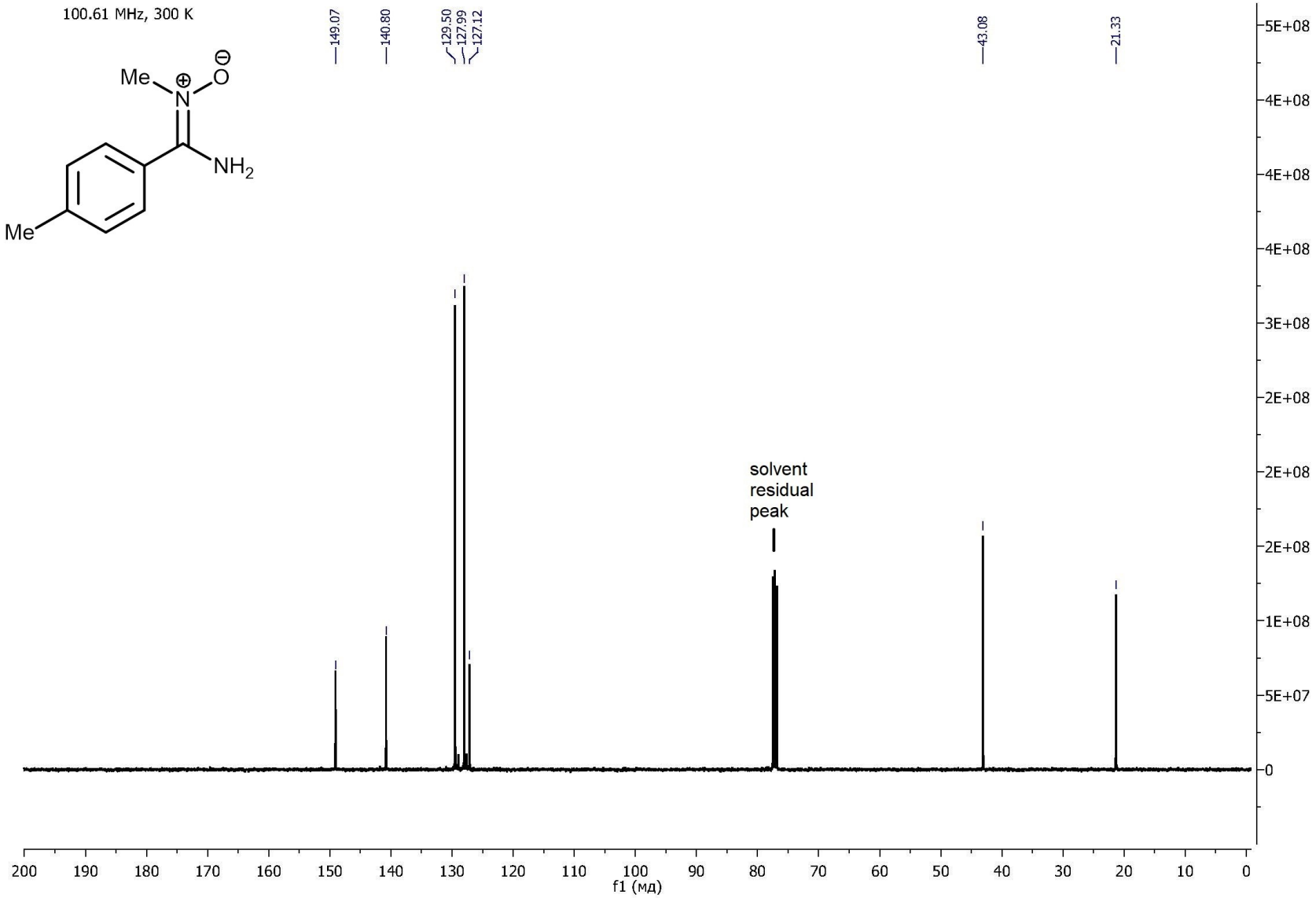

Figure 12S. $^{13}C\{^{1}H\}$ NMR spectrum of *p*-$MeC_6H_4C(NH_2)=N^+(Me)O^-$.

Acquisition Parameter

Source Type	ESI	Ion Polarity	Positive	Set Nebulizer	1.0 Bar
Focus	Active	Set Capillary	4500 V	Set Dry Heater	180 °C
Scan Begin	50 m/z	Set End Plate Offset	-500 V	Set Dry Gas	4.0 l/min
Scan End	1200 m/z	Set Collision Cell RF	300.0 Vpp	Set Divert Valve	Source

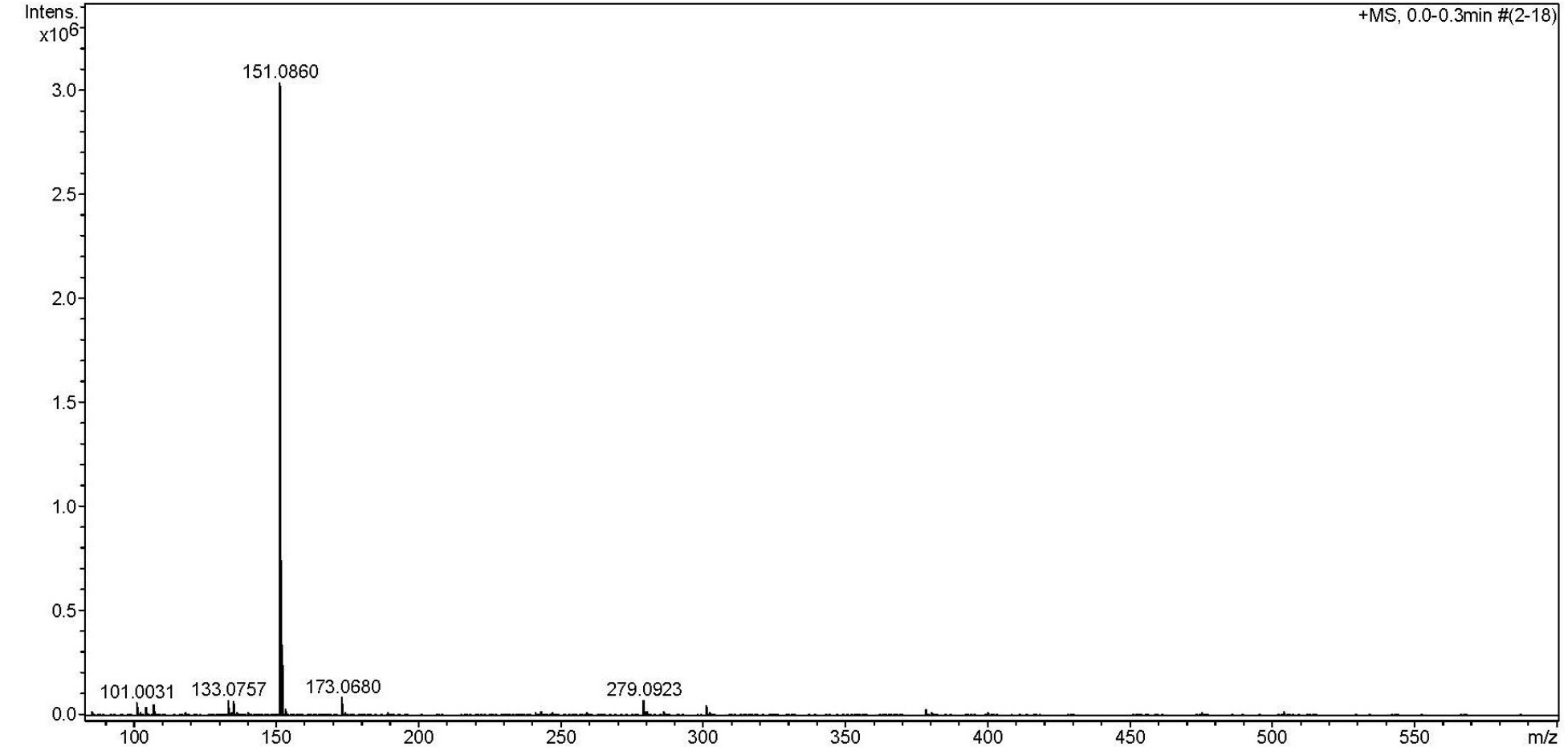

Figure 13S. HRESI$^+$-MS of $C_6H_5C(NH_2)=N^+(Me)O^-$.

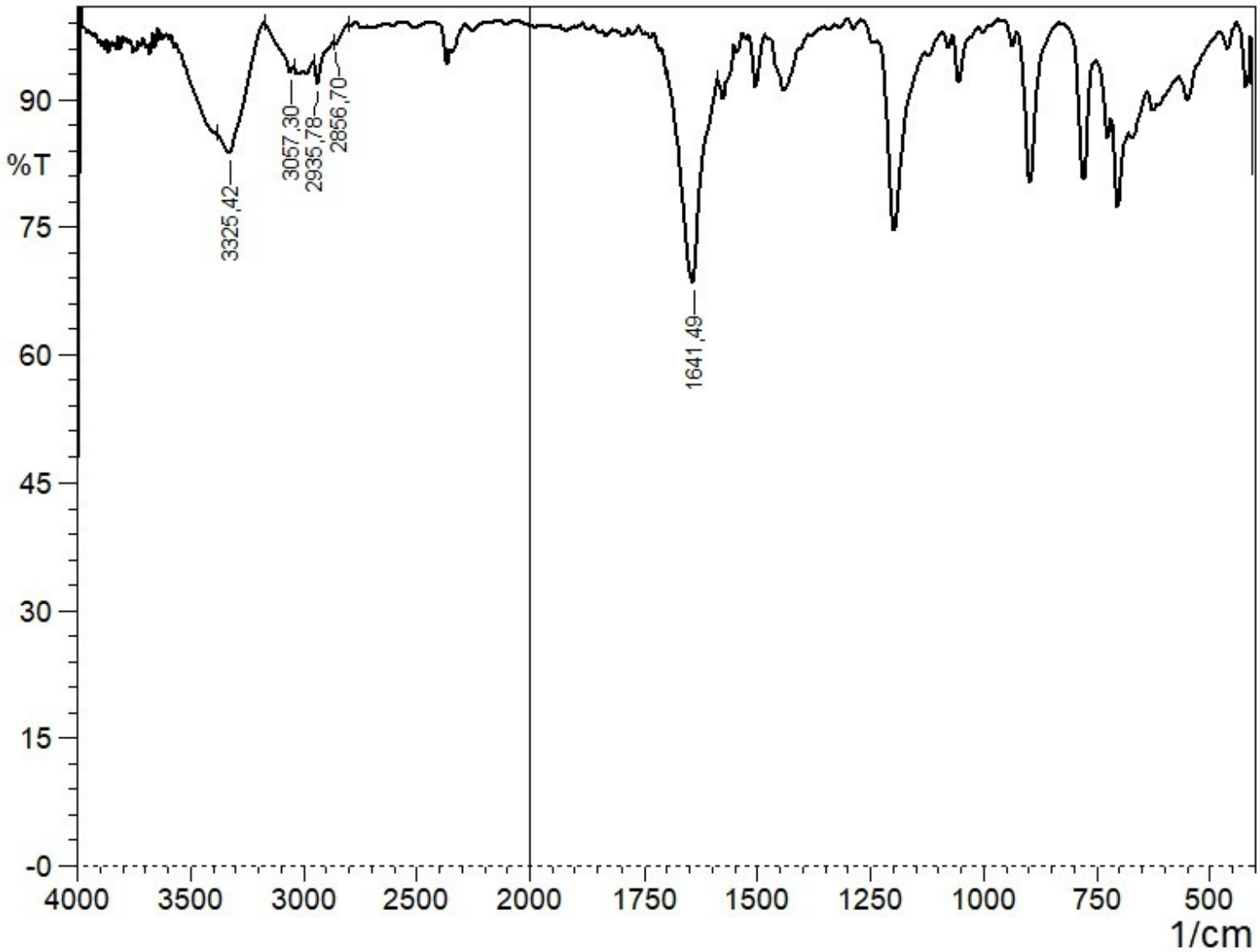

Figure 14S. IR spectrum of $C_6H_5C(NH_2)=N^+(Me)O^-$

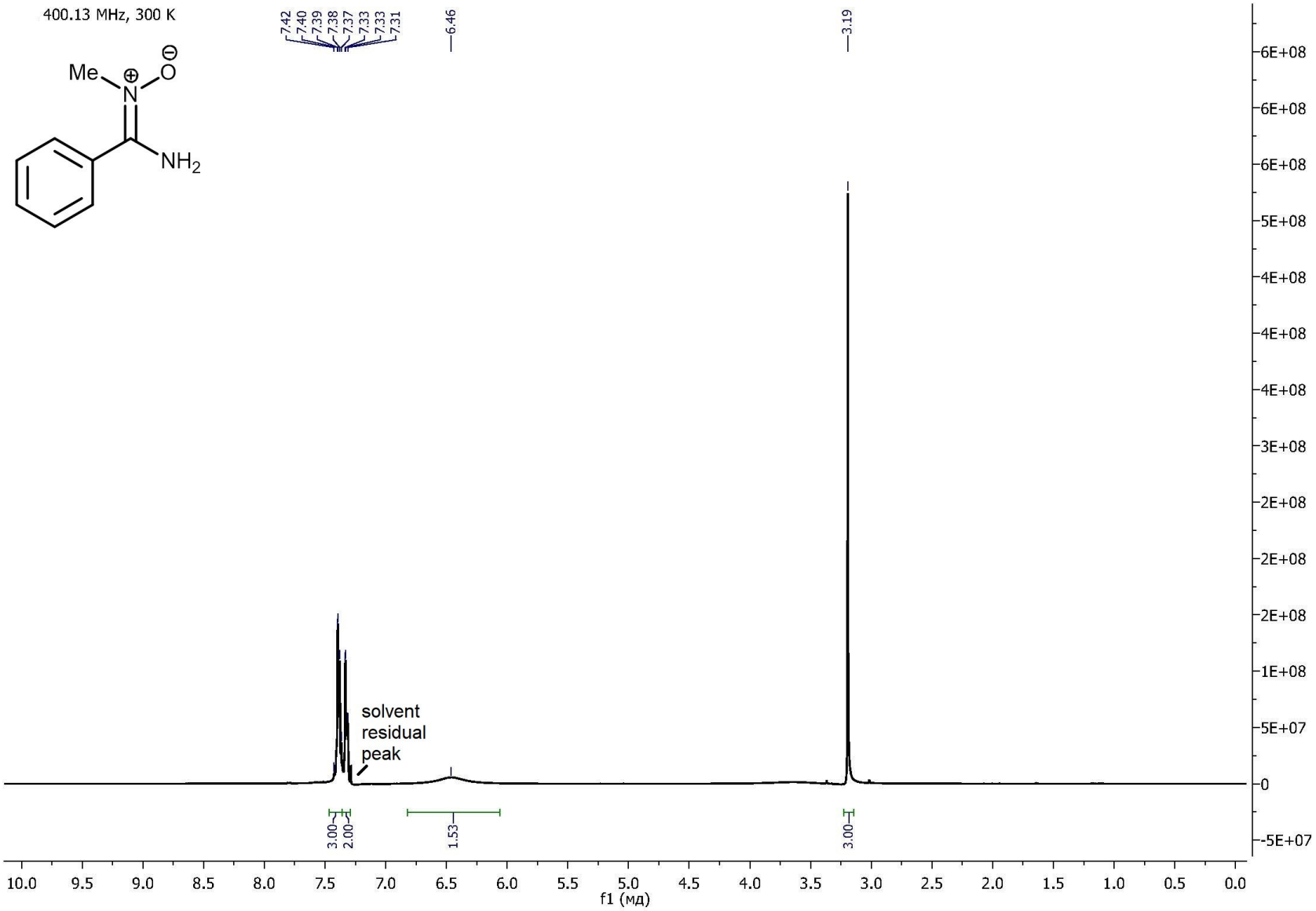

Figure 15S. ^{1}H NMR spectrum of $C_6H_5C(NH_2)=N^+(Me)O^-$.

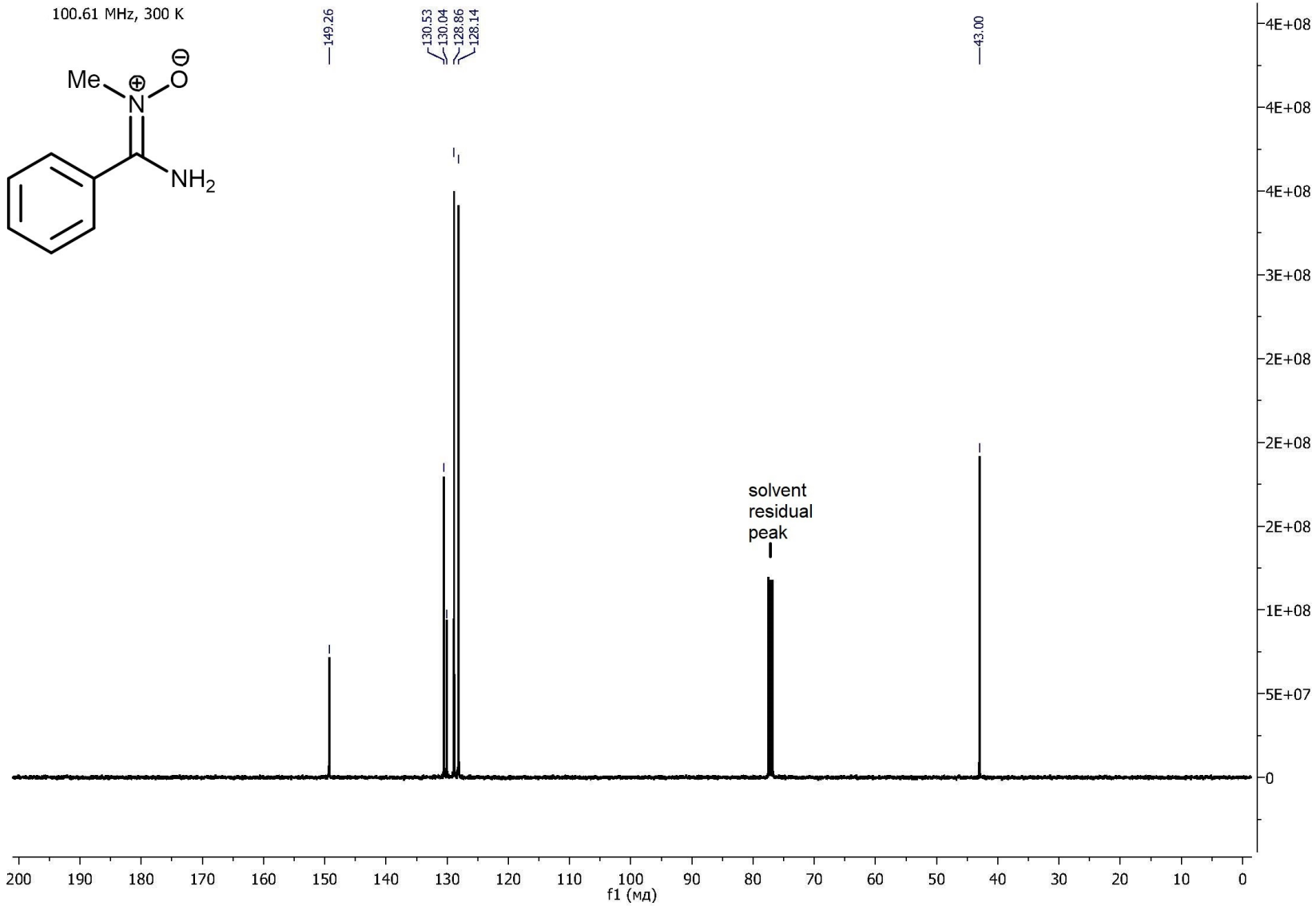

Figure 16S. $^{13}C\{^{1}H\}$ NMR spectrum of $C_6H_5C(NH_2)=N^+(Me)O^-$.

Acquisition Parameter

Source Type	ESI	Ion Polarity	Positive	Set Nebulizer	1.0 Bar
Focus	Active	Set Capillary	4500 V	Set Dry Heater	180 °C
Scan Begin	50 m/z	Set End Plate Offset	-500 V	Set Dry Gas	4.0 l/min
Scan End	1200 m/z	Set Collision Cell RF	300.0 Vpp	Set Divert Valve	Source

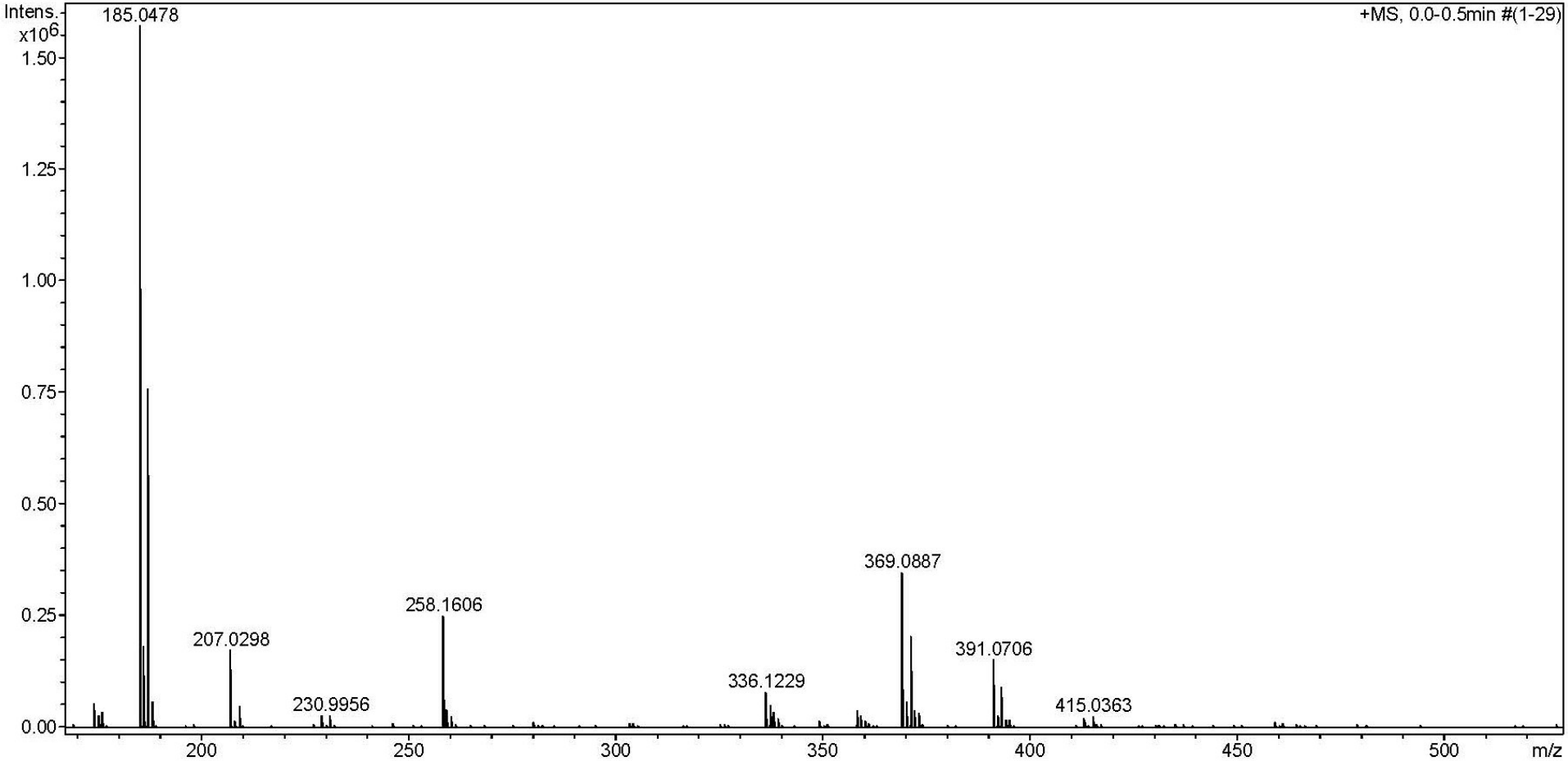

Figure 17S. HRESI$^+$-MS of *p*-$ClC_6H_4C(NH_2)=N^+(Me)O^-$.

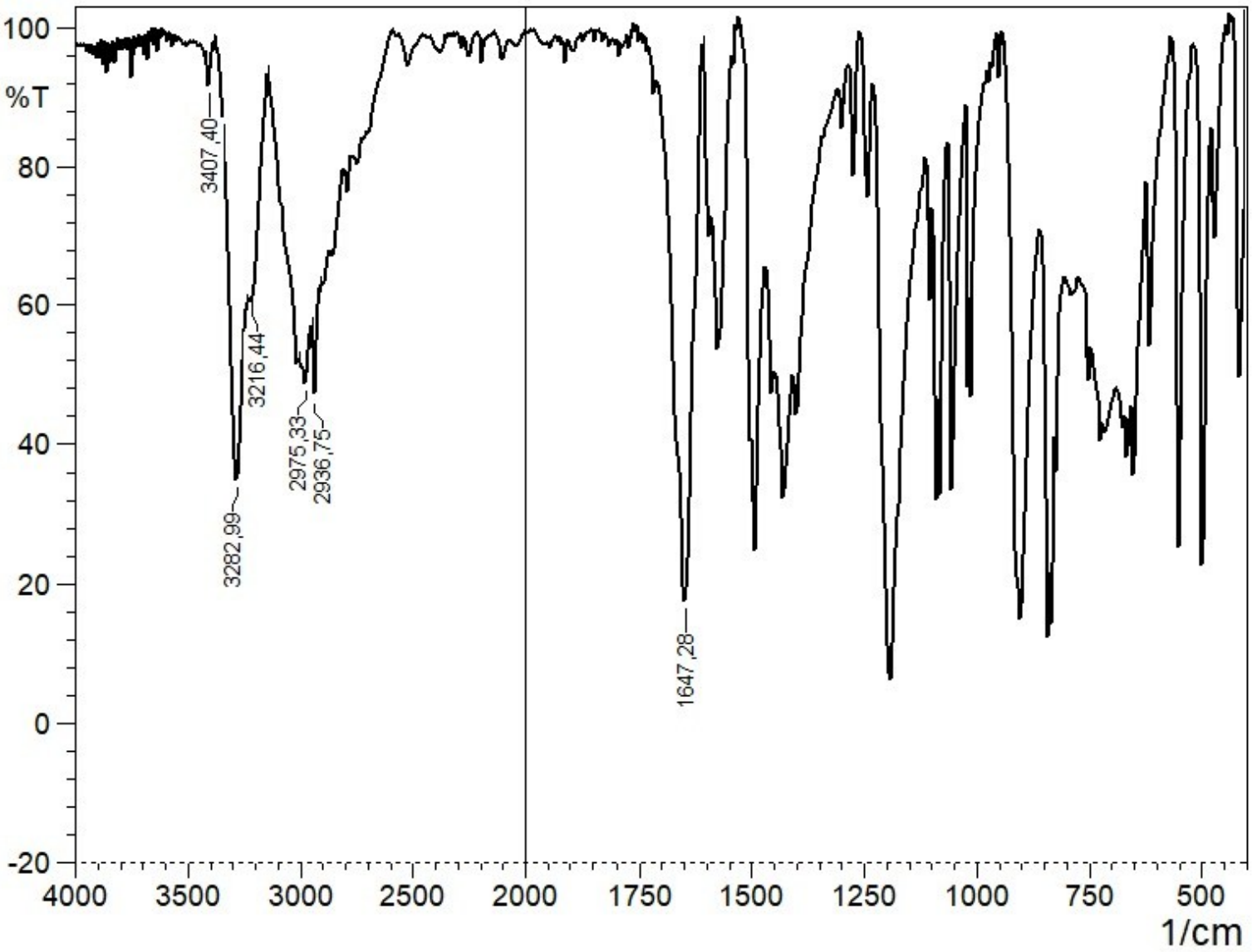

Figure 18S. IR spectrum of *p*-$ClC_6H_4C(NH_2)=N^+(Me)O^-$.

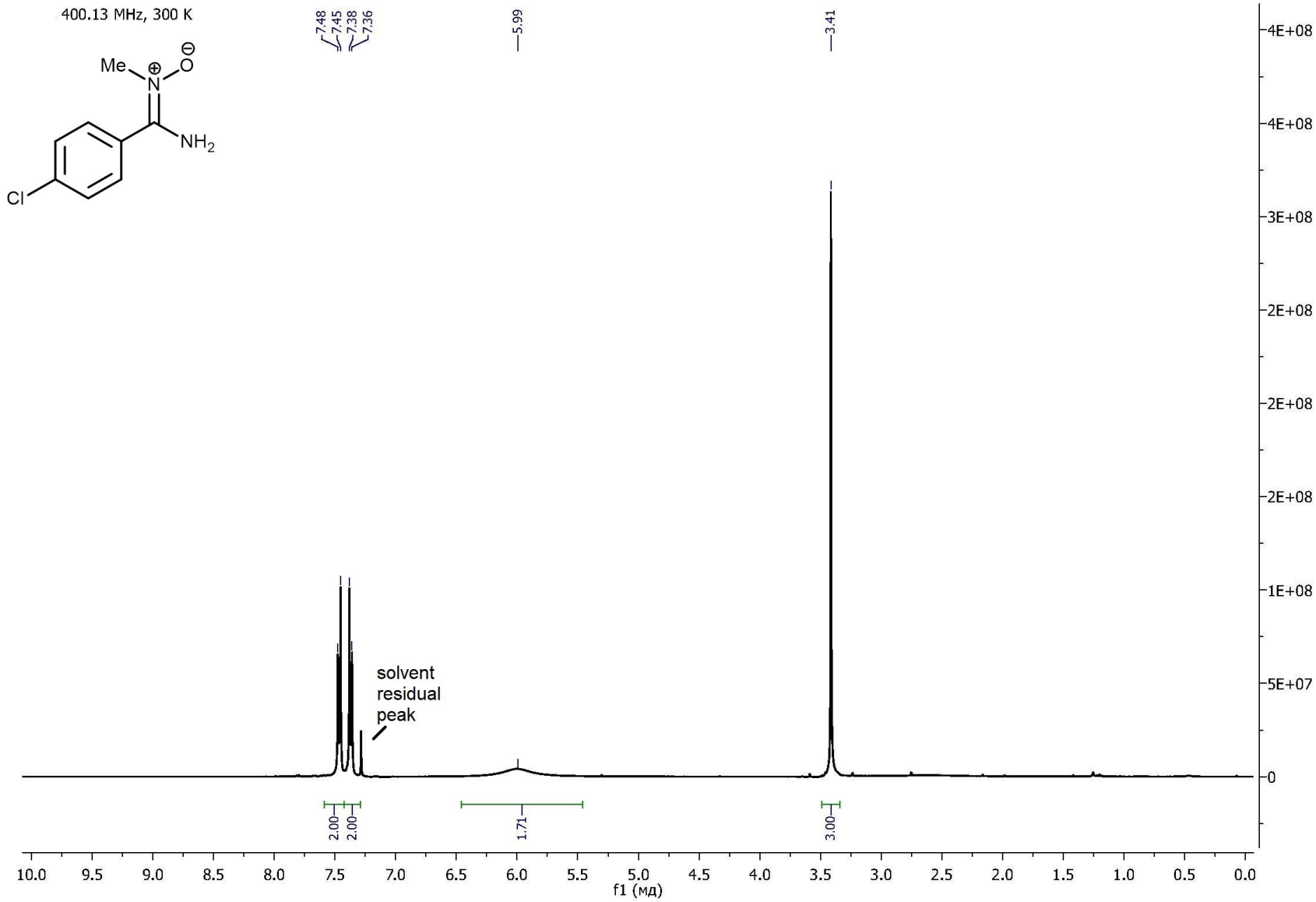

Figure 19S. ^{1}H NMR spectrum of *p*-$ClC_6H_4C(NH_2)=N^+(Me)O^-$.

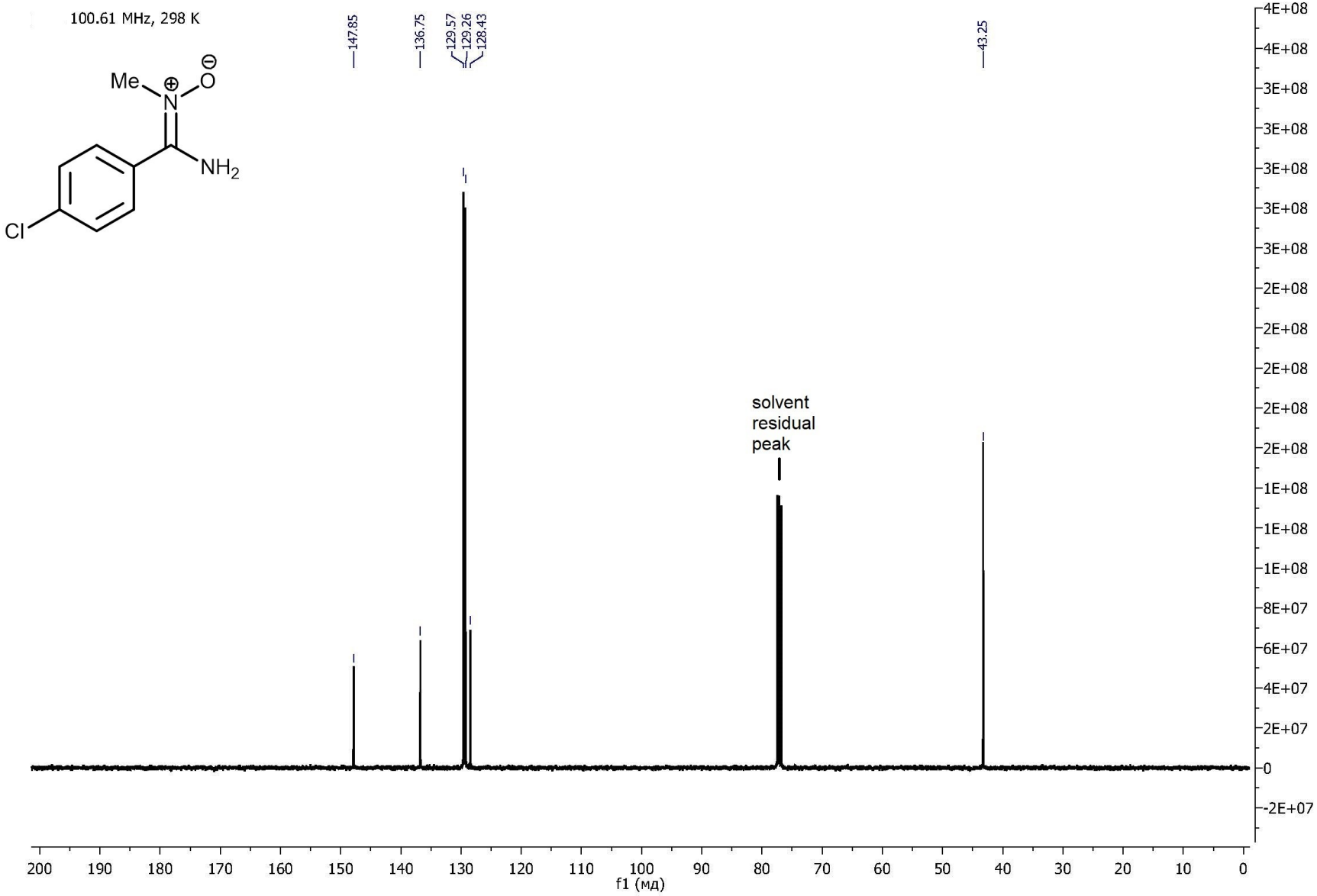

Figure 20S. $^{13}C\{^{1}H\}$ NMR spectrum of *p*-$ClC_6H_4C(NH_2)=N^+(Me)O^-$.

Acquisition Parameter

Source Type	ESI	Ion Polarity	Positive	Set Nebulizer	1.0 Bar
Focus	Active	Set Capillary	4500 V	Set Dry Heater	180 °C
Scan Begin	50 m/z	Set End Plate Offset	-500 V	Set Dry Gas	4.0 l/min
Scan End	1200 m/z	Set Collision Cell RF	300.0 Vpp	Set Divert Valve	Source

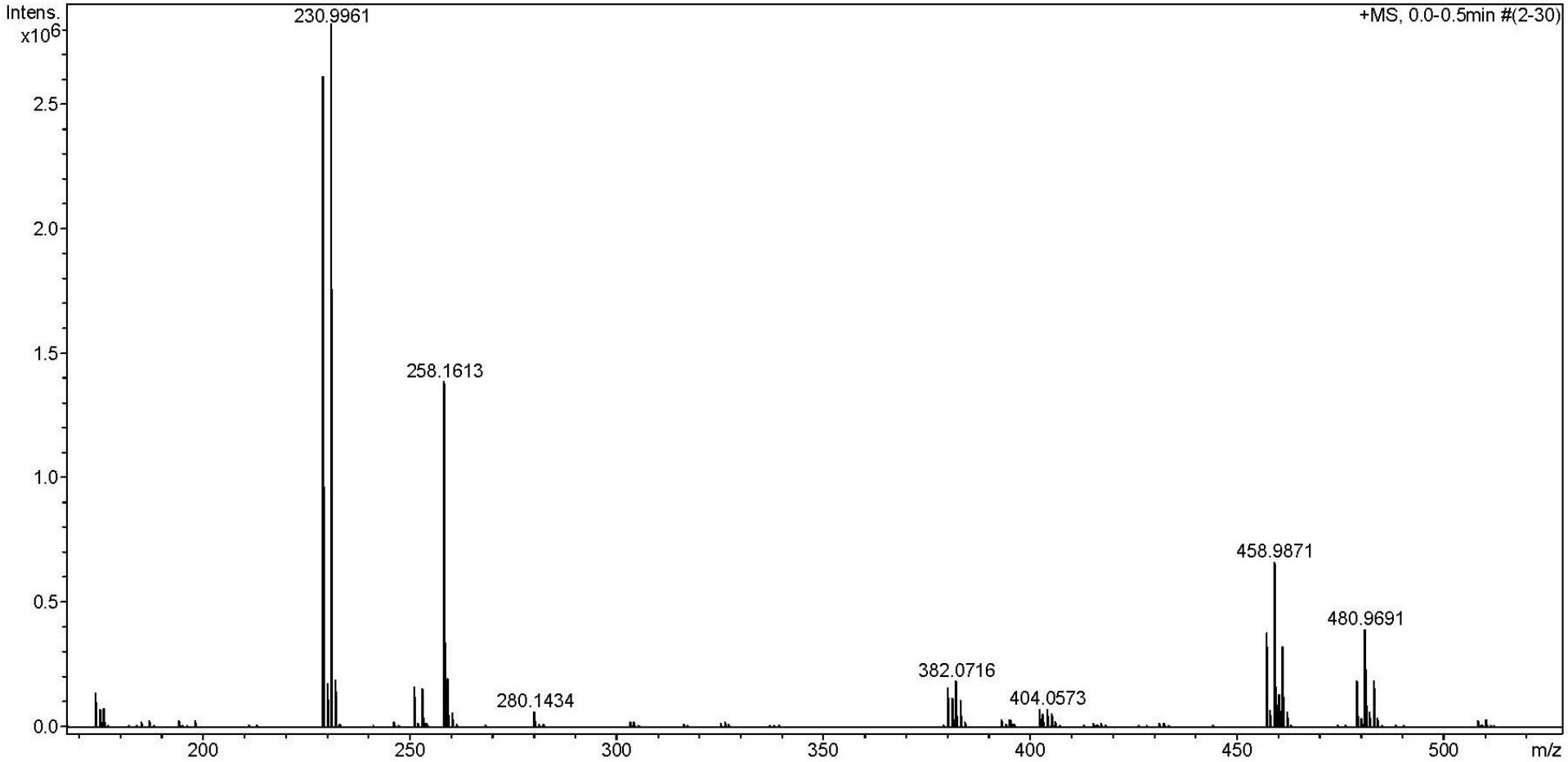

Figure 21S. HRESI$^+$-MS of *p*-$BrC_6H_4C(NH_2)=N^+(Me)O^-$.

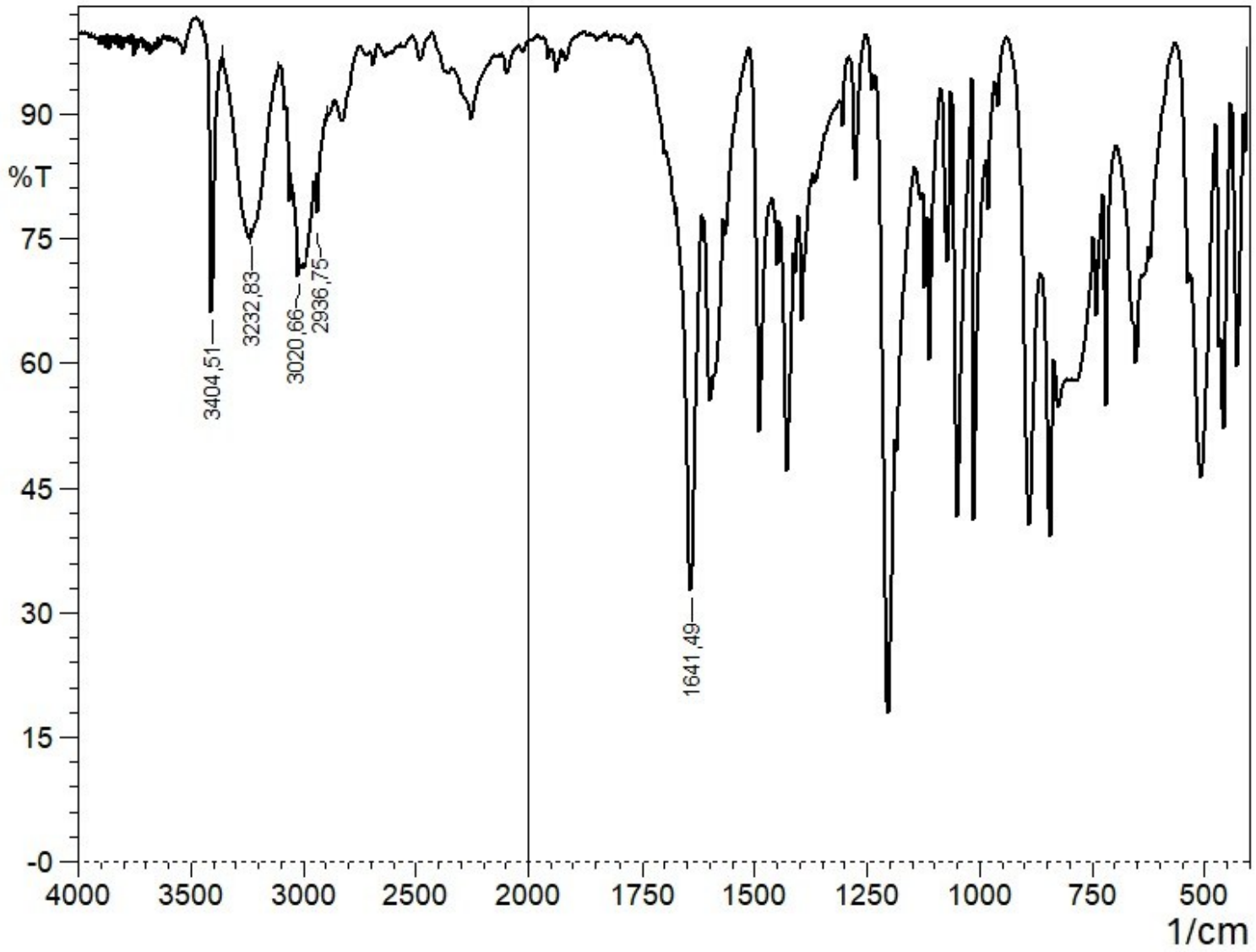

Figure 22S. IR spectrum of *p*-$BrC_6H_4C(NH_2)=N^+(Me)O^-$.

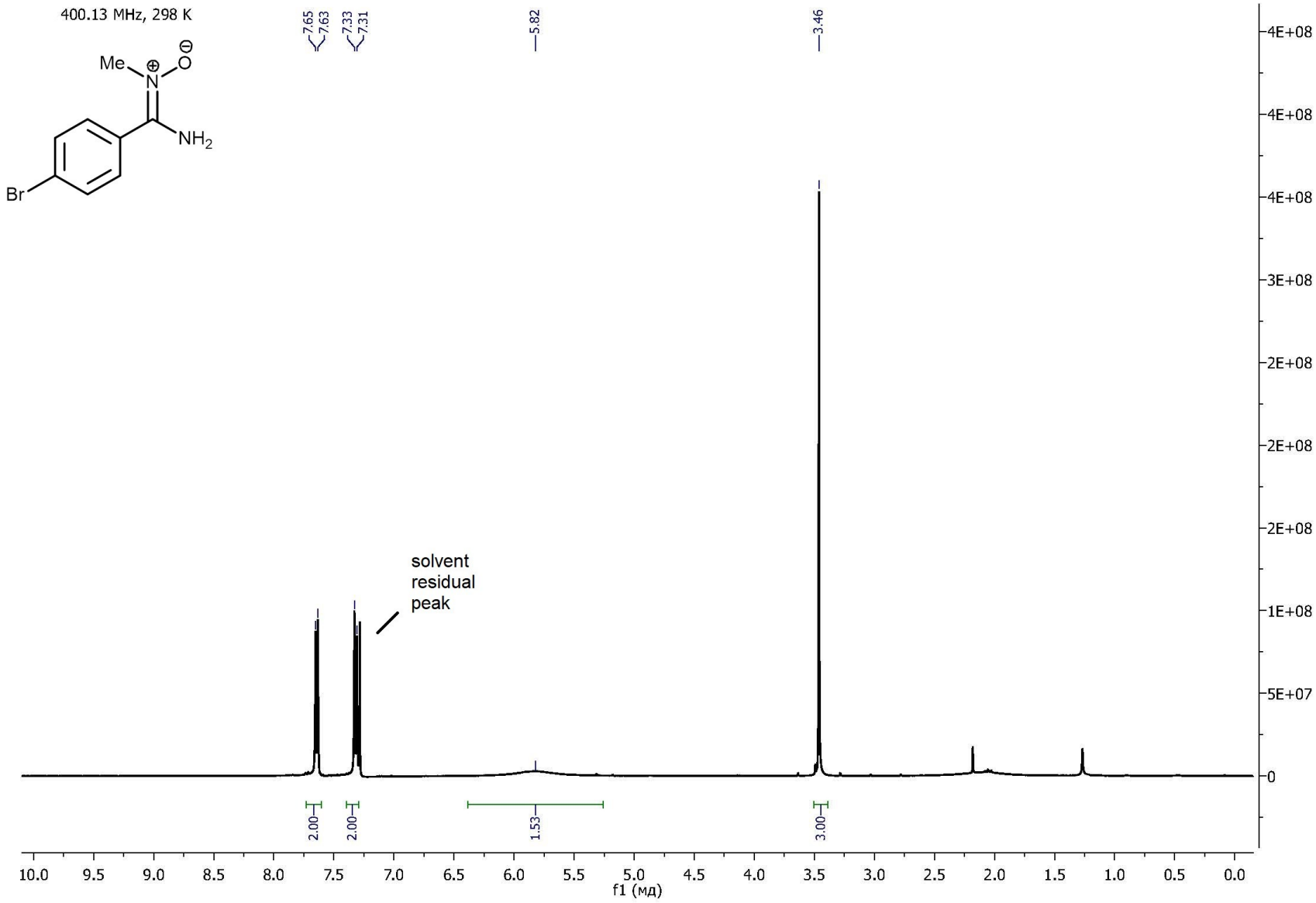

Figure 23S. ^{1}H NMR spectrum of *p*-$BrC_6H_4C(NH_2)=N^+(Me)O^-$.

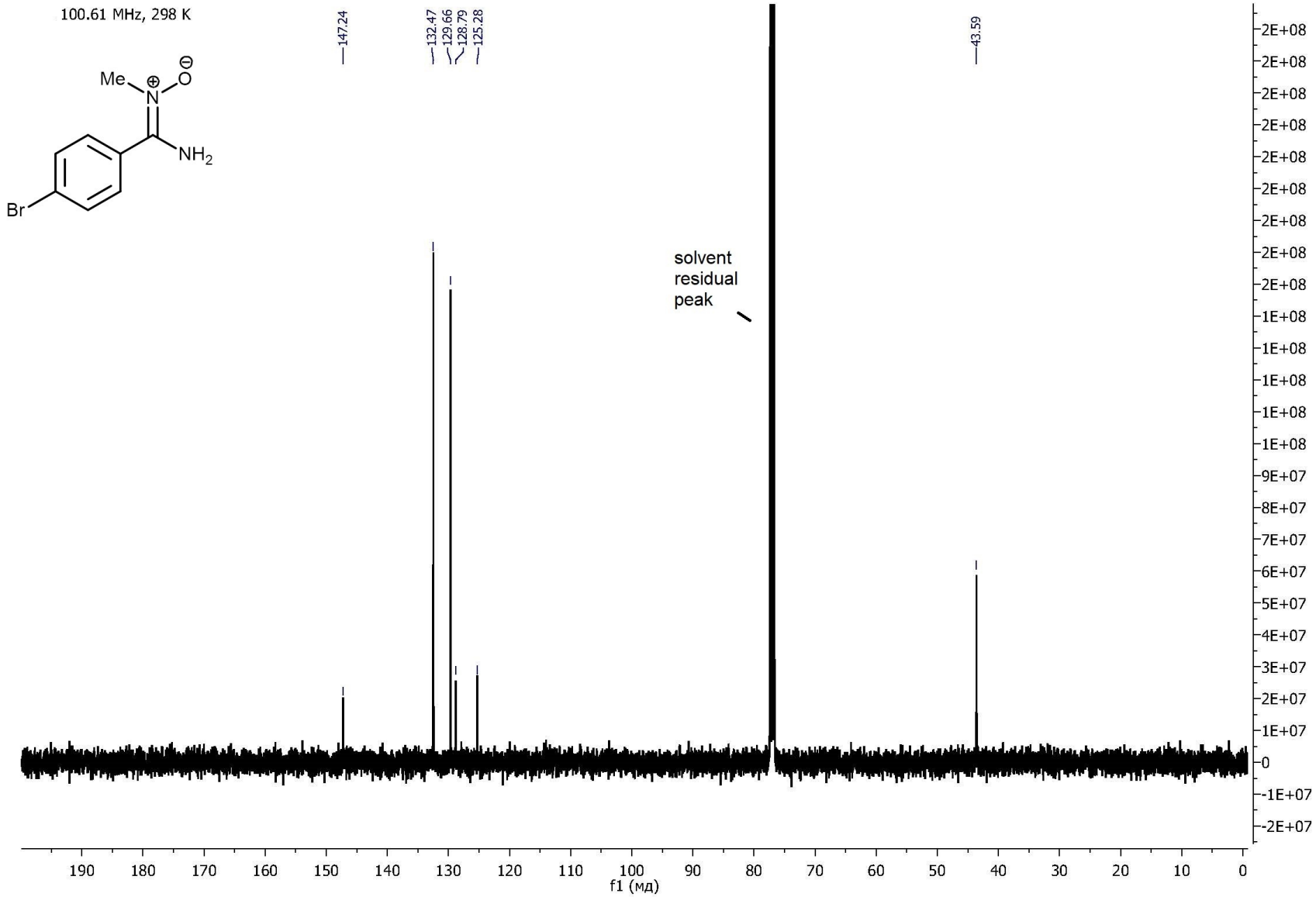

Figure 24S. $^{13}C\{^{1}H\}$ NMR spectrum of *p*-$BrC_6H_4C(NH_2)=N^+(Me)O^-$.

Acquisition Parameter

Source Type	ESI	Ion Polarity	Positive	Set Nebulizer	1.0 Bar
Focus	Active	Set Capillary	4500 V	Set Dry Heater	180 °C
Scan Begin	50 m/z	Set End Plate Offset	-500 V	Set Dry Gas	4.0 l/min
Scan End	1200 m/z	Set Collision Cell RF	300.0 Vpp	Set Divert Valve	Source

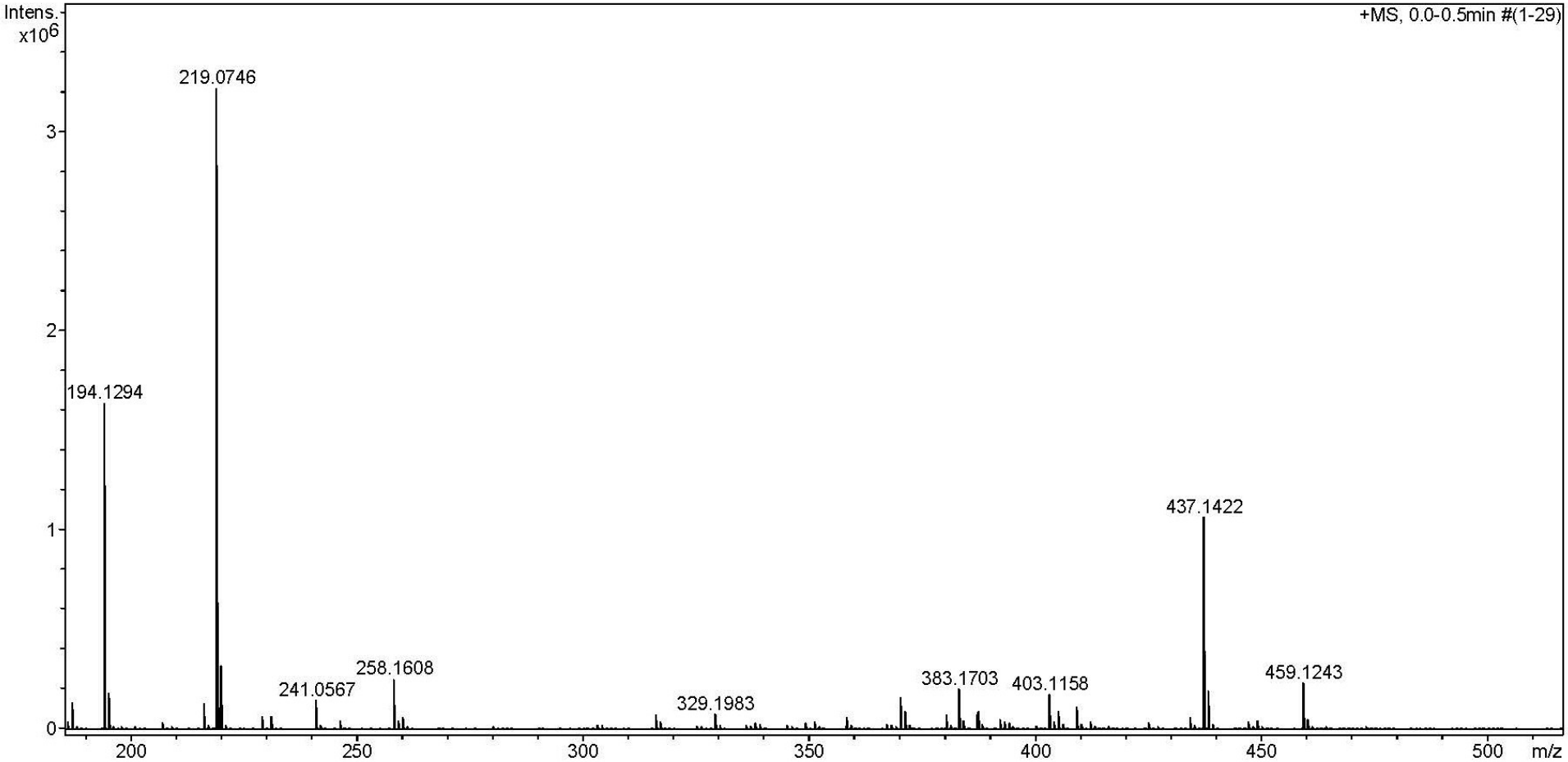

Figure 25S. HRESI$^+$-MS of *m*-$CF_3C_6H_4C(NH_2)=N^+(Me)O^-$.

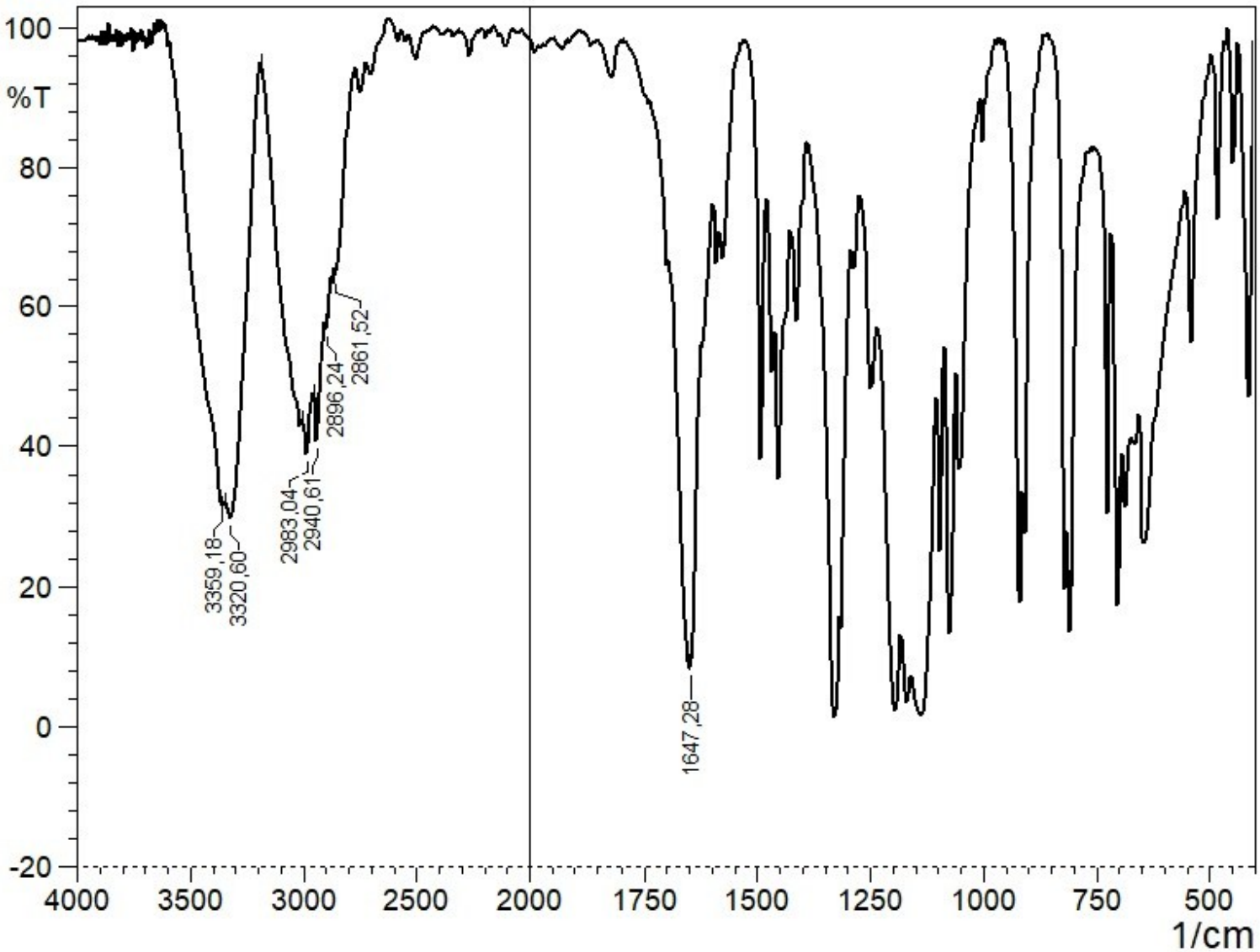

Figure 26S. IR spectrum of *m*-$CF_3C_6H_4C(NH_2)=N^+(Me)O^-$.

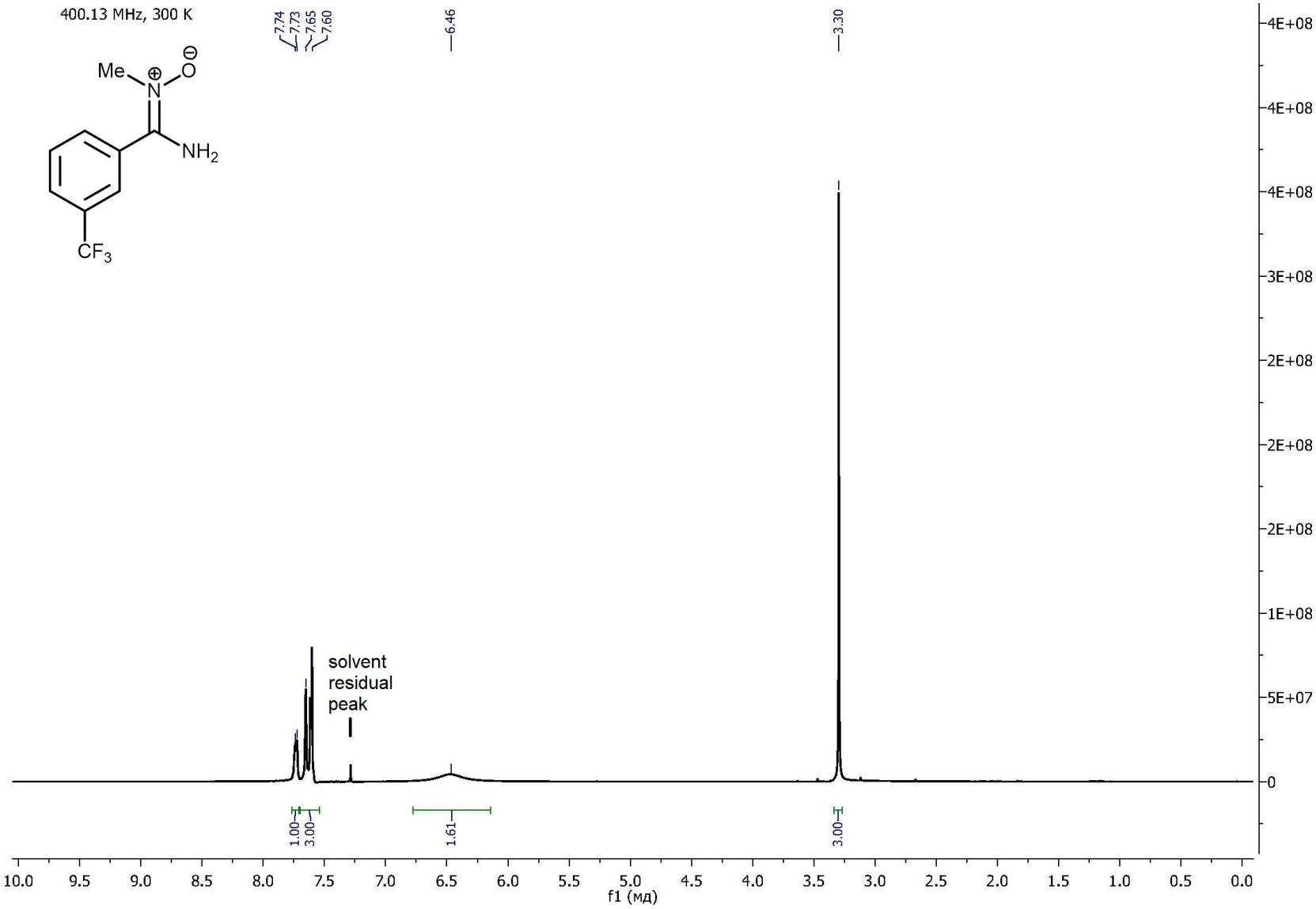

Figure 27S. ^{1}H NMR spectrum of *m*-$CF_3C_6H_4C(NH_2)=N^+(Me)O^-$.

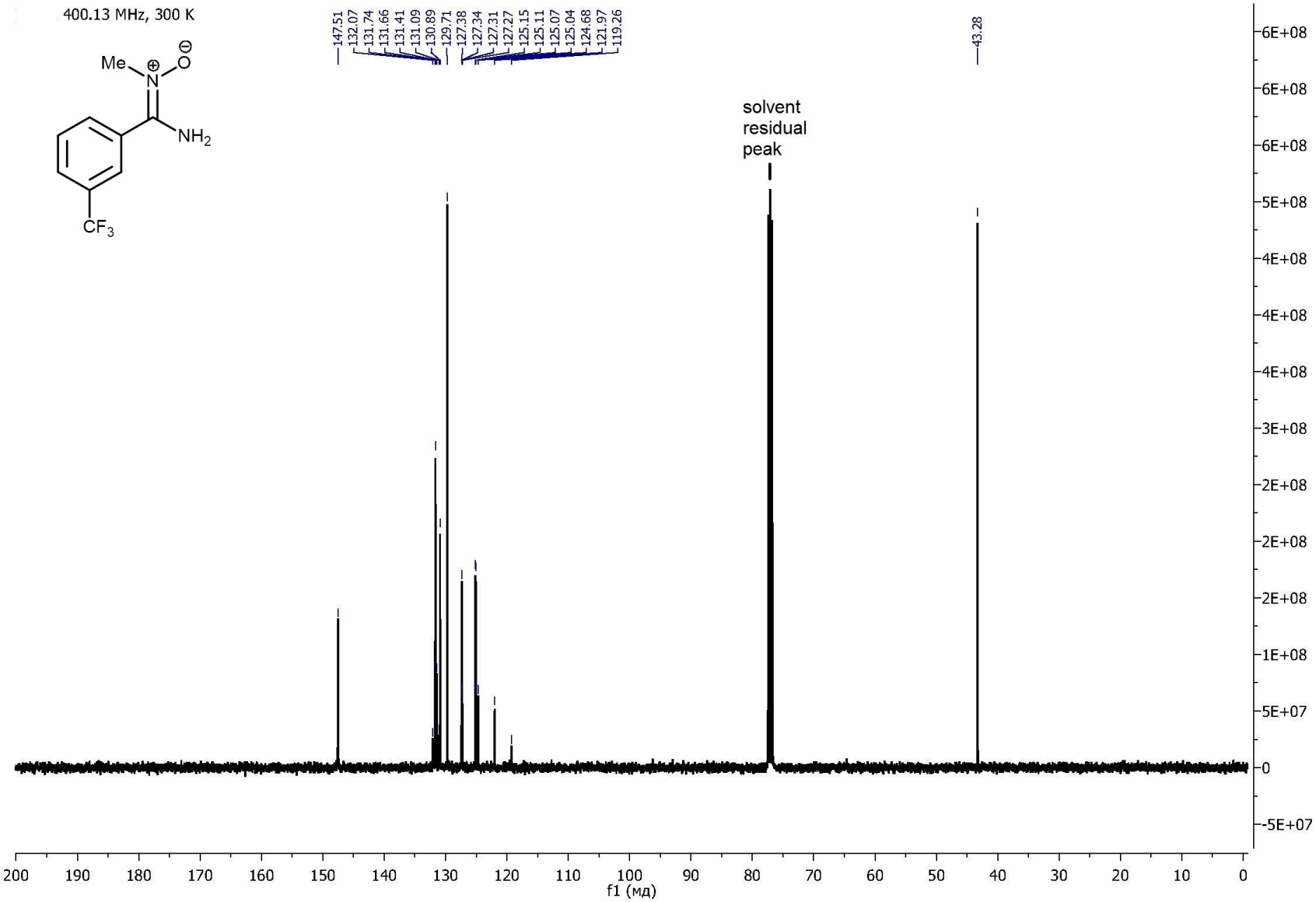

Figure 28S. $^{13}C\{^{1}H\}$ NMR spectrum of *m*-$CF_3C_6H_4C(NH_2)=N^+(Me)O^-$.

Acquisition Parameter

Source Type	ESI	Ion Polarity	Positive	Set Nebulizer	1.0 Bar
Focus	Active	Set Capillary	4500 V	Set Dry Heater	180 °C
Scan Begin	50 m/z	Set End Plate Offset	-500 V	Set Dry Gas	4.0 l/min
Scan End	1200 m/z	Set Collision Cell RF	300.0 Vpp	Set Divert Valve	Source

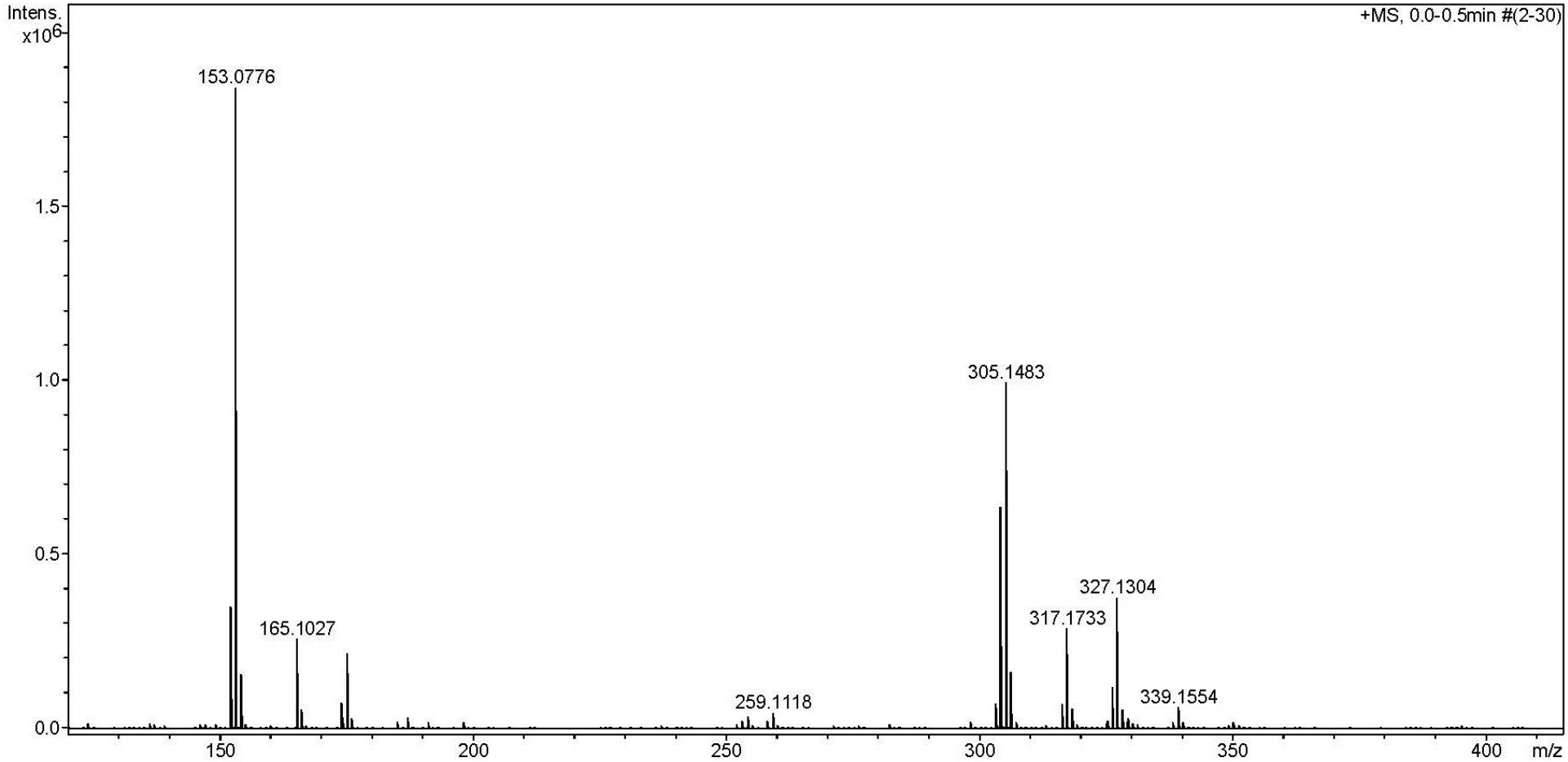

Figure 29S. HRESI$^+$-MS of $N_2C_4H_3C(NH_2)=N^+(Me)O^-$.

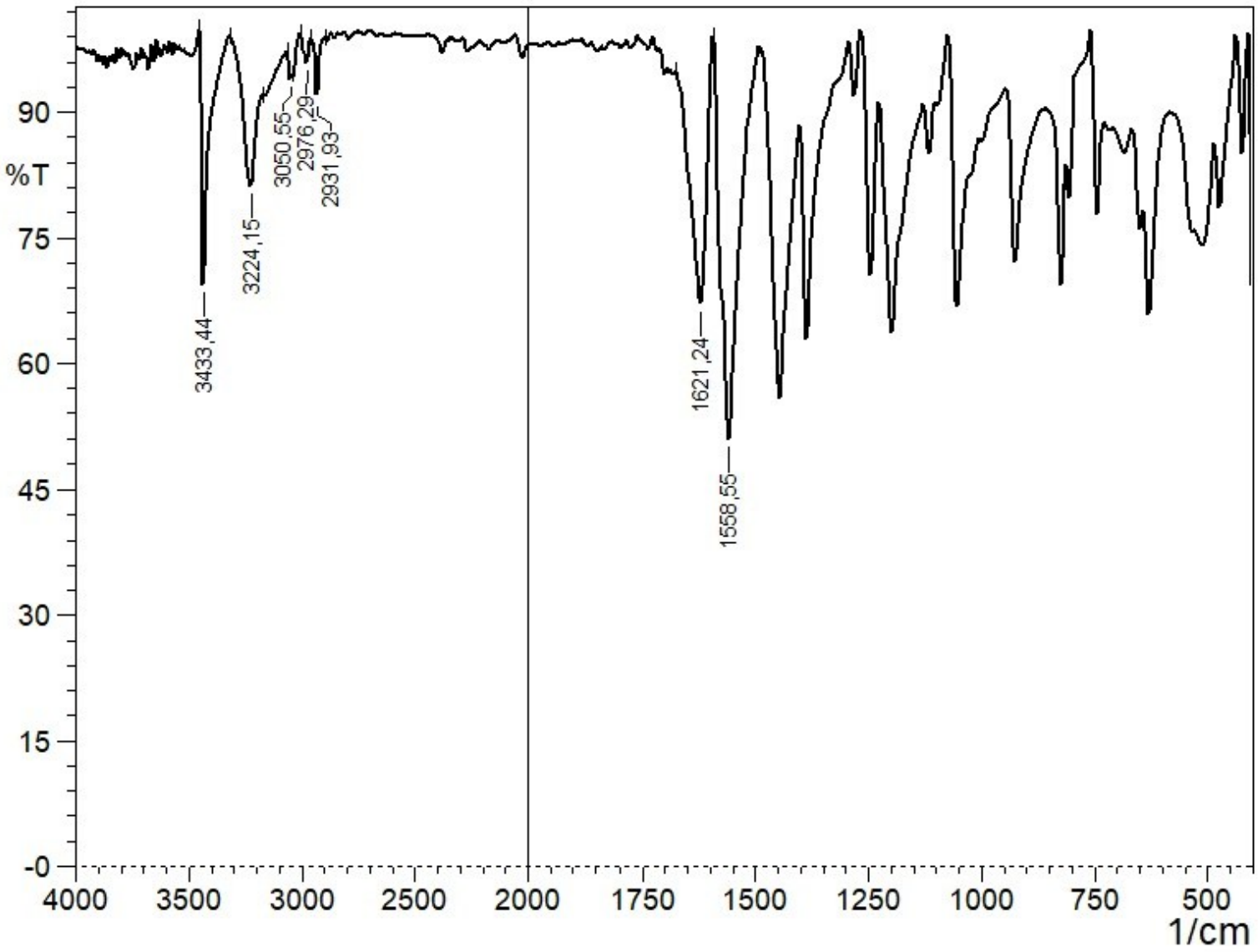

Figure 30S. IR spectrum of $N_2C_4H_3C(NH_2)=N^+(Me)O^-$.

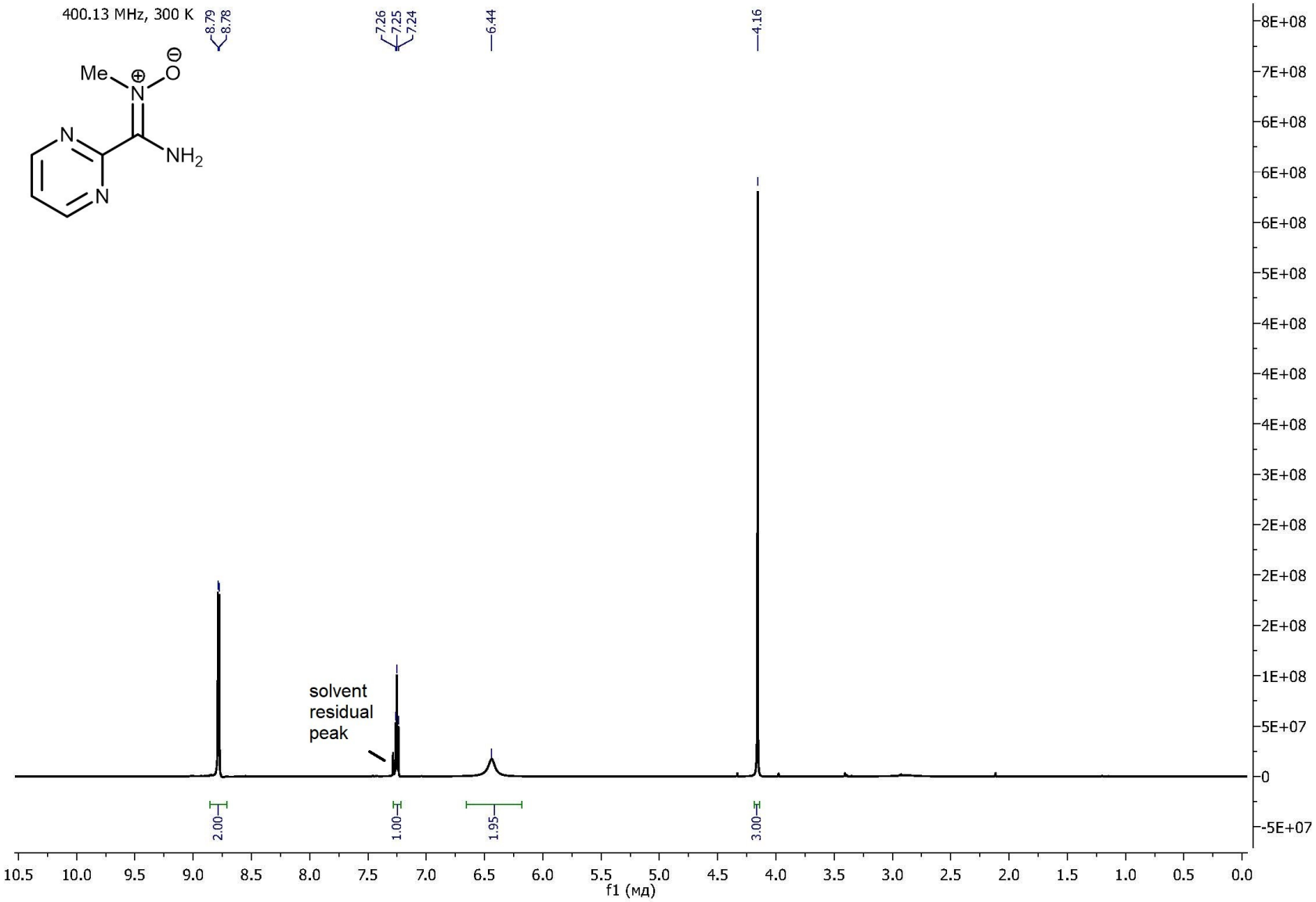

Figure 31S. ^{1}H NMR spectrum of $N_2C_4H_3C(NH_2)=N^{+}(Me)O^{-}$.

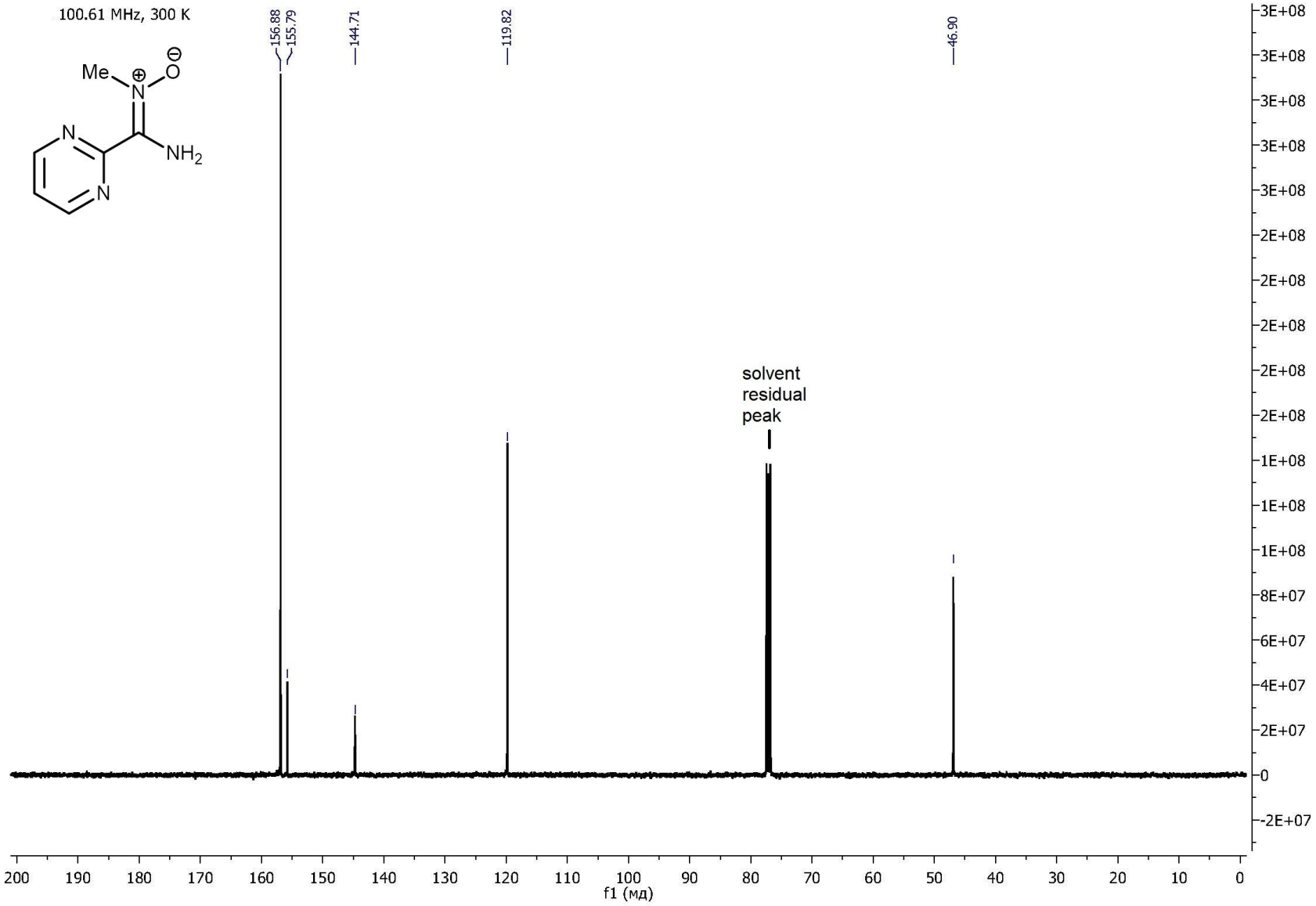

Figure 32S. $^{13}C\{^{1}H\}$ NMR spectrum of $N_2C_4H_3C(NH_2)=N^+(Me)O^-$.

Spectra of 1−20

Acquisition Parameter

Source Type	ESI	Ion Polarity	Positive	Set Nebulizer	0.4 Bar
Focus	Not active			Set Dry Heater	180 °C
Scan Begin	50 m/z	Set Capillary	4500 V	Set Dry Gas	4.0 l/min
Scan End	1000 m/z	Set End Plate Offset	-500 V	Set Divert Valve	Source

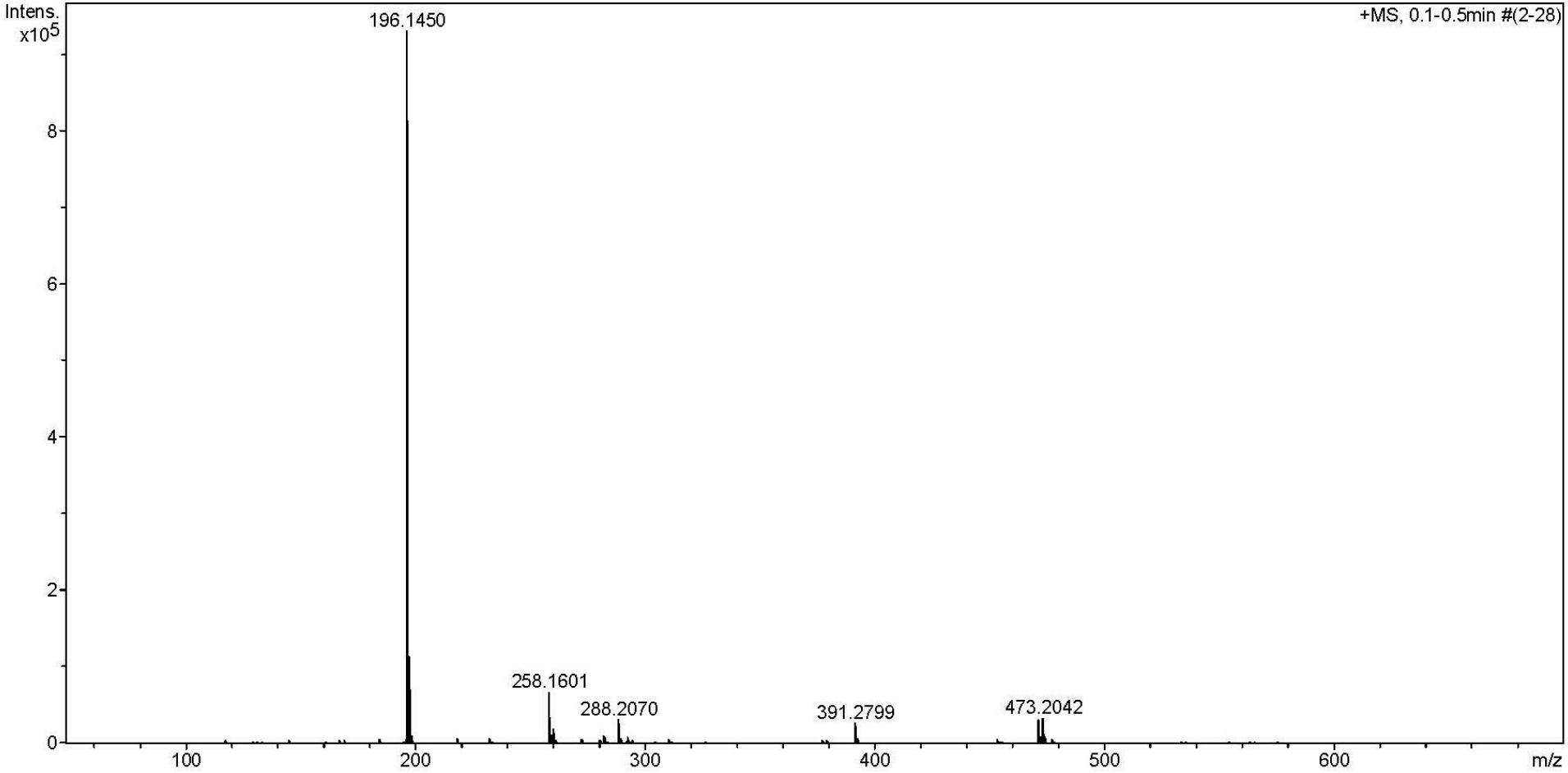

Figure 33S. HRESI$^+$-MS of **1**.

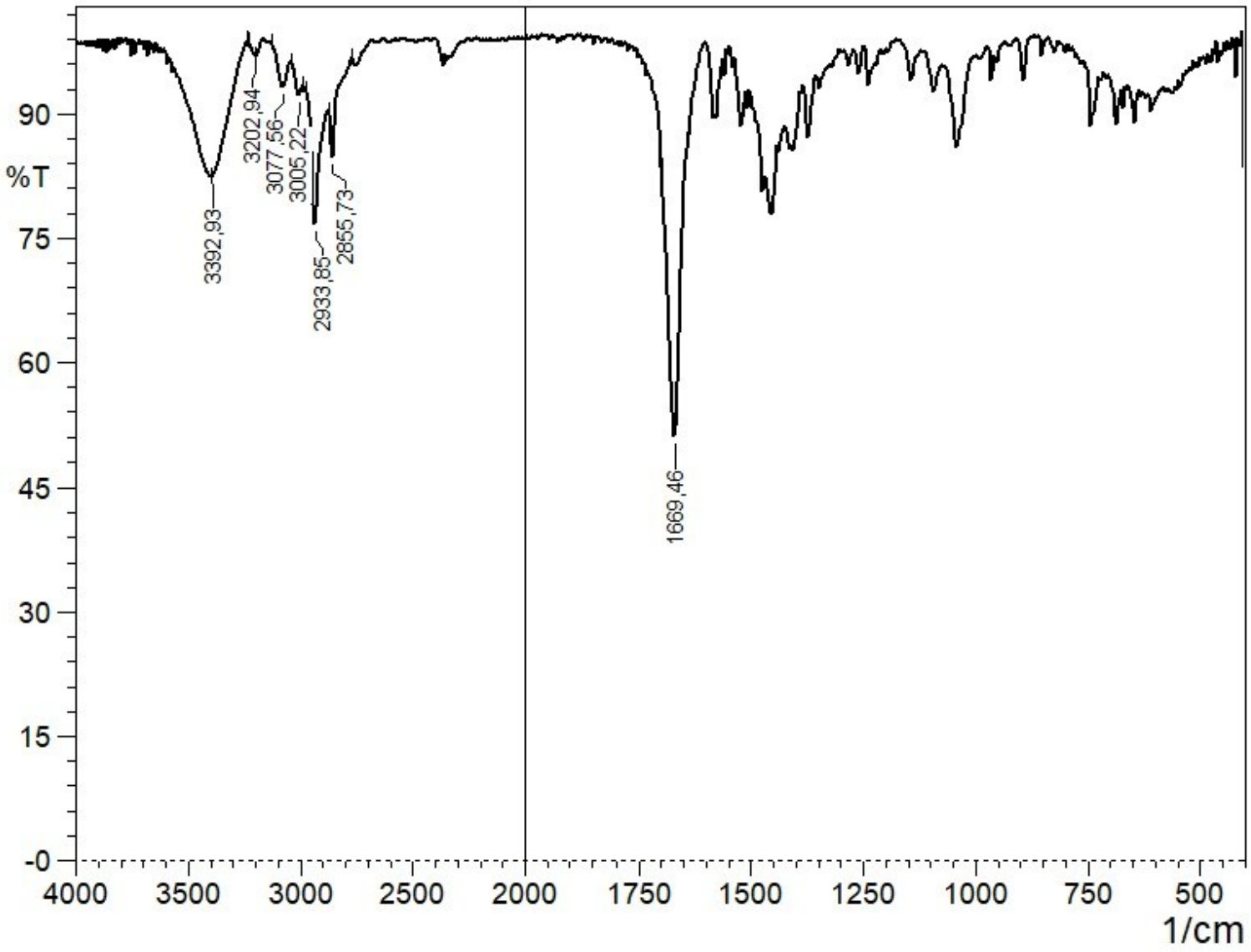

Figure 34S. IR spectrum of **1**.

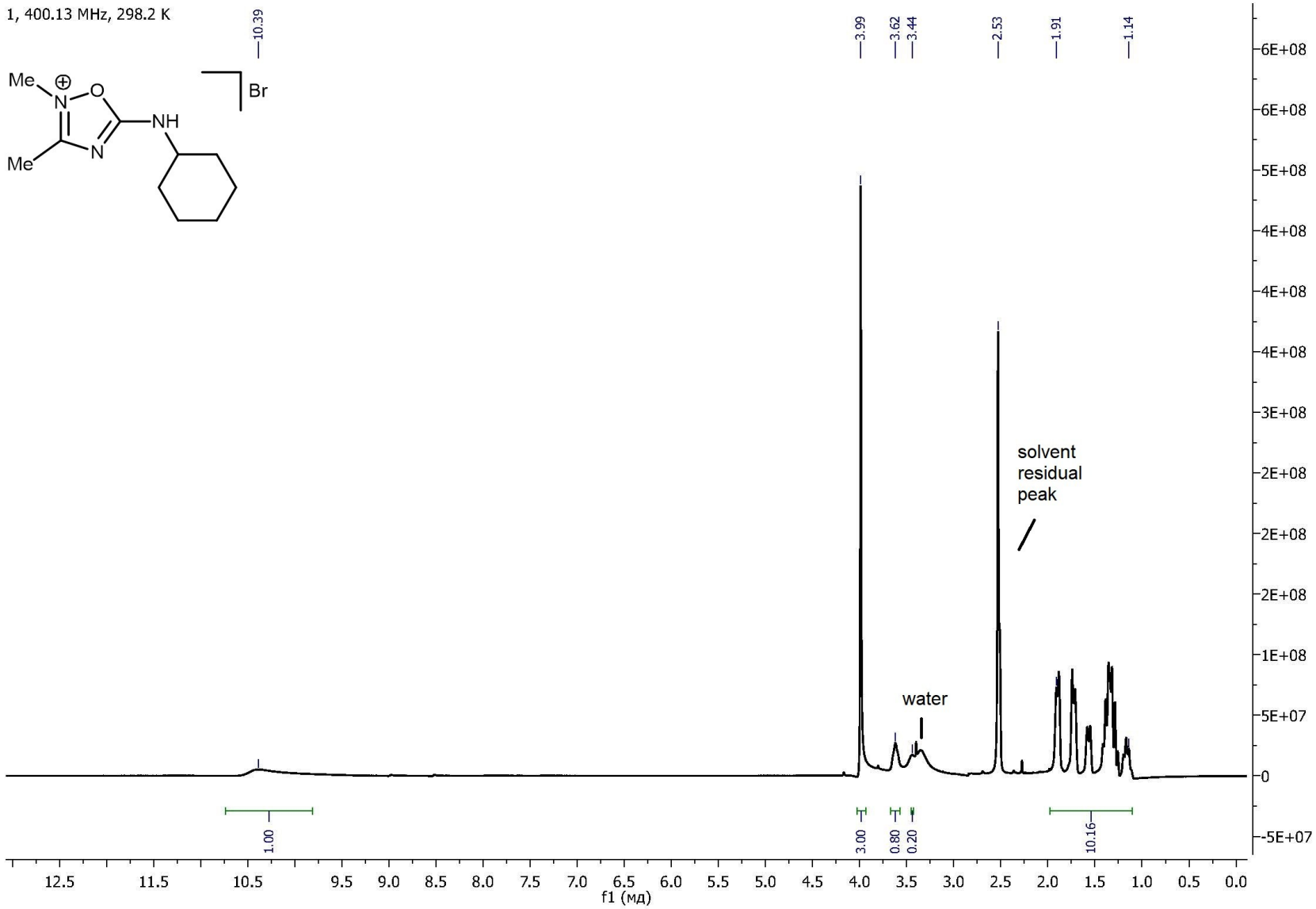

Figure 35S. ^{1}H NMR spectrum of **1** in DMSO.

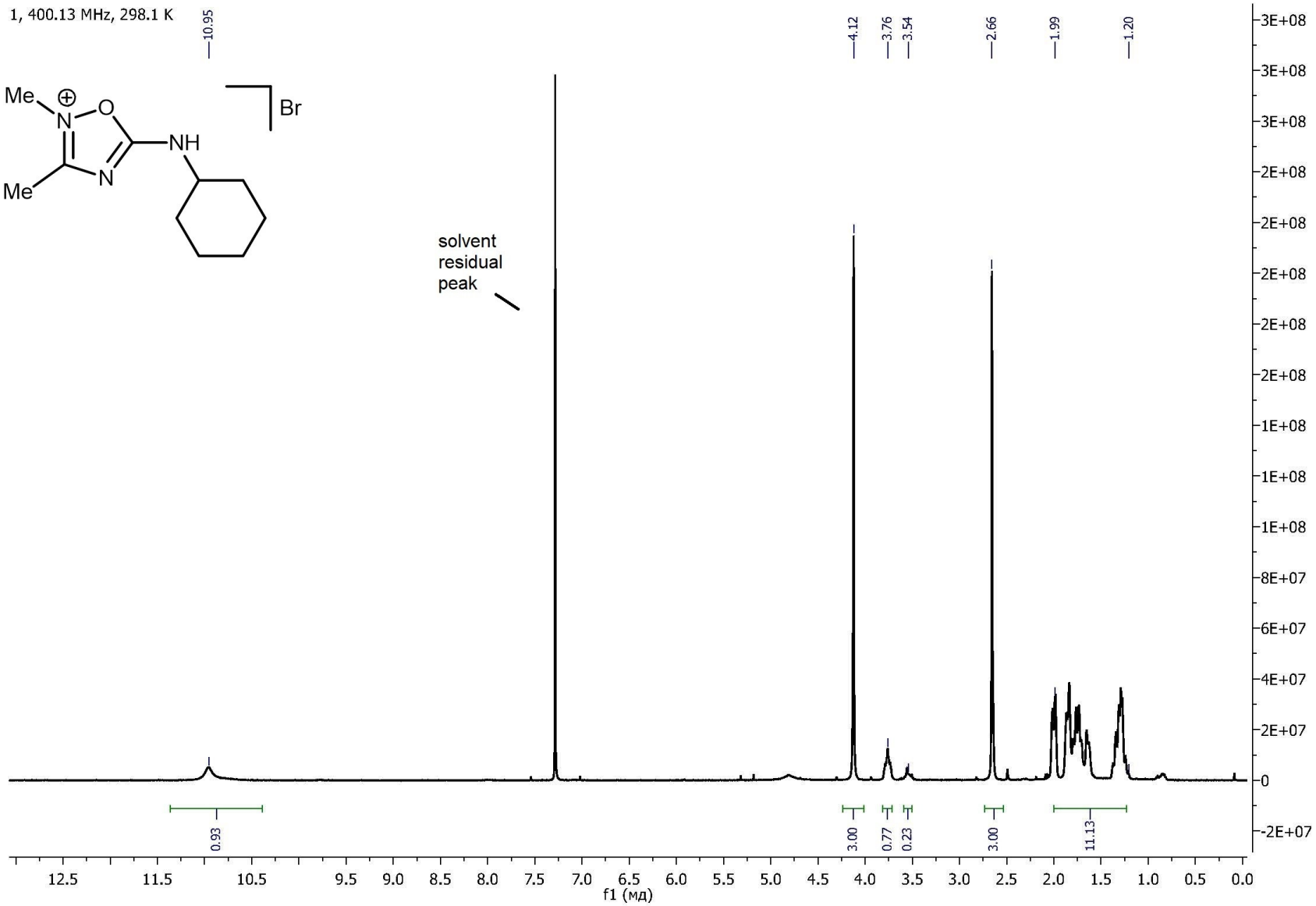

Figure 36S. ^{1}H NMR spectrum of **1** in $CDCl_3$.

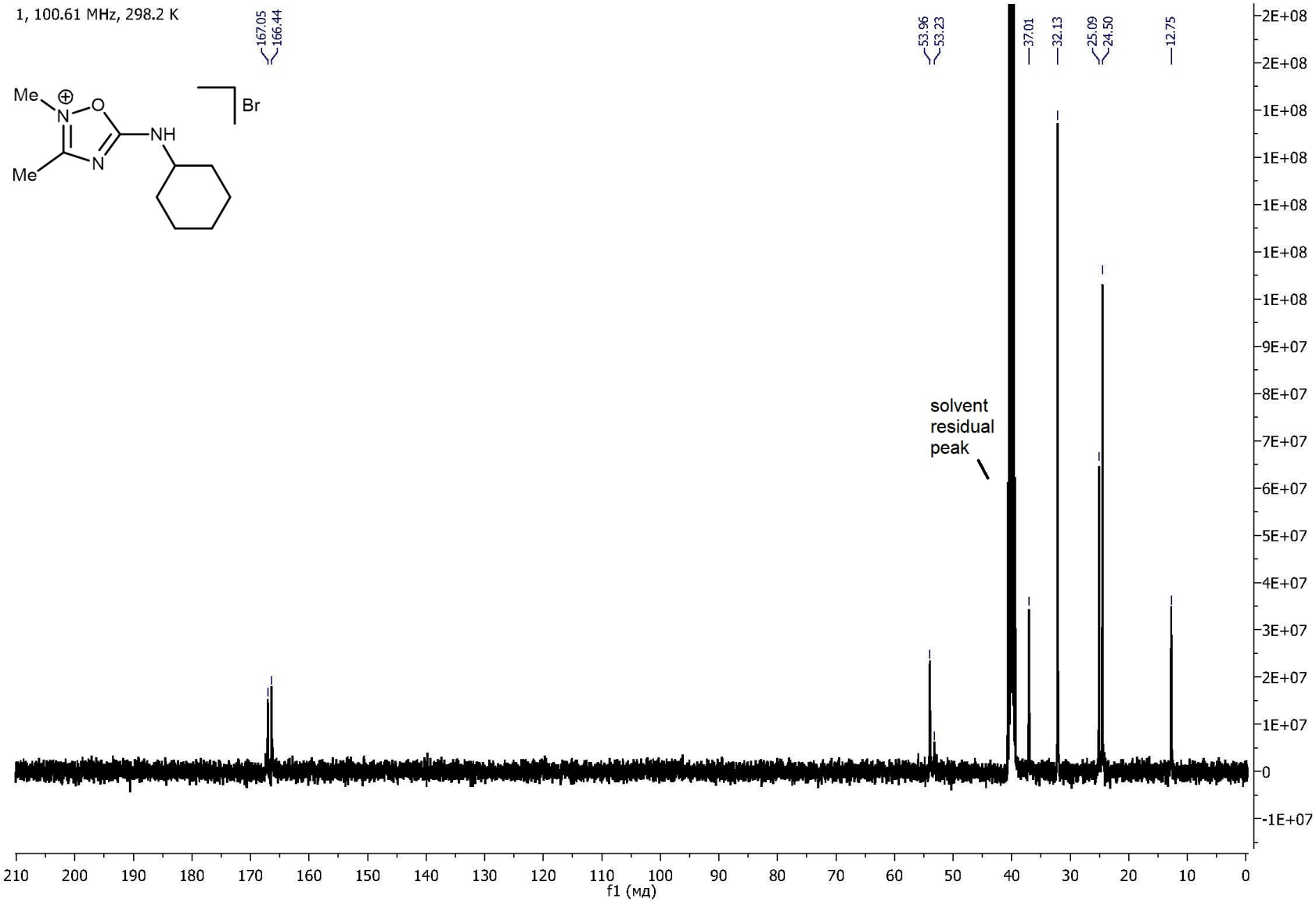

Figure 37S. $^{13}C\{^{1}H\}$ NMR spectrum of **1**.

Acquisition Parameter

Source Type	ESI	Ion Polarity	Positive	Set Nebulizer	0.4 Bar
Focus	Not active			Set Dry Heater	180 °C
Scan Begin	50 m/z	Set Capillary	4500 V	Set Dry Gas	4.0 l/min
Scan End	1200 m/z	Set End Plate Offset	-500 V	Set Divert Valve	Source

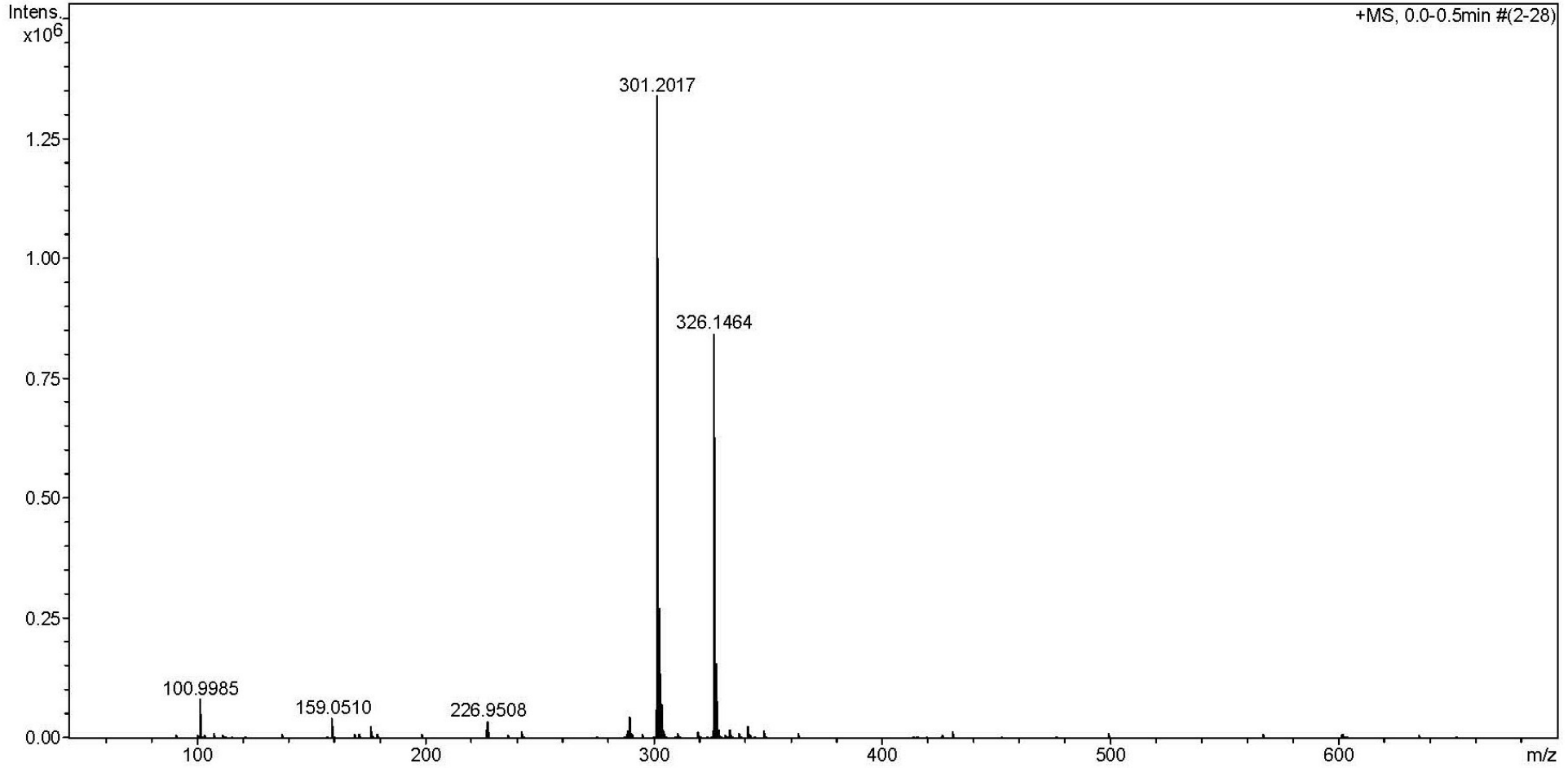

Figure 38S. HRESI$^+$-MS of **2**.

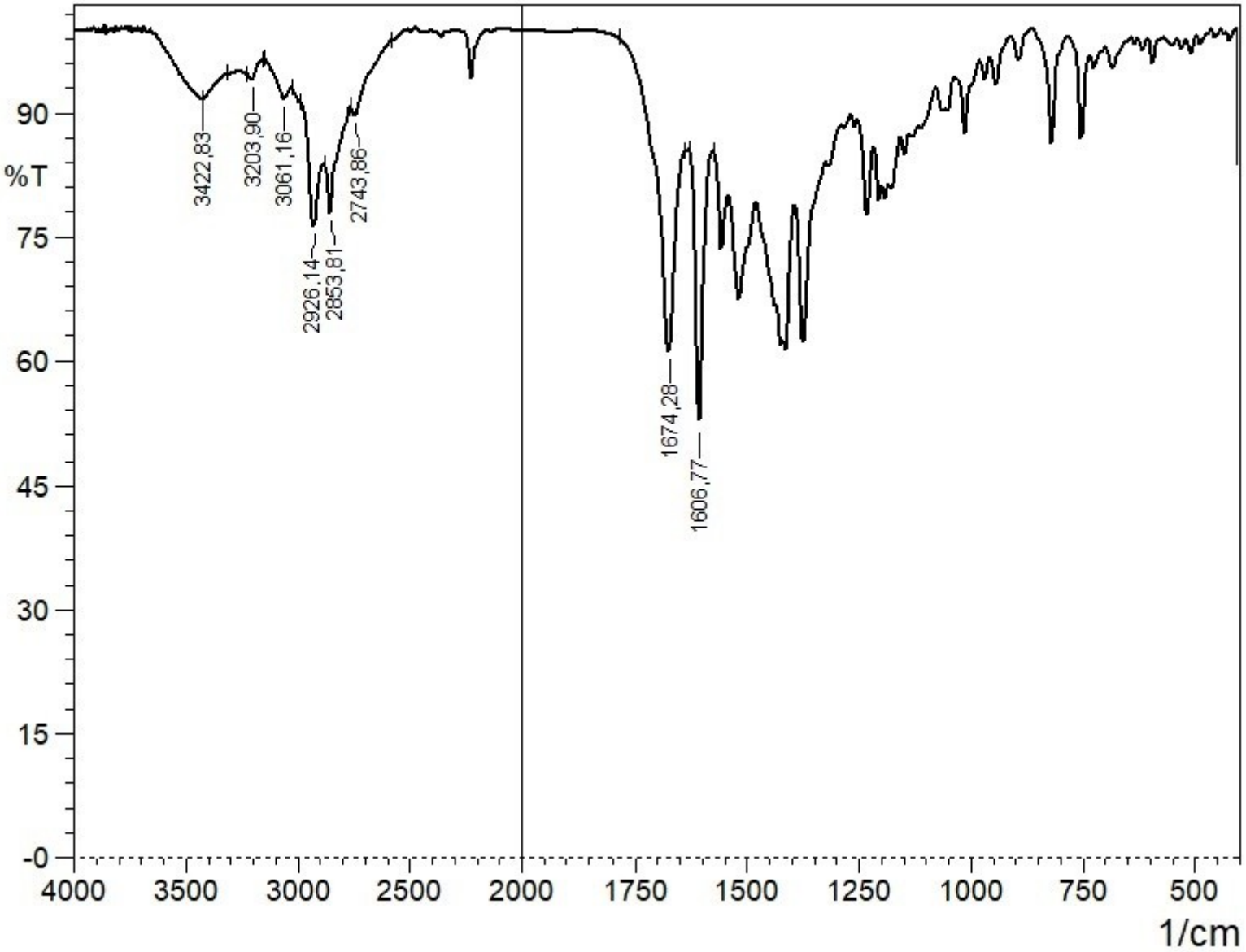

Figure 39S. IR spectrum of **2**.

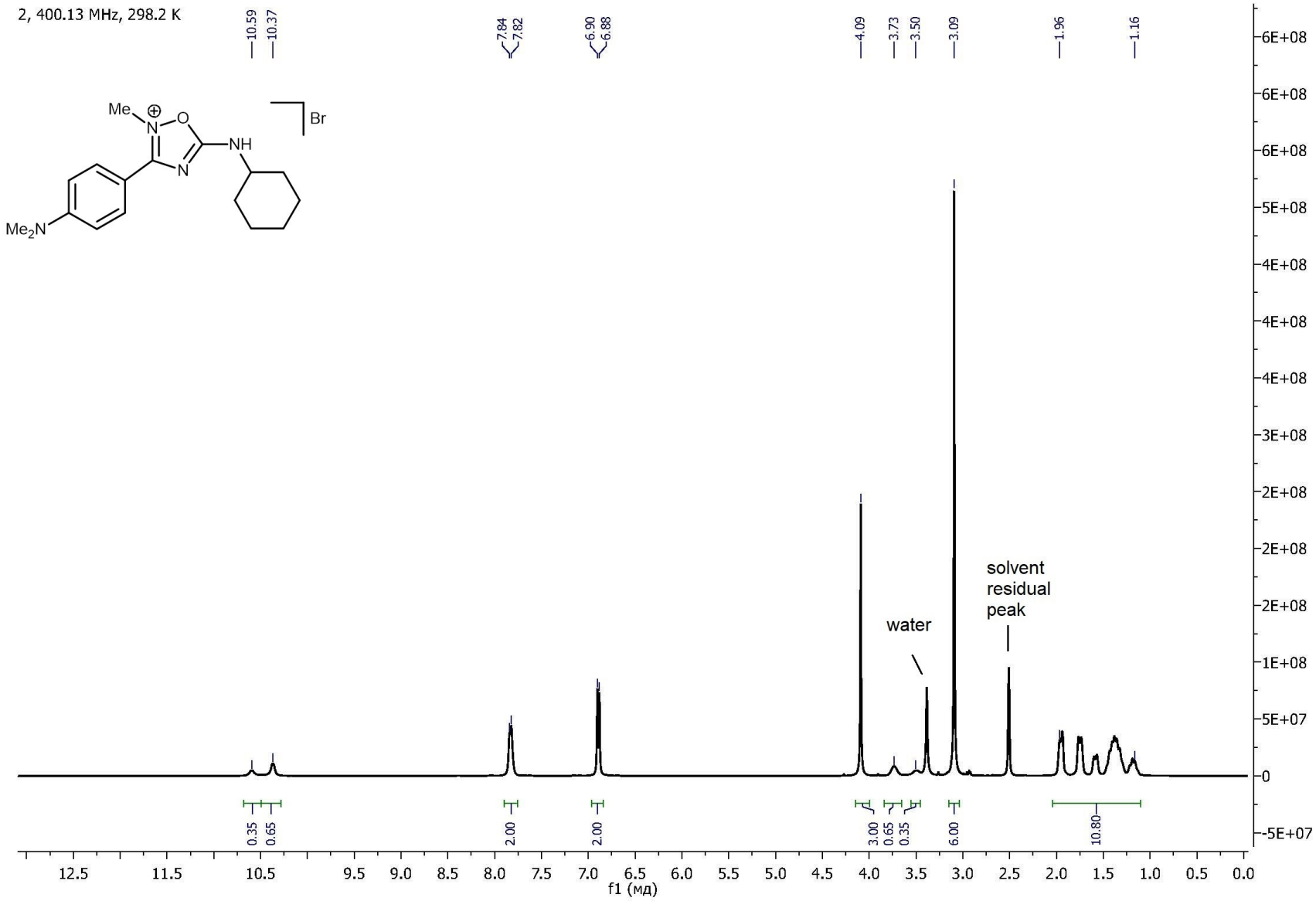

Figure 40S. ^{1}H NMR spectrum of **2**.

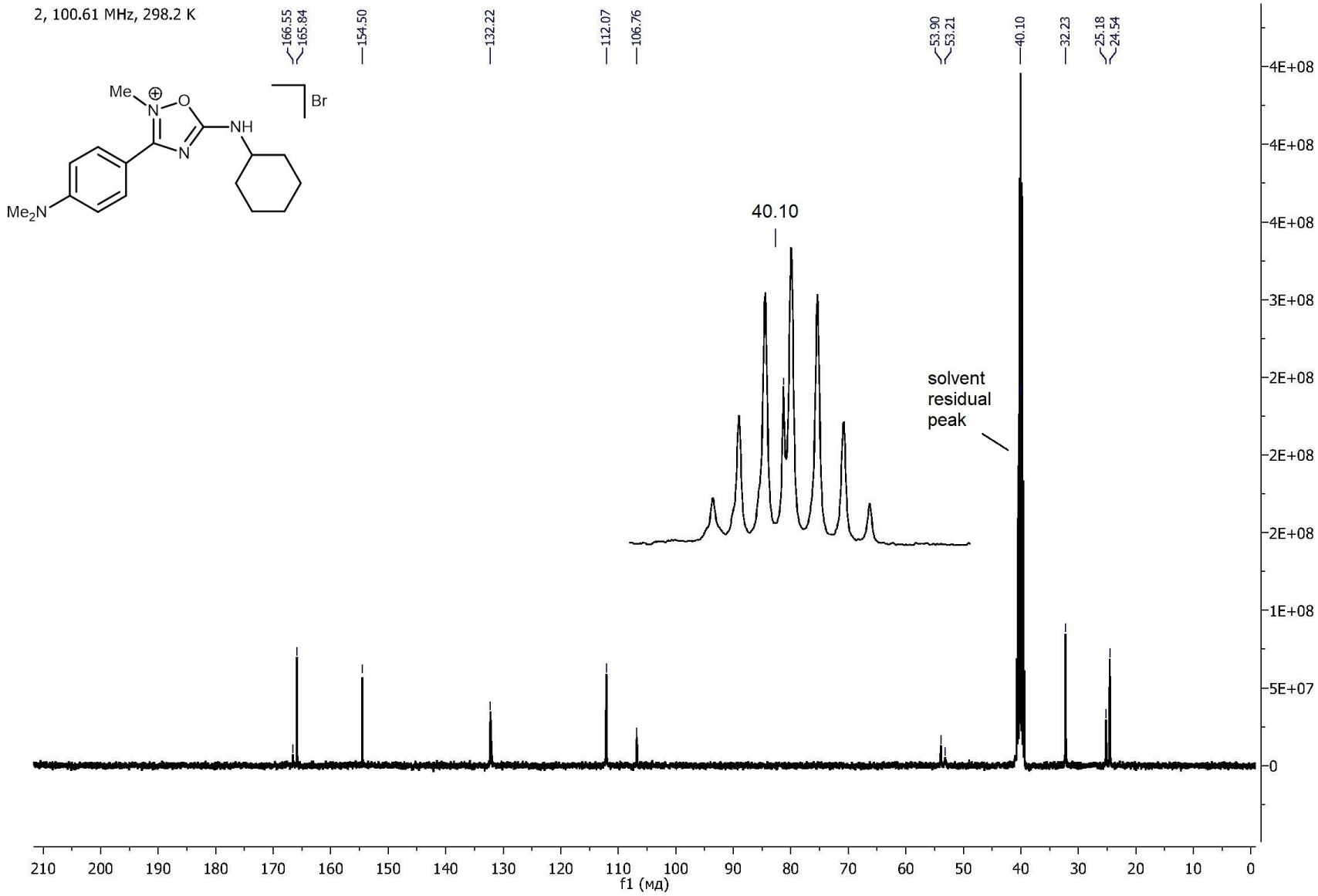

Figure 41S. $^{13}C\{^{1}H\}$ NMR spectrum of **2**.

Acquisition Parameter

Source Type	ESI	Ion Polarity	Positive	Set Nebulizer	0.4 Bar
Focus	Not active			Set Dry Heater	180 °C
Scan Begin	50 m/z	Set Capillary	4500 V	Set Dry Gas	4.0 l/min
Scan End	3000 m/z	Set End Plate Offset	-500 V	Set Divert Valve	Source

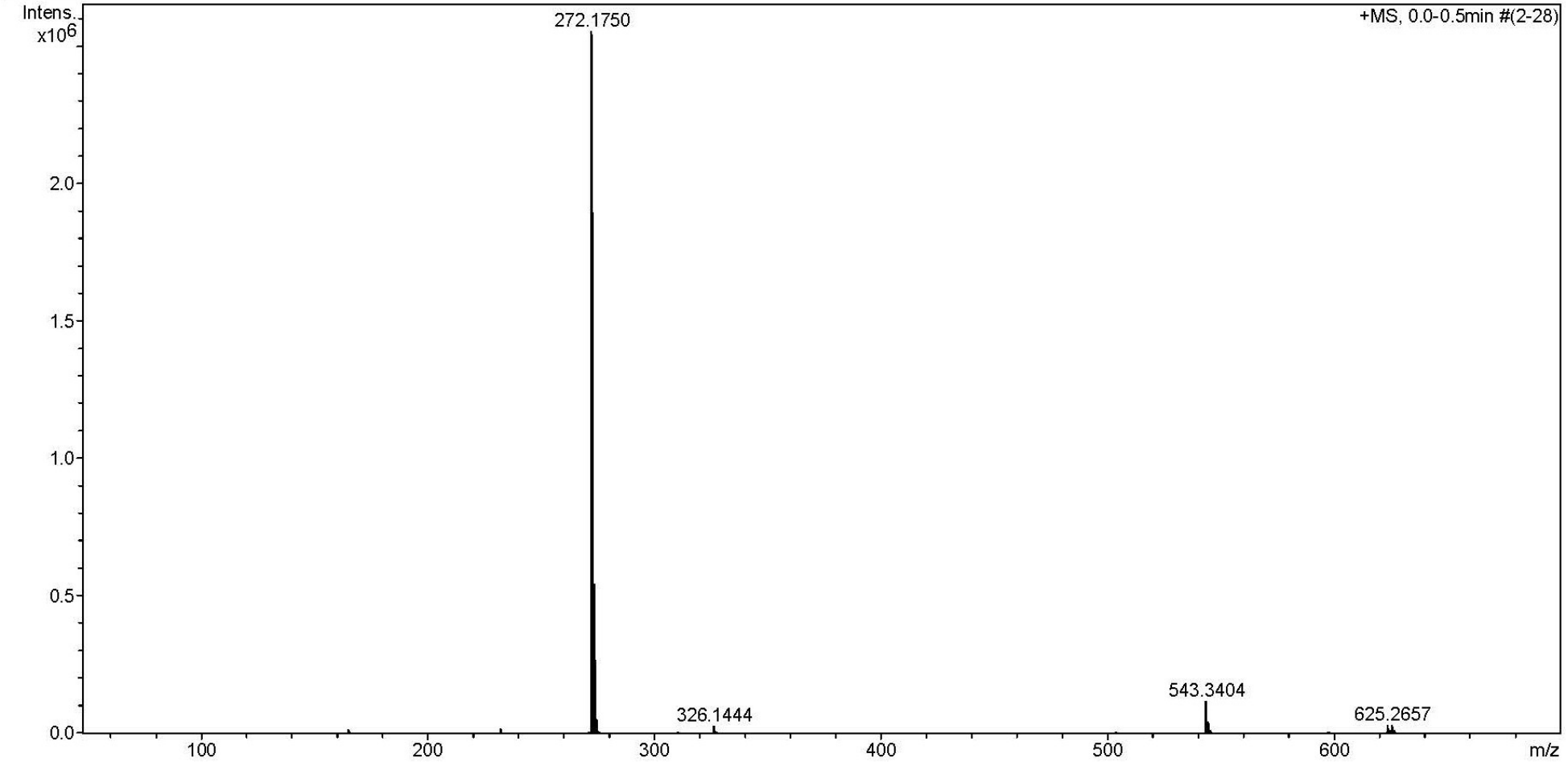

Figure 42S. HRESI^{+}-MS of **3**.

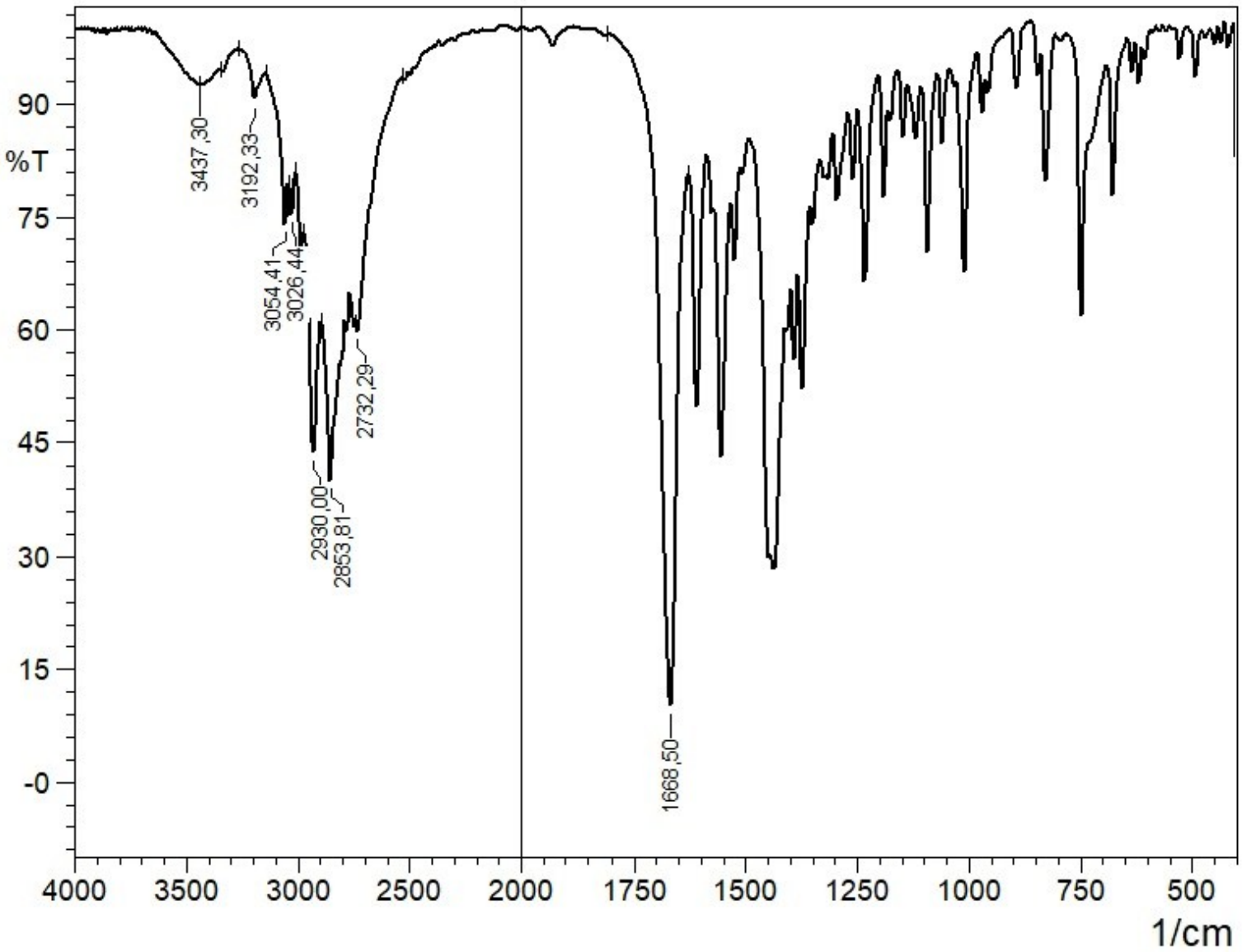

Figure 43S. IR spectrum of **3**.

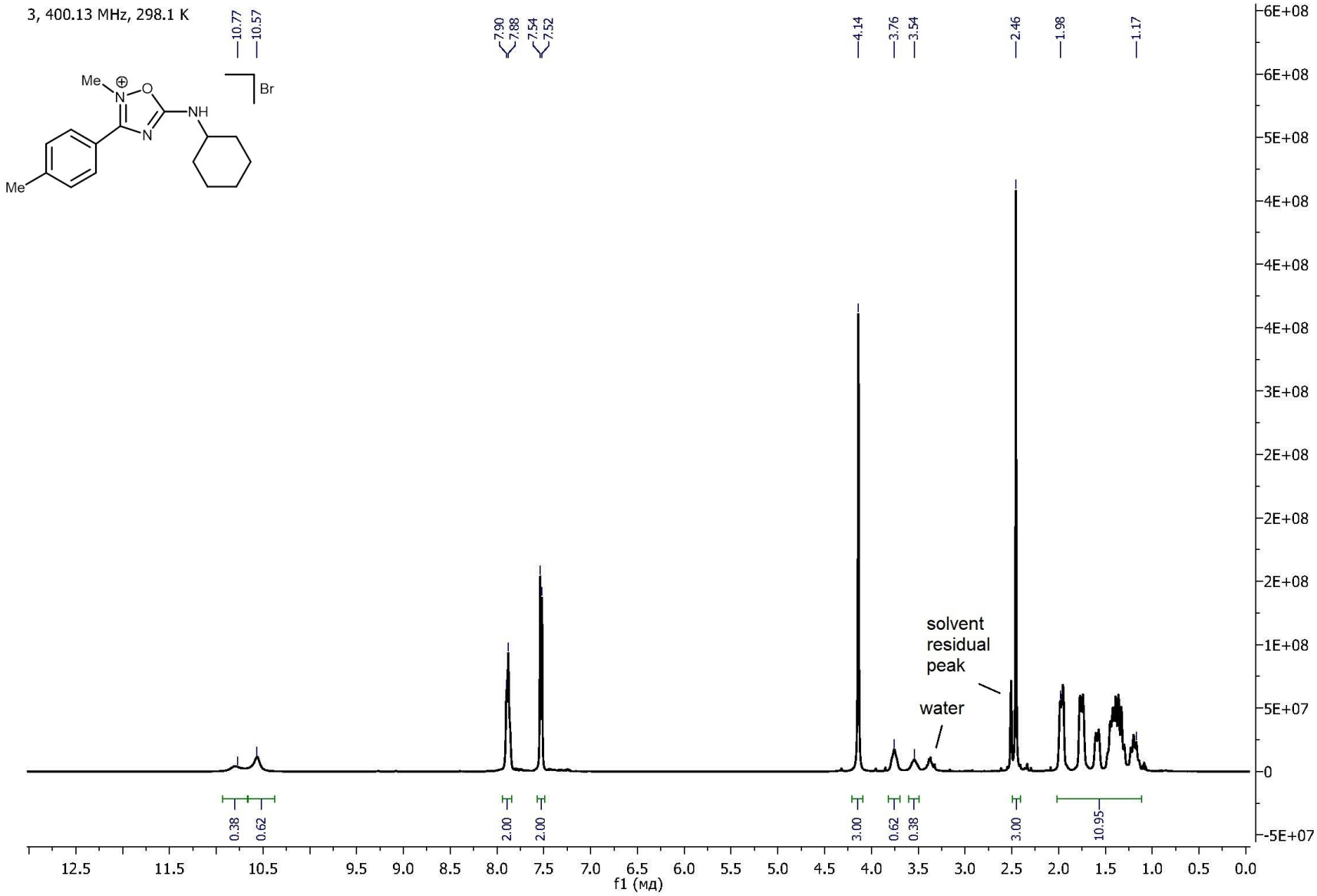

Figure 44S. ^{1}H NMR spectrum of **3**.

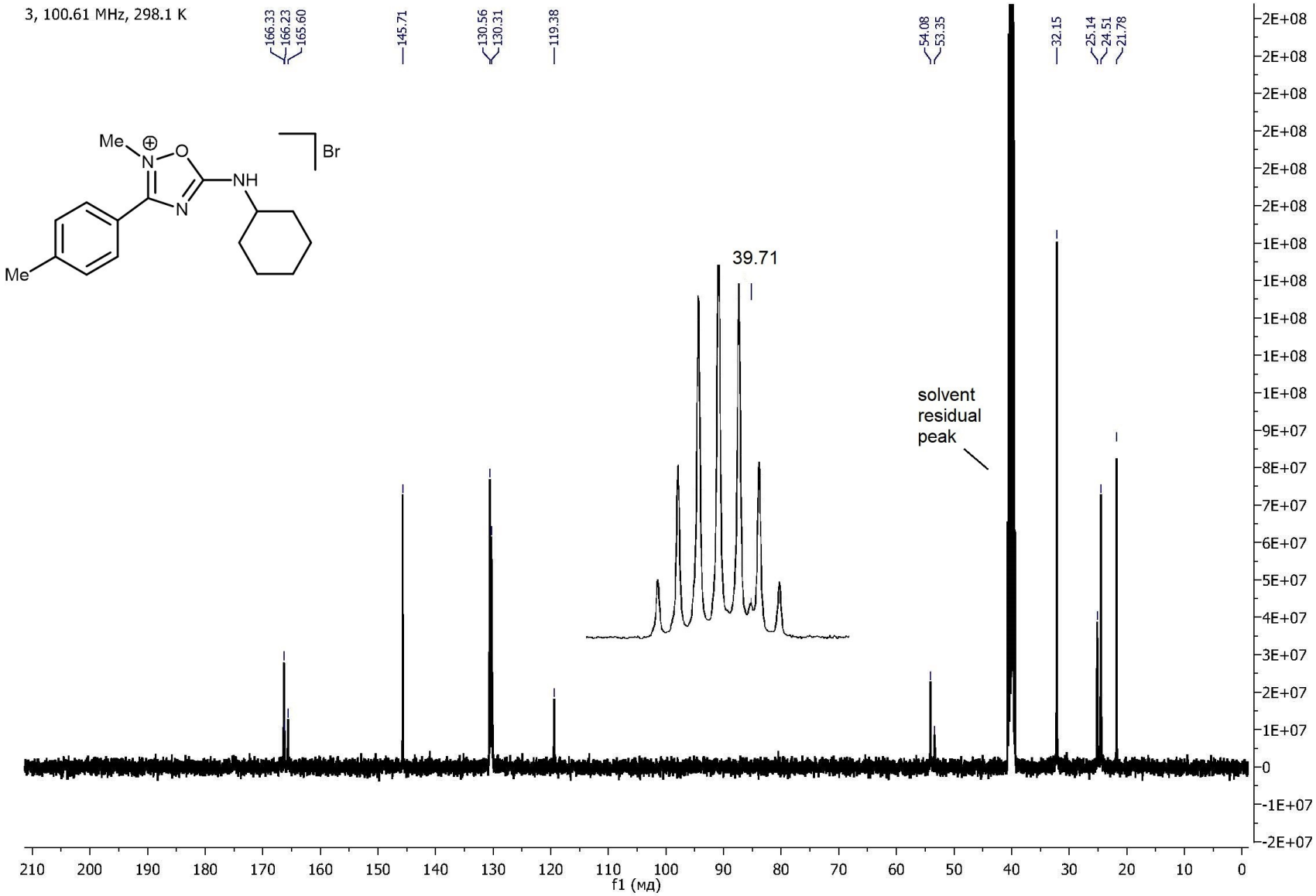

Figure 45S. $^{13}C\{^{1}H\}$ NMR spectrum of **3**.

Acquisition Parameter

Source Type	ESI	Ion Polarity	Positive	Set Nebulizer	0.4 Bar
Focus	Not active			Set Dry Heater	180 °C
Scan Begin	50 m/z	Set Capillary	4500 V	Set Dry Gas	4.0 l/min
Scan End	1000 m/z	Set End Plate Offset	-500 V	Set Divert Valve	Source

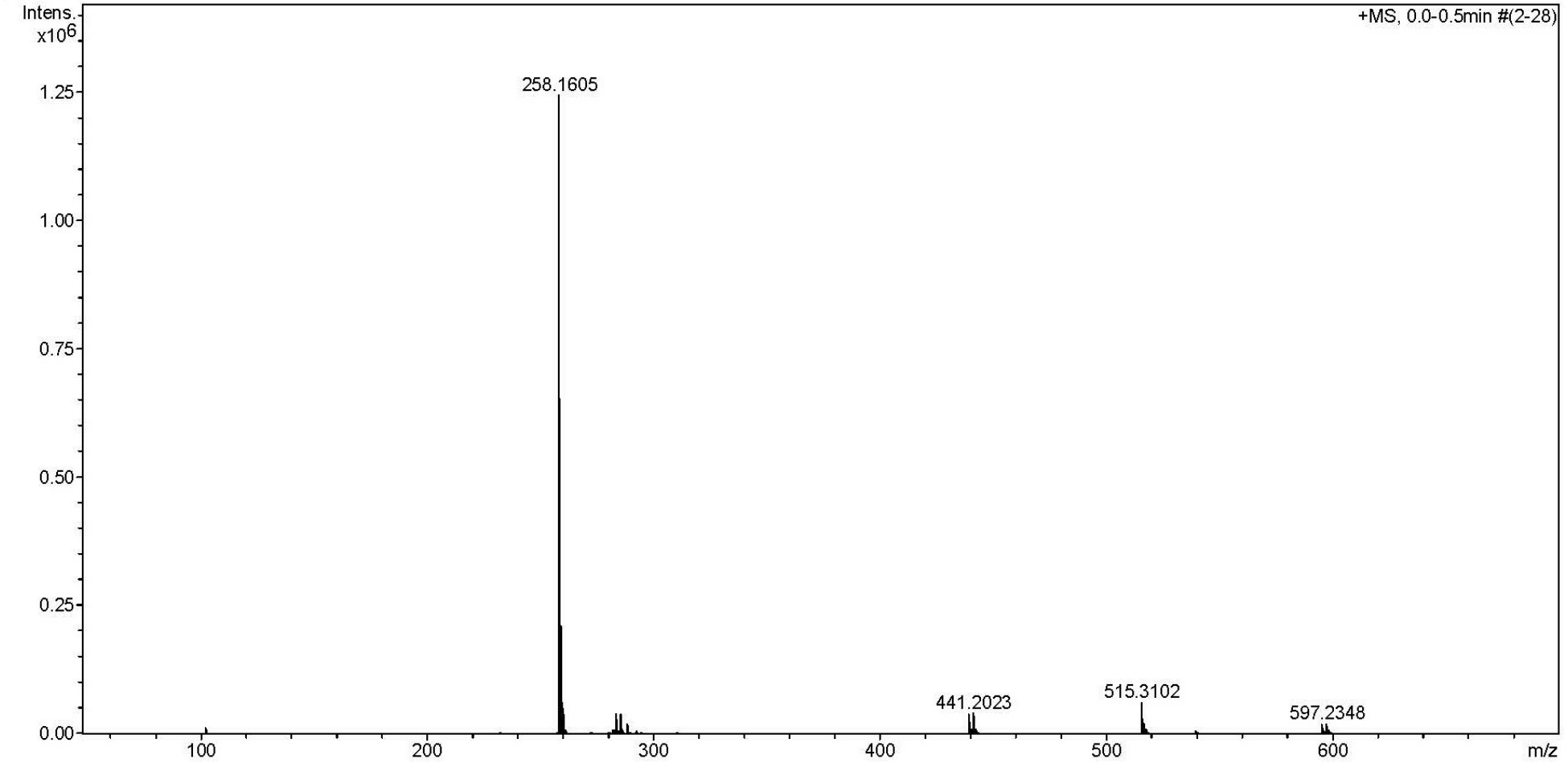

Figure 46S. HRESI^{+}-MS of **4**.

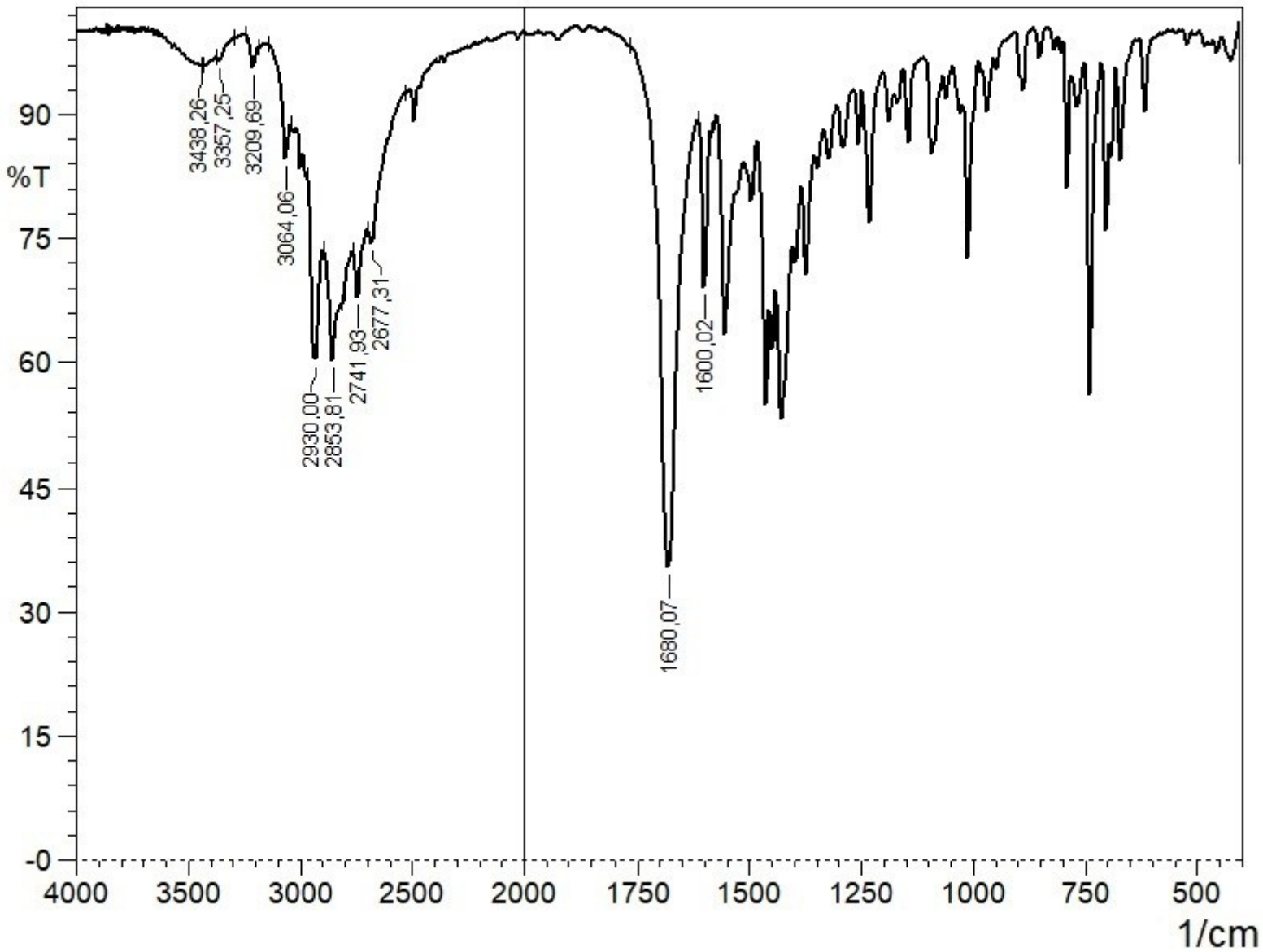

Figure 47S. IR spectrum of **4**.

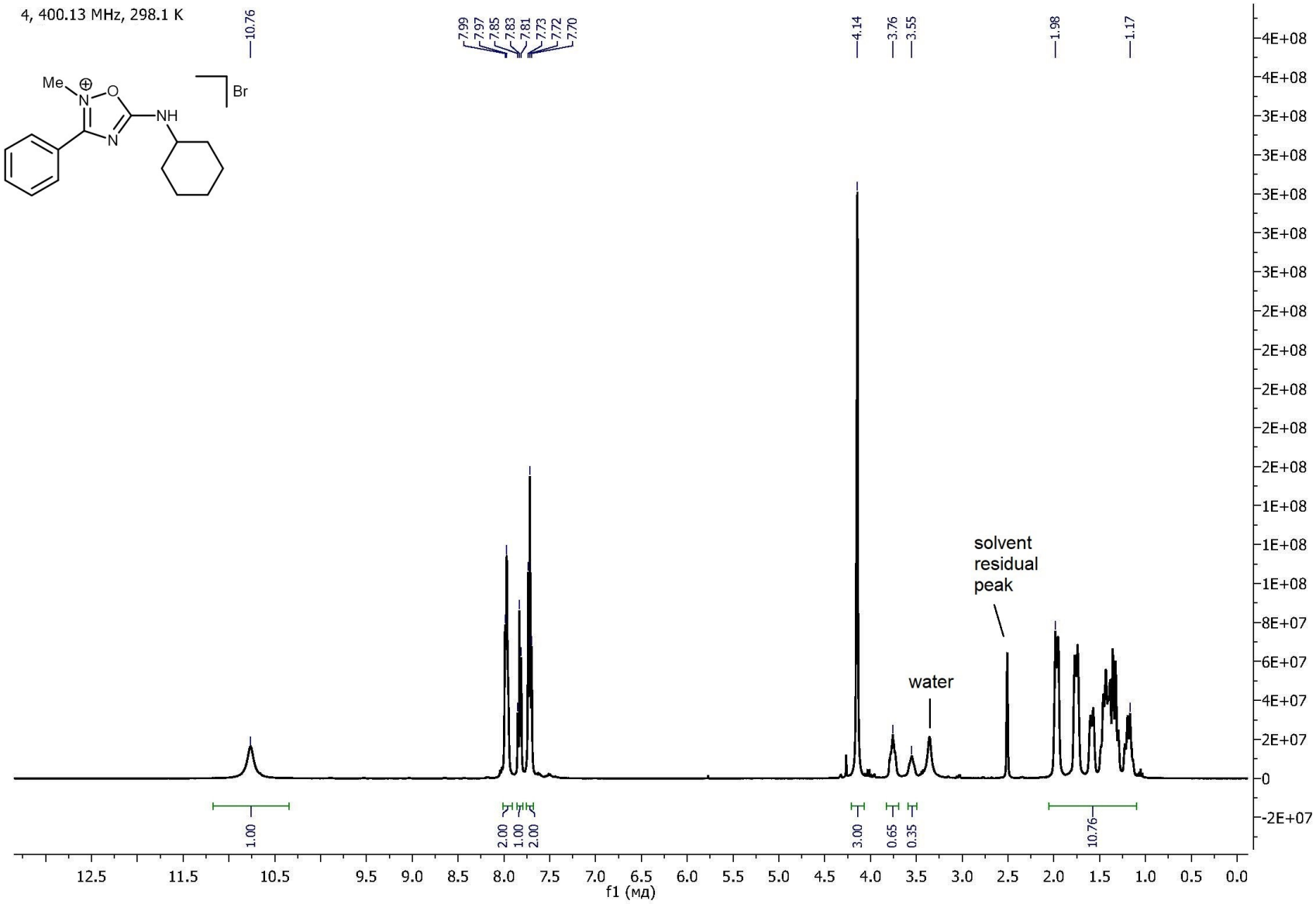

Figure 48S. ^{1}H NMR spectrum of **4**.

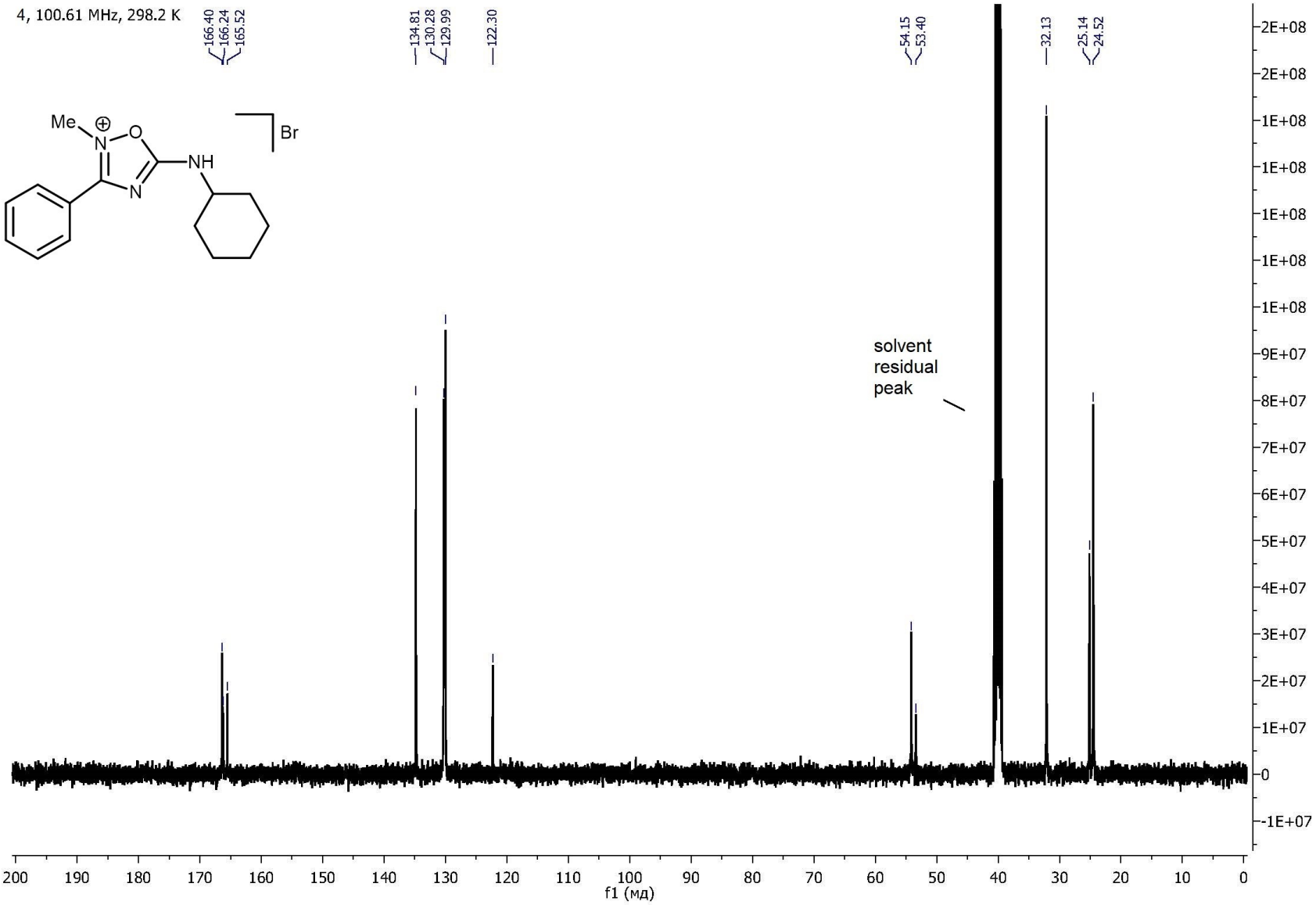

Figure 49S. $^{13}C\{^{1}H\}$ NMR spectrum of **4**.

Acquisition Parameter

Source Type	ESI	Ion Polarity	Positive	Set Nebulizer	0.4 Bar
Focus	Not active			Set Dry Heater	180 °C
Scan Begin	50 m/z	Set Capillary	4500 V	Set Dry Gas	4.0 l/min
Scan End	1000 m/z	Set End Plate Offset	-500 V	Set Divert Valve	Source

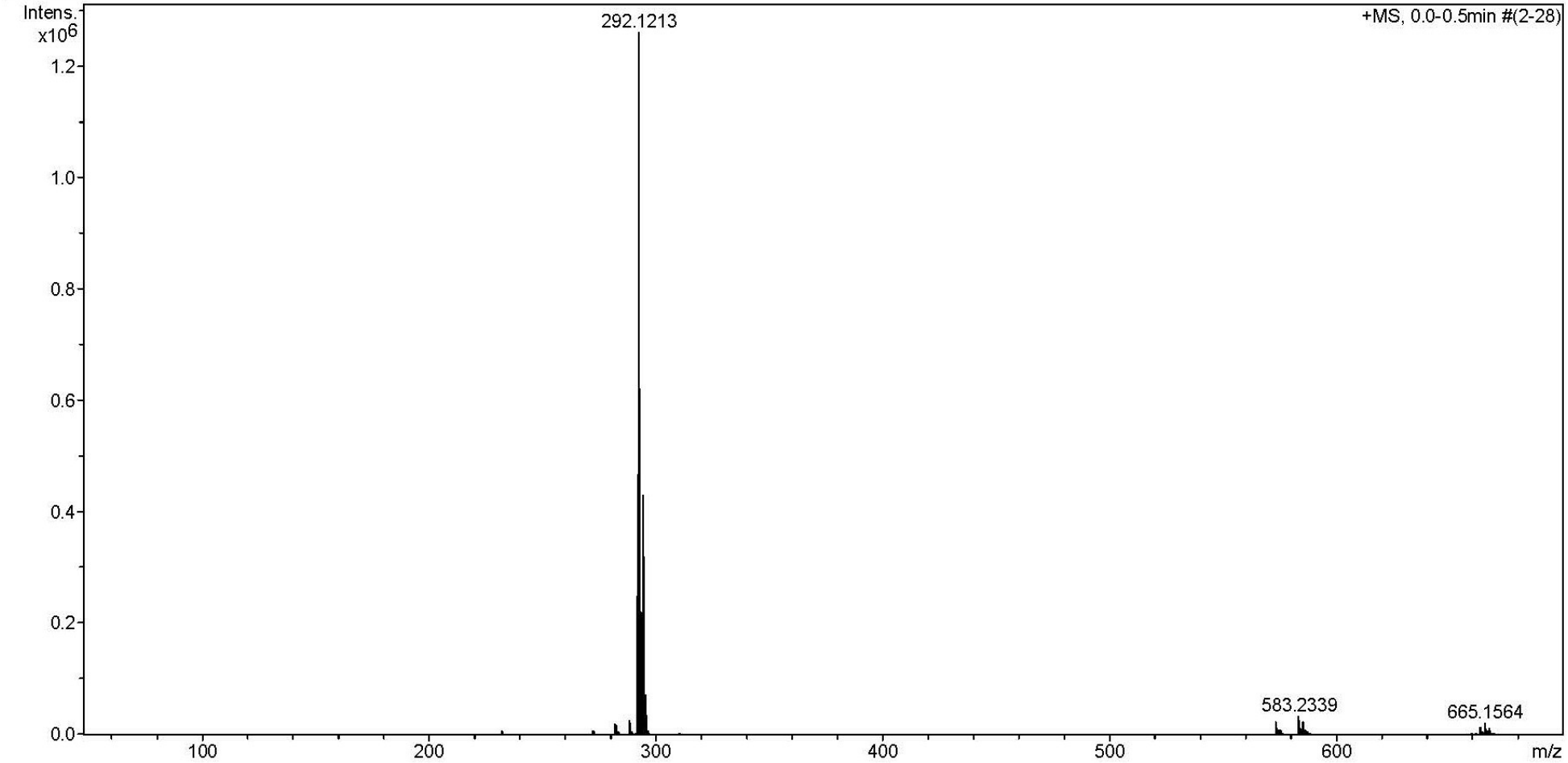

Figure 50S. HRESI^{+}-MS of **5**.

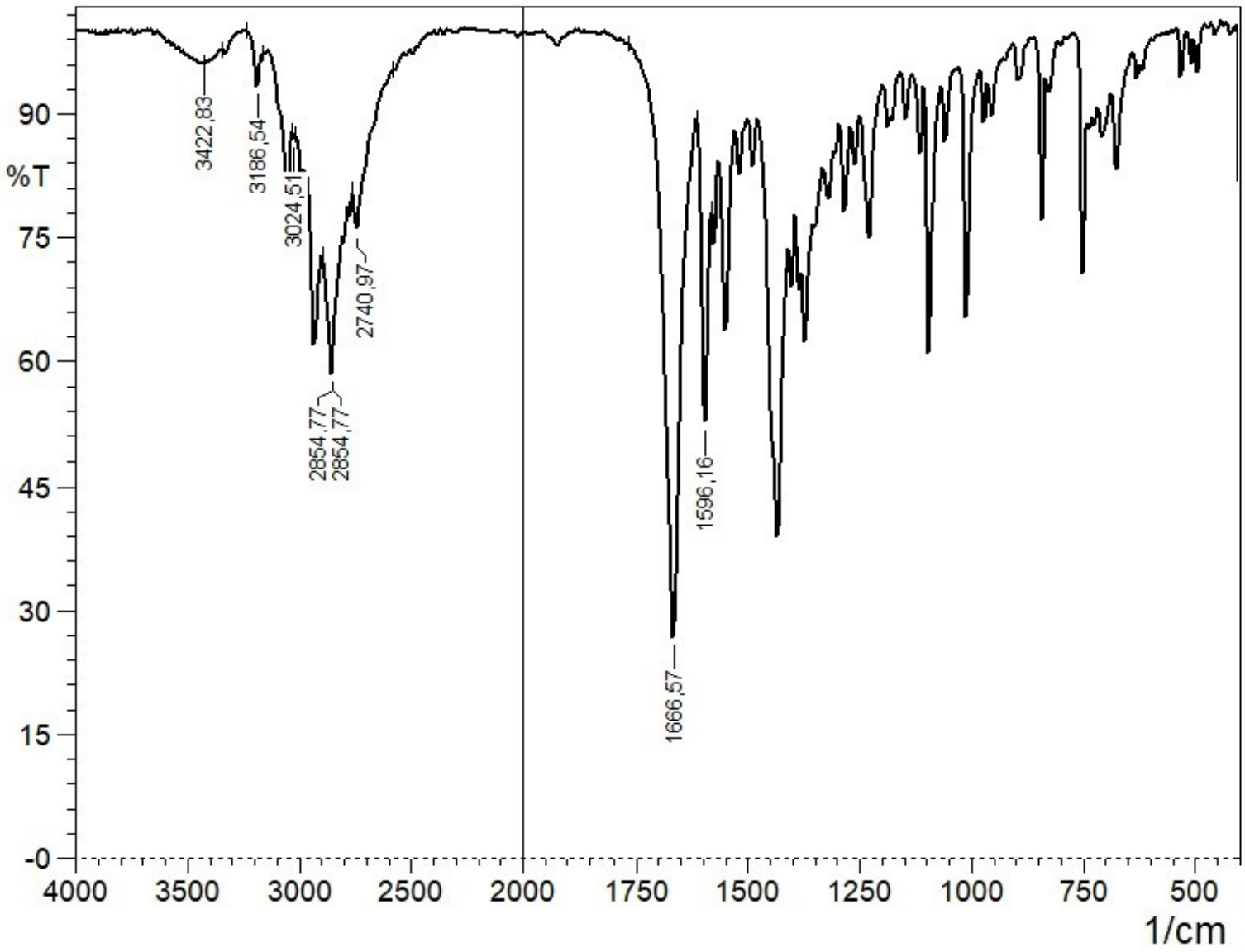

Figure 51S. IR spectrum of **5**.

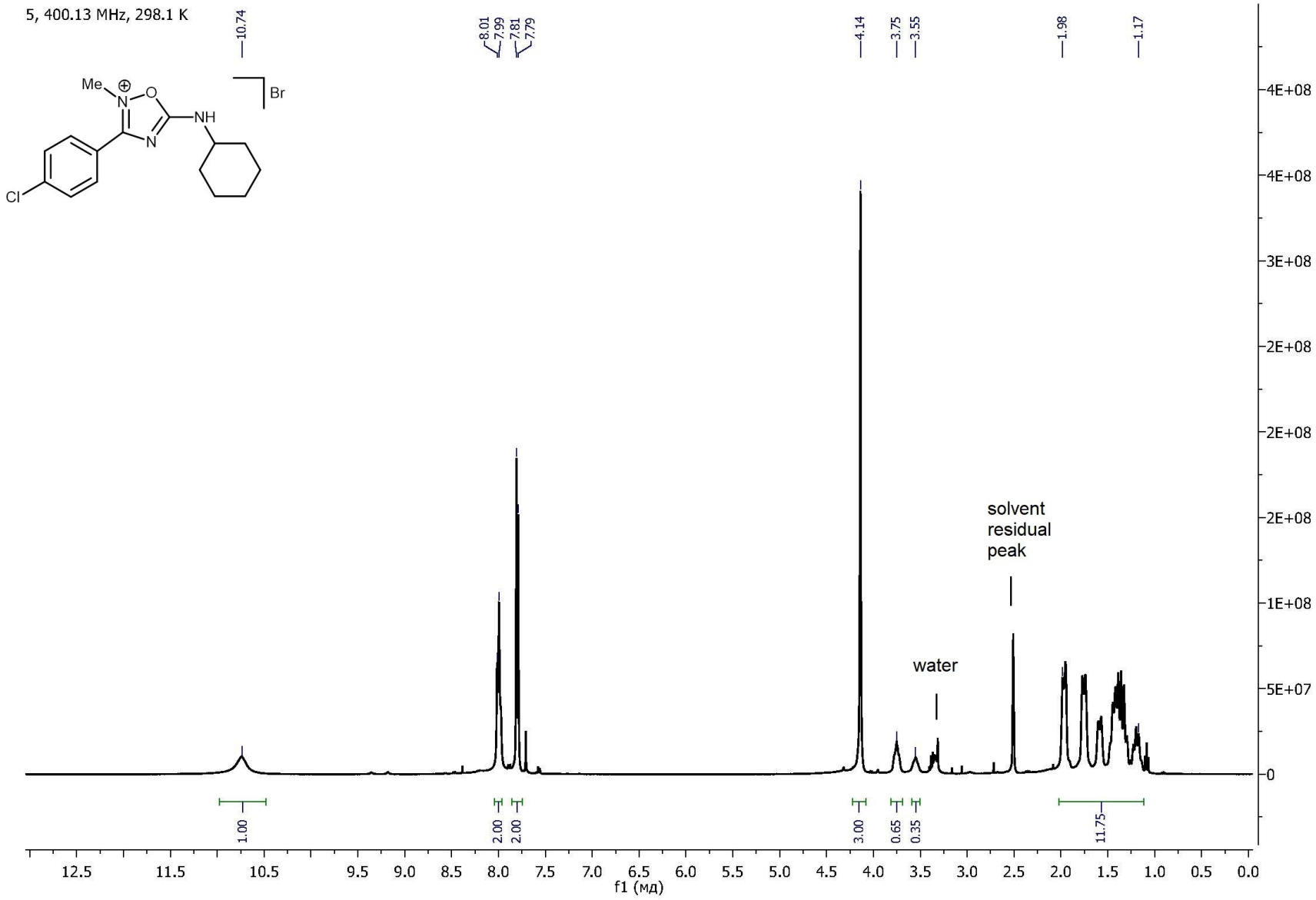

Figure 52S. ^{1}H NMR spectrum of **5**.

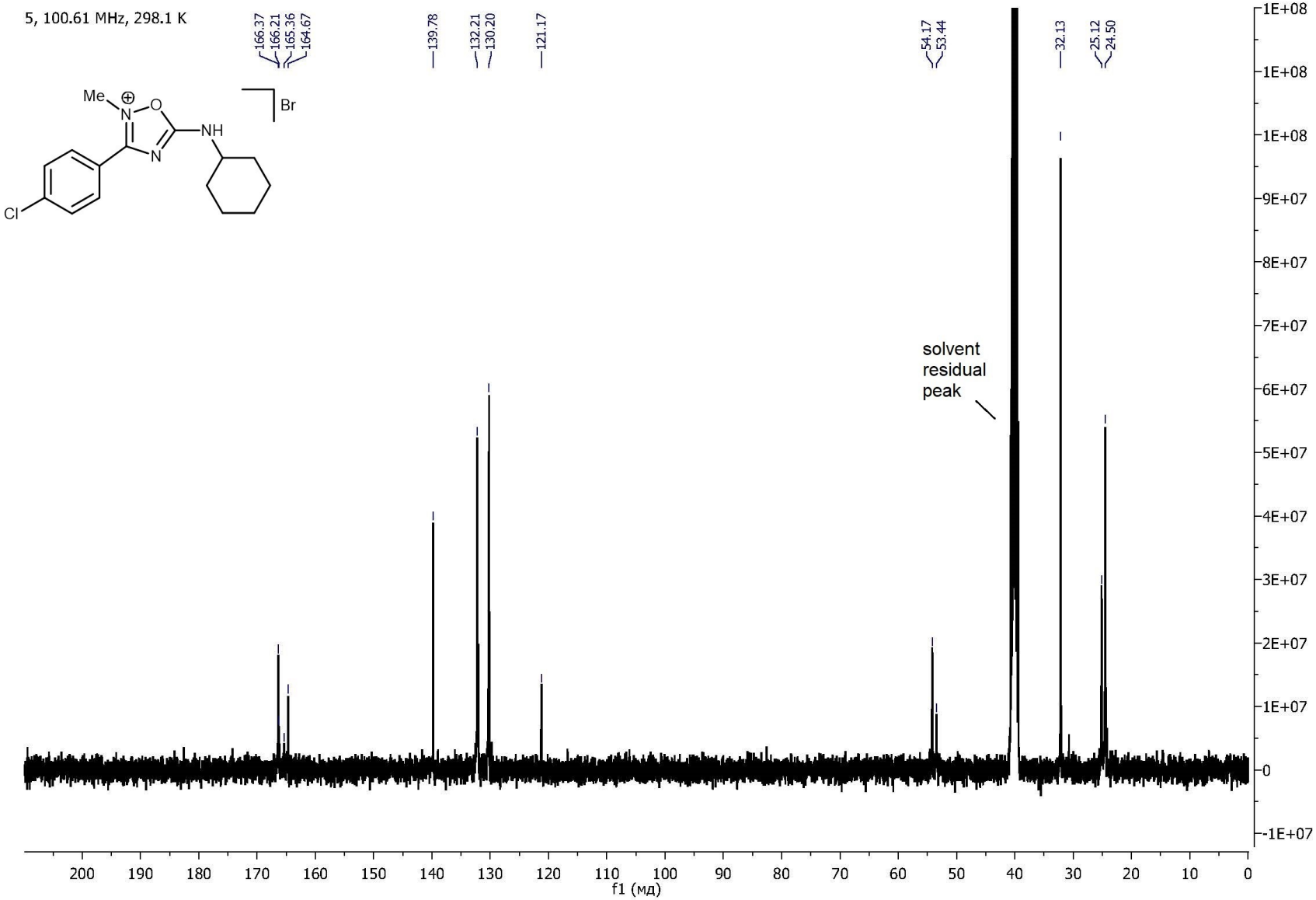

Figure 53S. $^{13}C\{^{1}H\}$ NMR spectrum of **5**.

Acquisition Parameter

Source Type	ESI	Ion Polarity	Positive	Set Nebulizer	0.4 Bar
Focus	Not active			Set Dry Heater	180 °C
Scan Begin	50 m/z	Set Capillary	4500 V	Set Dry Gas	4.0 l/min
Scan End	1000 m/z	Set End Plate Offset	-500 V	Set Divert Valve	Source

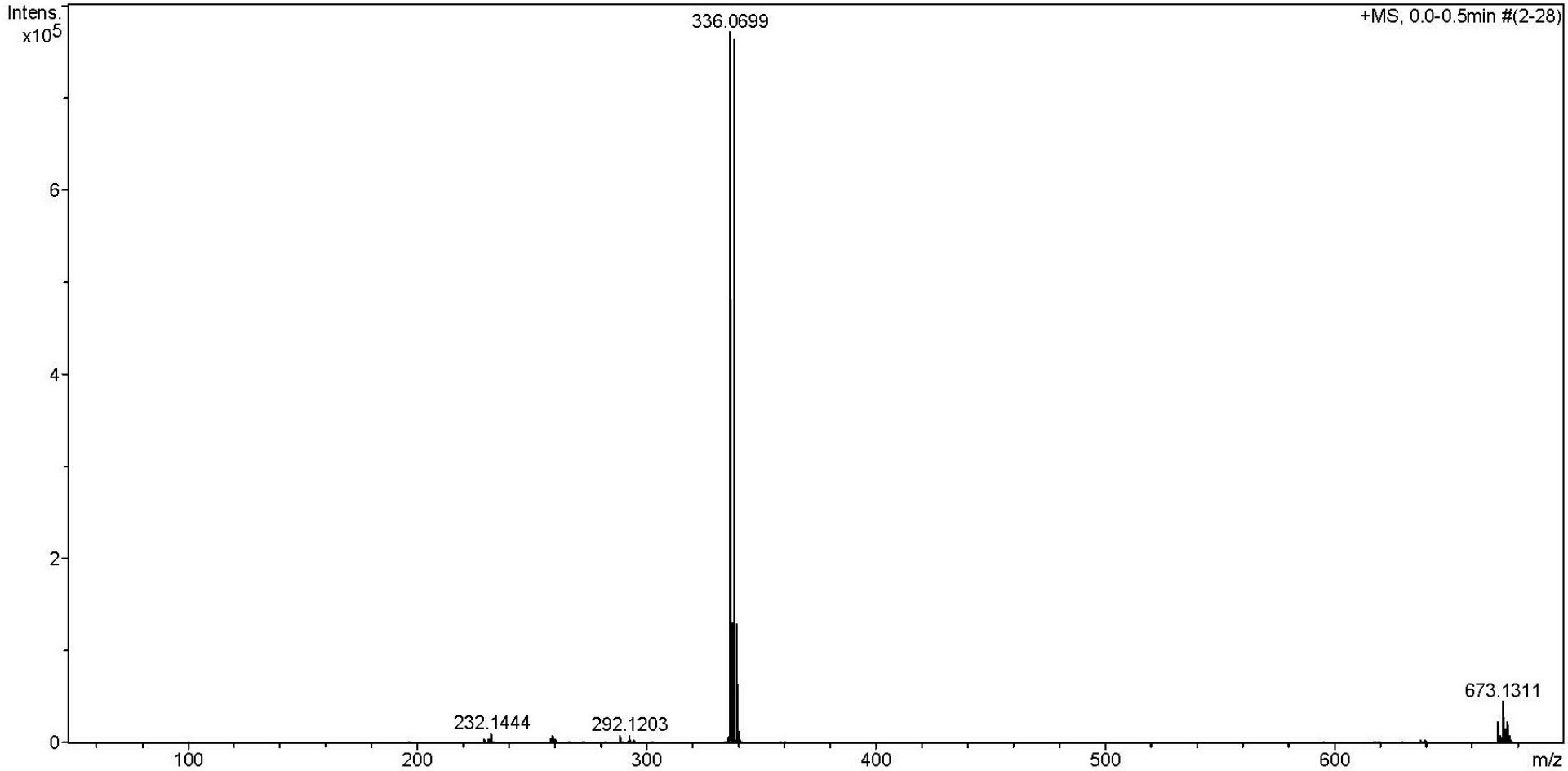

Figure 54S. HRESI^{+}-MS of **6**.

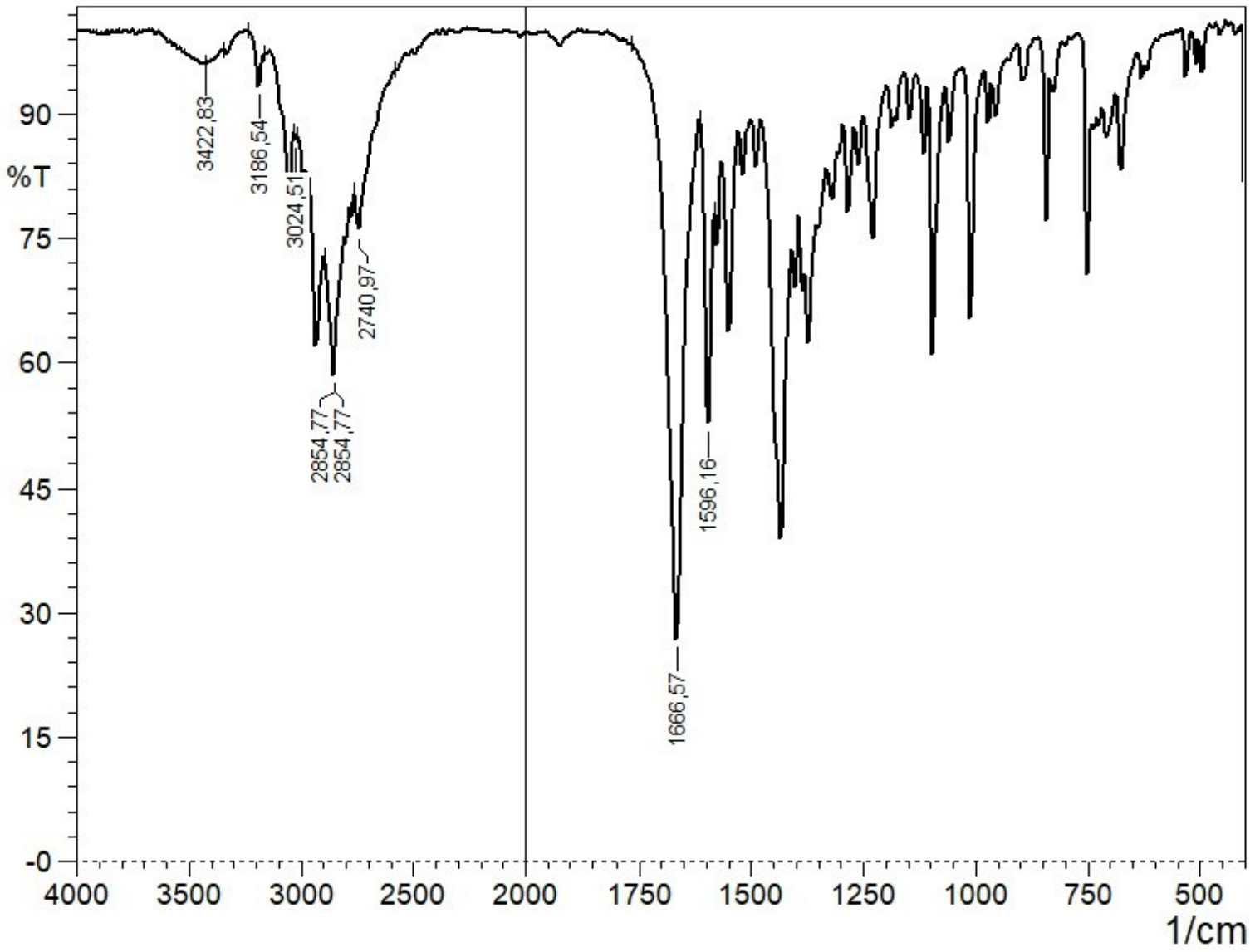

Figure 55S. IR spectrum of **6**.

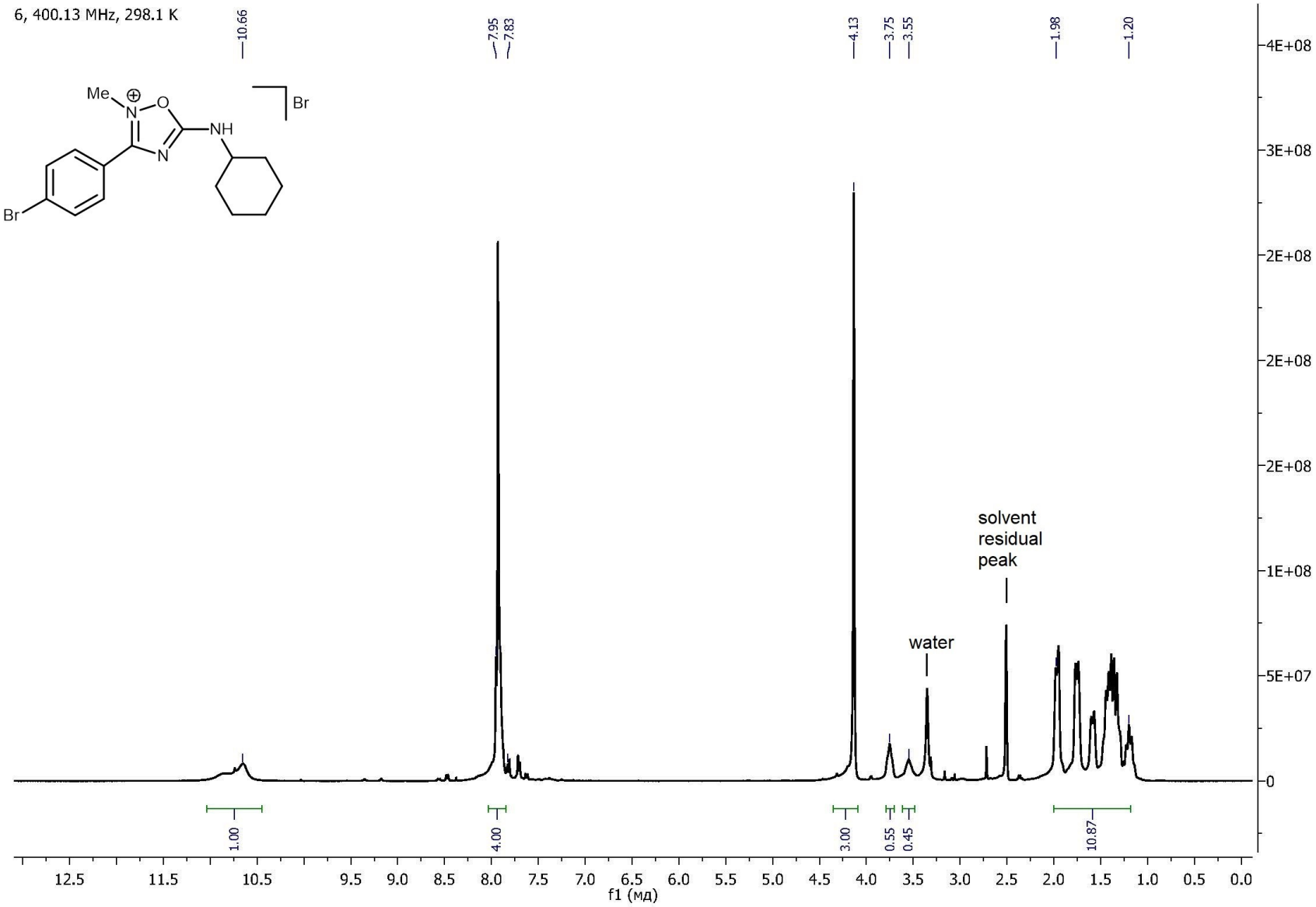

Figure 56S. ^{1}H NMR spectrum of **6**.

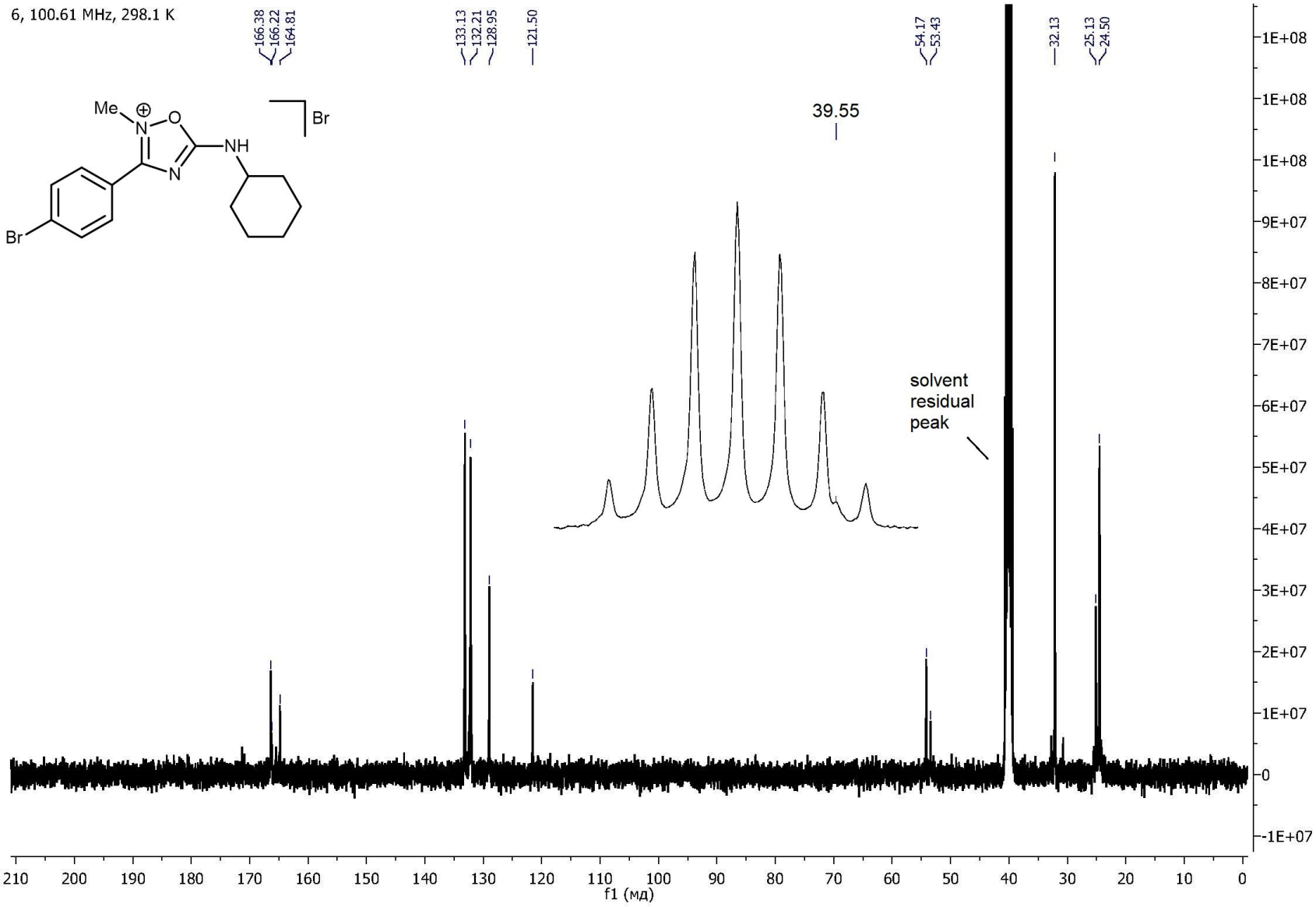

Figure 57S. $^{13}C\{^{1}H\}$ NMR spectrum of **6**.

Acquisition Parameter

Source Type	ESI	Ion Polarity	Positive	Set Nebulizer	0.4 Bar
Focus	Not active			Set Dry Heater	180 °C
Scan Begin	50 m/z	Set Capillary	4500 V	Set Dry Gas	4.0 l/min
Scan End	3000 m/z	Set End Plate Offset	-500 V	Set Divert Valve	Source

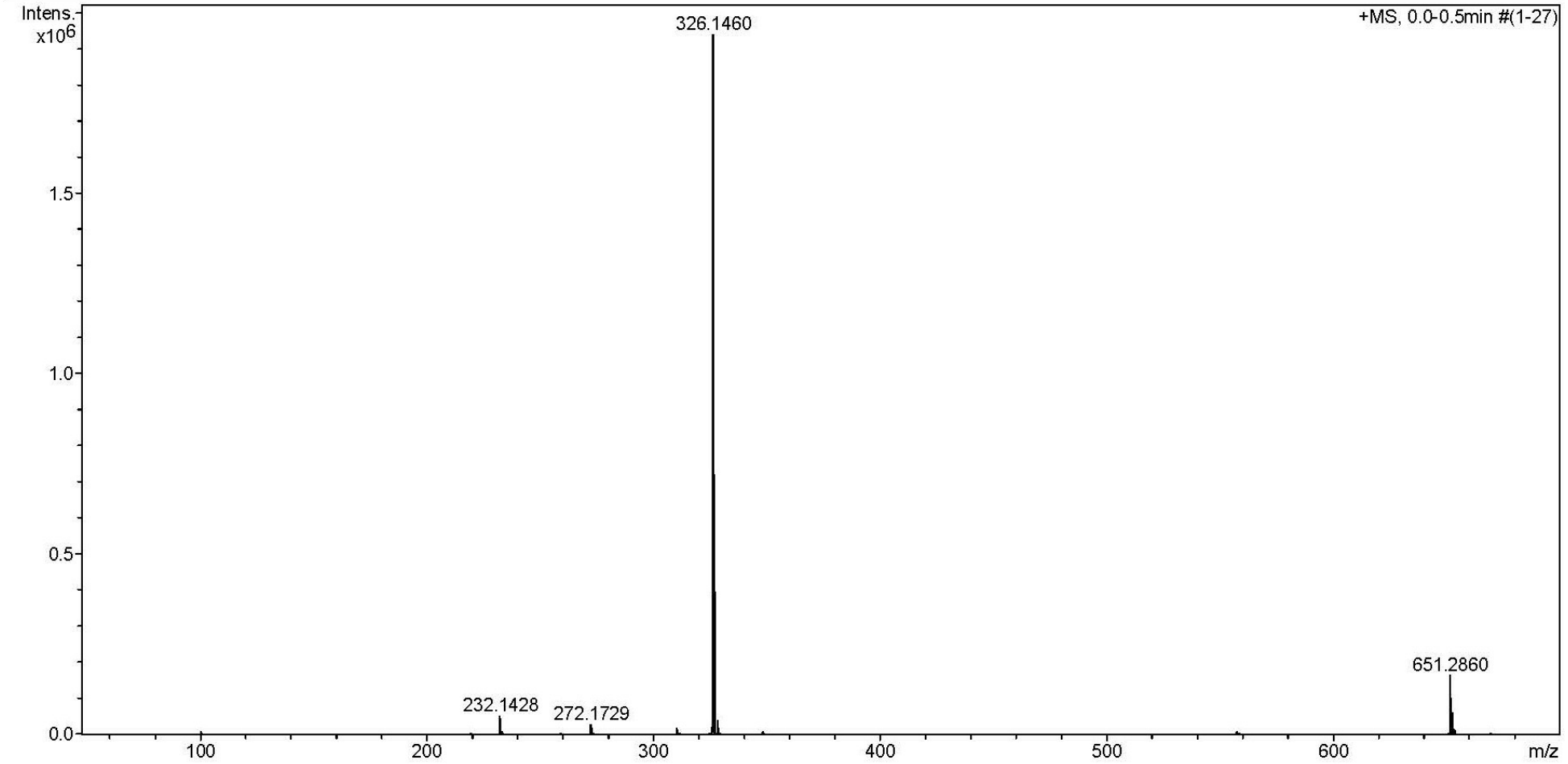

Figure 58S. HRESI$^+$-MS of **7**.

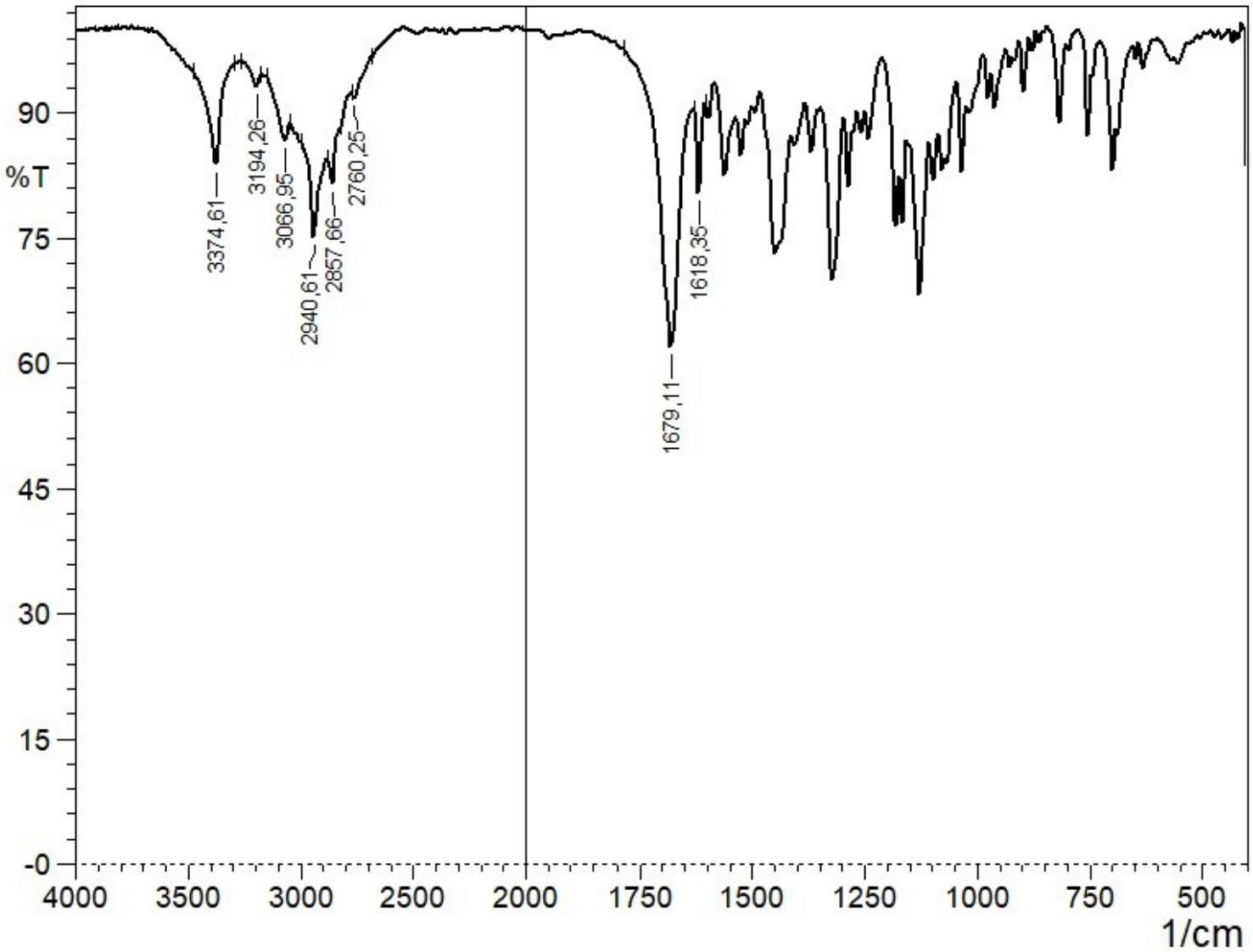

Figure 59S. IR spectrum of **7**.

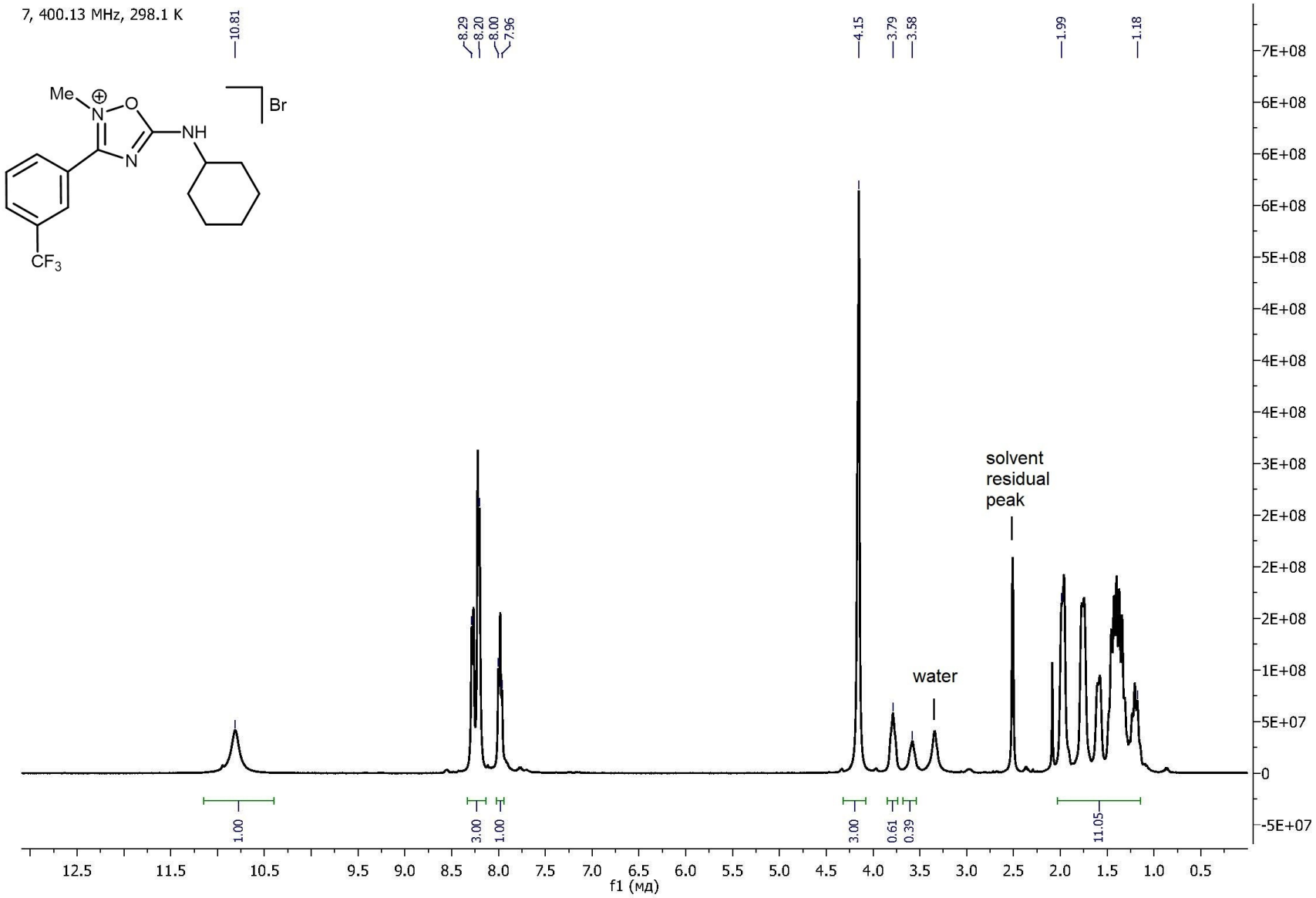

Figure 60S. ^{1}H NMR spectrum of **7**.

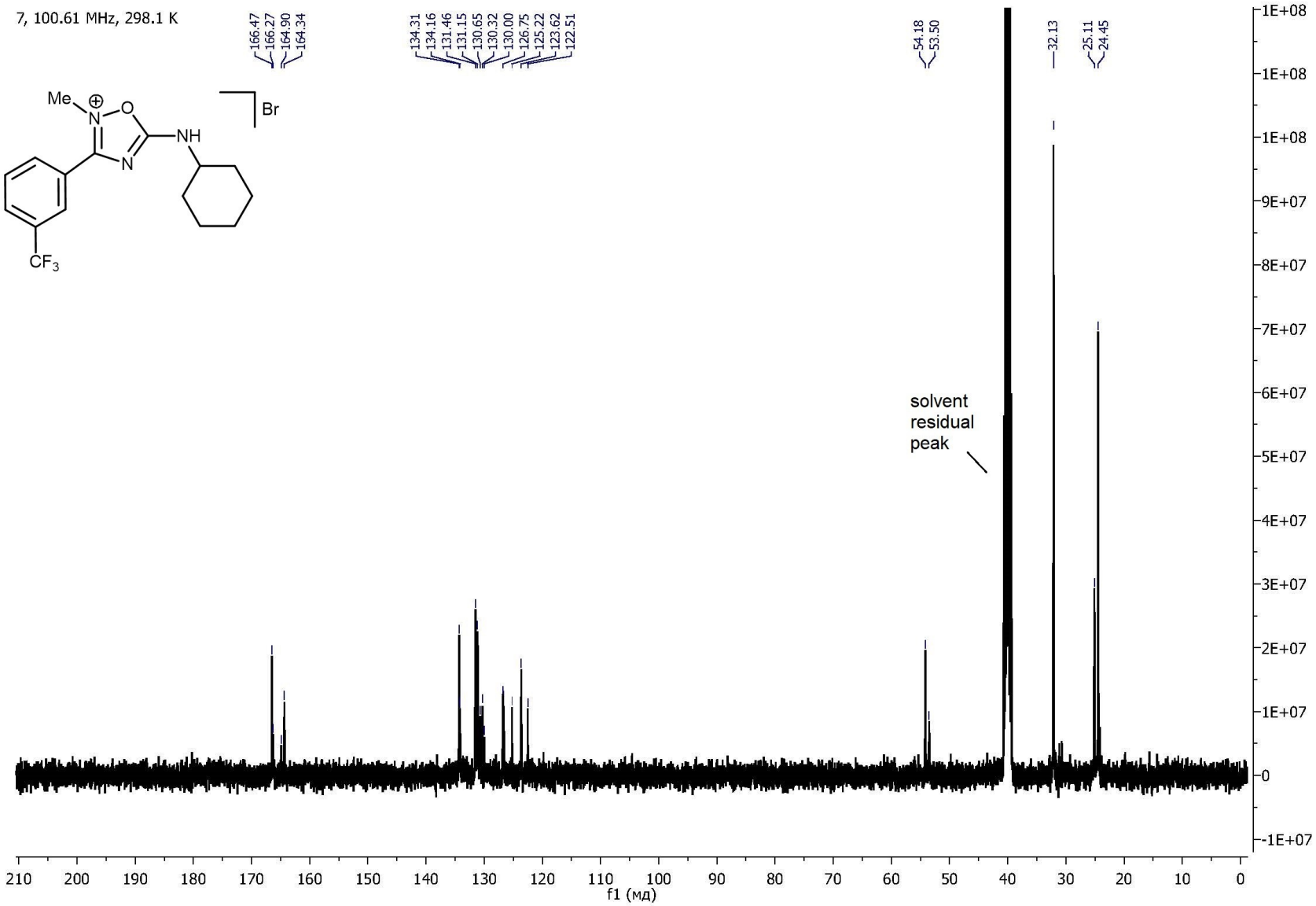

Figure 61S. $^{13}C\{^{1}H\}$ NMR spectrum of **7**.

Acquisition Parameter

Source Type	ESI	Ion Polarity	Positive	Set Nebulizer	0.4 Bar
Focus	Not active			Set Dry Heater	180 °C
Scan Begin	50 m/z	Set Capillary	4500 V	Set Dry Gas	4.0 l/min
Scan End	1000 m/z	Set End Plate Offset	-500 V	Set Divert Valve	Source

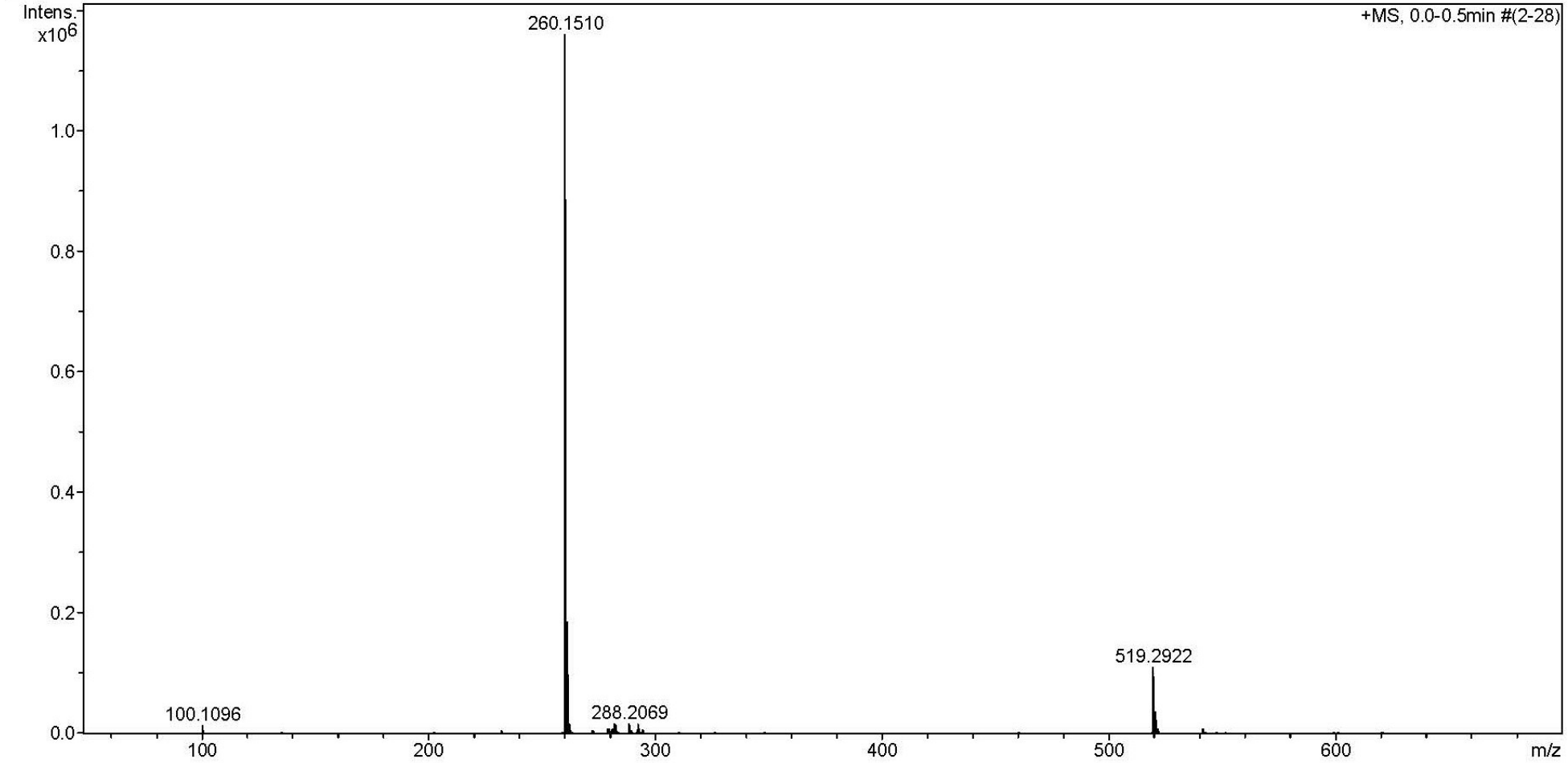

Figure 62S. HRESI$^+$-MS of **8**.

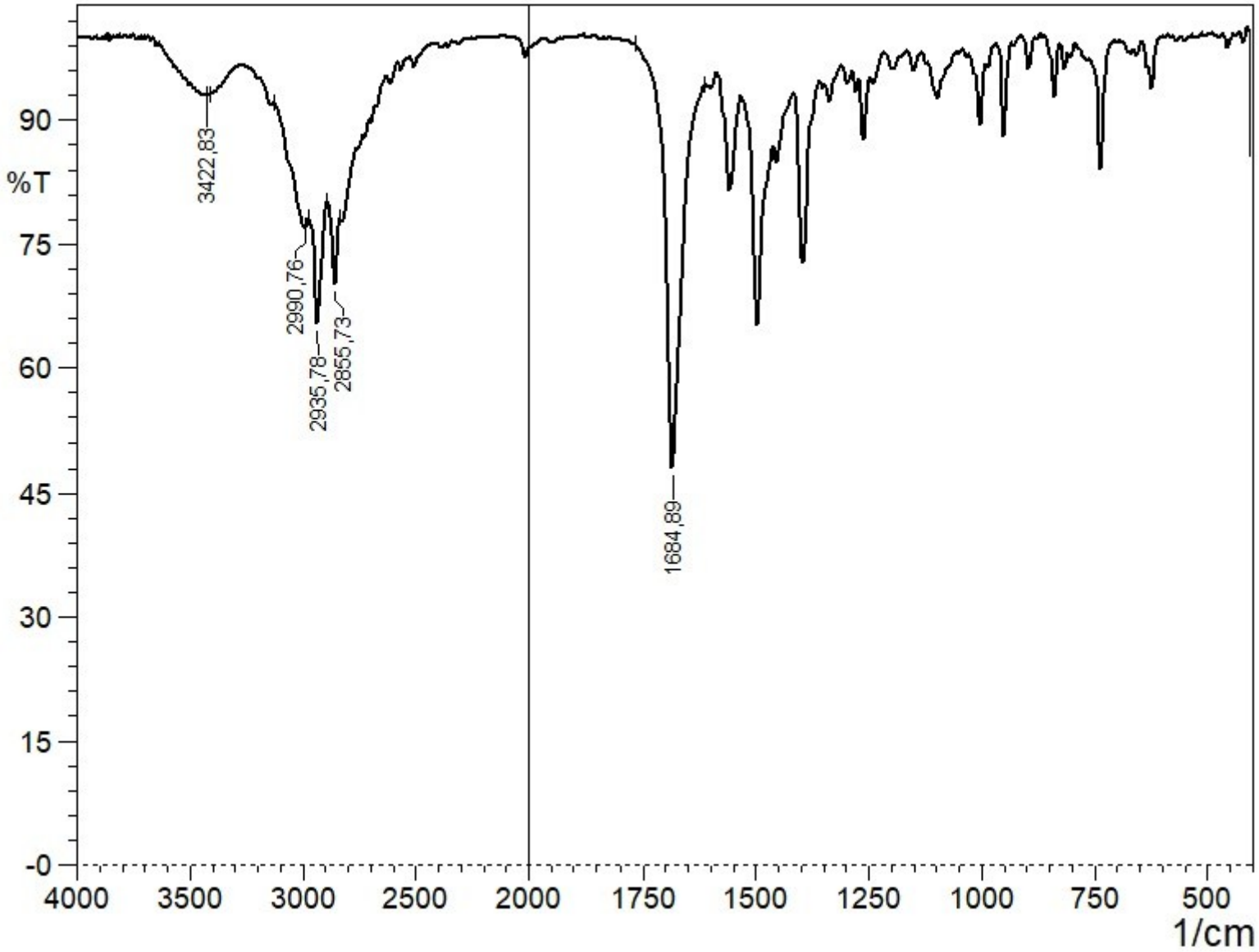

Figure 63S. IR spectrum of **8**.

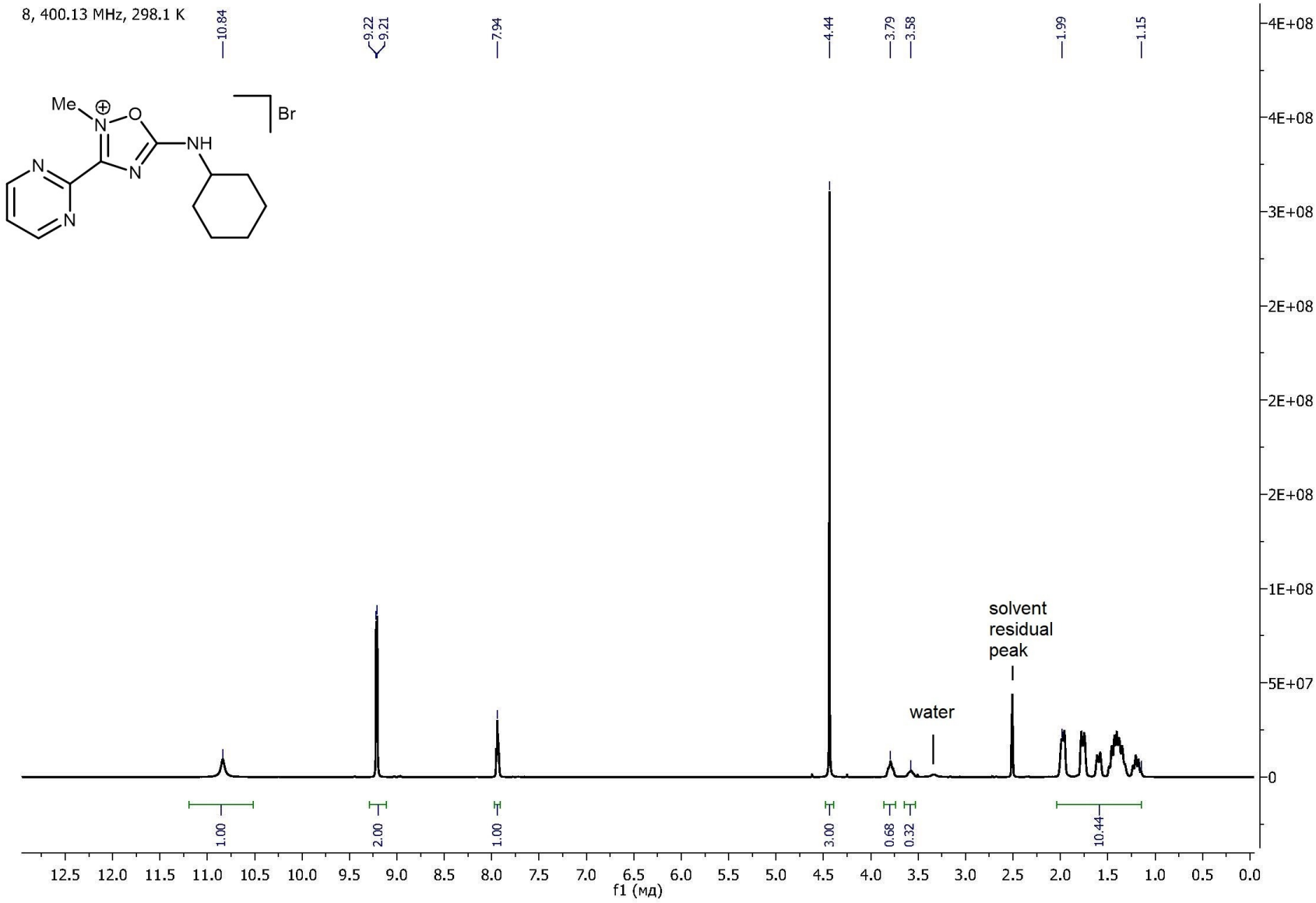

Figure 64S. ^{1}H NMR spectrum of **8**.

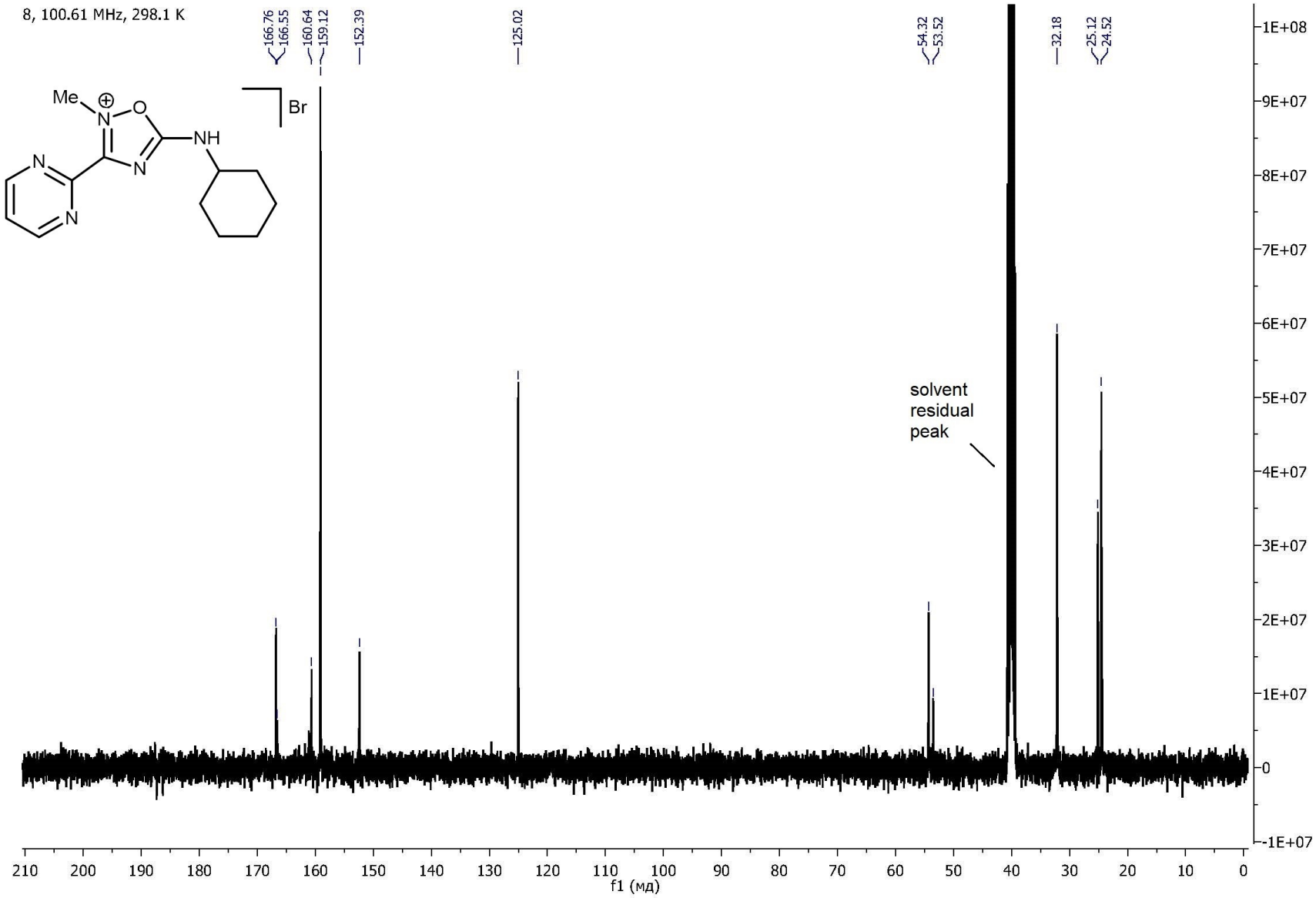

Figure 65S. $^{13}C\{^{1}H\}$ NMR spectrum of **8**.

Acquisition Parameter

Source Type	ESI	Ion Polarity	Positive	Set Nebulizer	0.4 Bar
Focus	Not active			Set Dry Heater	180 °C
Scan Begin	50 m/z	Set Capillary	4500 V	Set Dry Gas	4.0 l/min
Scan End	3000 m/z	Set End Plate Offset	-500 V	Set Divert Valve	Source

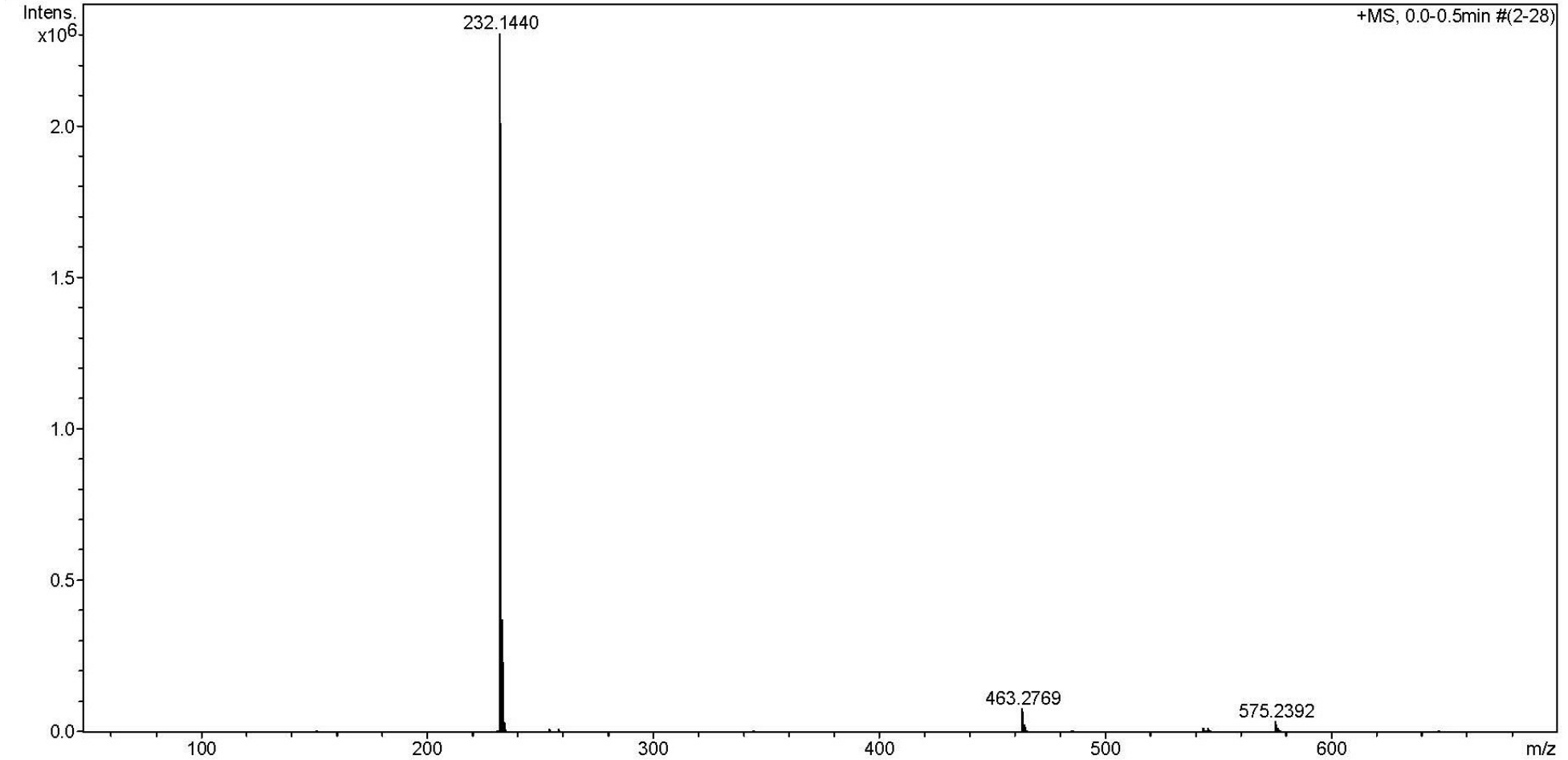

Figure 66S. HRESI$^+$-MS of **9**.

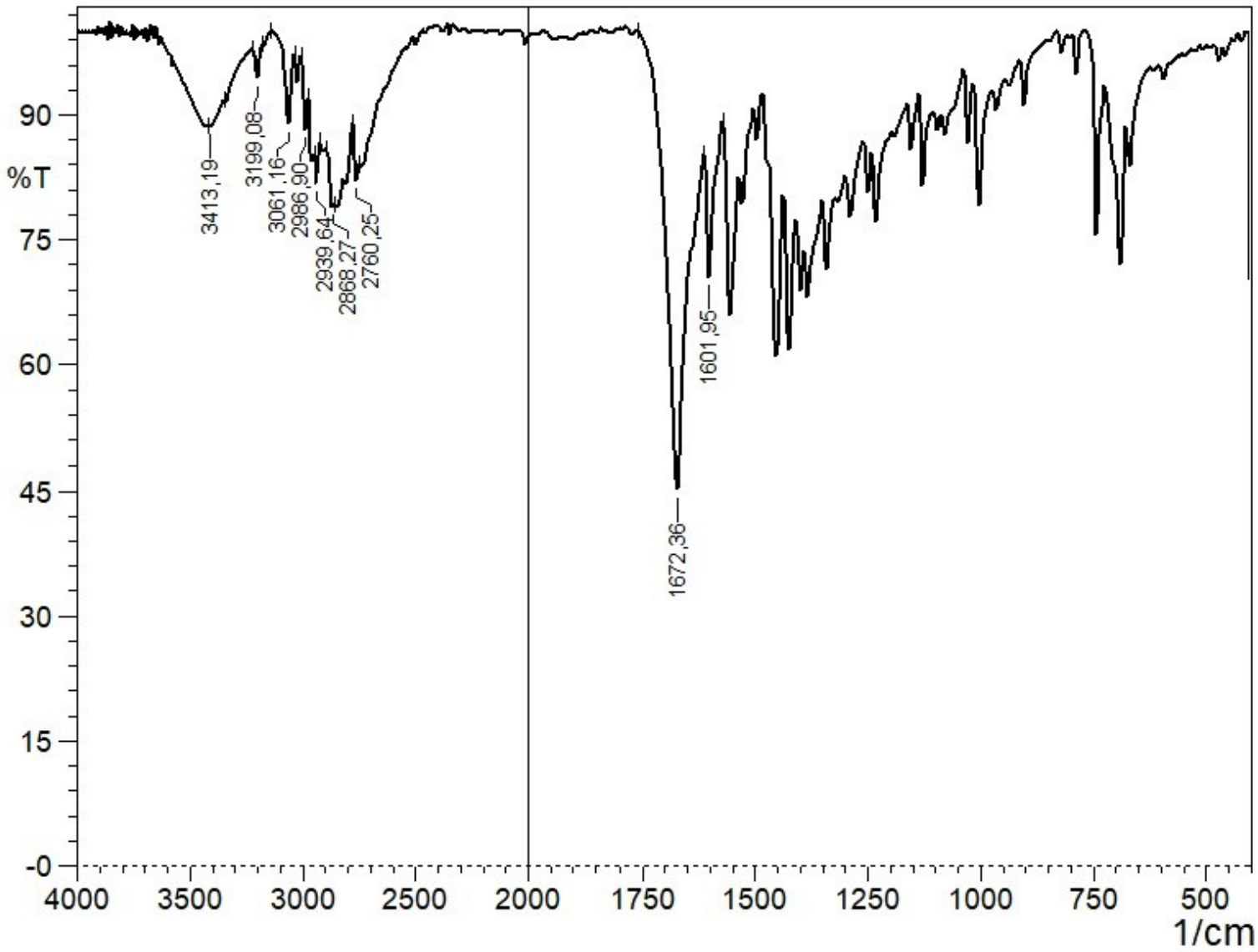

Figure 67S. IR spectrum of **9**.

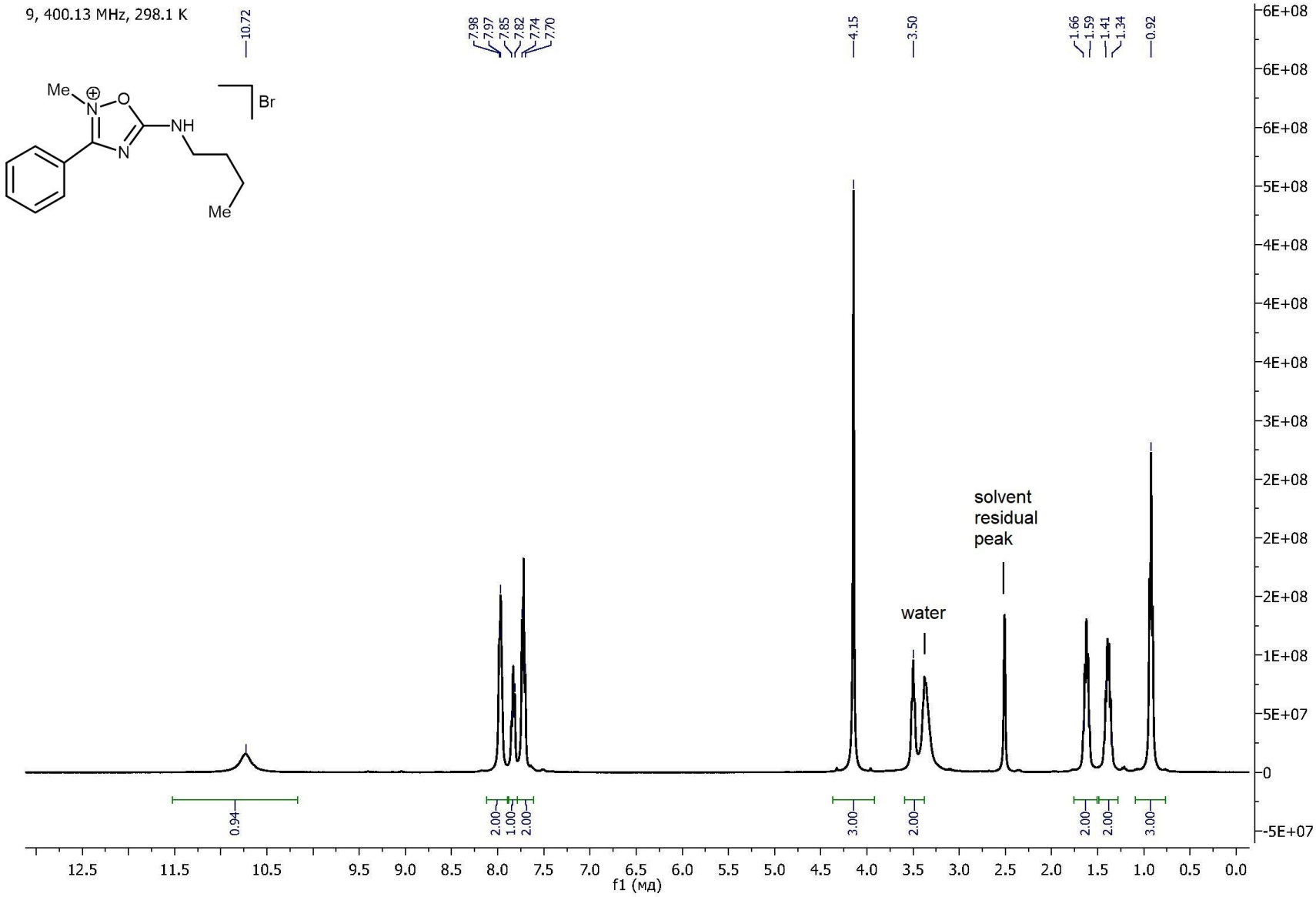

Figure 68S. ^{1}H NMR spectrum of **9**.

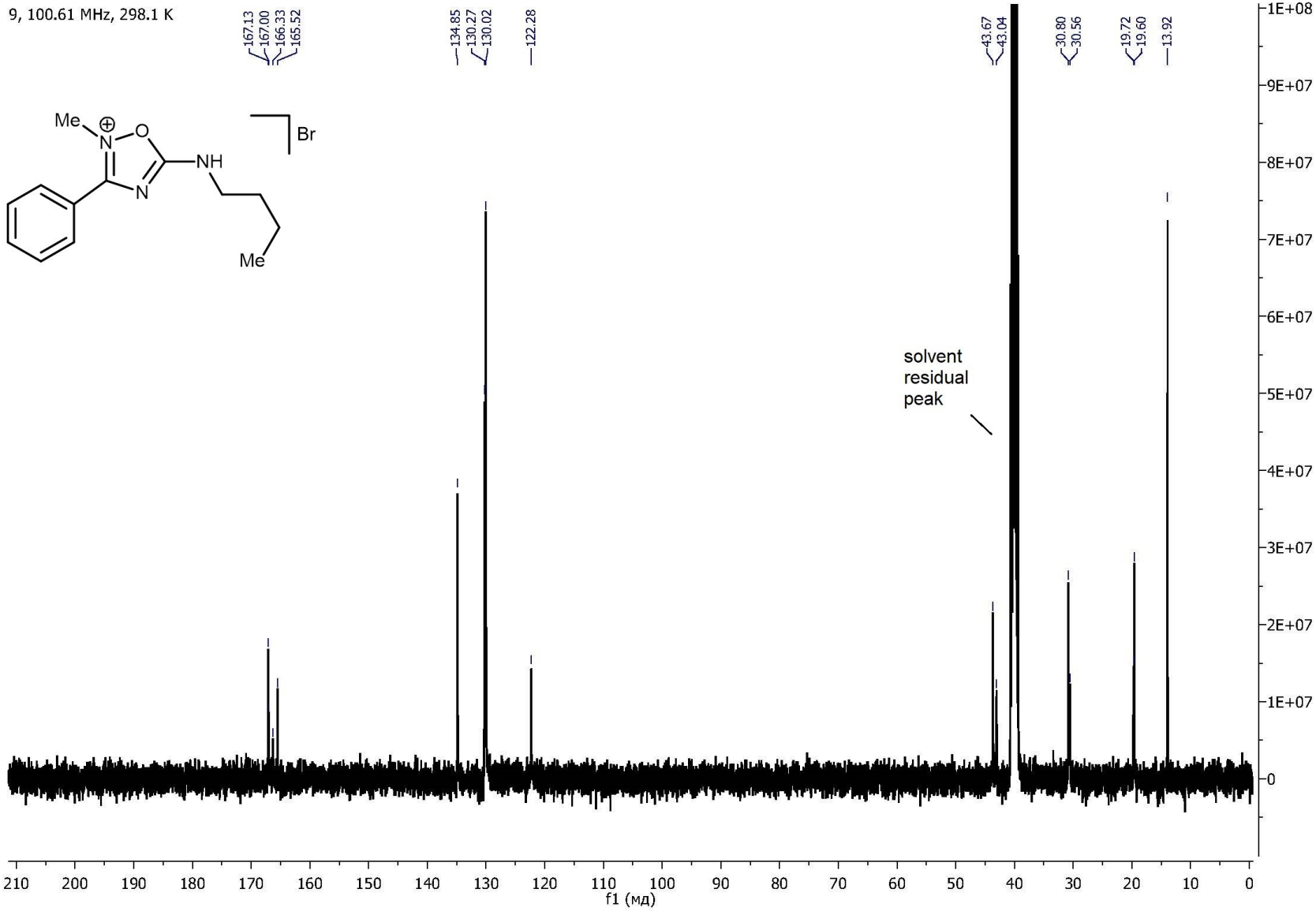

Figure 69S. $^{13}C\{^{1}H\}$ NMR spectrum of **9**.

Acquisition Parameter

Source Type	ESI	Ion Polarity	Positive	Set Nebulizer	0.4 Bar
Focus	Not active			Set Dry Heater	180 °C
Scan Begin	50 m/z	Set Capillary	4500 V	Set Dry Gas	4.0 l/min
Scan End	1000 m/z	Set End Plate Offset	-500 V	Set Divert Valve	Source

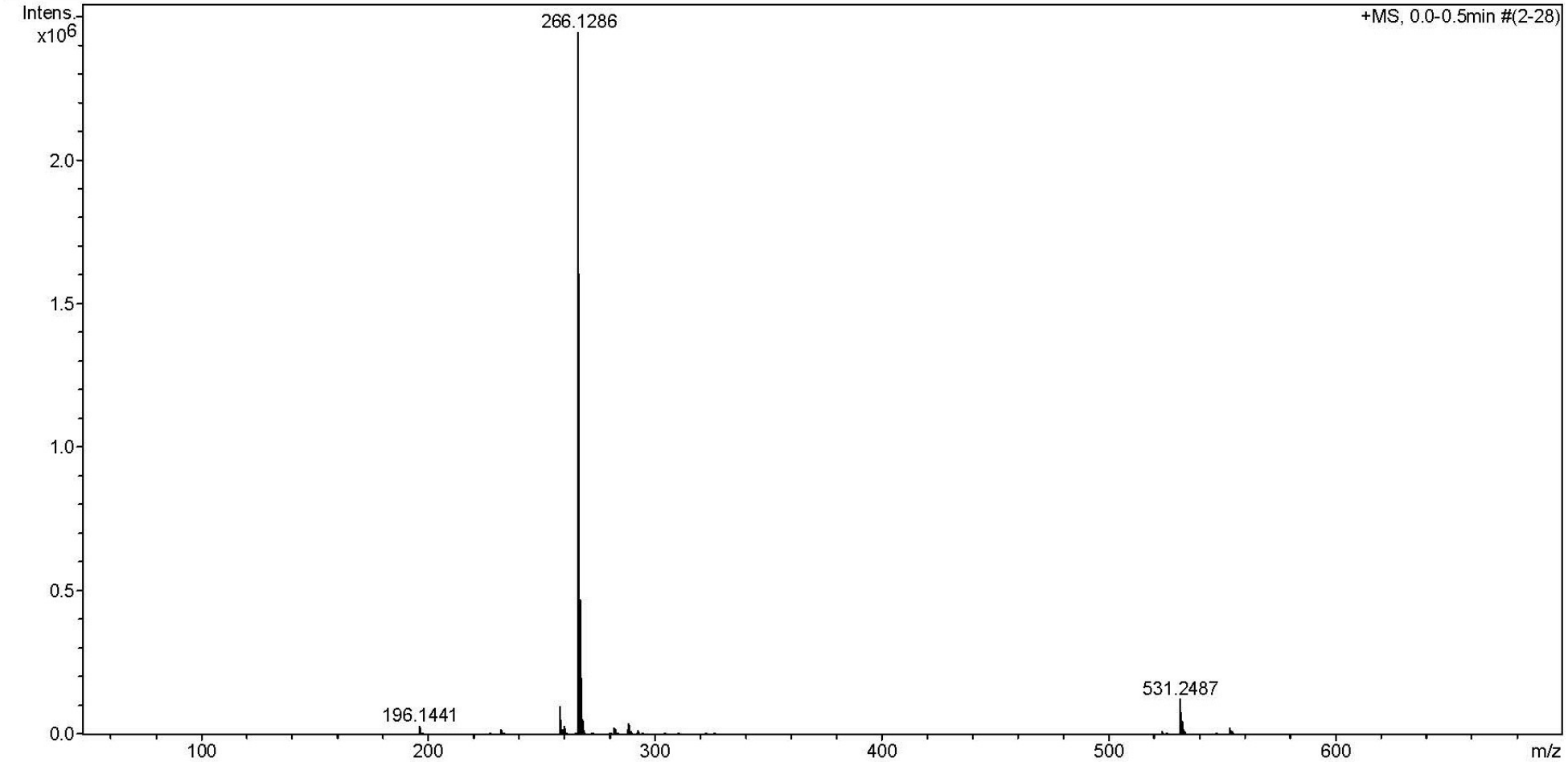

Figure 70S. HRESI^{+}-MS of **10**.

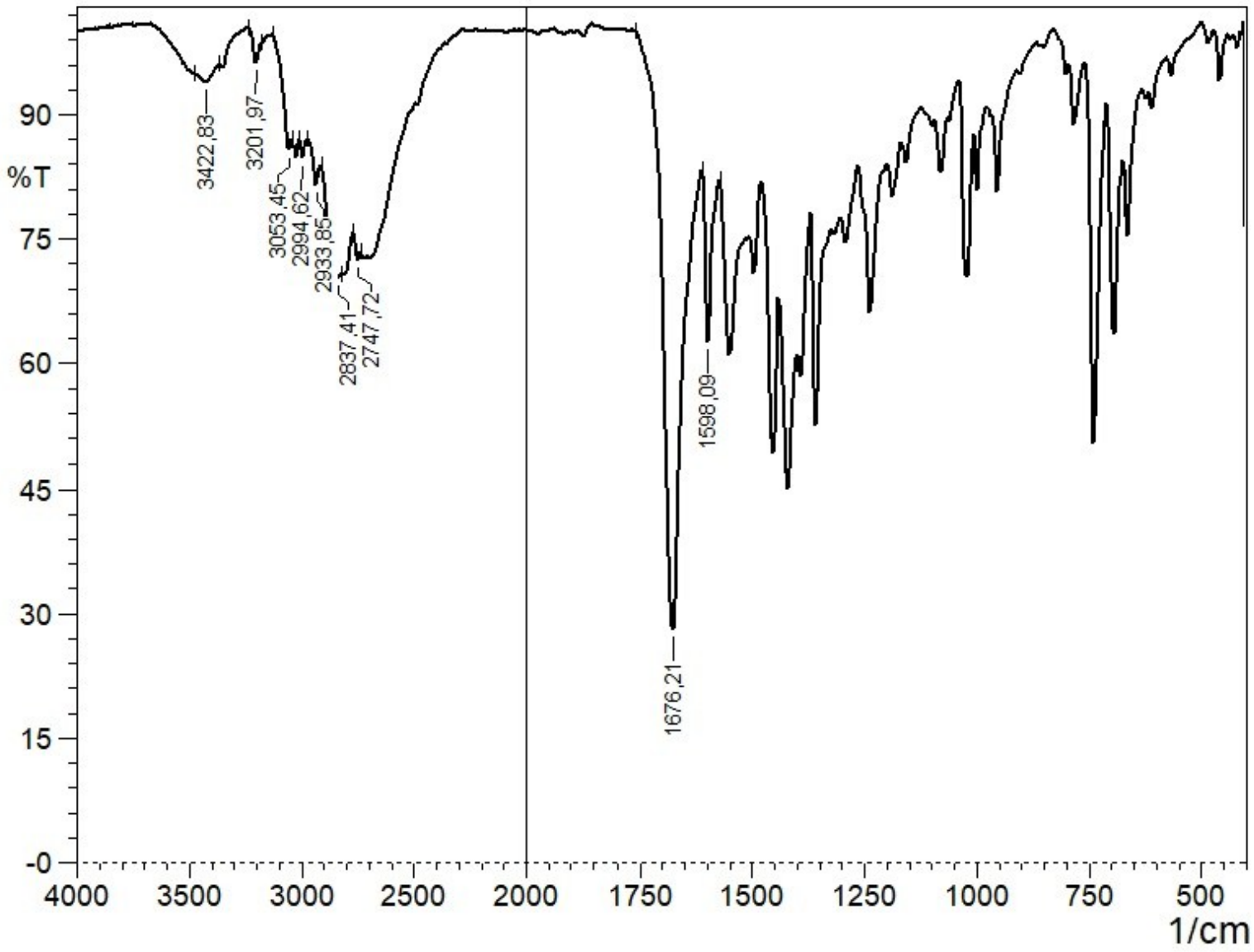

Figure 71S. IR spectrum of **10**.

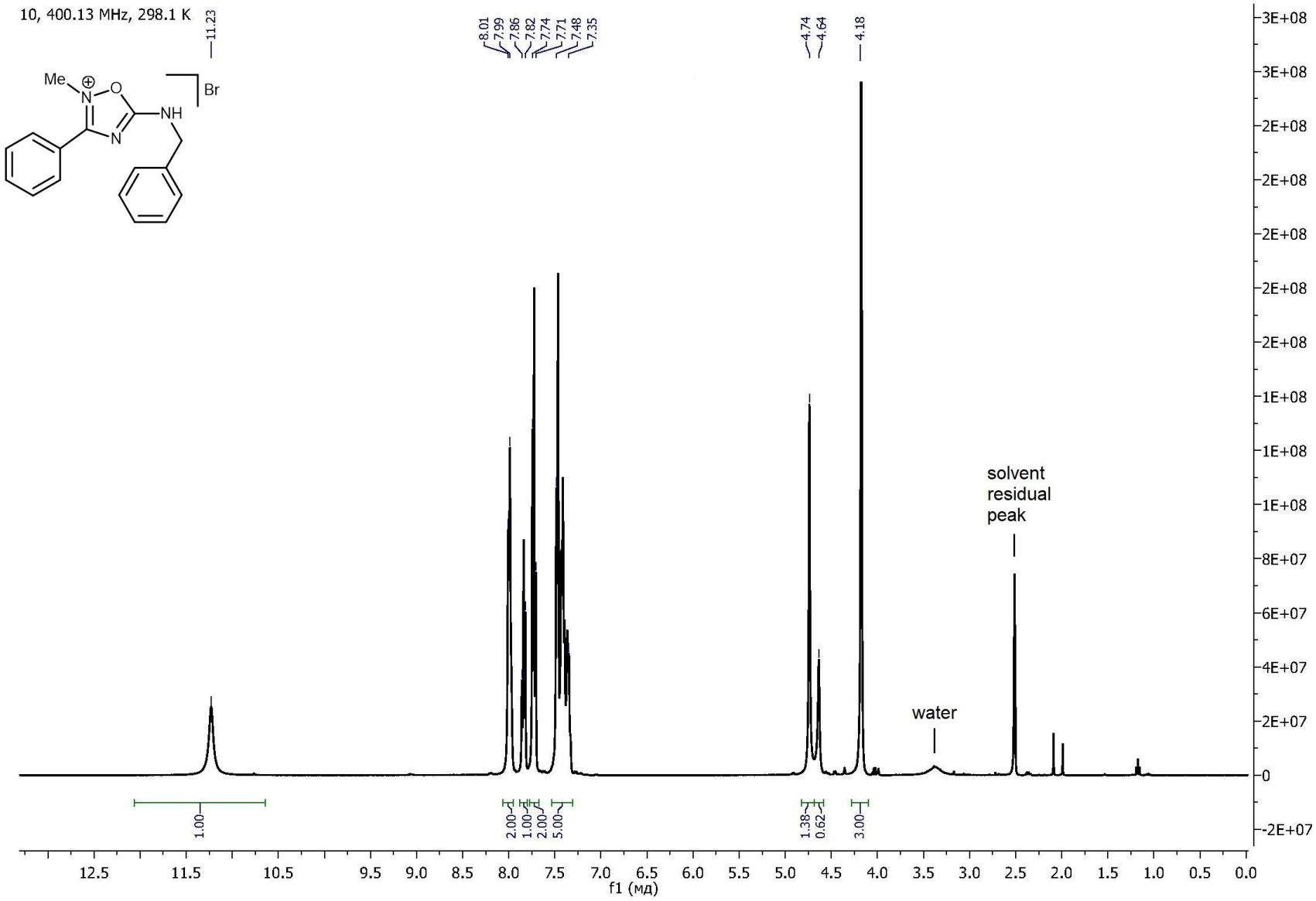

Figure 72S. ^{1}H NMR spectrum of **10**.

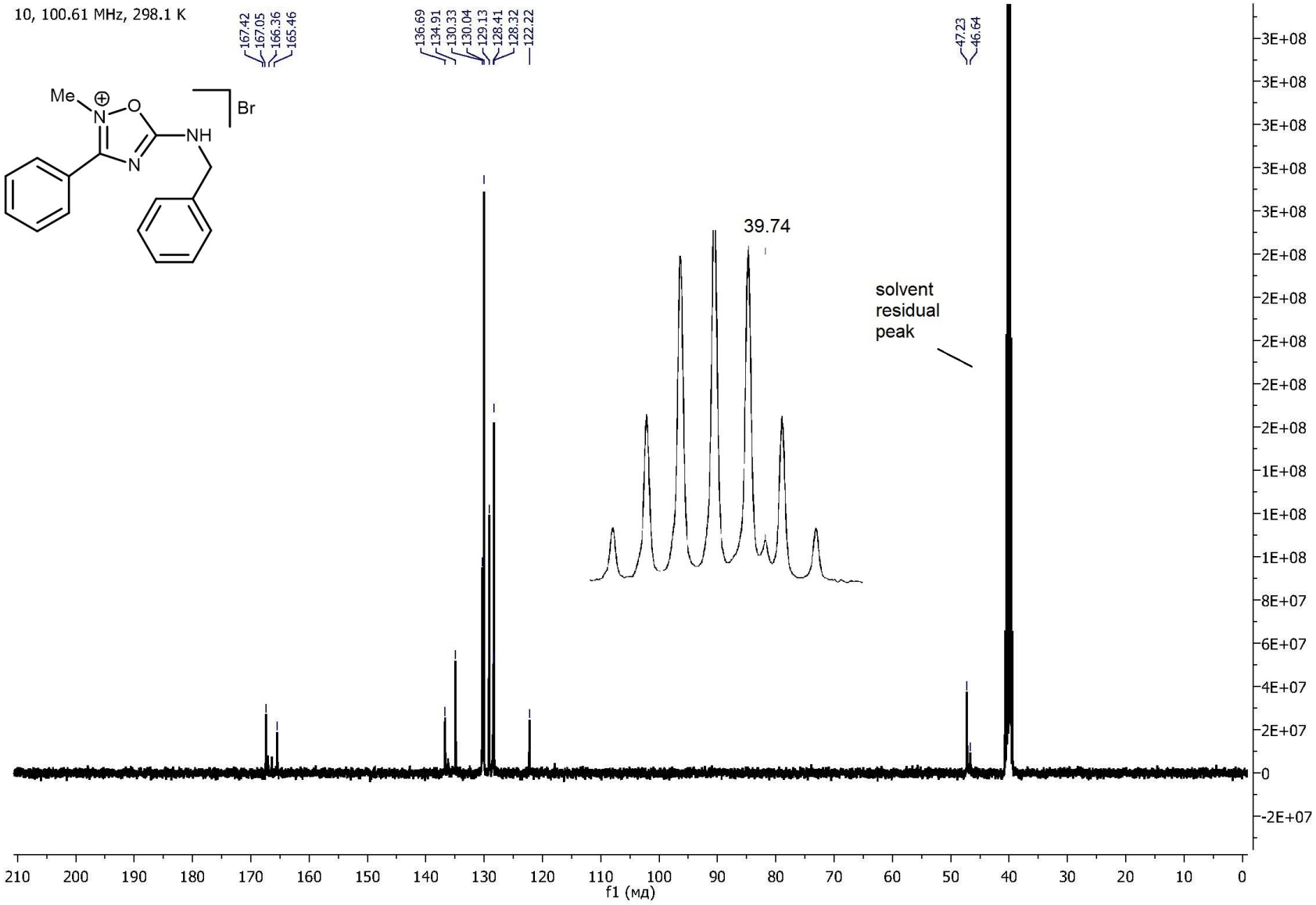

Figure 73S. $^{13}C\{^{1}H\}$ NMR spectrum of **10**.

Acquisition Parameter

Source Type	ESI	Ion Polarity	Positive	Set Nebulizer	0.4 Bar
Focus	Not active			Set Dry Heater	180 °C
Scan Begin	50 m/z	Set Capillary	4500 V	Set Dry Gas	4.0 l/min
Scan End	1000 m/z	Set End Plate Offset	-500 V	Set Divert Valve	Source

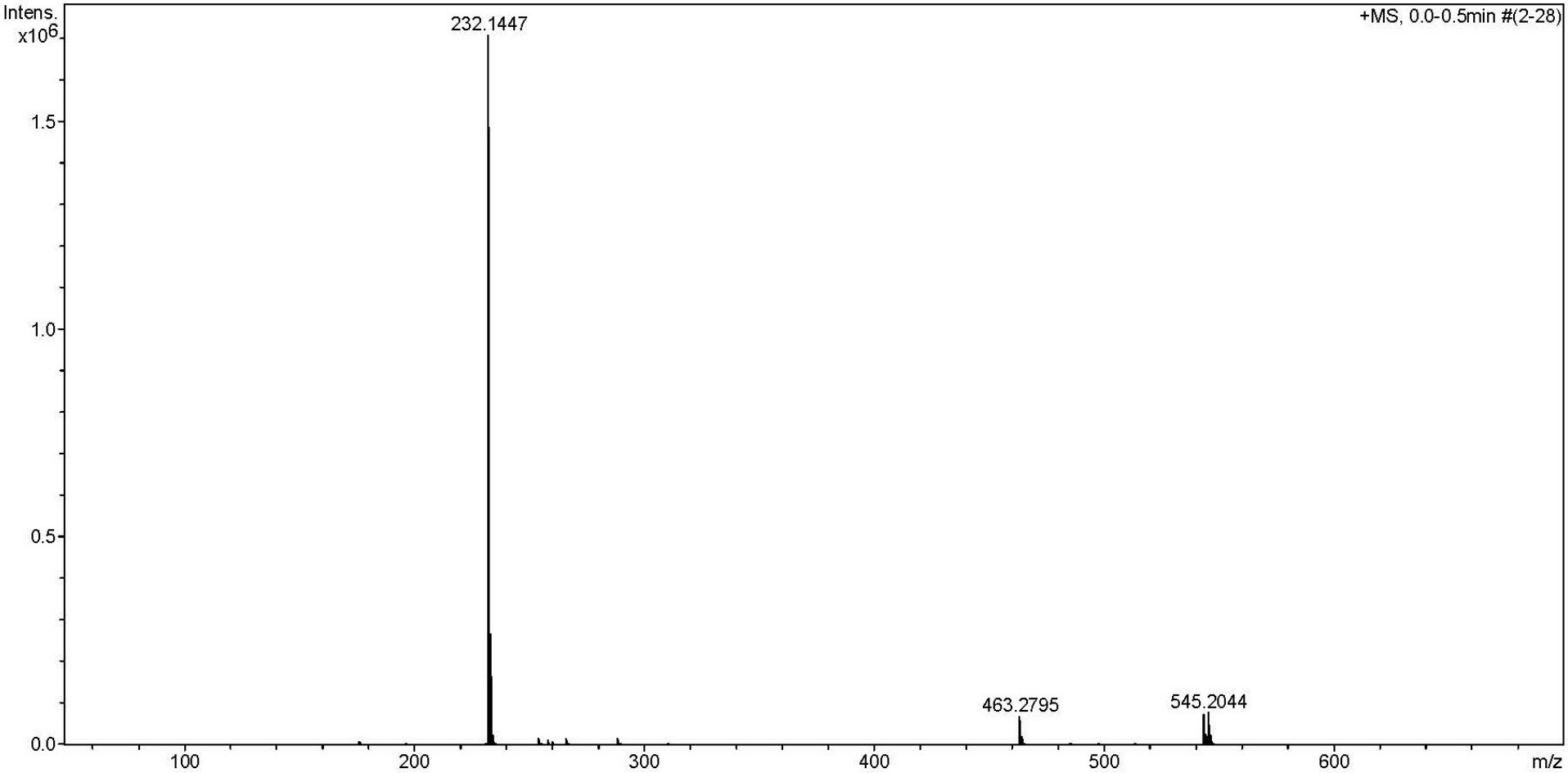

Figure 74S. HRESI^{+}-MS of **11**.

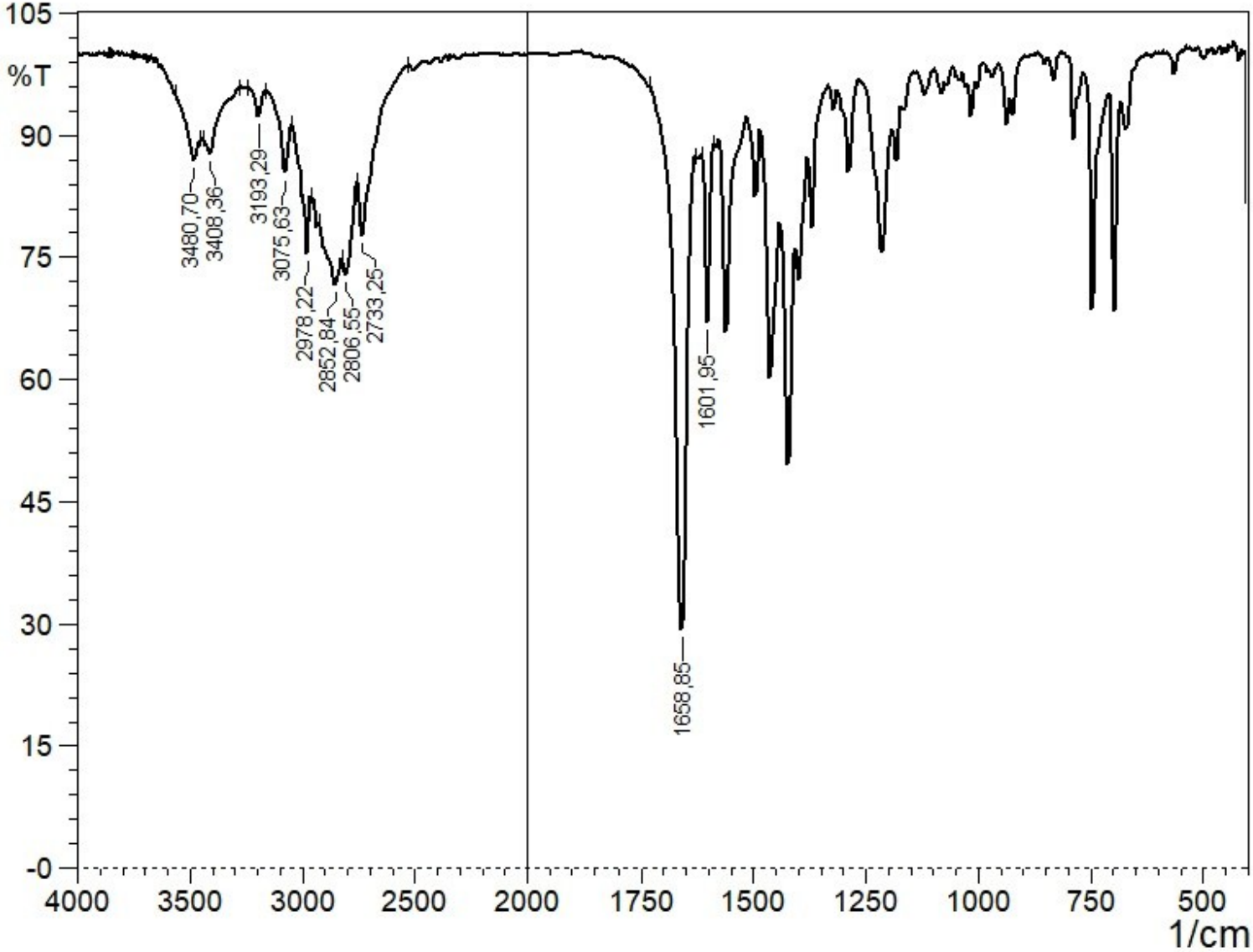

Figure 75S. IR spectrum of **11**.

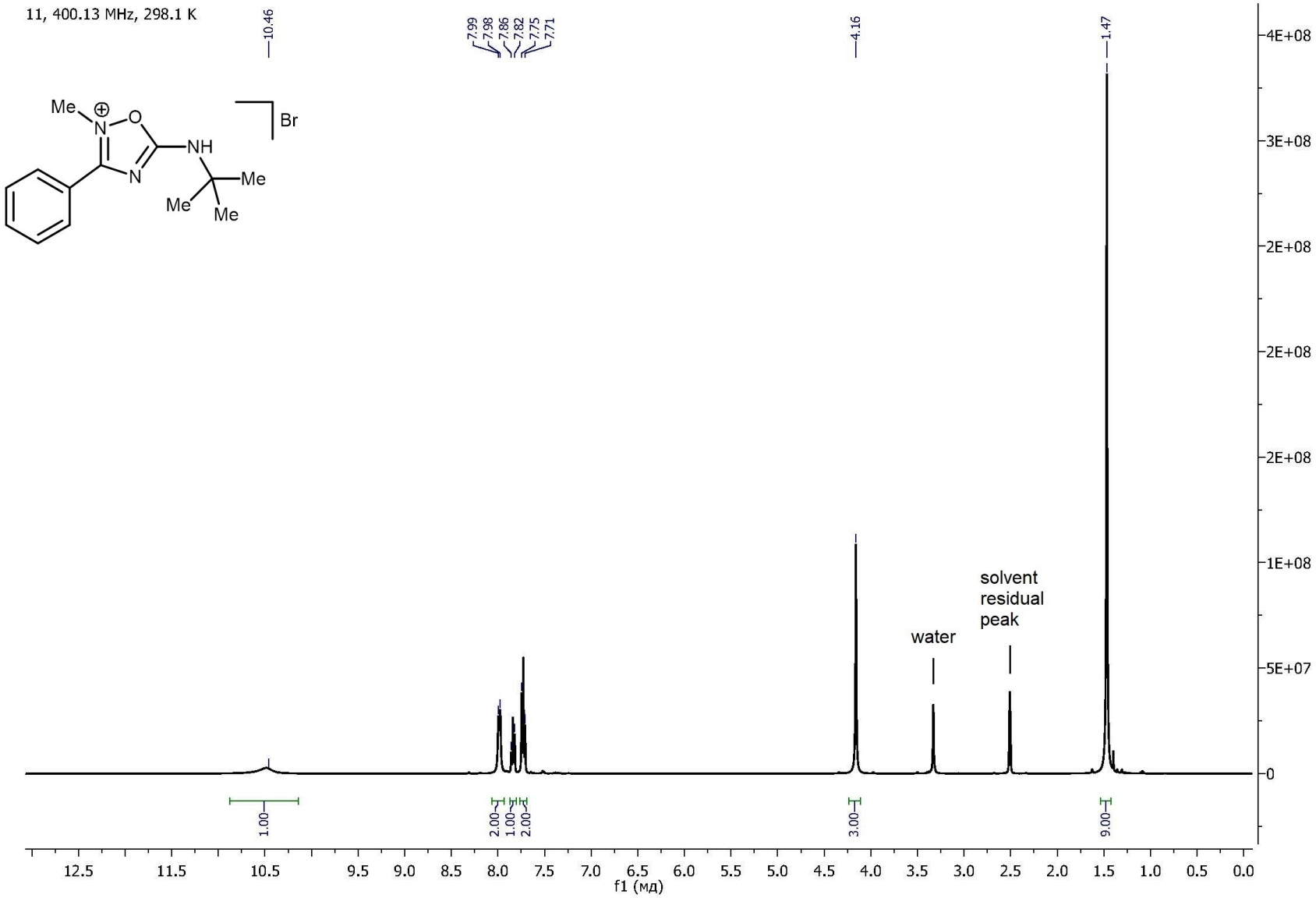

Figure 76S. ^{1}H NMR spectrum of **11**.

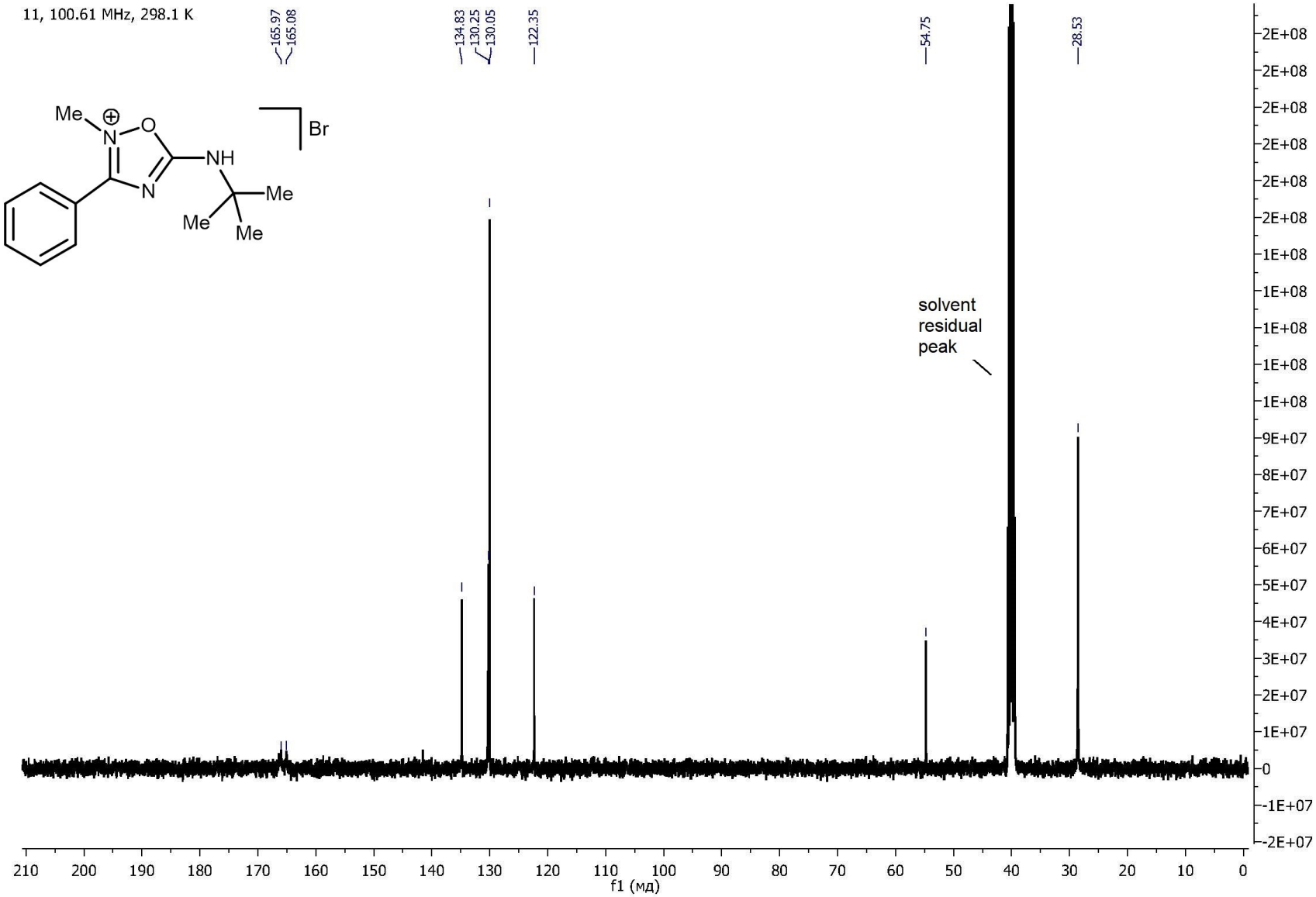

Figure 77S. $^{13}C\{^{1}H\}$ NMR spectrum of **11**.

Acquisition Parameter

Source Type	ESI	Ion Polarity	Positive	Set Nebulizer	0.4 Bar
Focus	Not active			Set Dry Heater	180 °C
Scan Begin	50 m/z	Set Capillary	4500 V	Set Dry Gas	4.0 l/min
Scan End	1200 m/z	Set End Plate Offset	-500 V	Set Divert Valve	Source

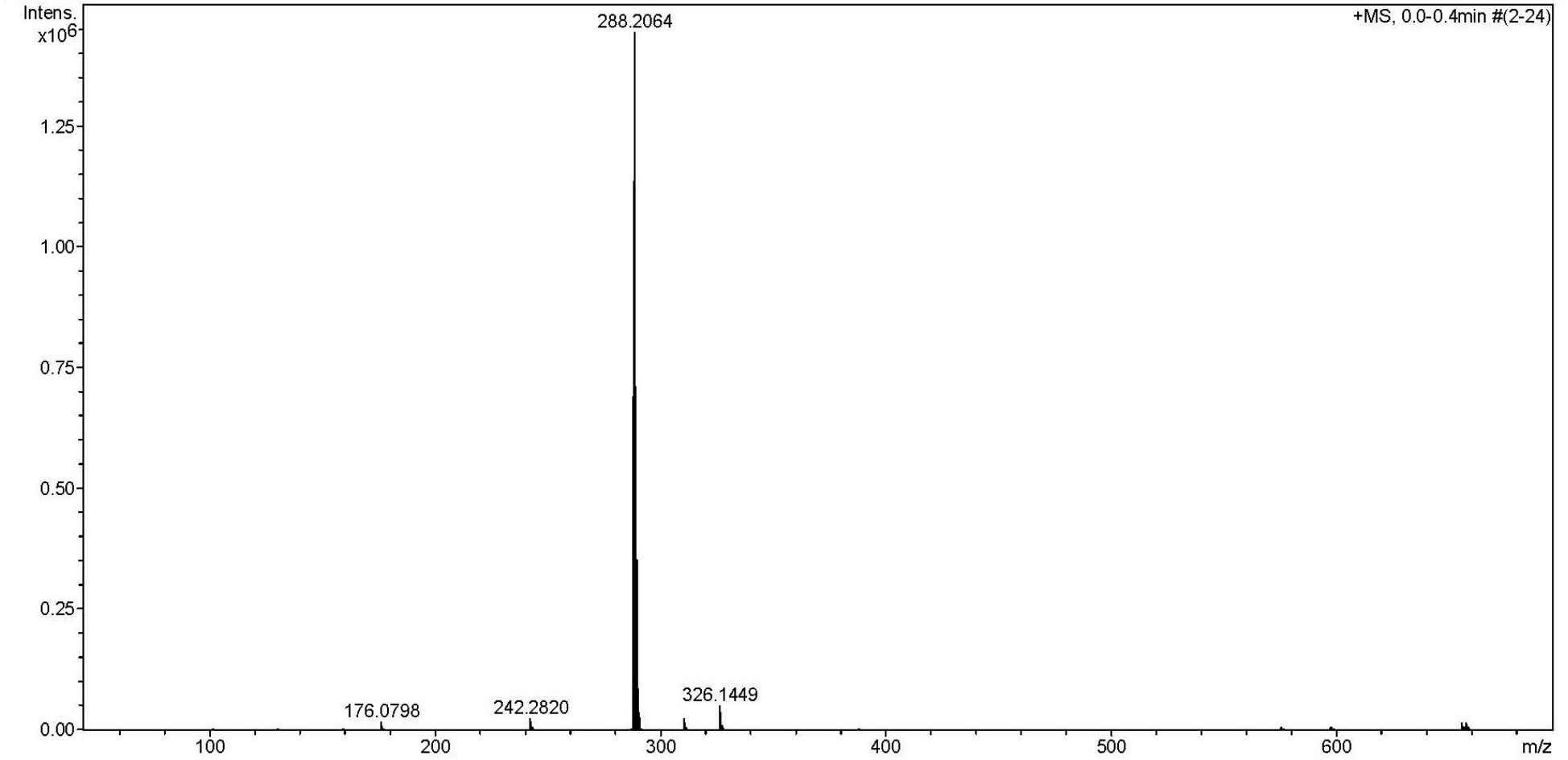

Figure 78S. HRESI^{+}-MS of **12**.

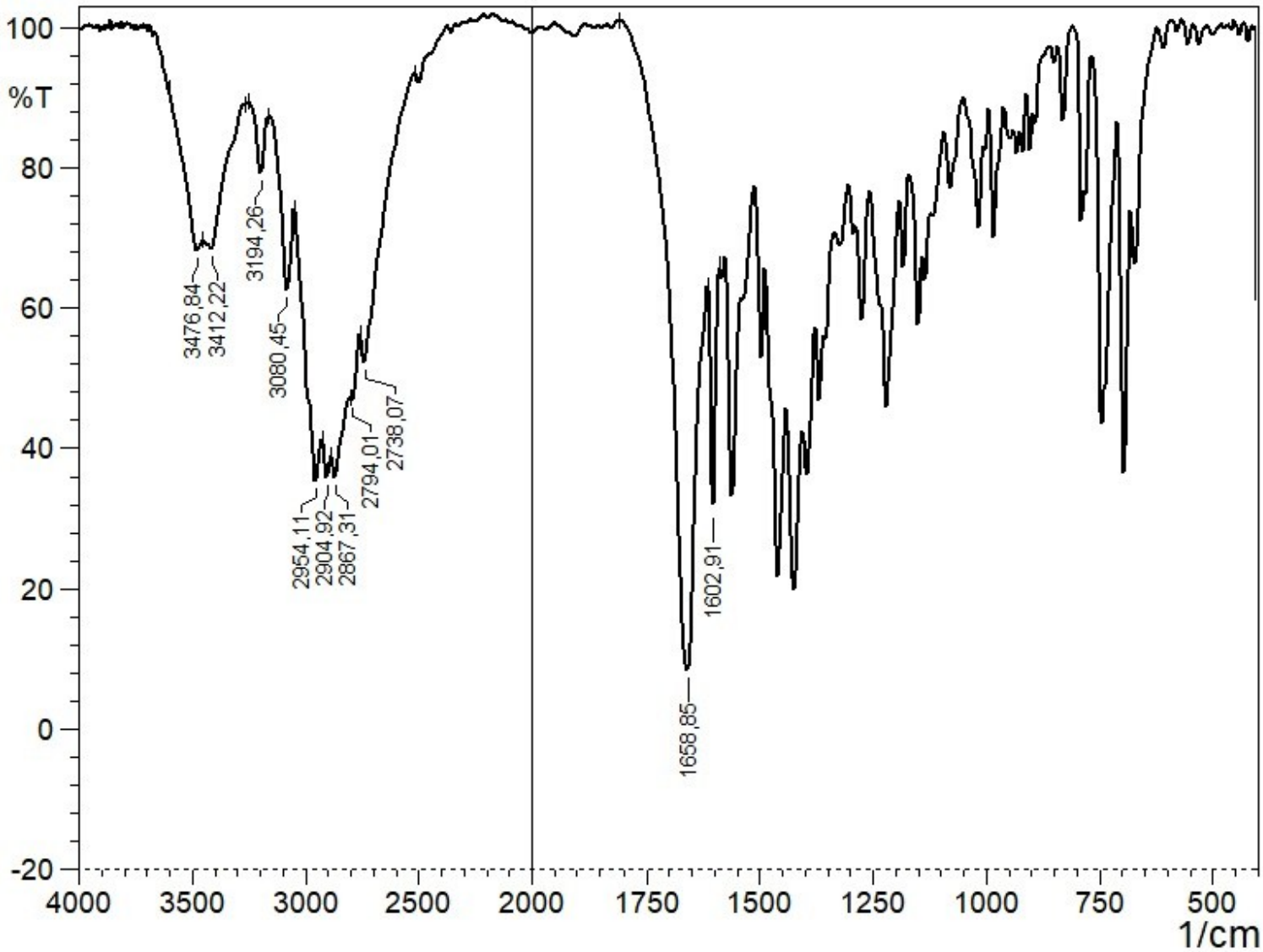

Figure 79S. IR spectrum of **12**.

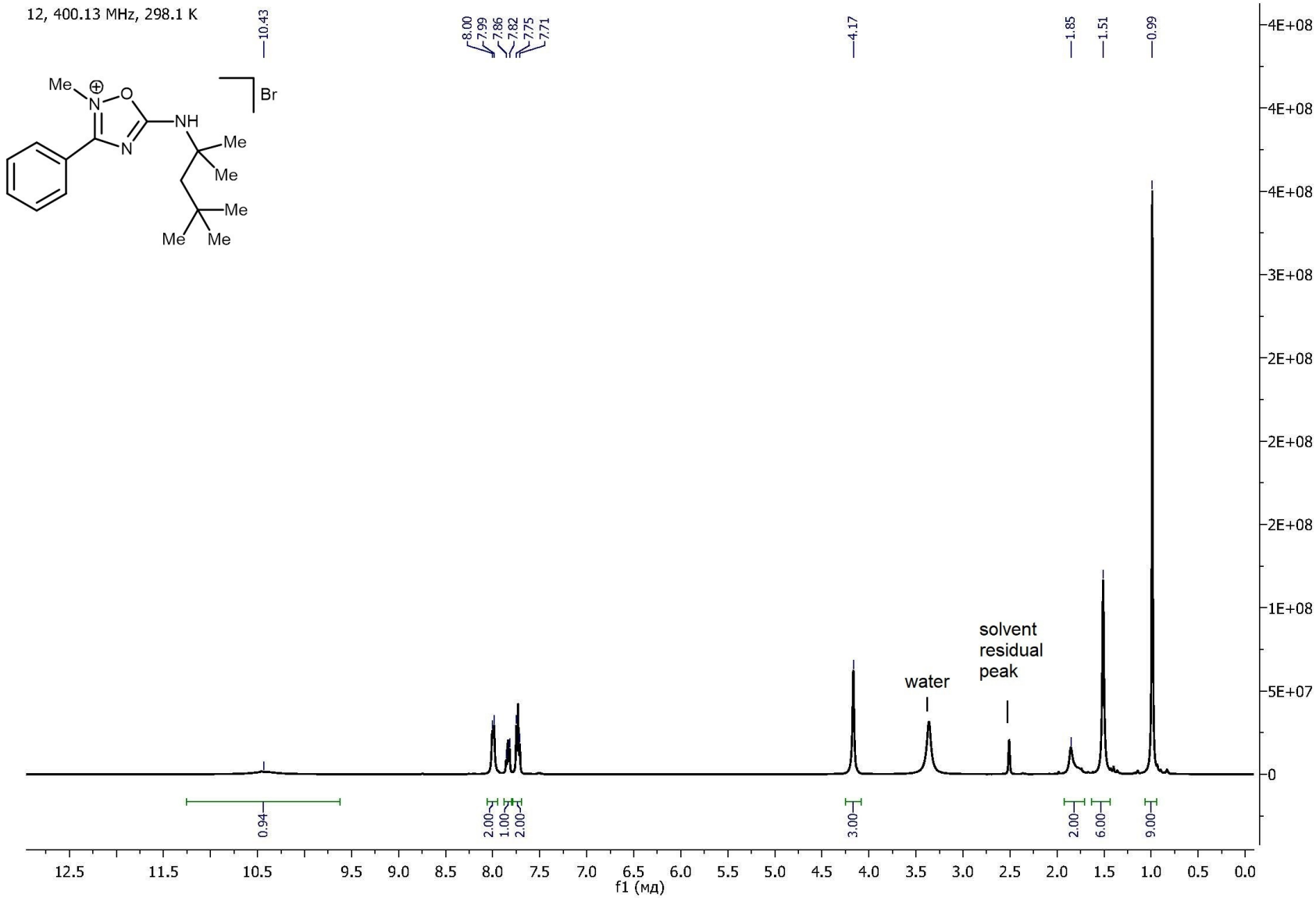

Figure 80S. ^{1}H NMR spectrum of **12**.

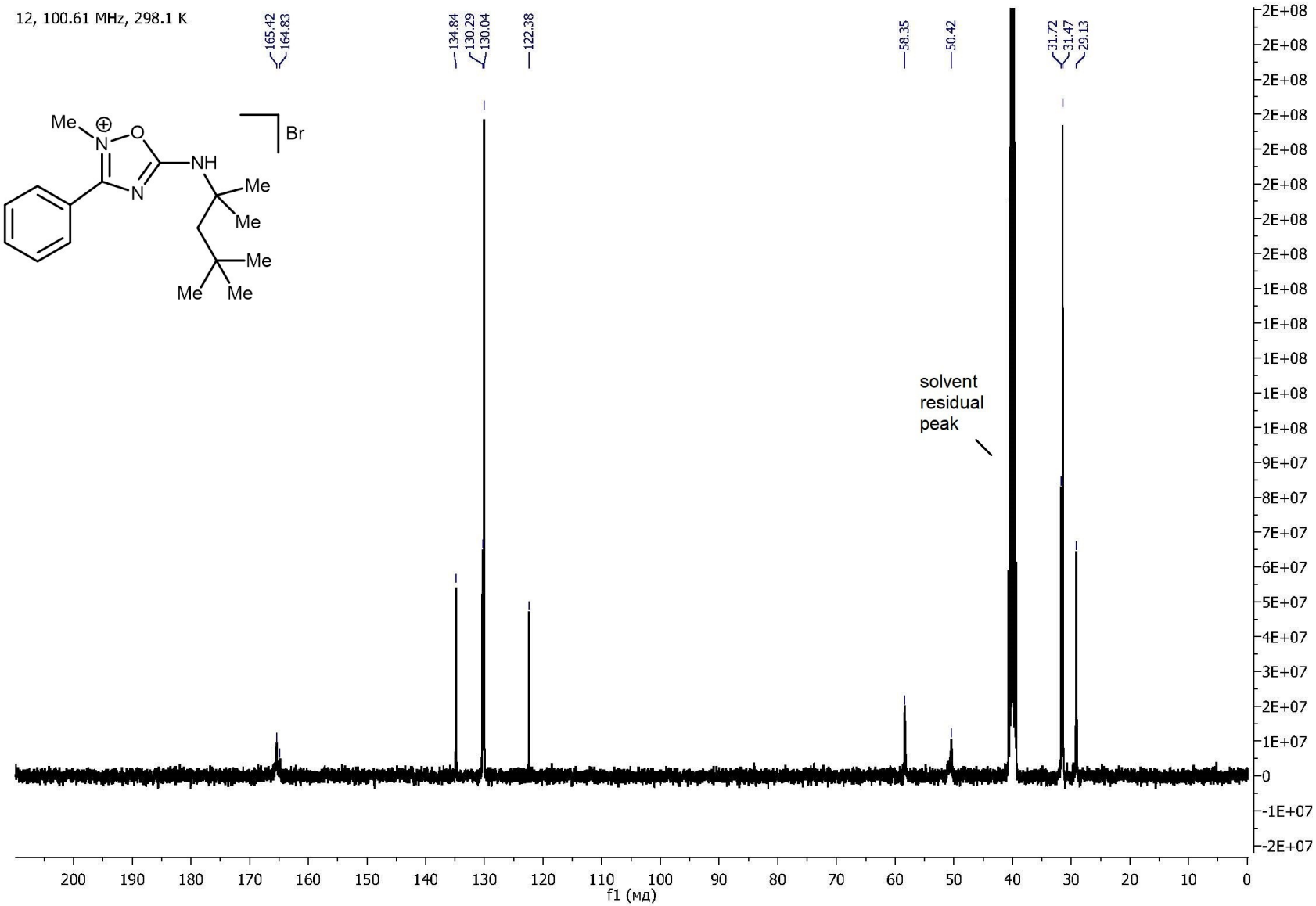

Figure 81S. $^{13}C\{^{1}H\}$ NMR spectrum of **12**.

Acquisition Parameter

Source Type	ESI	Ion Polarity	Positive	Set Nebulizer	0.4 Bar
Focus	Not active			Set Dry Heater	180 °C
Scan Begin	50 m/z	Set Capillary	4500 V	Set Dry Gas	4.0 l/min
Scan End	1200 m/z	Set End Plate Offset	-500 V	Set Divert Valve	Source

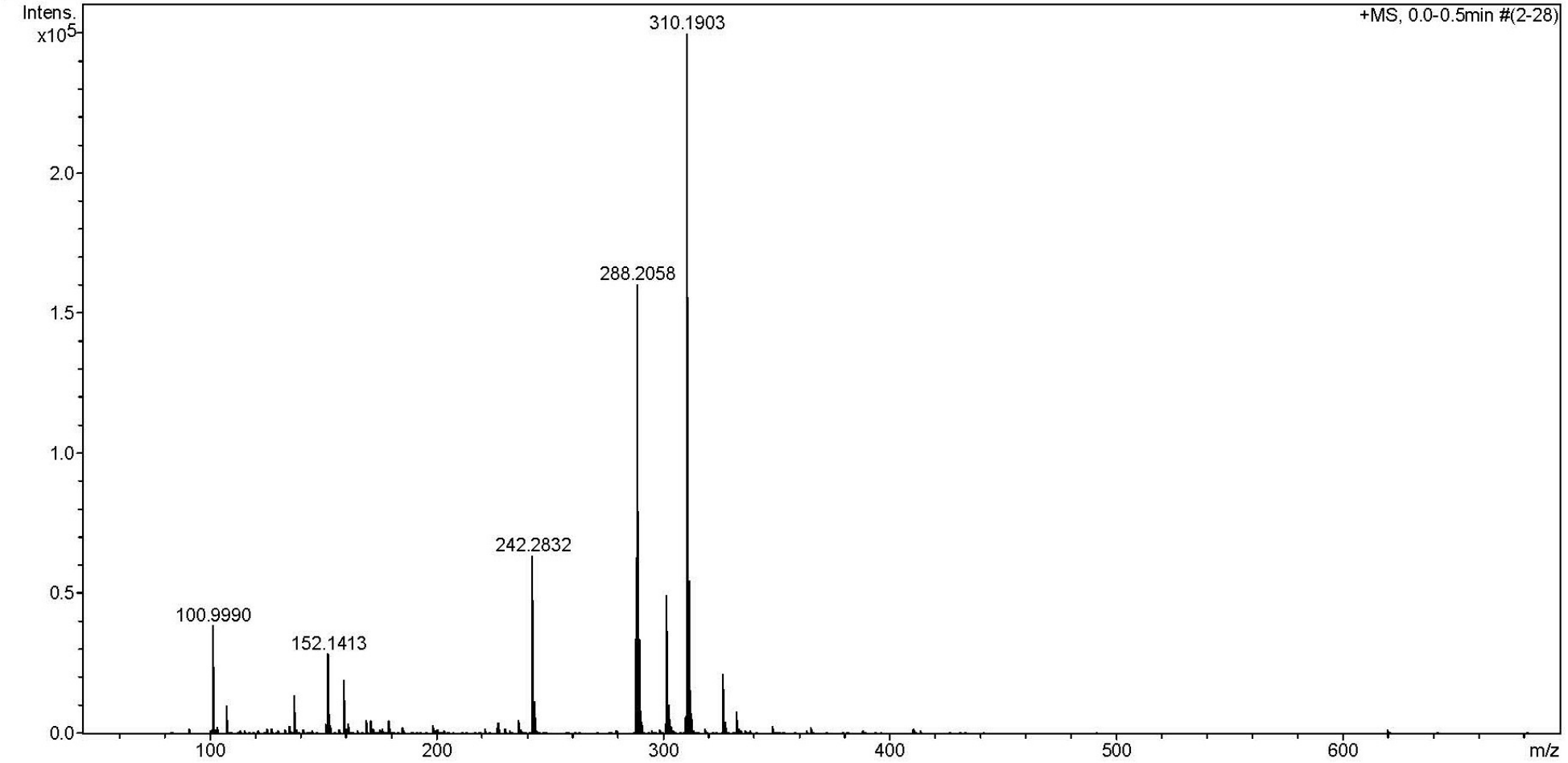

Figure 82S. HRESI^{+}-MS of **13**.

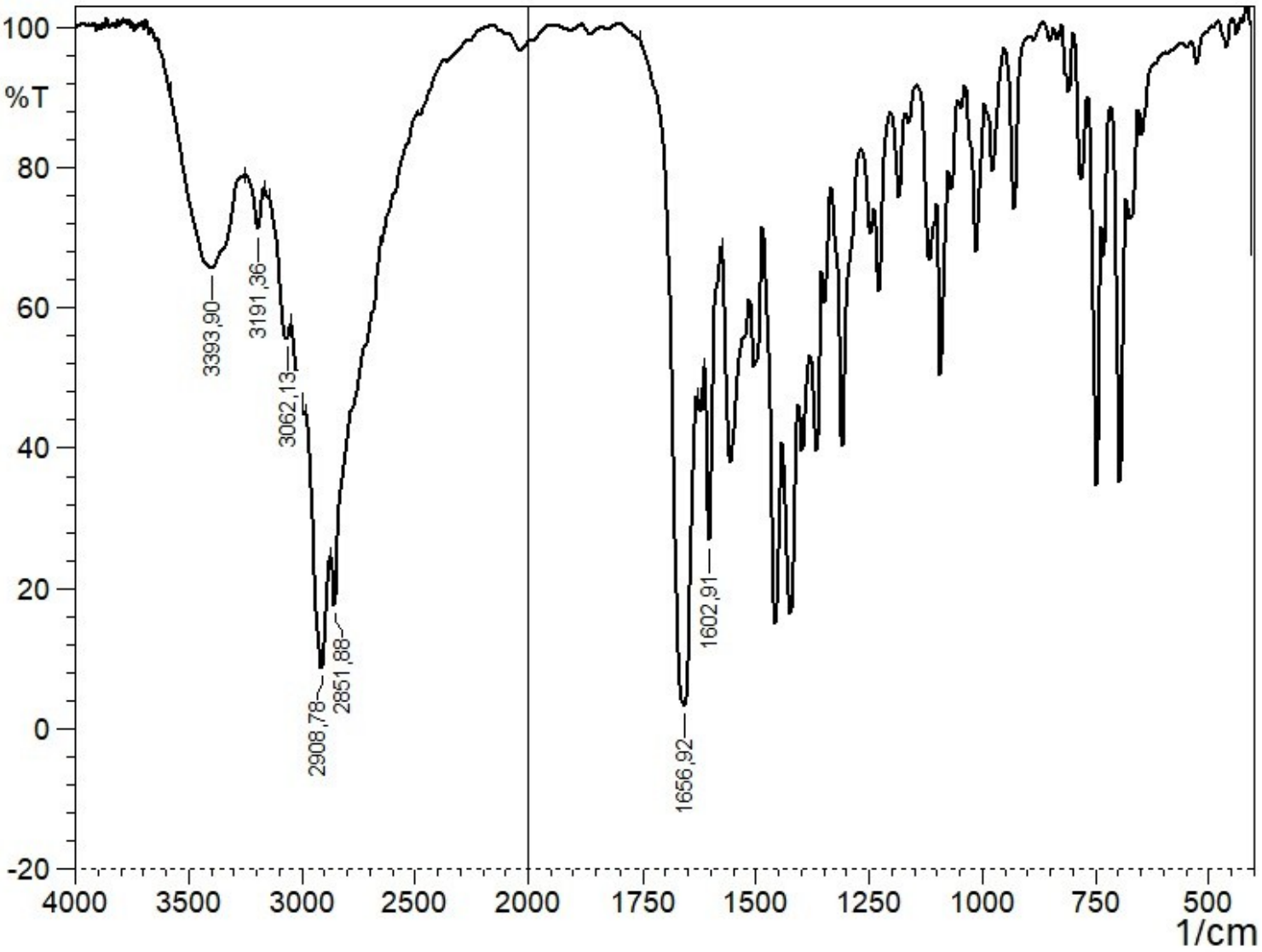

Figure 83S. IR spectrum of **13**.

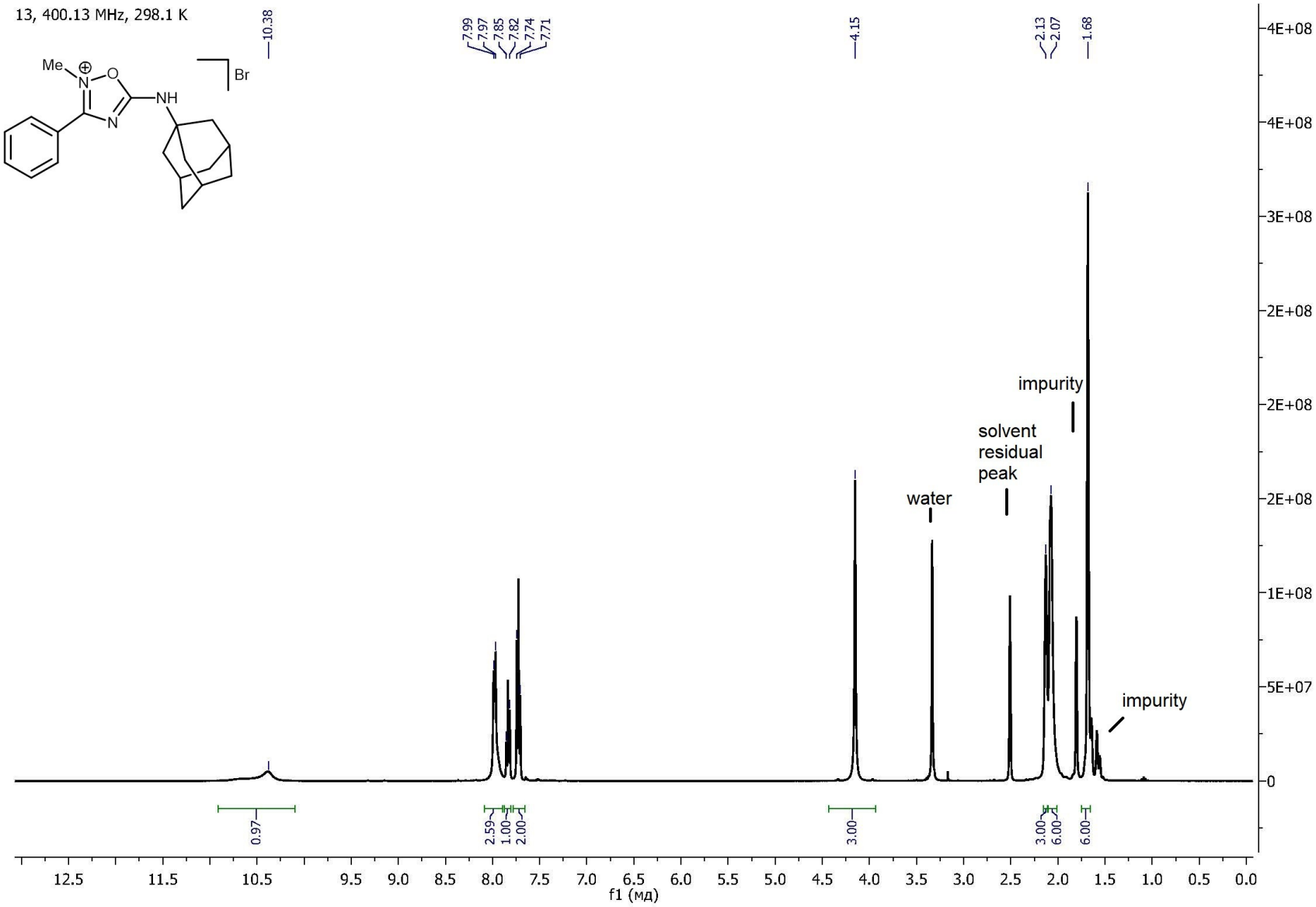

Figure 84S. ^{1}H NMR spectrum of **13**.

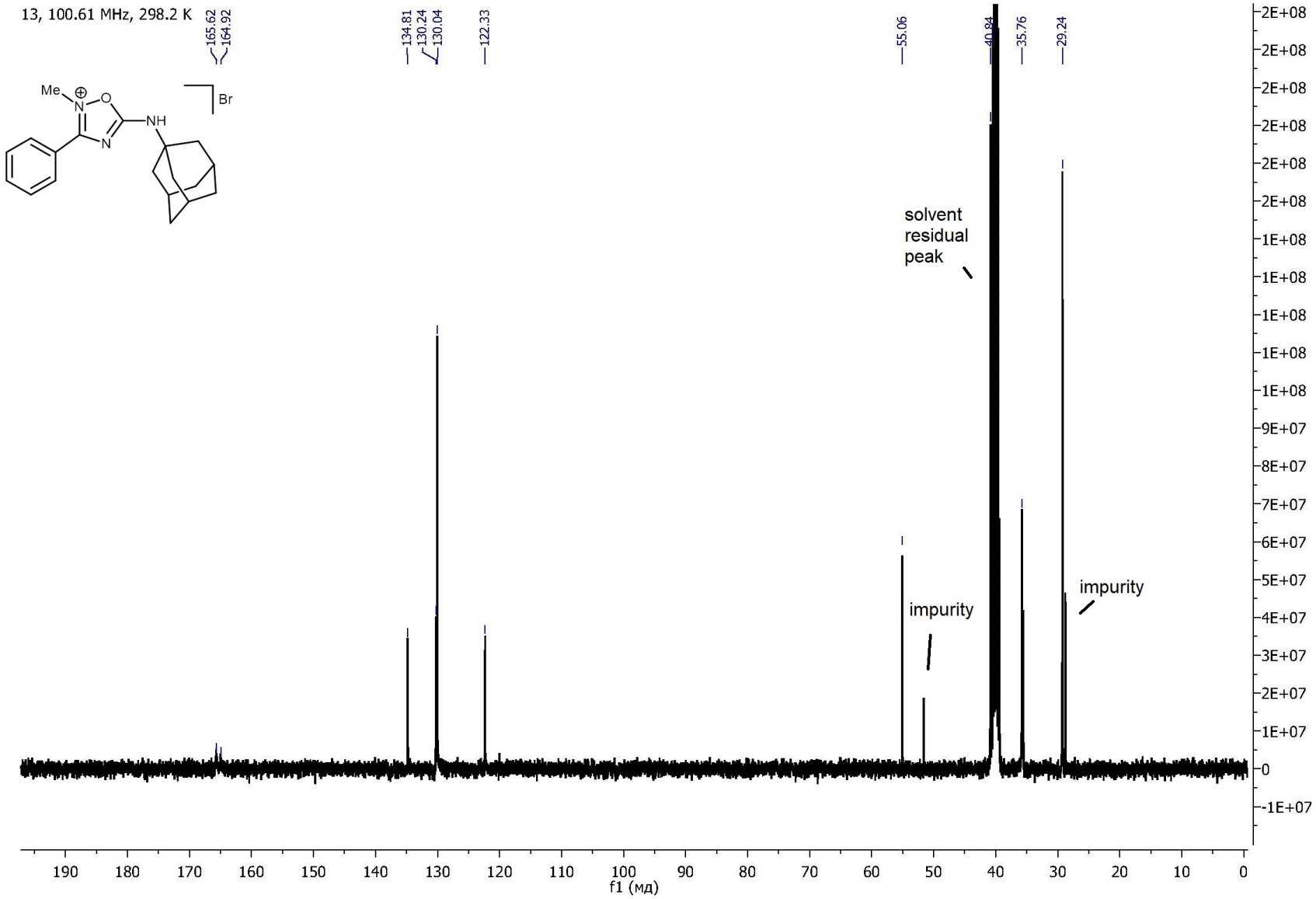

Figure 85S. $^{13}C\{^{1}H\}$ NMR spectrum of **13**.

Acquisition Parameter

Source Type	ESI	Ion Polarity	Positive	Set Nebulizer	0.4 Bar
Focus	Not active			Set Dry Heater	180 °C
Scan Begin	50 m/z	Set Capillary	4500 V	Set Dry Gas	4.0 l/min
Scan End	3000 m/z	Set End Plate Offset	-500 V	Set Divert Valve	Source

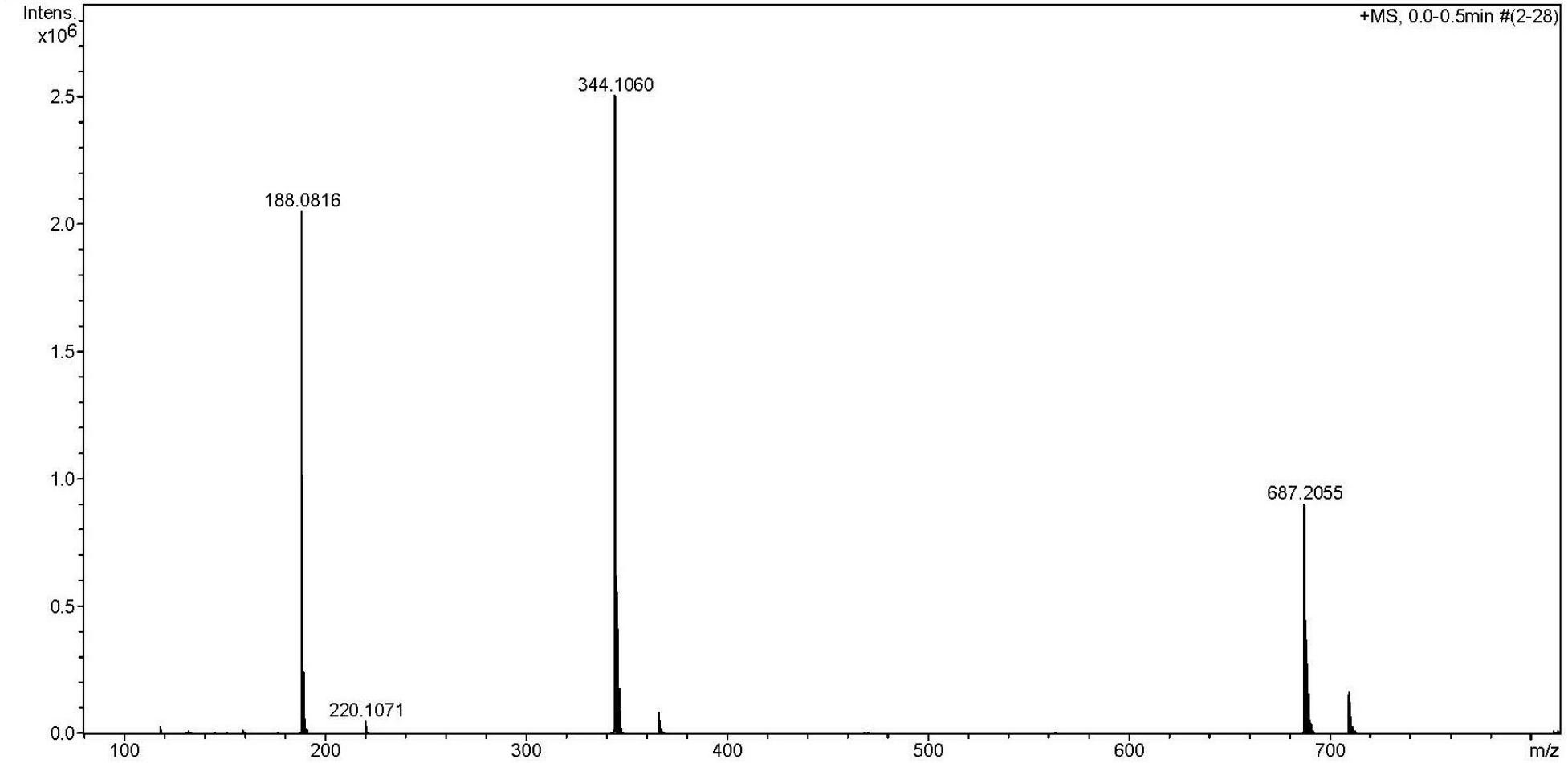

Figure 86S. HRESI^{+}-MS of **14**.

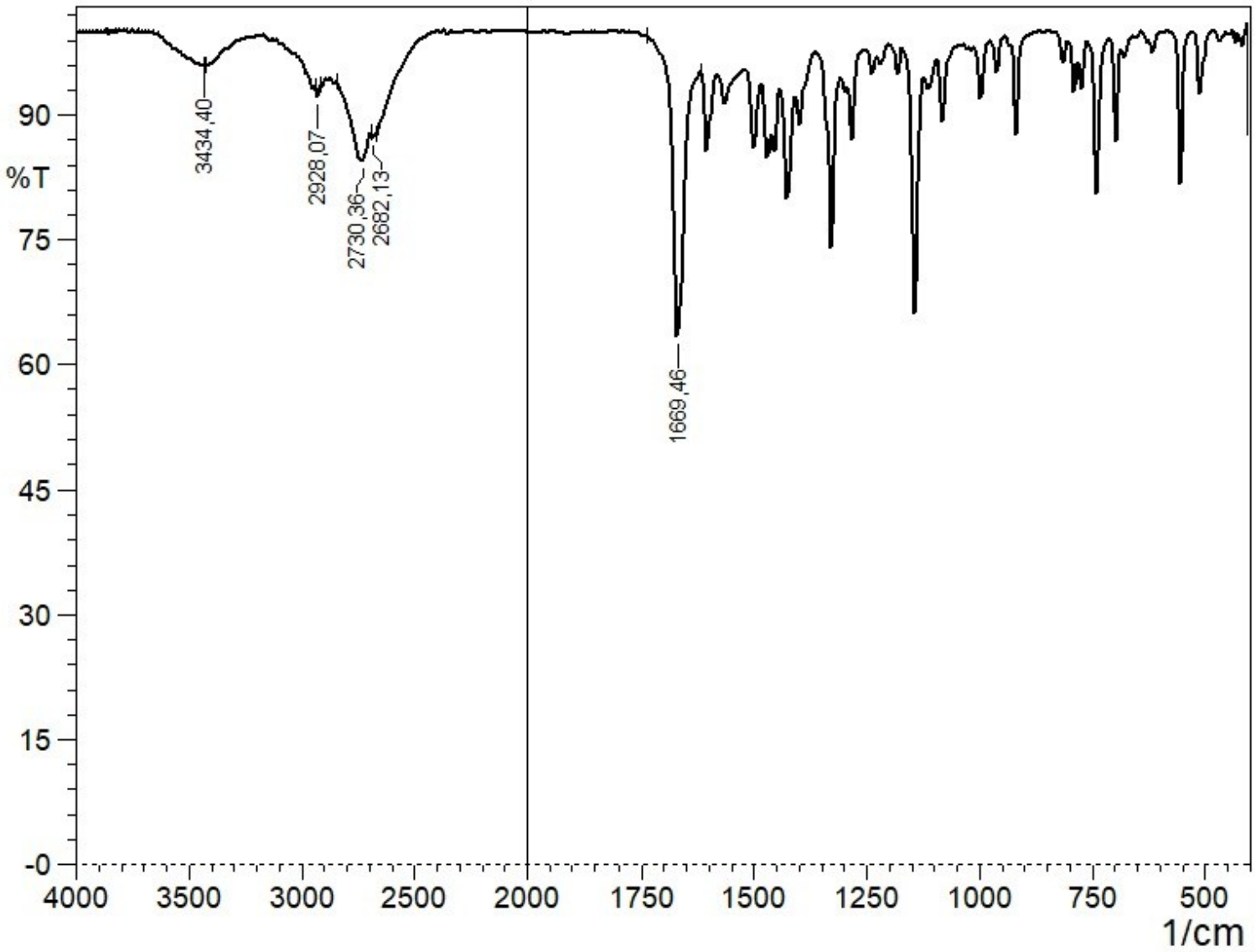

Figure 87S. IR spectrum of **14**.

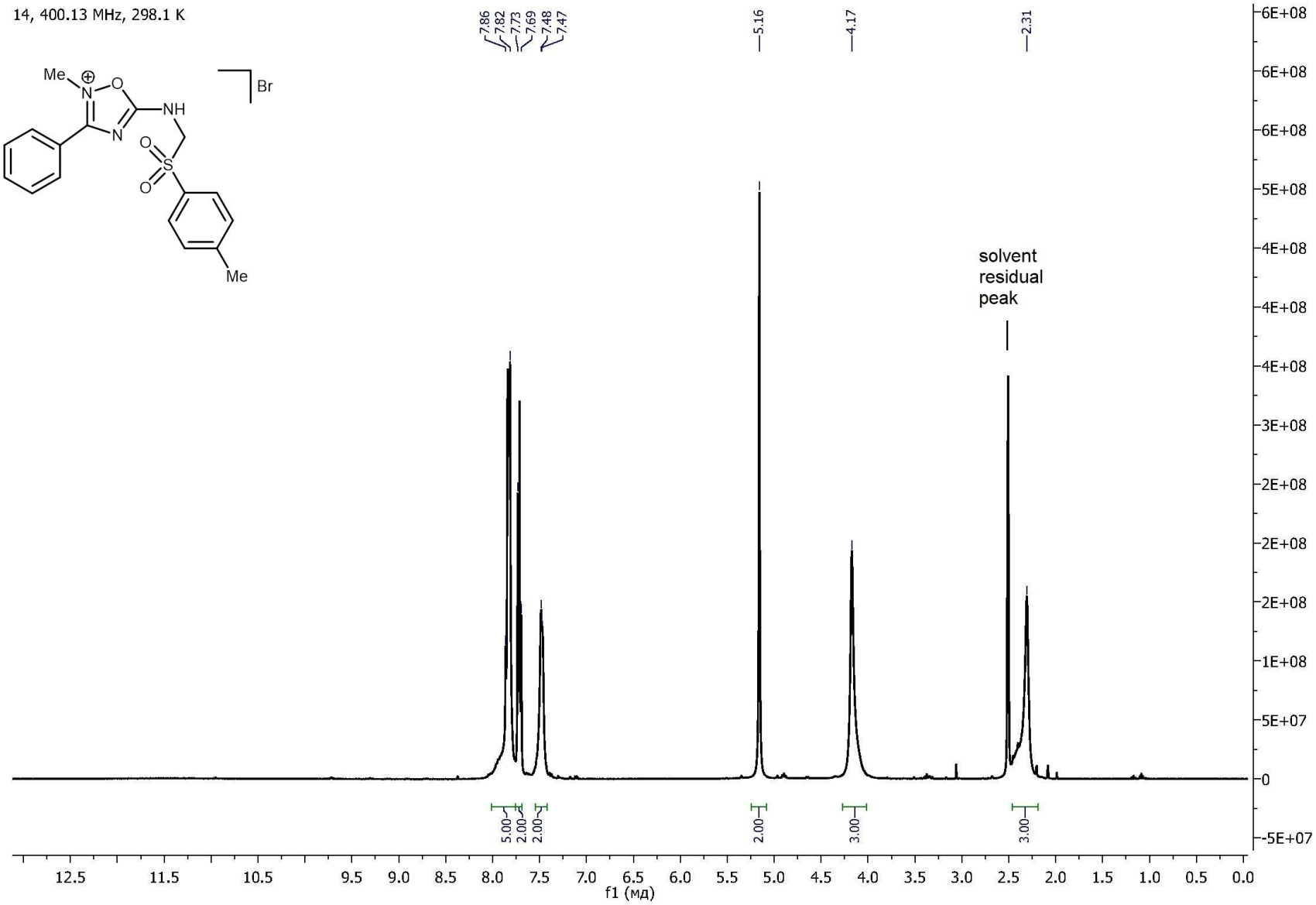

Figure 88S. ^{1}H NMR spectrum of **14**.

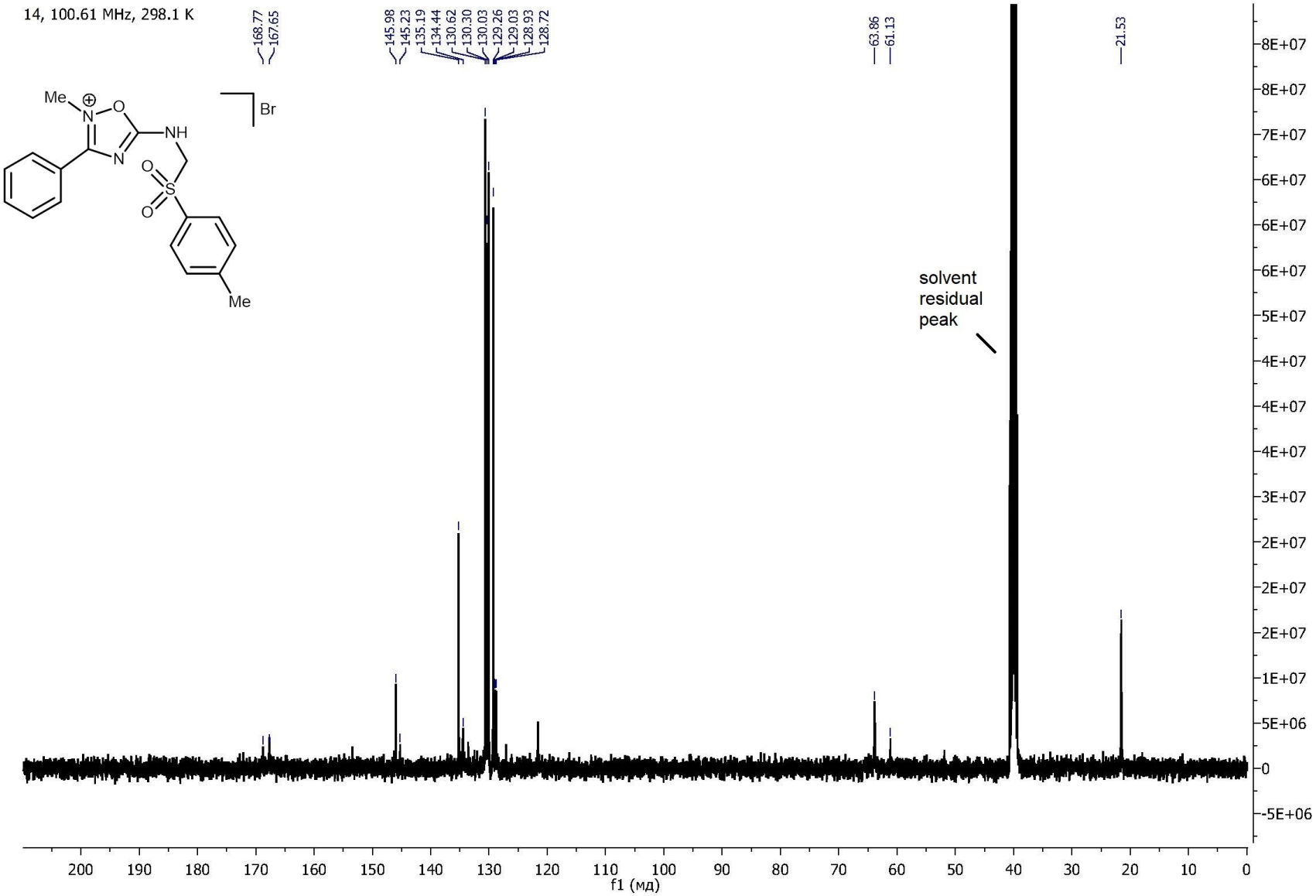

Figure 89S. $^{13}C\{^{1}H\}$ NMR spectrum of **14**.

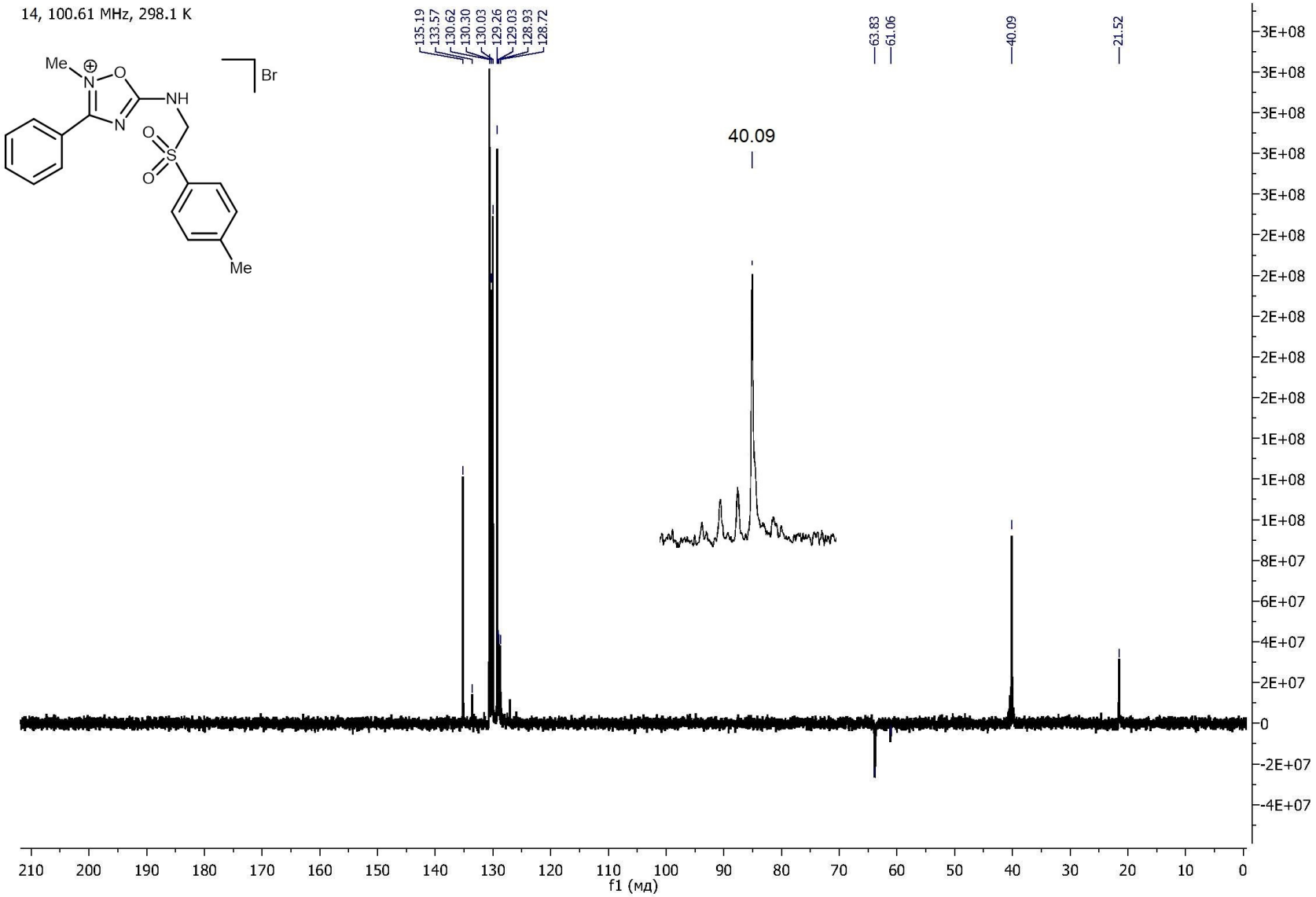

Figure 90S. $^{13}C\{^{1}H\}$ DEPT 135° NMR spectrum of **14**.

Acquisition Parameter

Source Type	ESI	Ion Polarity	Positive	Set Nebulizer	0.4 Bar
Focus	Not active			Set Dry Heater	180 °C
Scan Begin	50 m/z	Set Capillary	4500 V	Set Dry Gas	4.0 l/min
Scan End	1000 m/z	Set End Plate Offset	-500 V	Set Divert Valve	Source

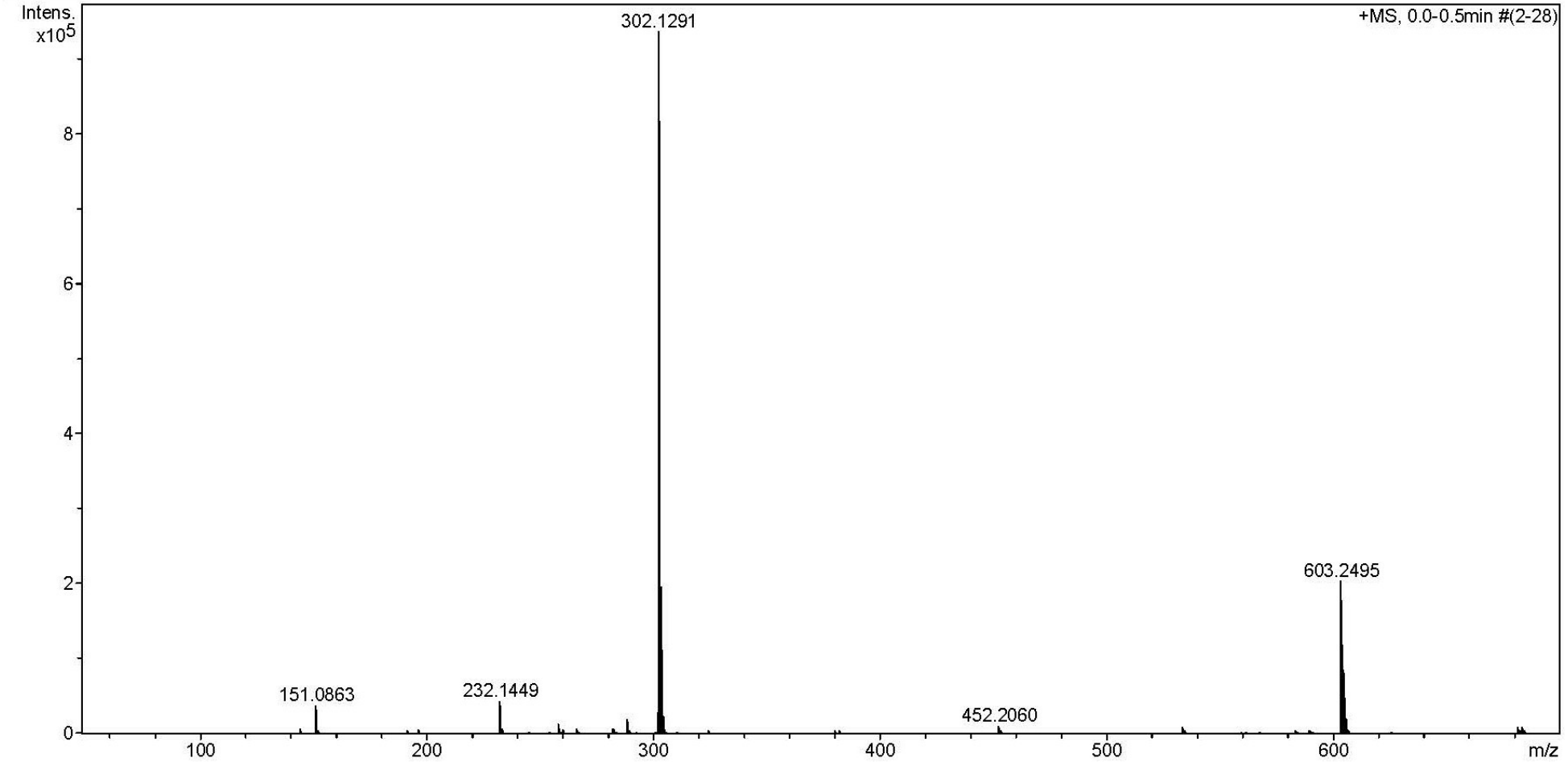

Figure 91S. HRESI^{+}-MS of **15**.

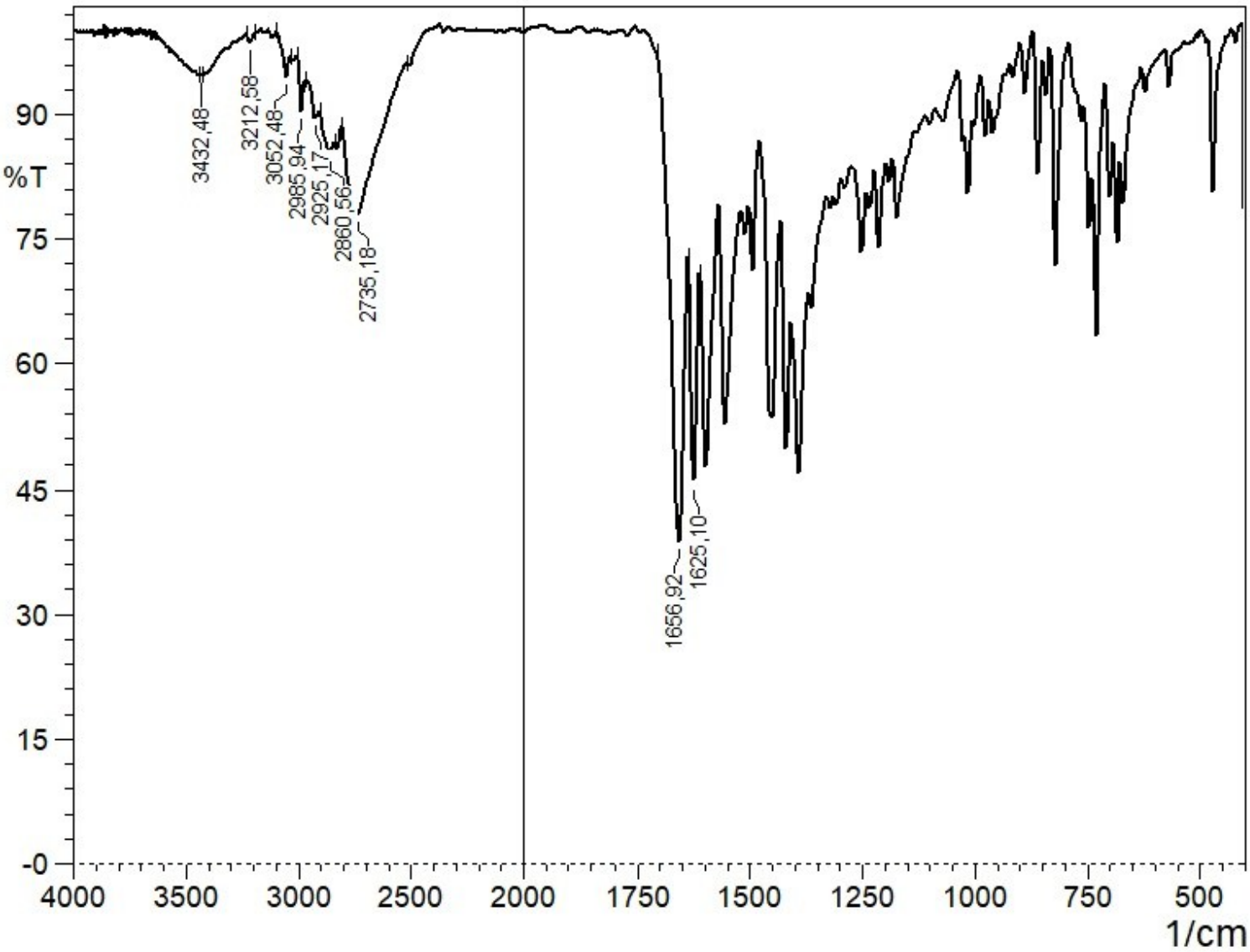

Figure 92S. IR spectrum of **15**.

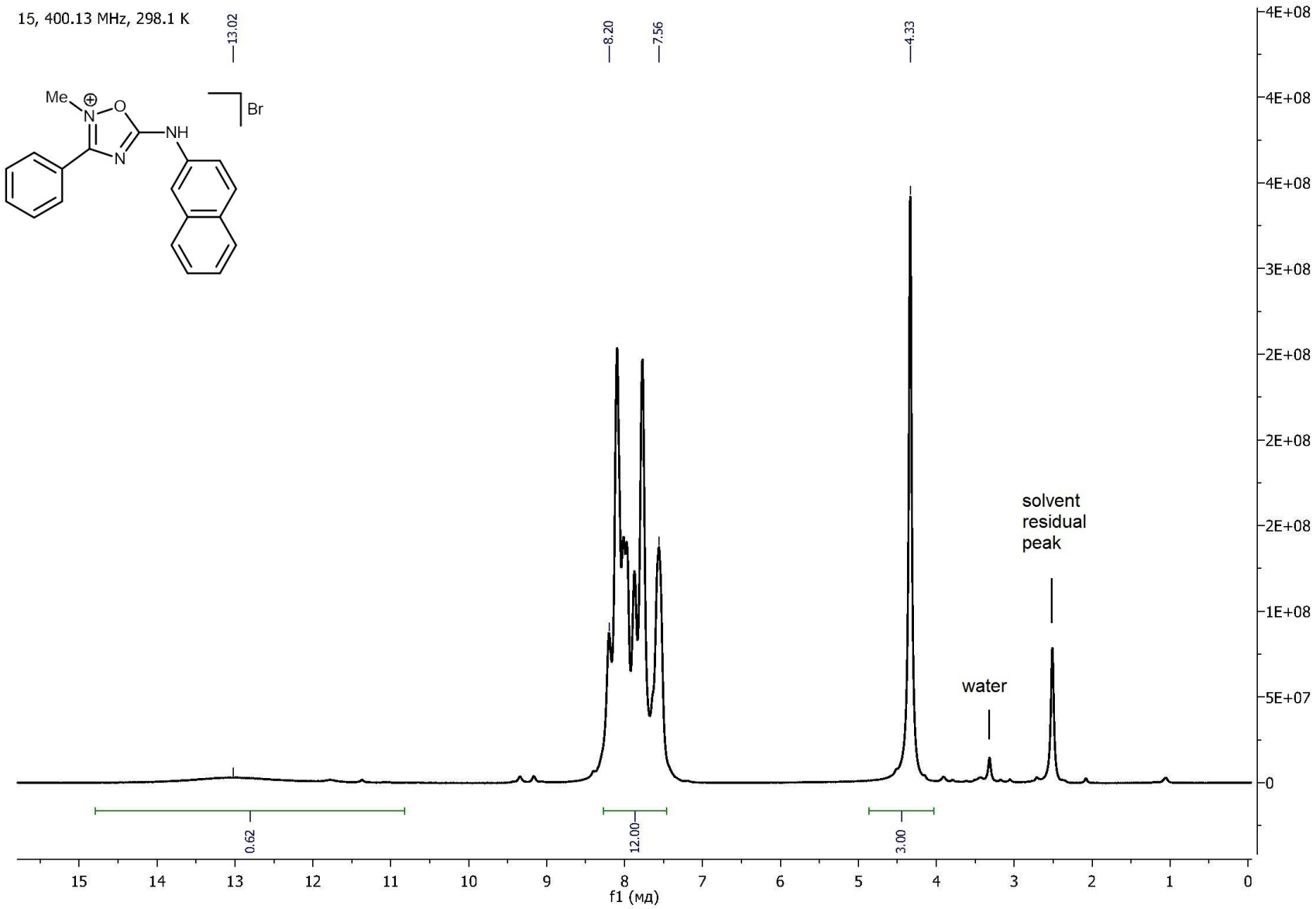

Figure 93S. ^{1}H NMR spectrum of **15**.

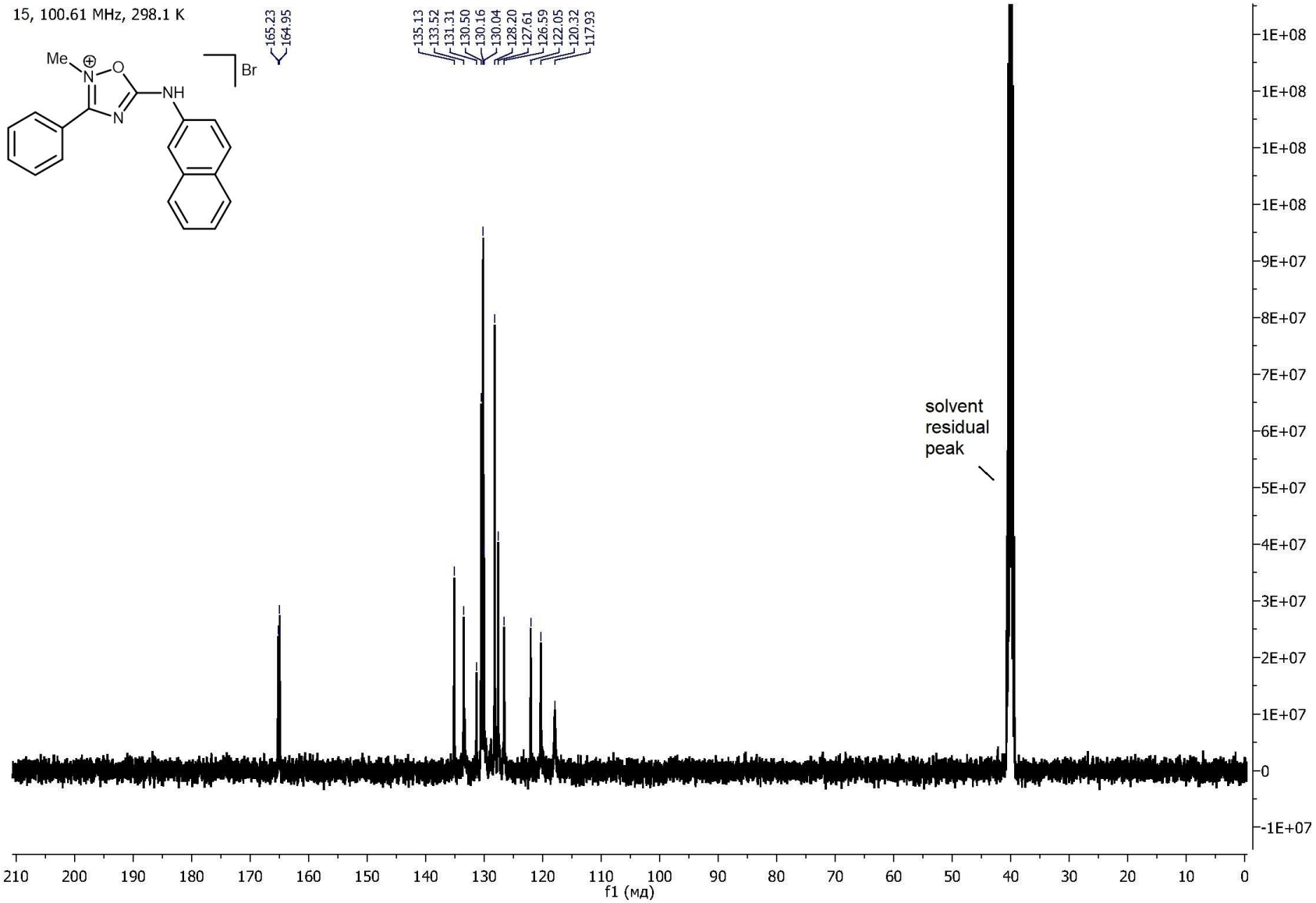

Figure 94S. $^{13}C\{^{1}H\}$ NMR spectrum of **15**.

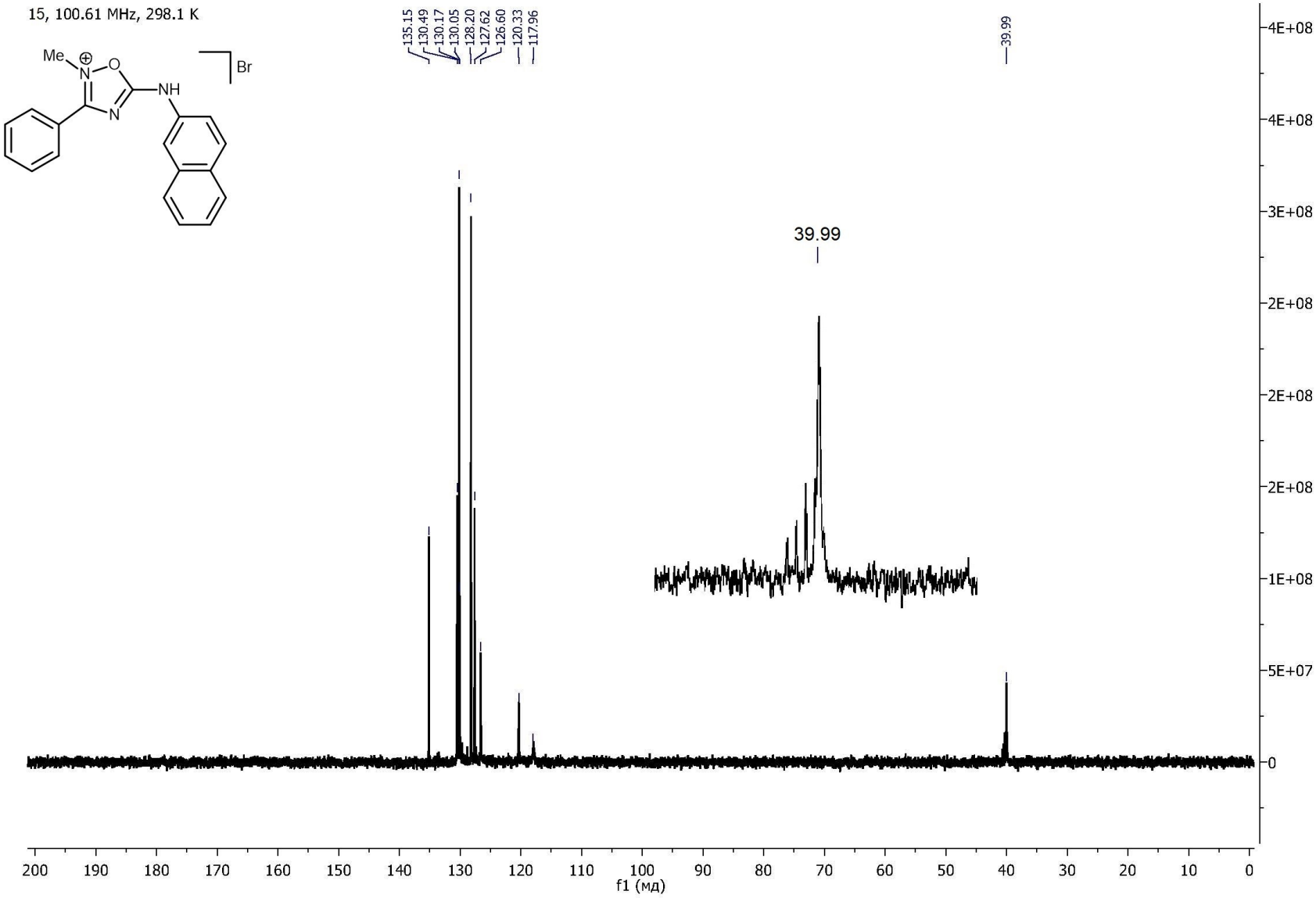

Figure 95S. $^{13}C\{^{1}H\}$ DEPT 135° NMR spectrum of **15**.

Acquisition Parameter

Source Type	ESI	Ion Polarity	Positive	Set Nebulizer	0.4 Bar
Focus	Not active			Set Dry Heater	180 °C
Scan Begin	50 m/z	Set Capillary	4500 V	Set Dry Gas	4.0 l/min
Scan End	1000 m/z	Set End Plate Offset	-500 V	Set Divert Valve	Source

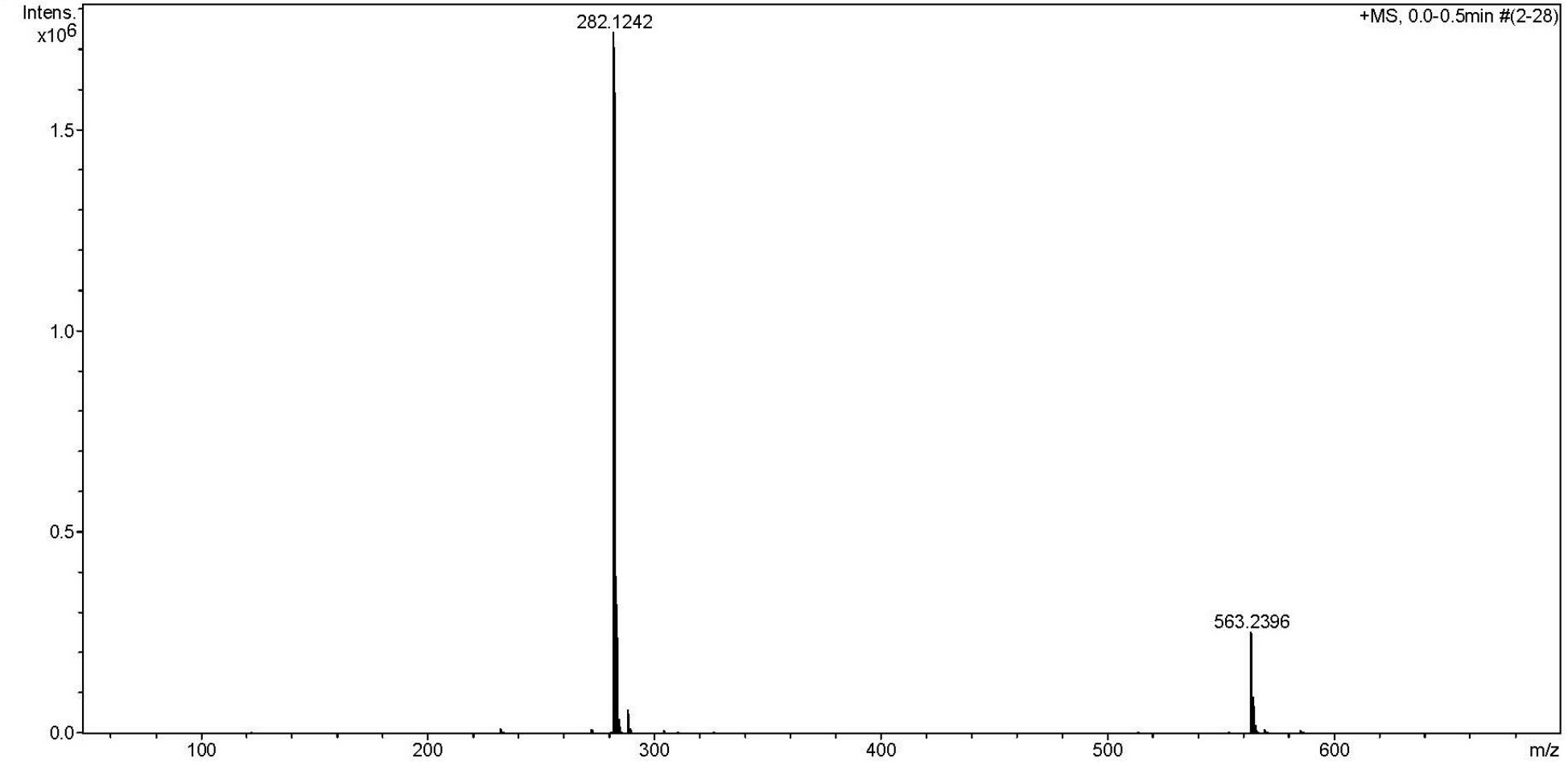

Figure 96S. HRESI^{+}-MS of **16**.

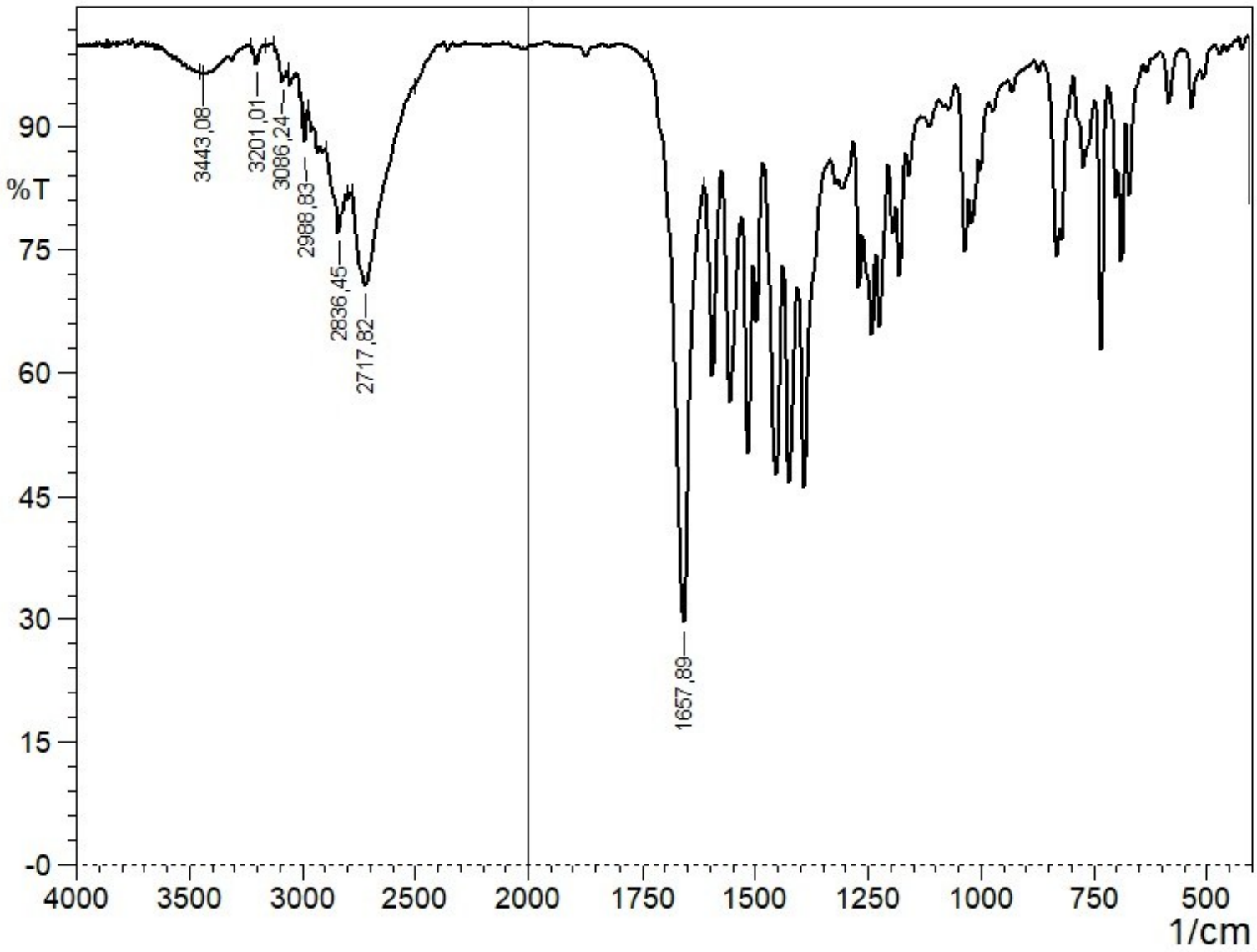

Figure 97S. IR spectrum of **16**.

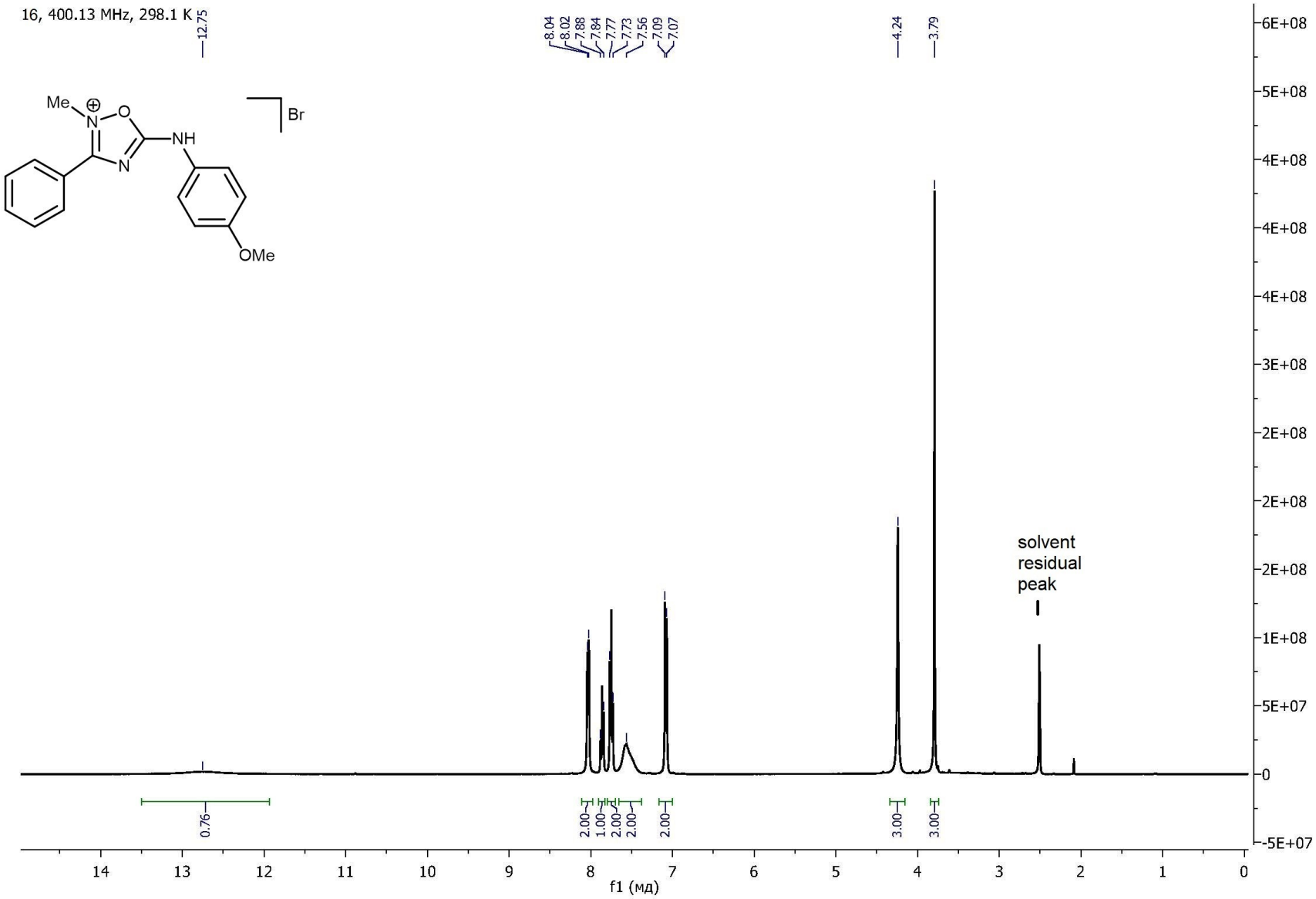

Figure 98S. ^{1}H NMR spectrum of **16**.

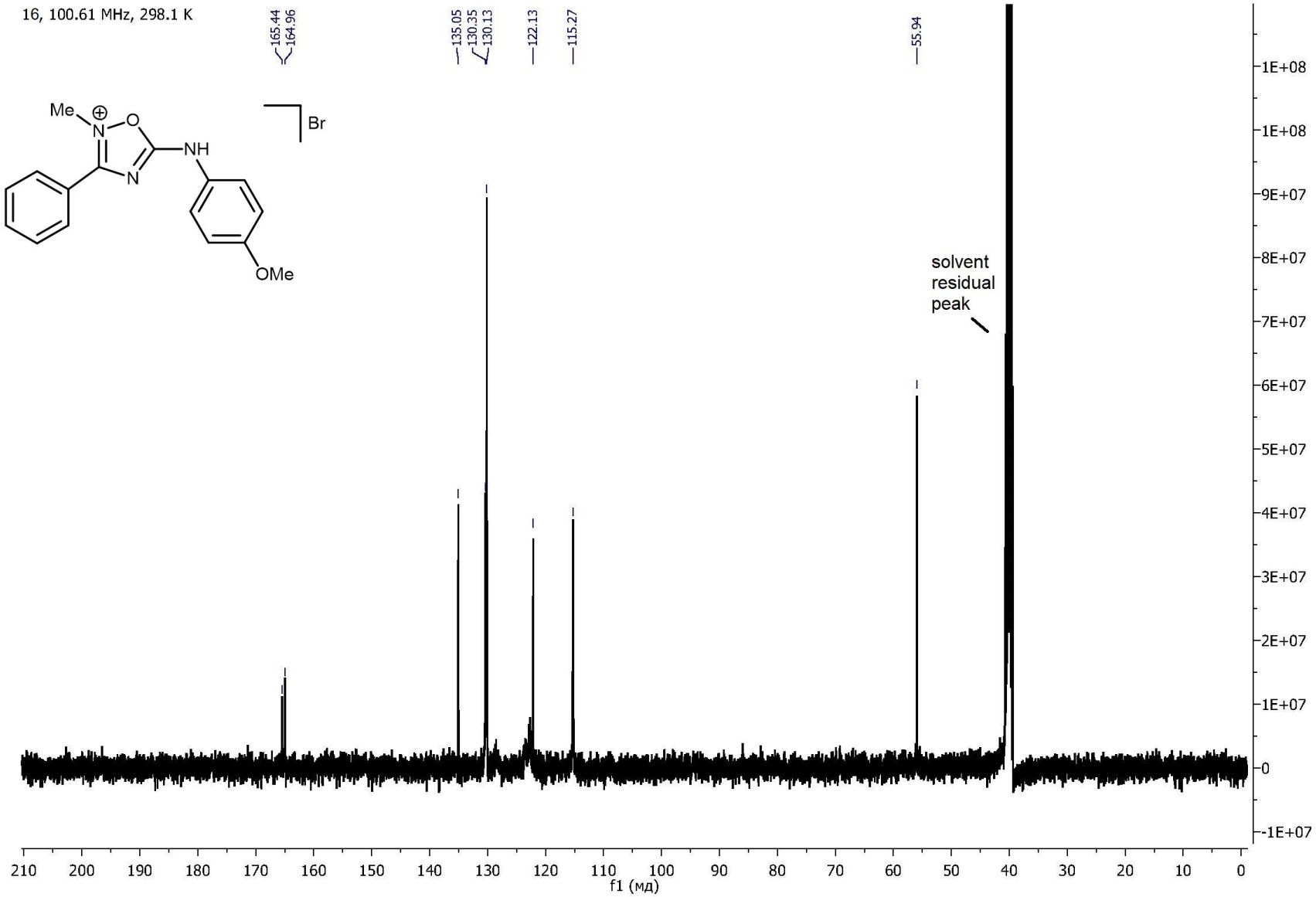

Figure 99S. $^{13}C\{^{1}H\}$ NMR spectrum of **16**.

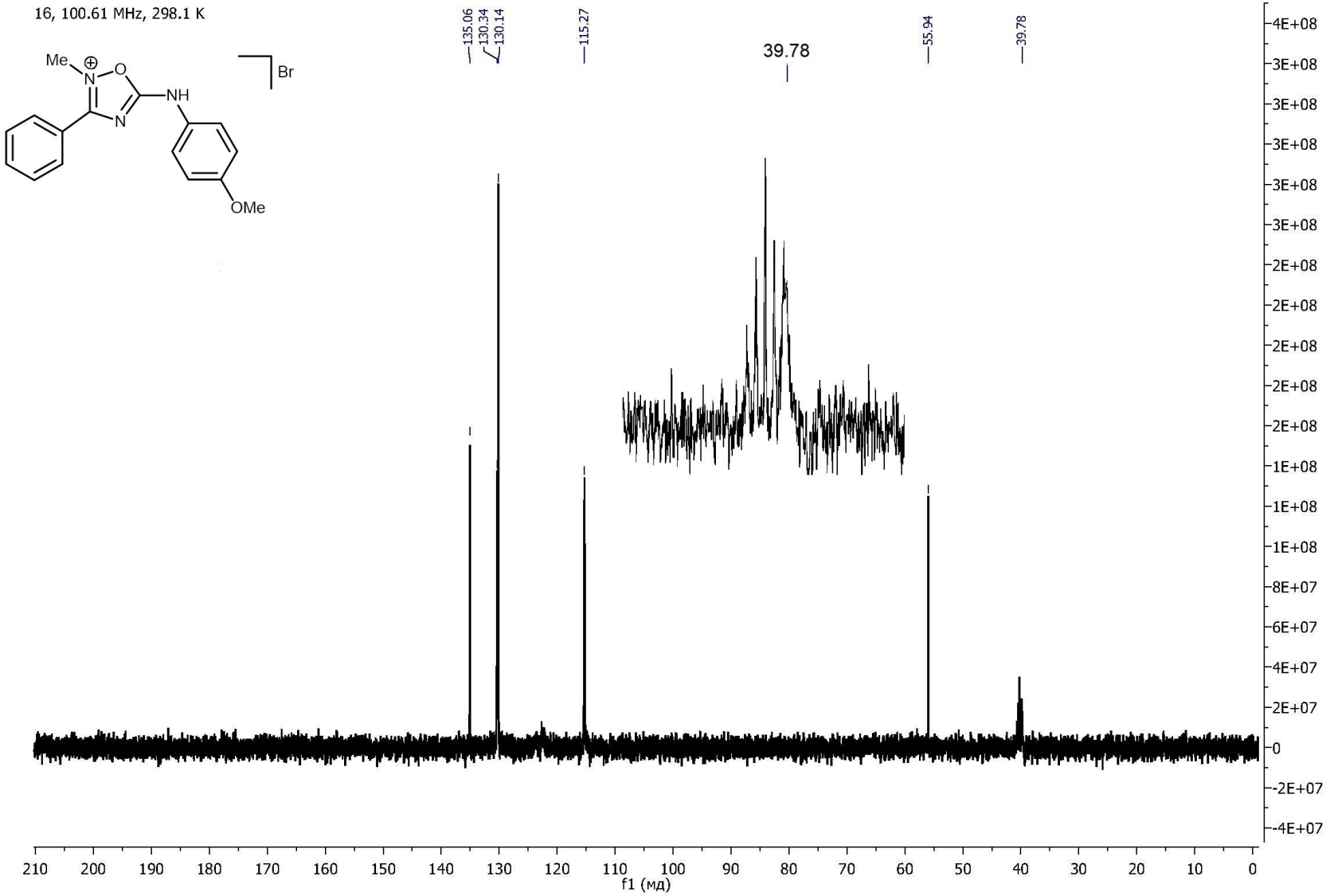

Figure 100S. $^{13}C\{^{1}H\}$ DEPT 135° NMR spectrum of **16**.

Acquisition Parameter

Source Type	ESI	Ion Polarity	Positive	Set Nebulizer	1.0 Bar
Focus	Active	Set Capillary	4500 V	Set Dry Heater	180 °C
Scan Begin	50 m/z	Set End Plate Offset	-500 V	Set Dry Gas	4.0 l/min
Scan End	1200 m/z	Set Collision Cell RF	300.0 Vpp	Set Divert Valve	Source

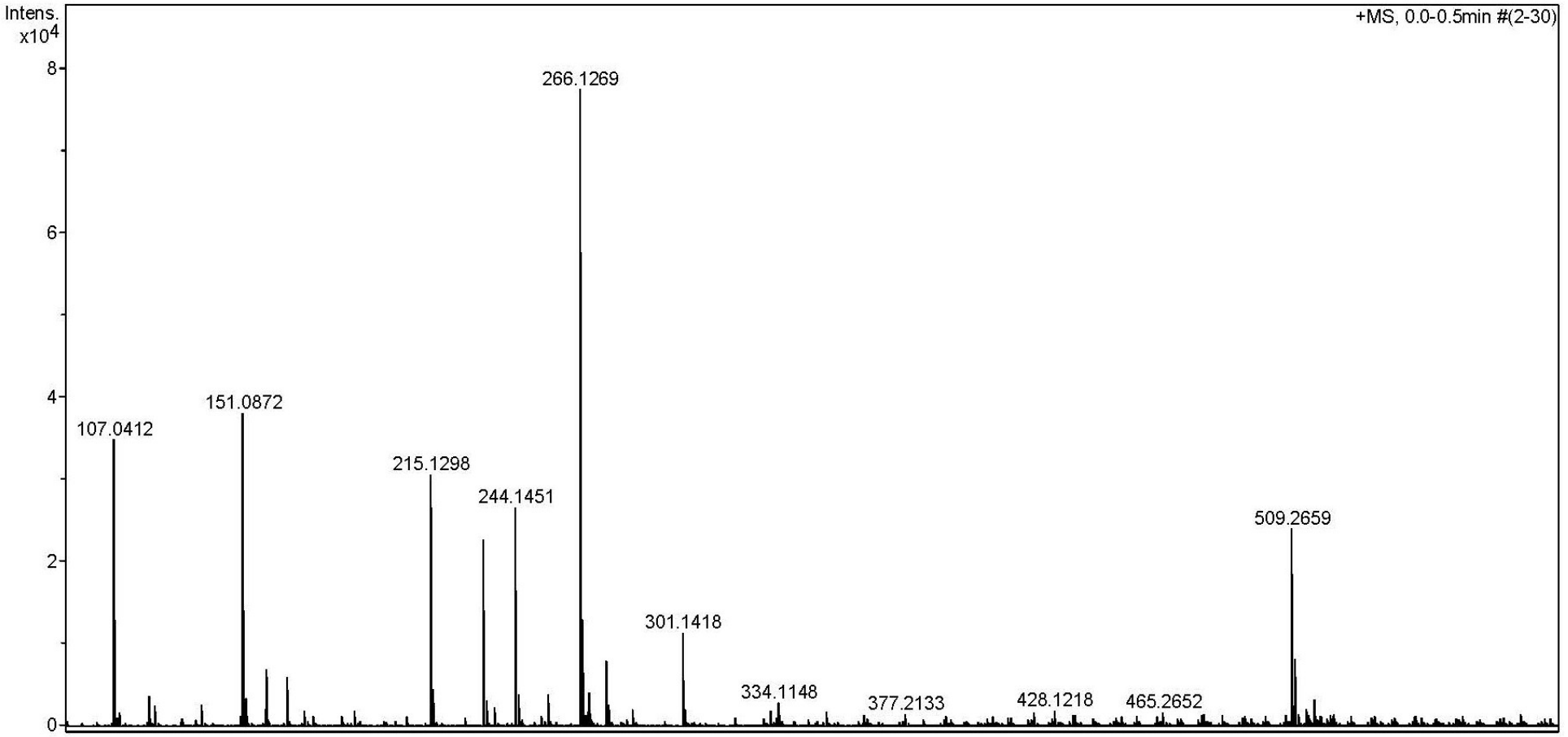

Figure 101S. HRESI$^+$-MS of **17**.

Acquisition Parameter

Source Type	ESI	Ion Polarity	Negative	Set Nebulizer	1.0 Bar
Focus	Active	Set Capillary	3500 V	Set Dry Heater	180 °C
Scan Begin	50 m/z	Set End Plate Offset	-500 V	Set Dry Gas	4.0 l/min
Scan End	1200 m/z	Set Collision Cell RF	300.0 Vpp	Set Divert Valve	Source

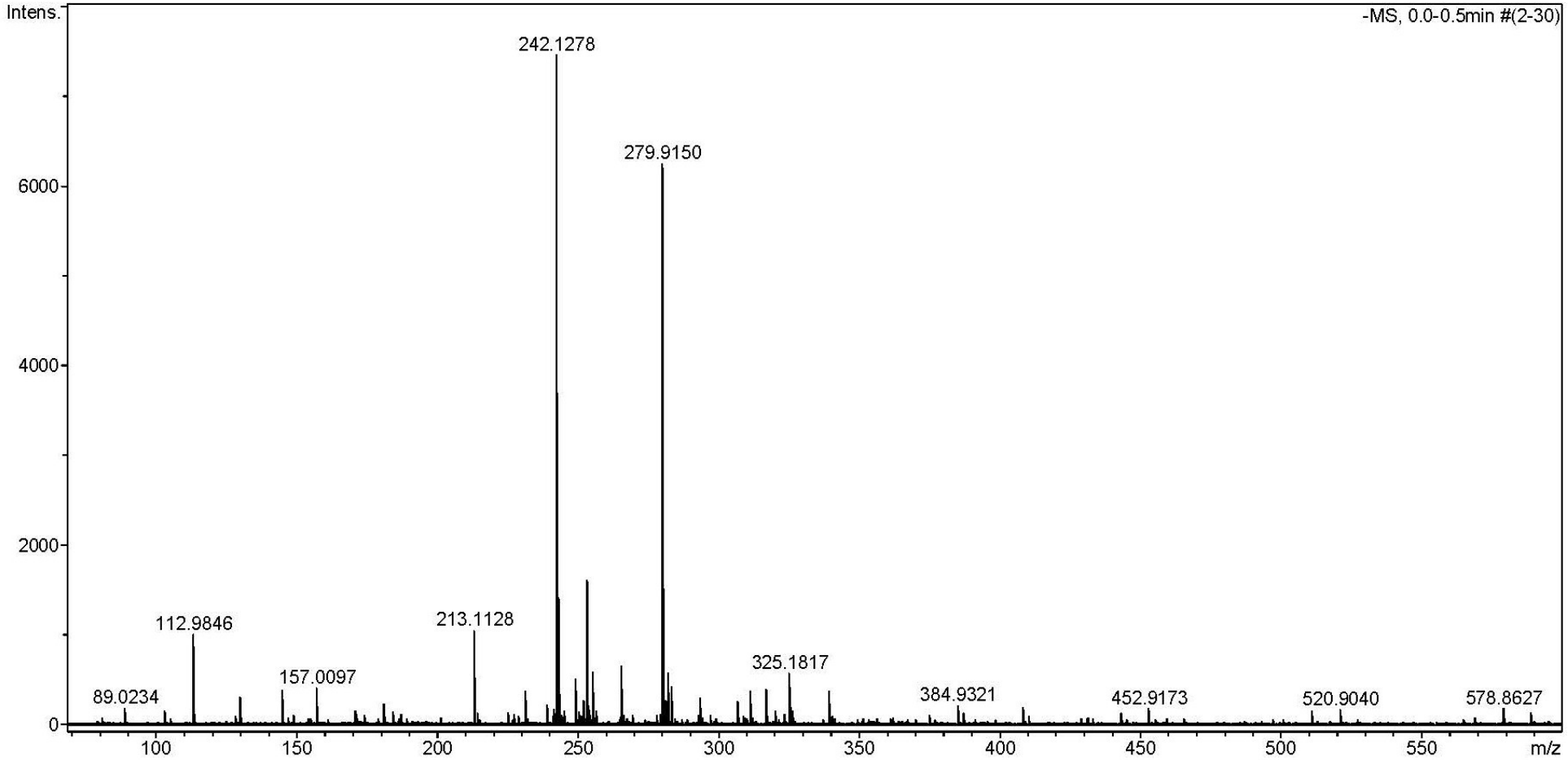

Figure 102S. HRESI⁻-MS of **17**.

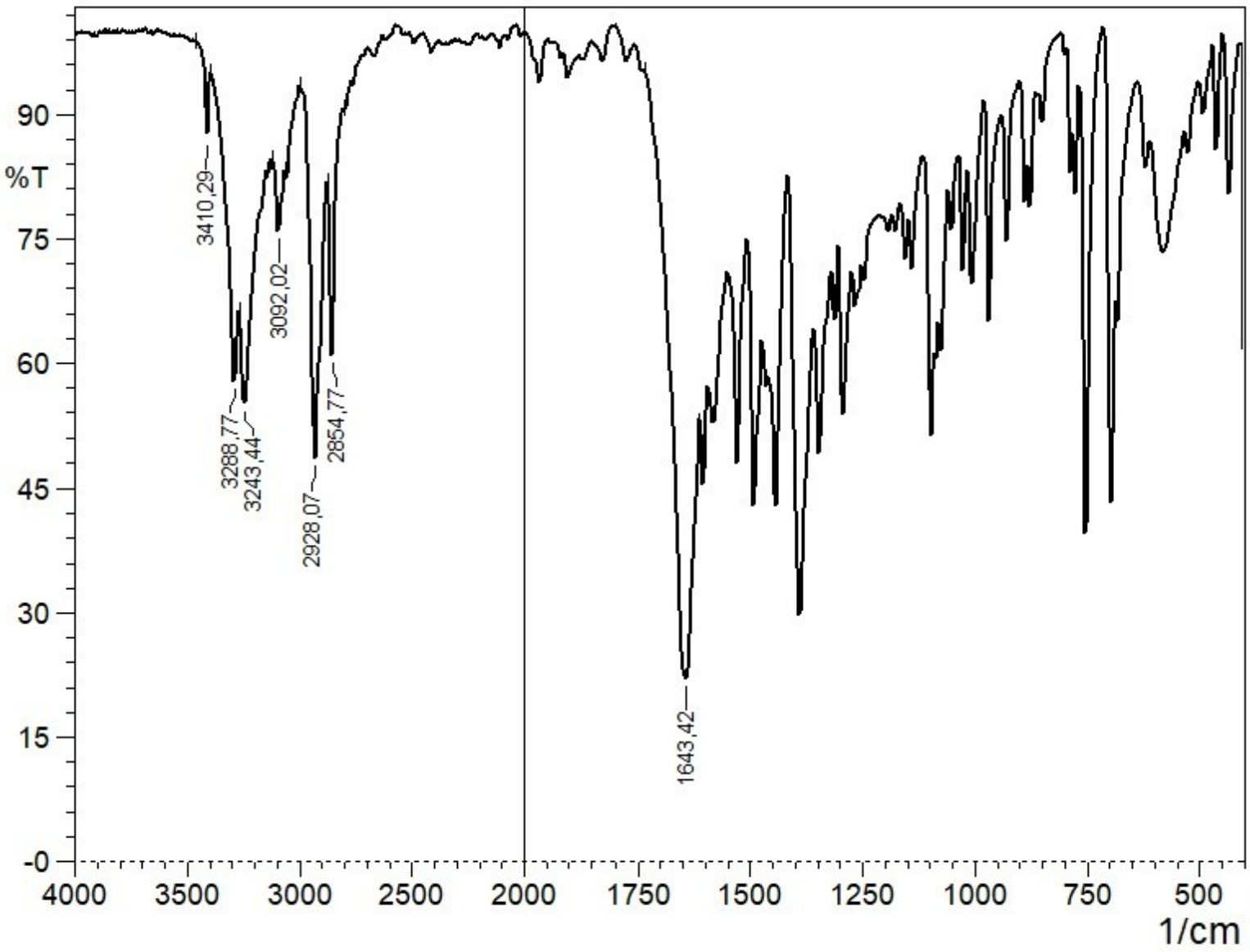

Figure 103S. IR spectrum of **17**.

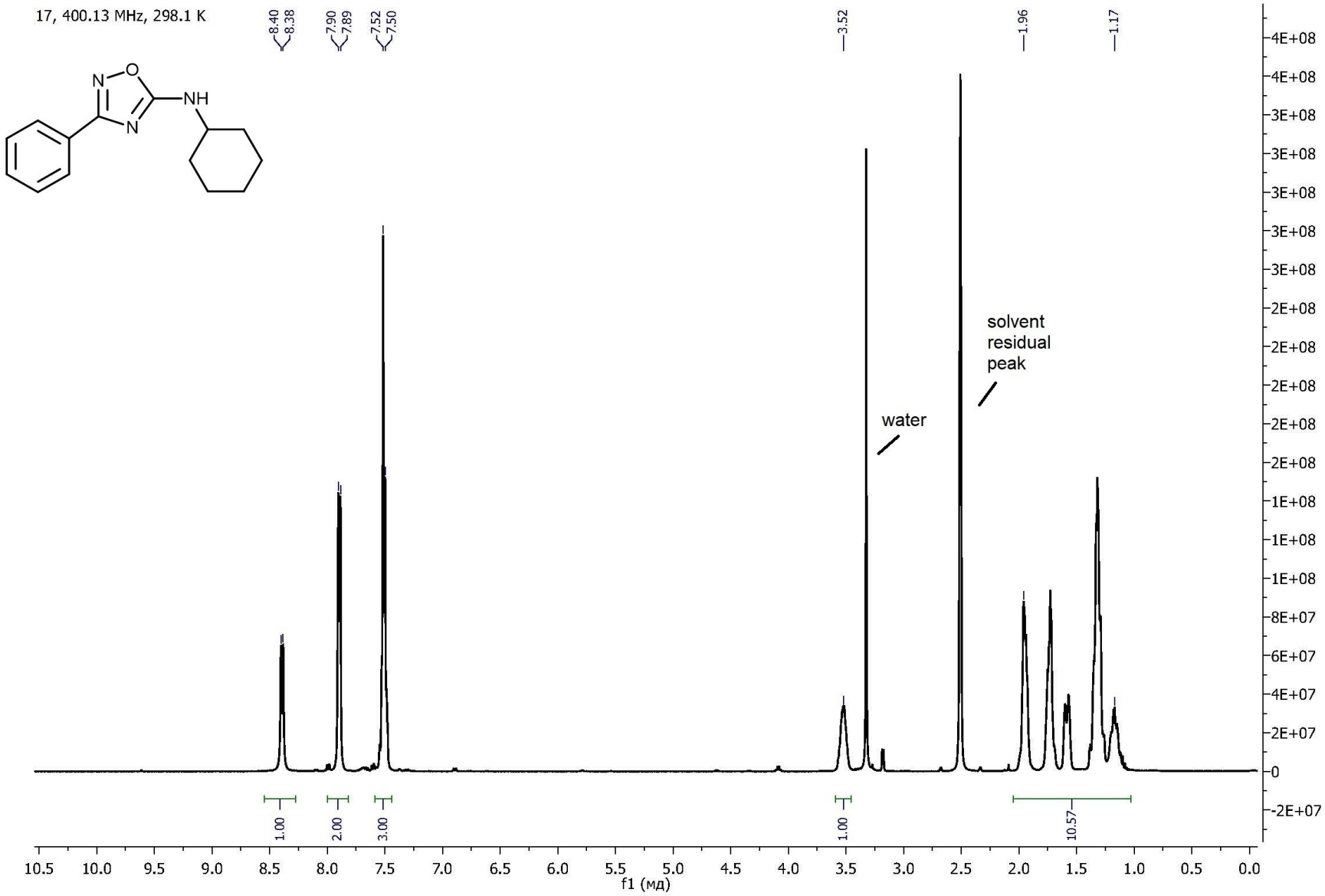

Figure 104S. ^{1}H NMR spectrum of **17**.

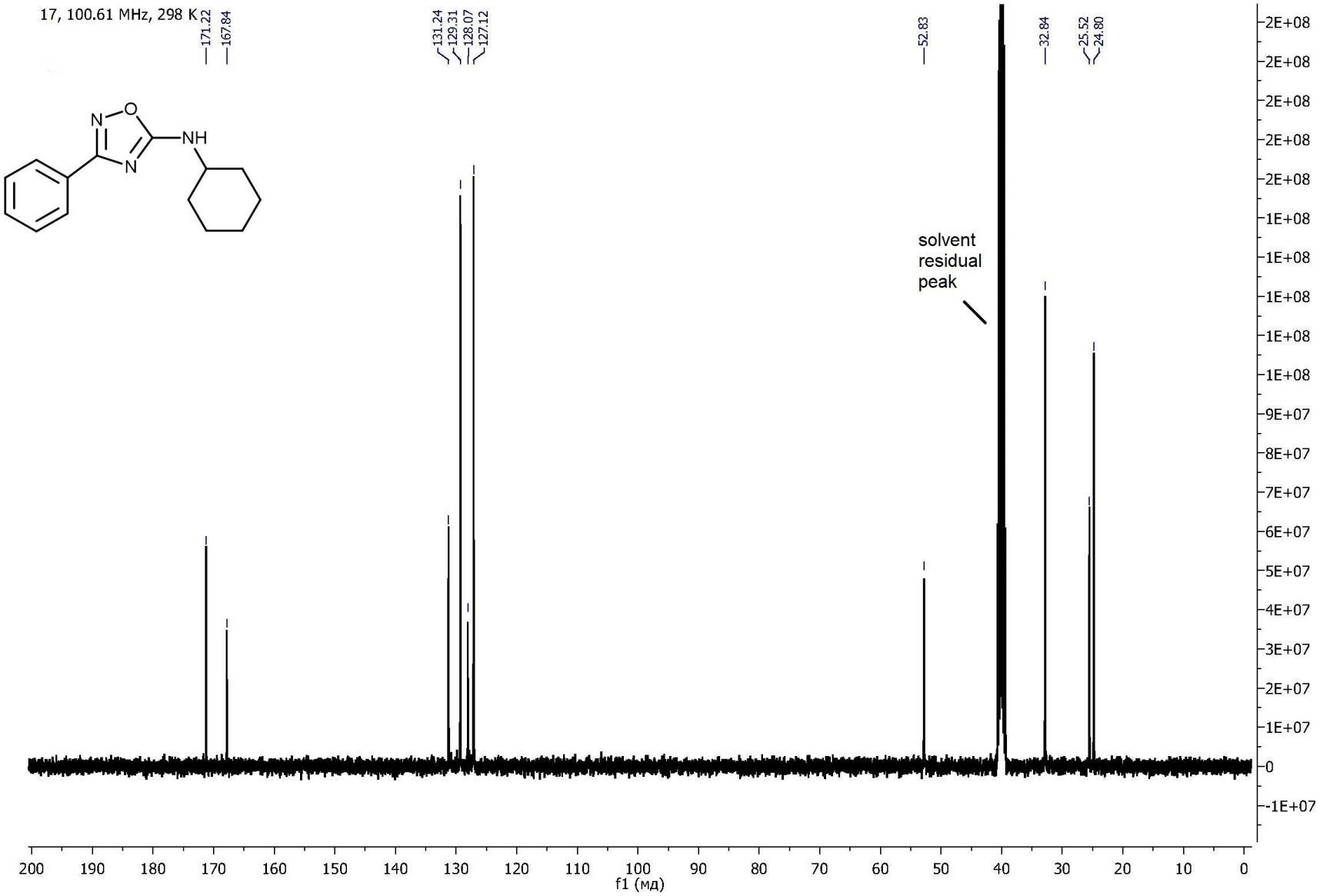

Figure 105S. $^{13}C\{^{1}H\}$ NMR spectrum of **17**.

Acquisition Parameter

Source Type	ESI	Ion Polarity	Positive	Set Nebulizer	1.0 Bar
Focus	Active	Set Capillary	4500 V	Set Dry Heater	180 °C
Scan Begin	50 m/z	Set End Plate Offset	-500 V	Set Dry Gas	4.0 l/min
Scan End	1200 m/z	Set Collision Cell RF	300.0 Vpp	Set Divert Valve	Source

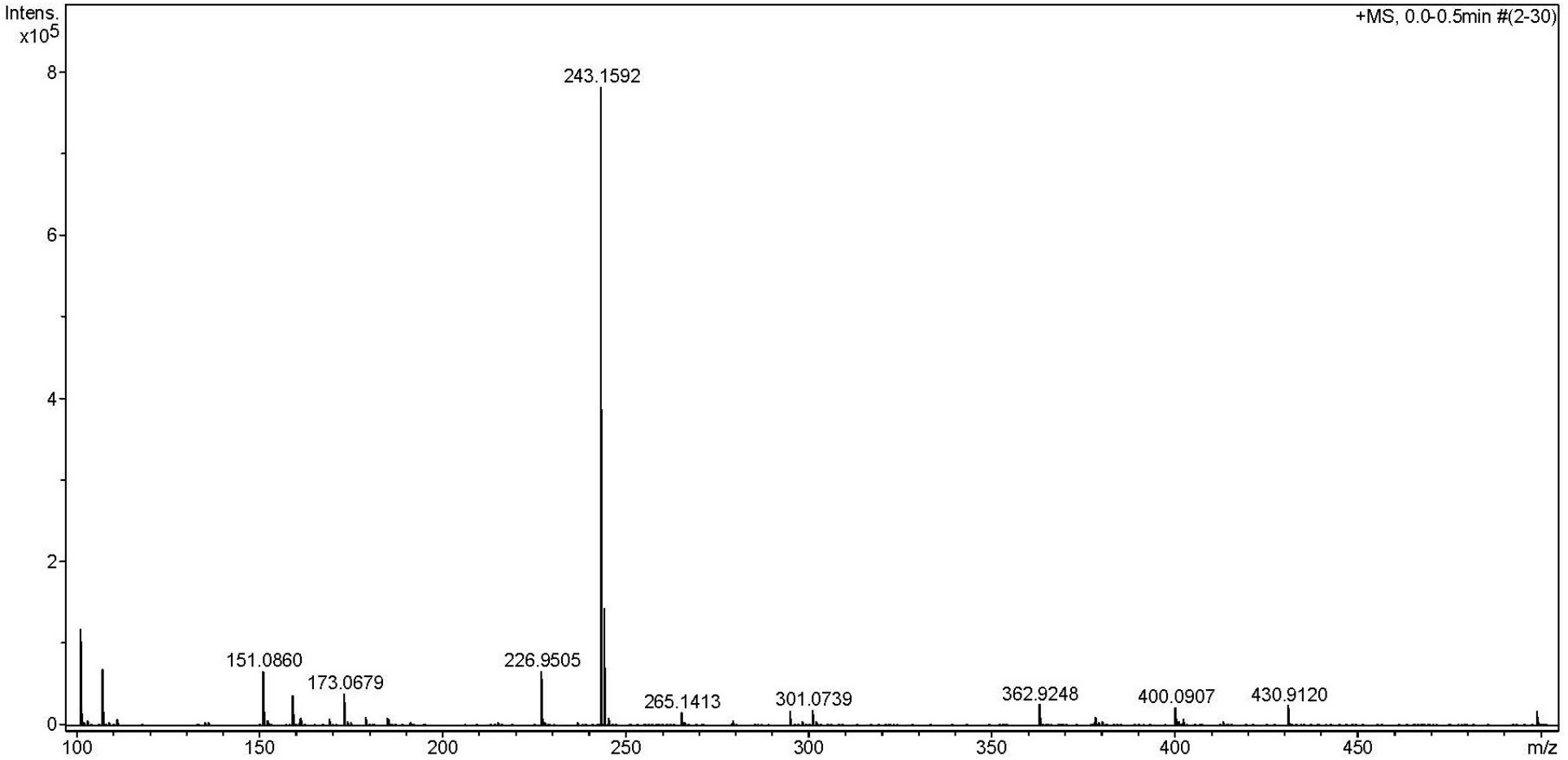

Figure 106S. HRESI$^+$-MS of **18**.

Acquisition Parameter

Source Type	ESI	Ion Polarity	Negative	Set Nebulizer	1.0 Bar
Focus	Active	Set Capillary	3500 V	Set Dry Heater	180 °C
Scan Begin	50 m/z	Set End Plate Offset	-500 V	Set Dry Gas	4.0 l/min
Scan End	1200 m/z	Set Collision Cell RF	300.0 Vpp	Set Divert Valve	Source

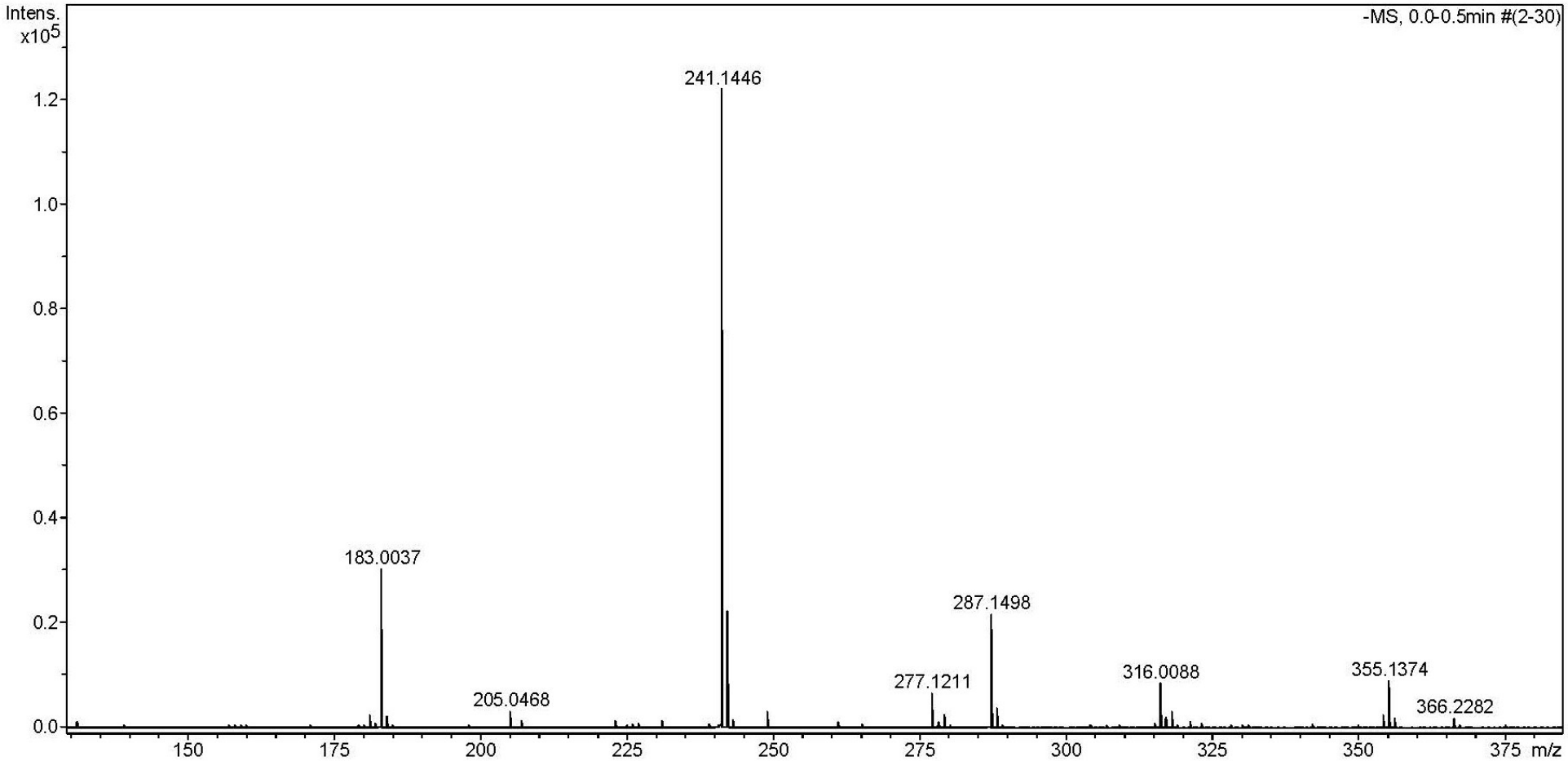

Figure 107S. HRESI⁻-MS of **18**.

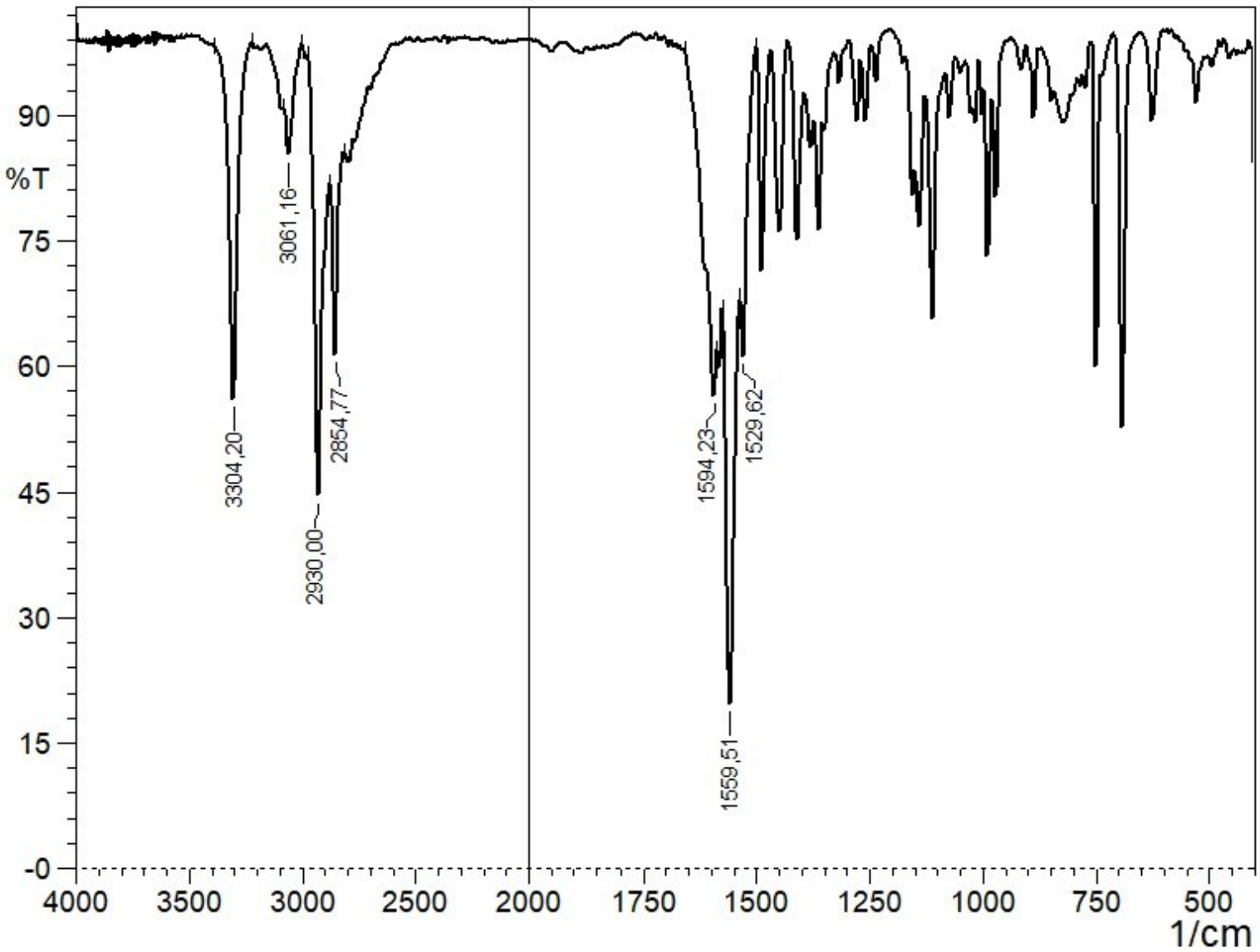

Figure 108S. IR spectrum of **18**.

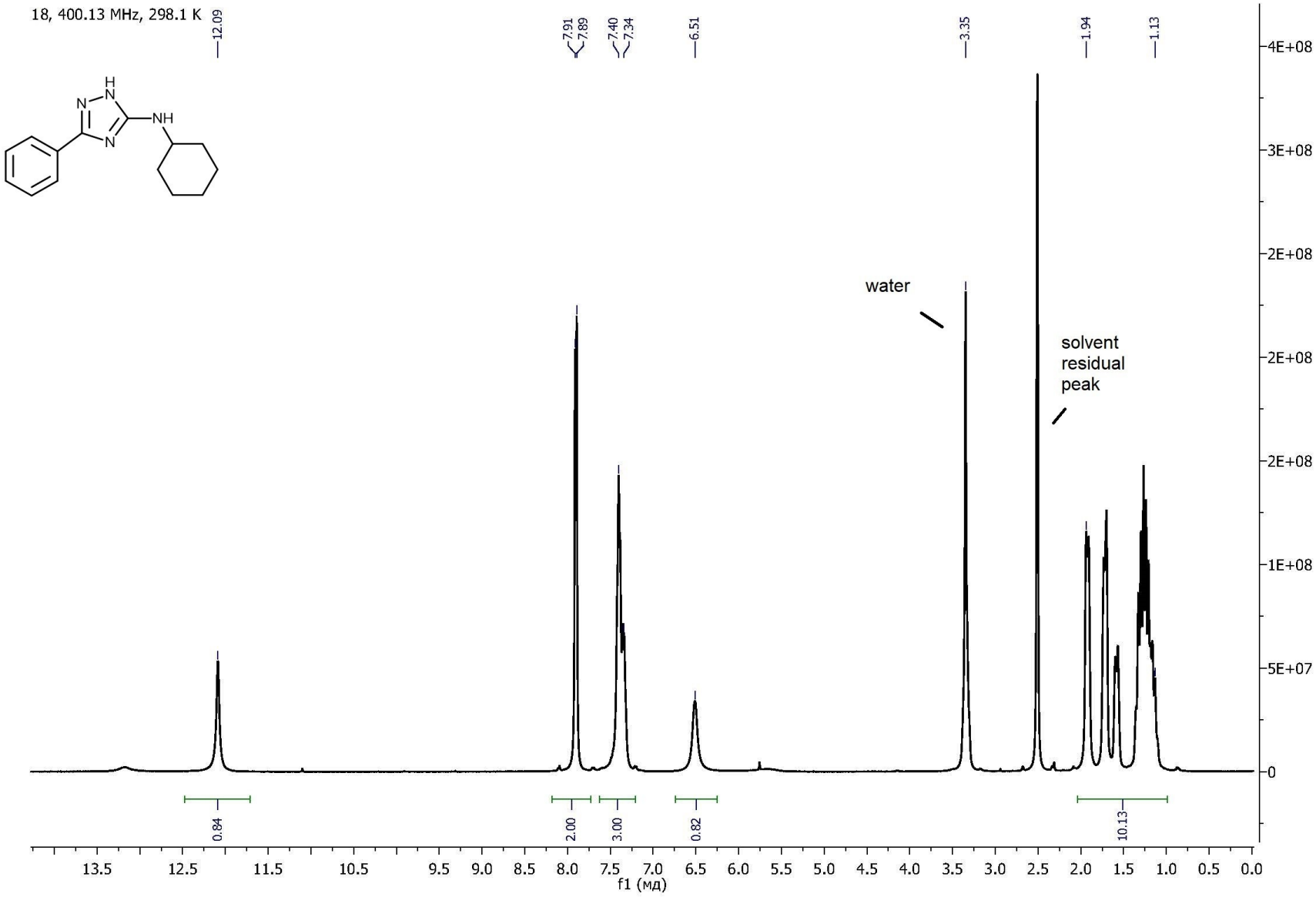

Figure 109S. ^{1}H NMR spectrum of **18**.

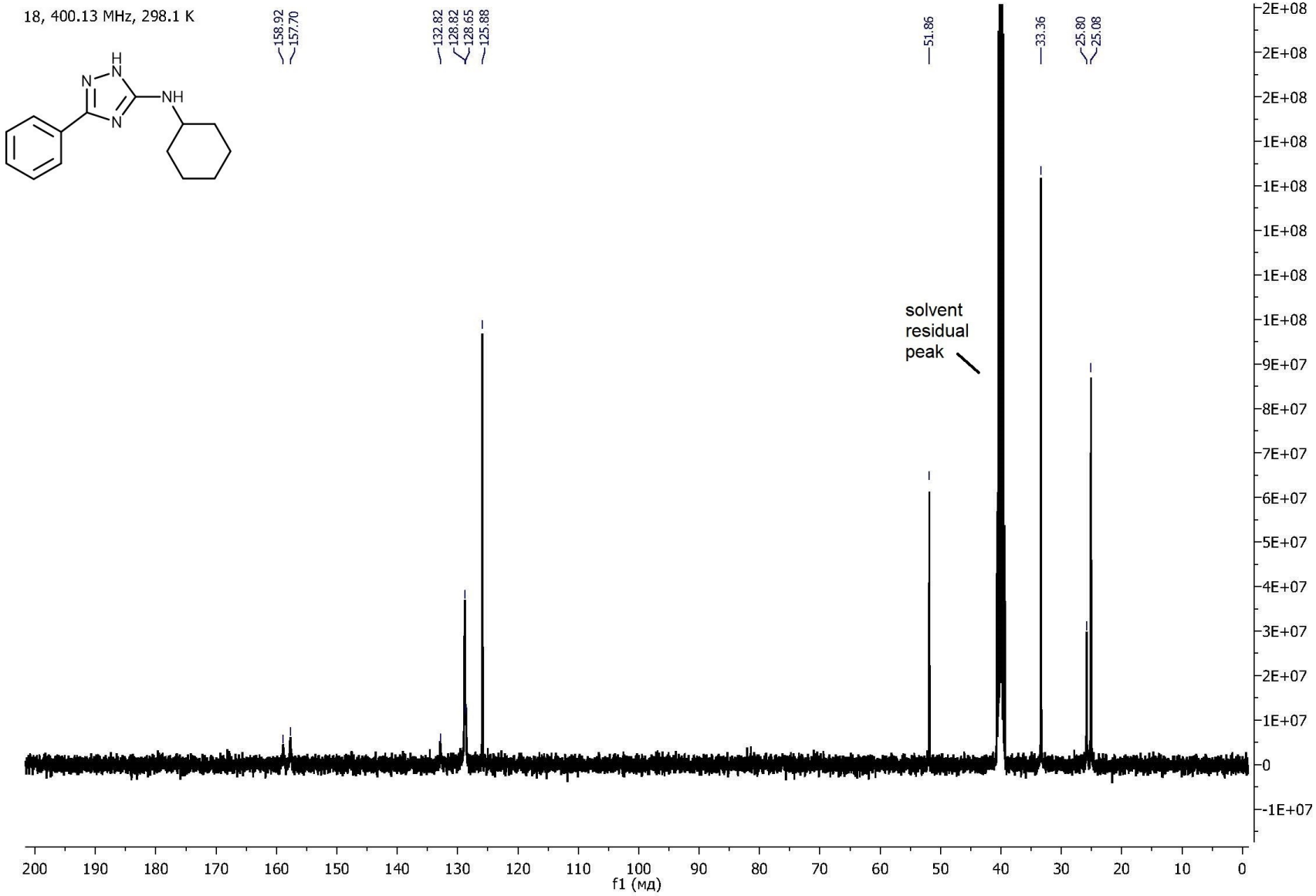

Figure 110S. $^{13}C\{^{1}H\}$ NMR spectrum of **18**.

Acquisition Parameter

Source Type	ESI	Ion Polarity	Positive	Set Nebulizer	1.0 Bar
Focus	Active	Set Capillary	4500 V	Set Dry Heater	180 °C
Scan Begin	50 m/z	Set End Plate Offset	-500 V	Set Dry Gas	4.0 l/min
Scan End	1200 m/z	Set Collision Cell RF	300.0 Vpp	Set Divert Valve	Source

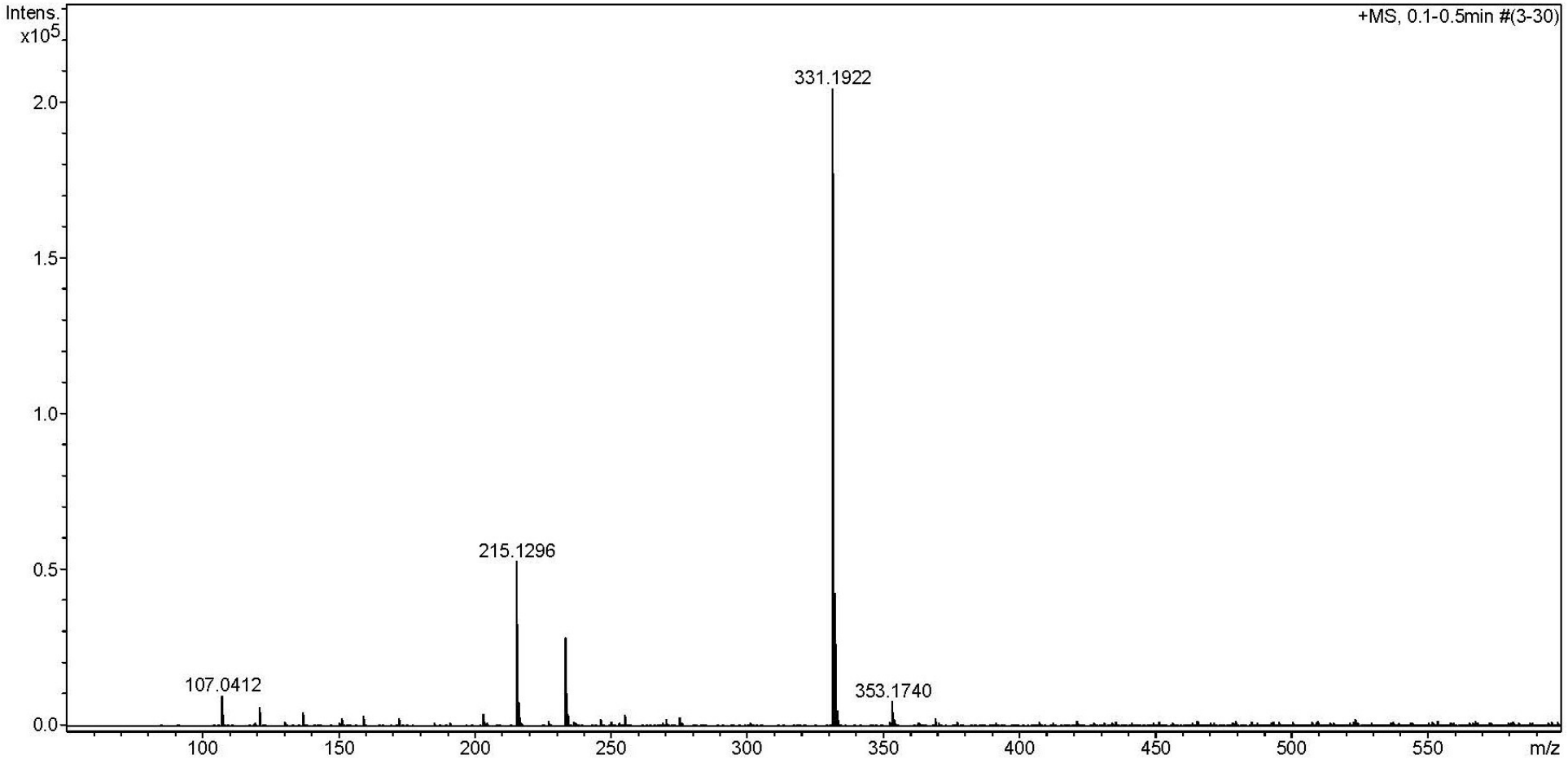

Figure 111S. HRESI$^+$-MS of **19**.

Acquisition Parameter

Source Type	ESI	Ion Polarity	Negative	Set Nebulizer	1.0 Bar
Focus	Active	Set Capillary	3500 V	Set Dry Heater	180 °C
Scan Begin	50 m/z	Set End Plate Offset	-500 V	Set Dry Gas	4.0 l/min
Scan End	1200 m/z	Set Collision Cell RF	300.0 Vpp	Set Divert Valve	Source

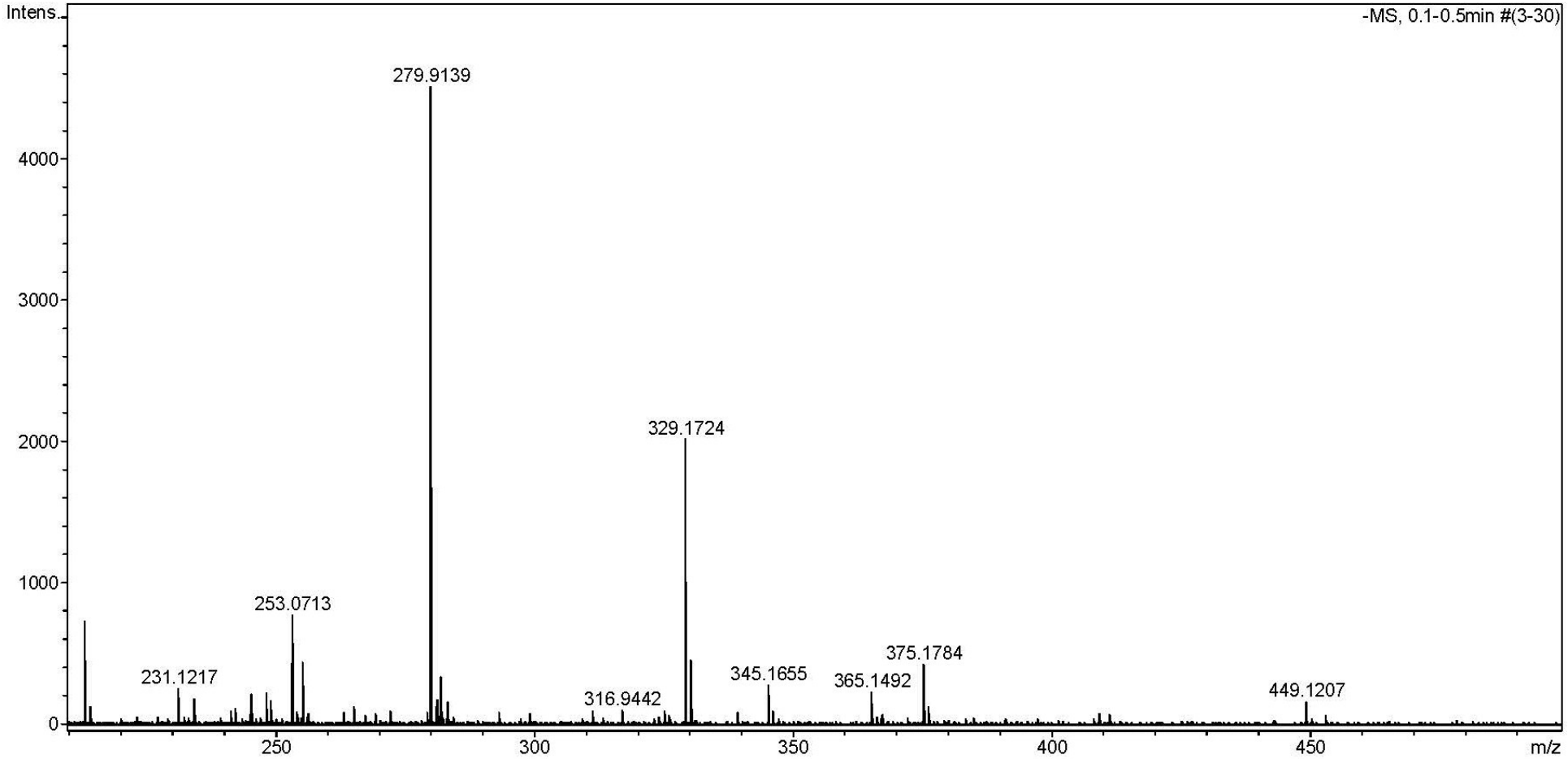

Figure 112S. HRESI⁻-MS of **19**.

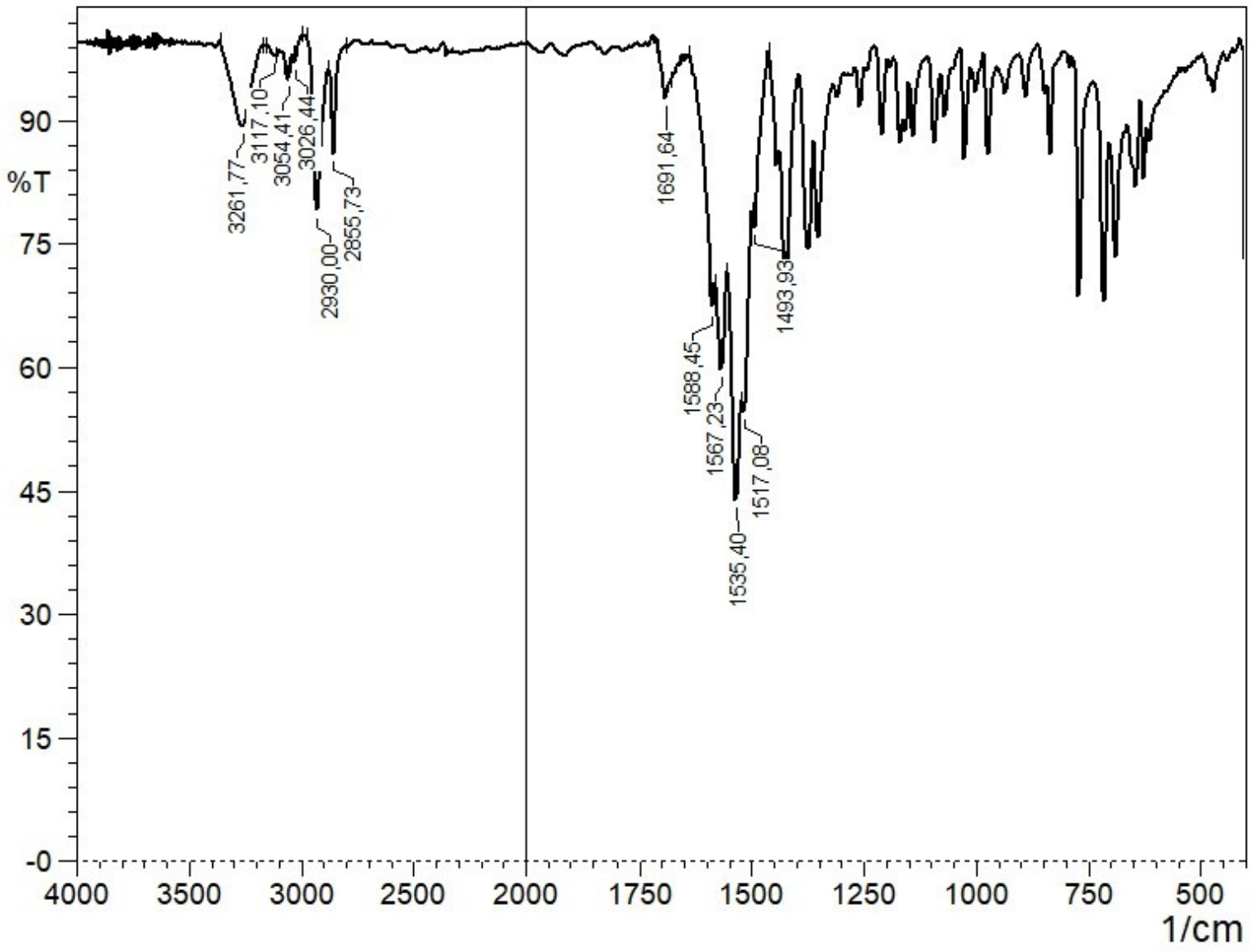

Figure 113S. IR spectrum of **19**.

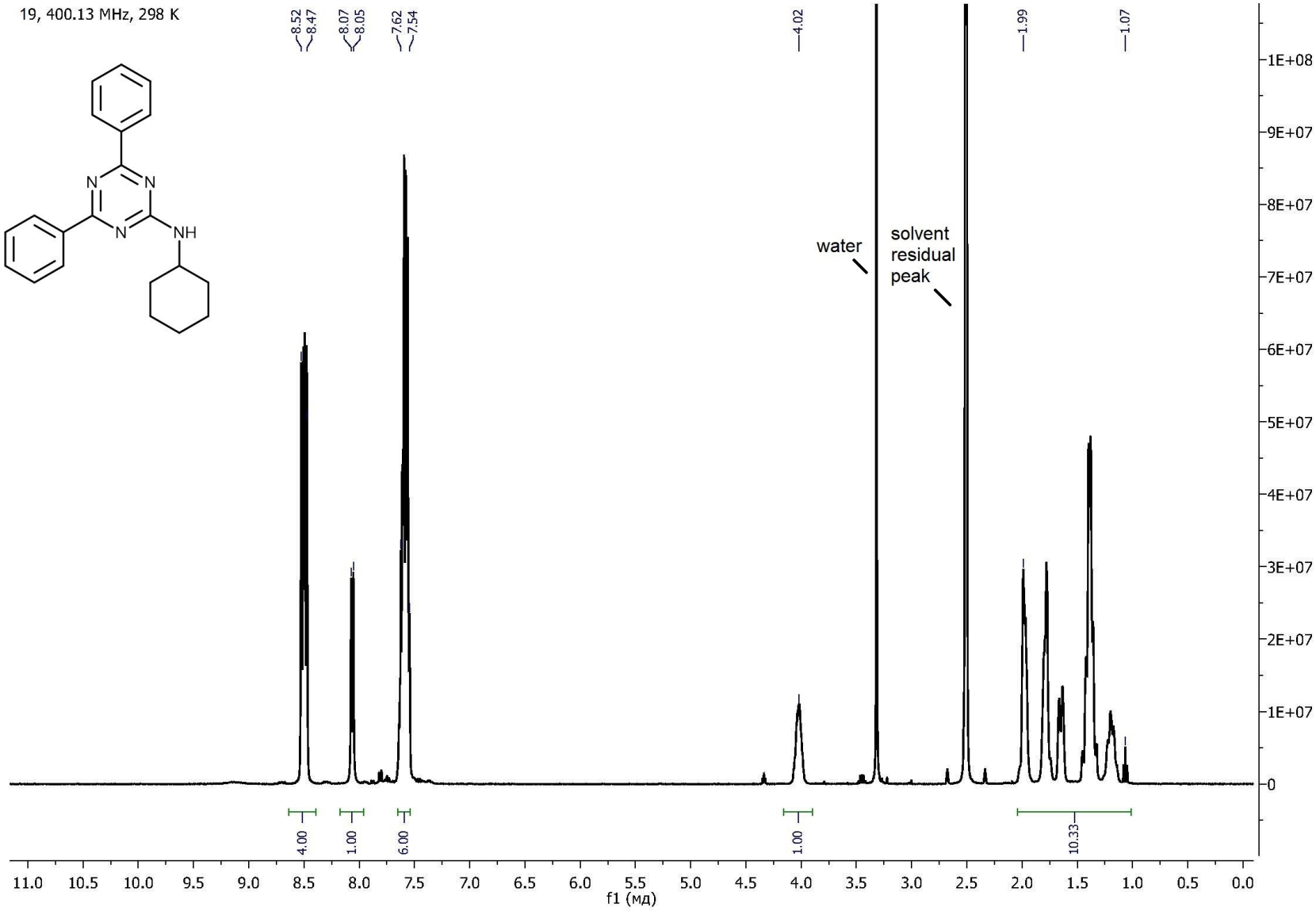

Figure 114S. ^{1}H NMR spectrum of **19**.

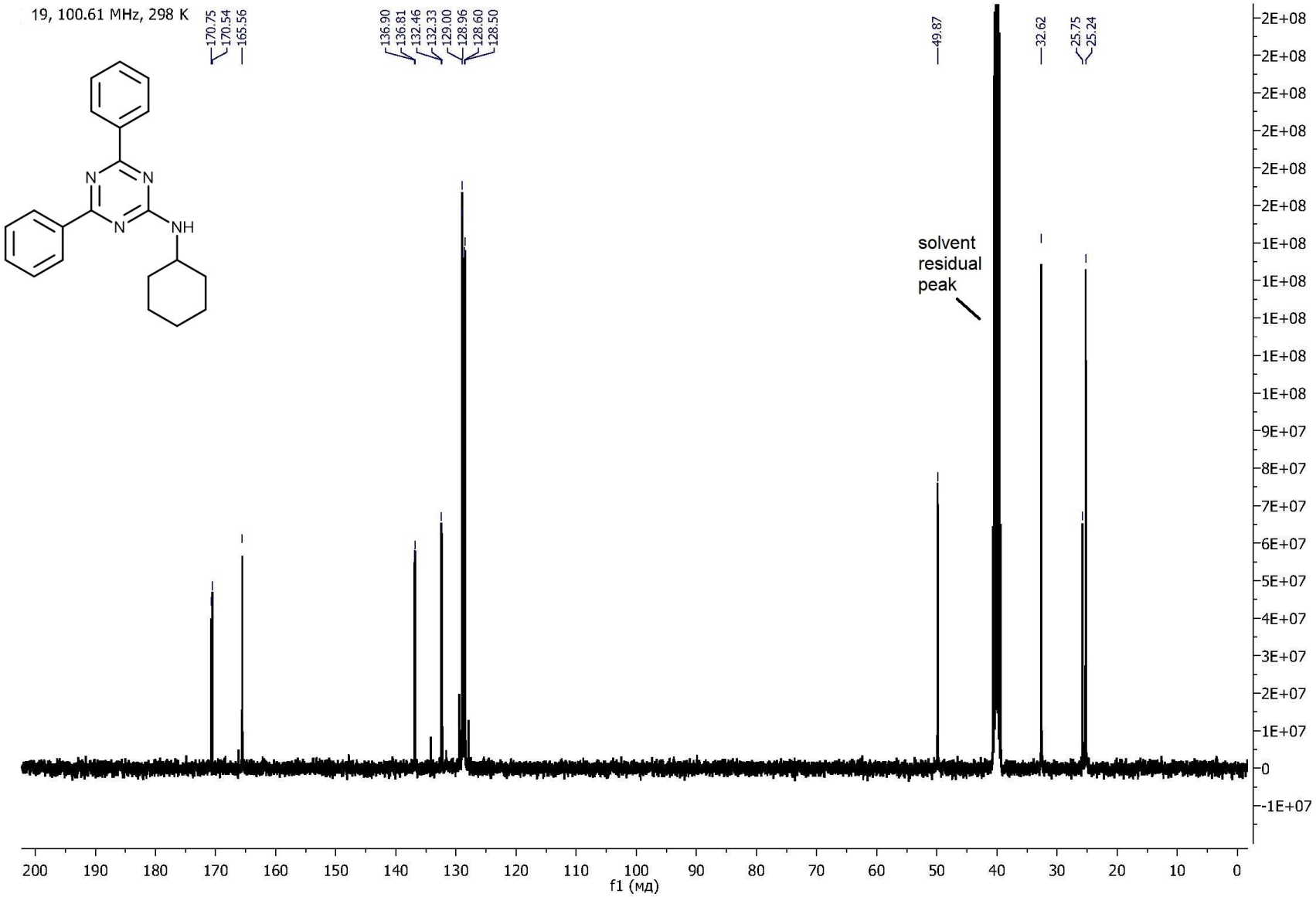

Figure 115S. $^{13}C\{^{1}H\}$ NMR spectrum of **19**.

Acquisition Parameter

Source Type	ESI	Ion Polarity	Positive	Set Nebulizer	1.0 Bar
Focus	Active	Set Capillary	4500 V	Set Dry Heater	180 °C
Scan Begin	50 m/z	Set End Plate Offset	-500 V	Set Dry Gas	4.0 l/min
Scan End	1200 m/z	Set Collision Cell RF	300.0 Vpp	Set Divert Valve	Source

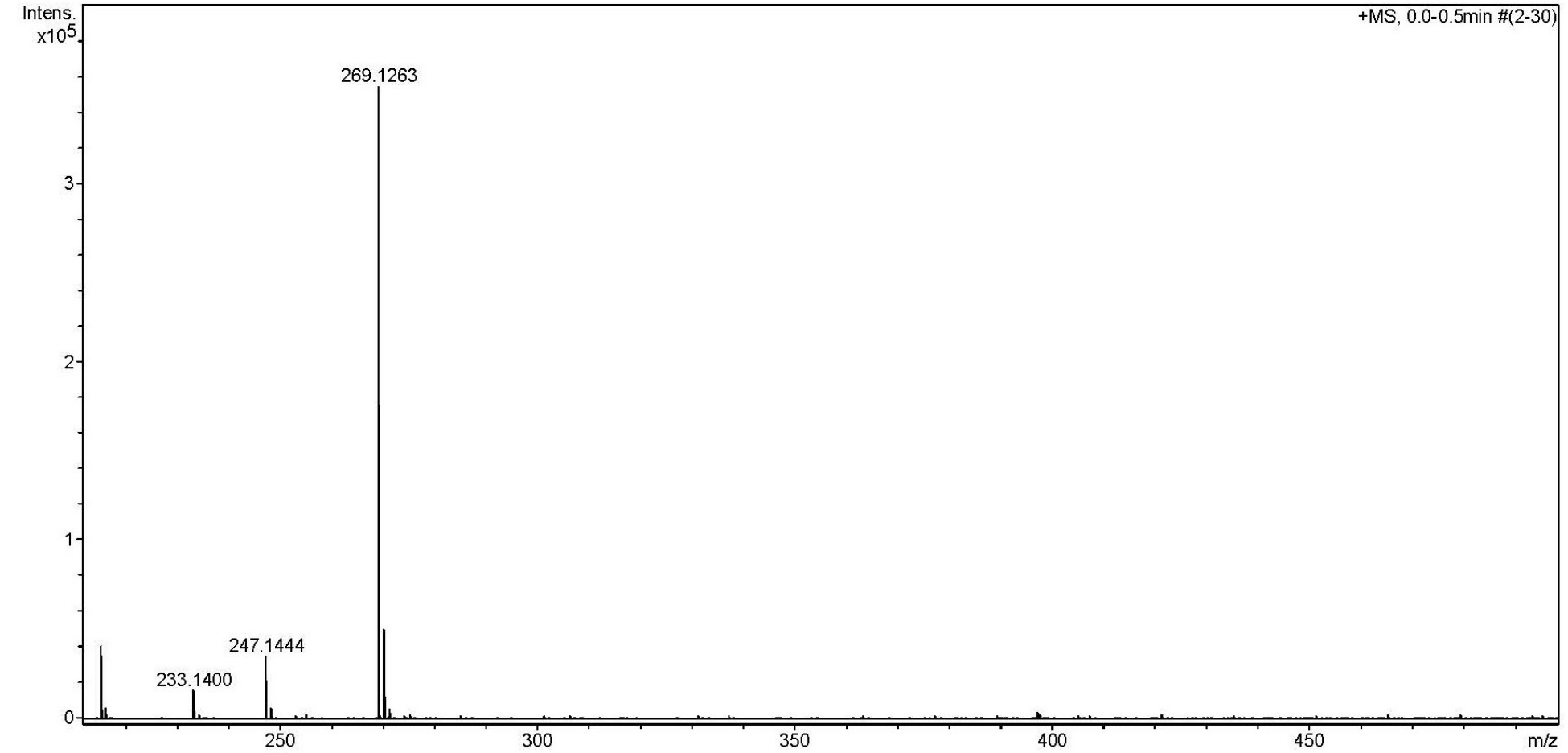

Figure 116S. HRESI^{+}-MS of **20**.

Acquisition Parameter

Source Type	ESI	Ion Polarity	Negative	Set Nebulizer	1.0 Bar
Focus	Active	Set Capillary	3500 V	Set Dry Heater	180 °C
Scan Begin	50 m/z	Set End Plate Offset	-500 V	Set Dry Gas	4.0 l/min
Scan End	1200 m/z	Set Collision Cell RF	300.0 Vpp	Set Divert Valve	Source

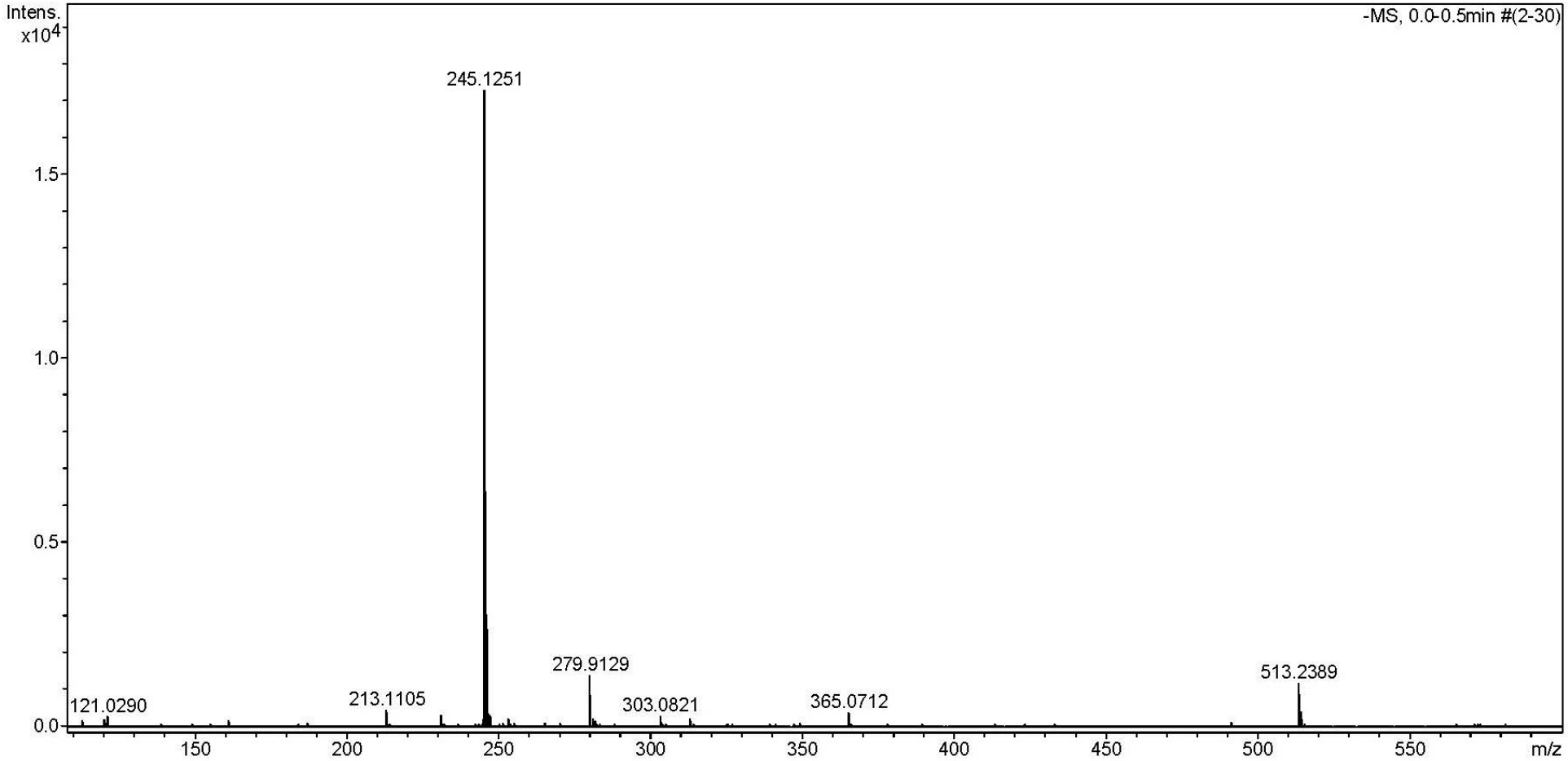

Figure 117S. HRESI⁻-MS of **20**.

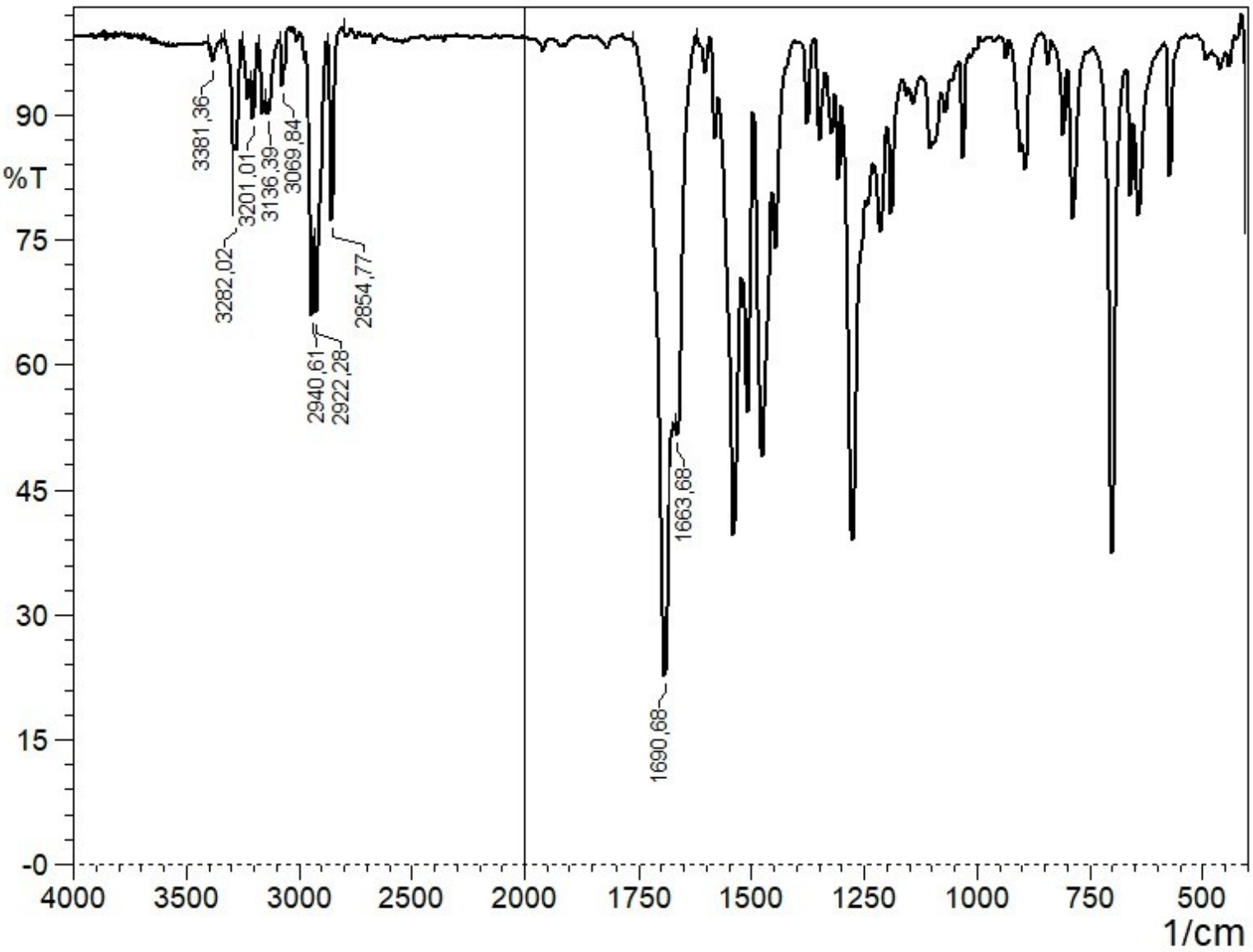

Figure 118S. IR spectrum of **20**.

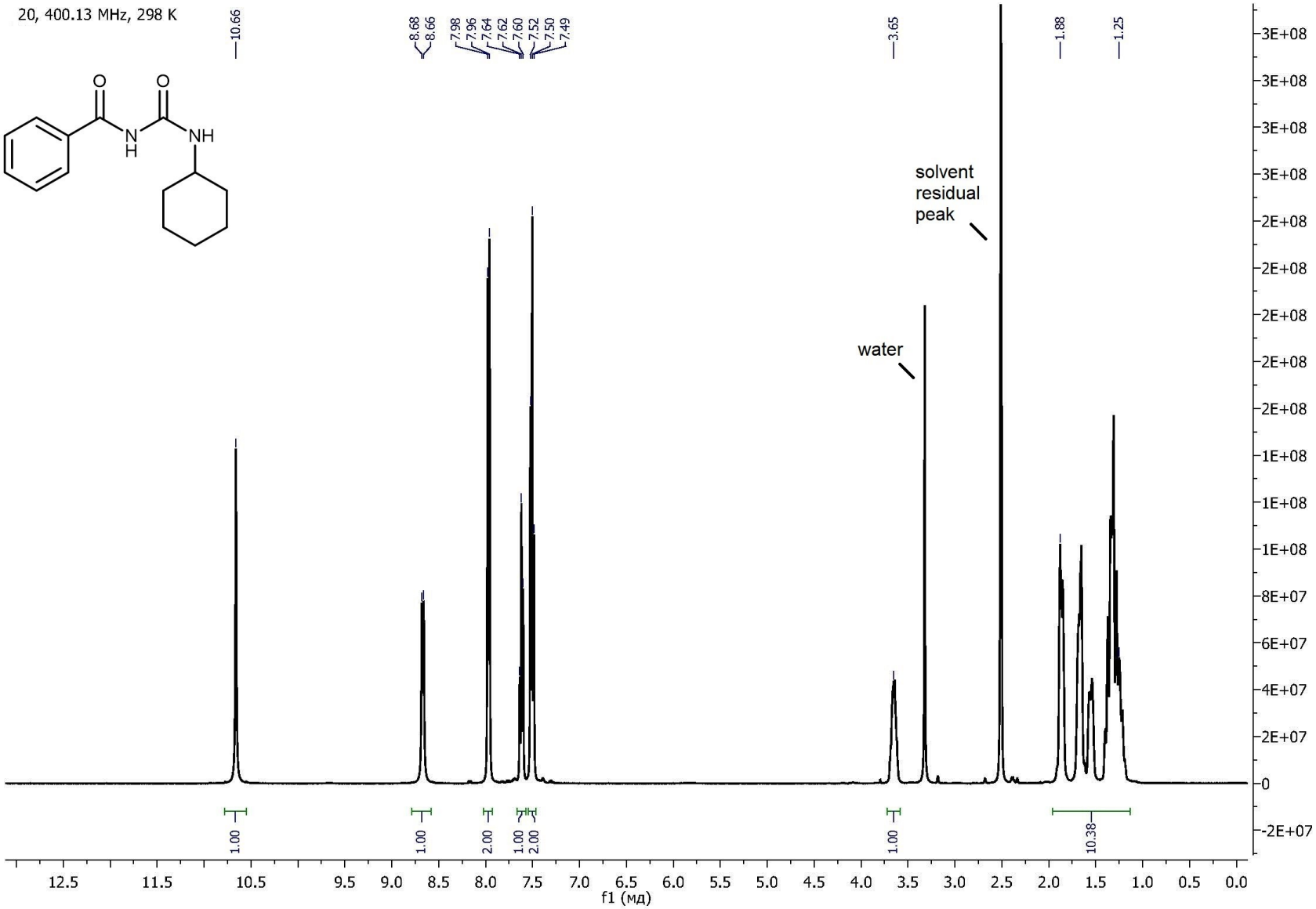

Figure 119S. ^{1}H NMR spectrum of **20**.

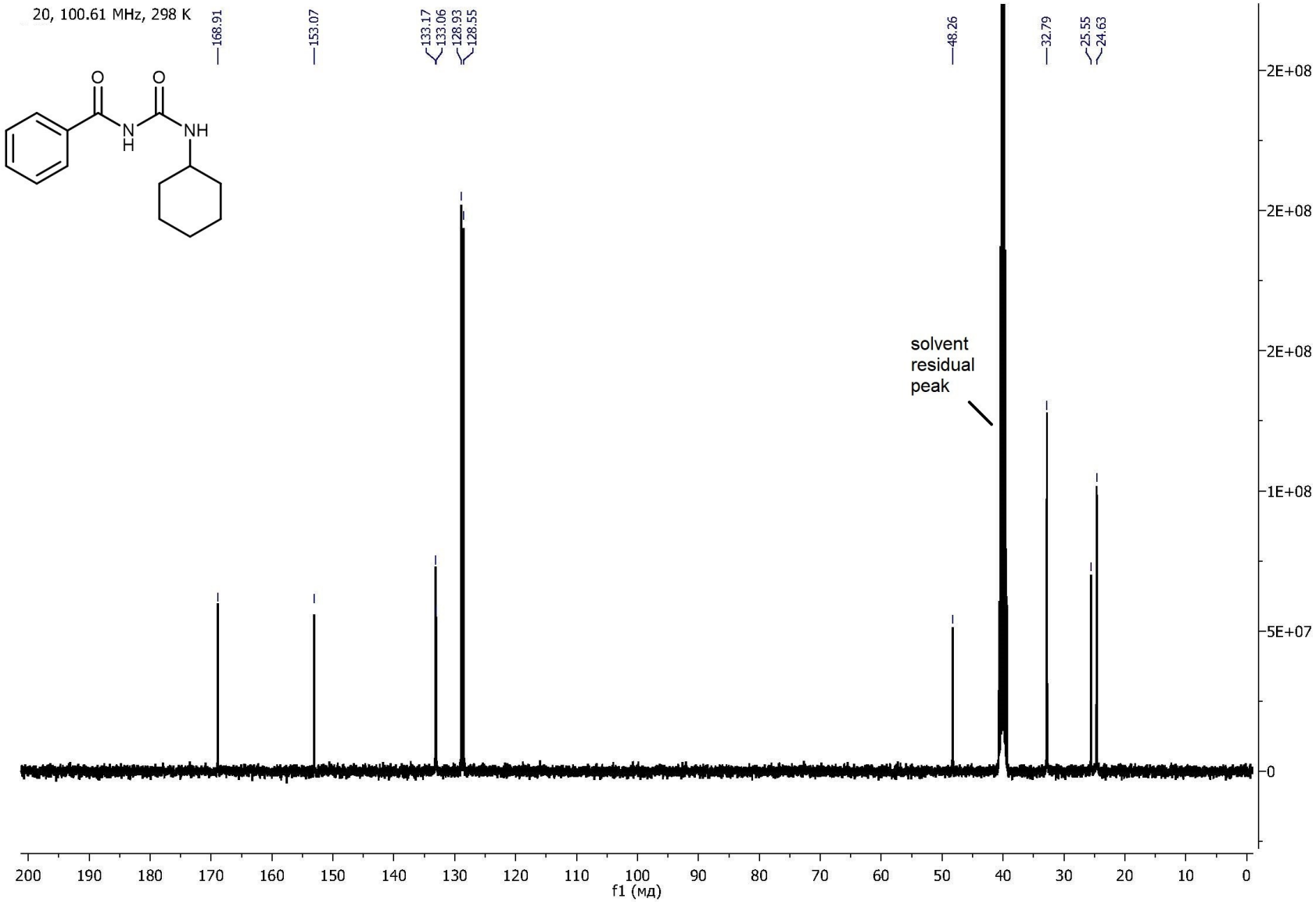

Figure 120S. $^{13}C\{^{1}H\}$ NMR spectrum of **20**.

Crystal data for 4, 6, 17, 18, 19, and 20

Identification code	**4**·H_2O	**6**	**17**
Empirical formula	$C_{15}H_{22}BrN_3O_2$	$C_{15}H_{19}Br_2N_3O$	$C_{14}H_{17}N_3O$
Formula weight	356.26	417.15	243.30
Temperature/K	100(2)	100(2)	100(2)
Crystal system	orthorhombic	trigonal	monoclinic
Space group	$P2_12_12_1$	R-3	$P2_1/n$
a/Å	5.56160(10)	36.6338(19)	5.8808(4)
b/Å	14.0149(4)	36.6338(19)	12.3009(8)
c/Å	20.3191(5)	6.4707(4)	17.6105(11)
α/°	90	90	90
β/°	90	90	91.401(7)
γ/°	90	120	90
Volume/$Å^3$	1583.78(7)	7520.5(9)	1273.55(15)
Z	4	18	4
ρ_{calc}g/cm^3	1.494	1.658	1.269
μ/mm^{-1}	3.609	6.171	0.083
F(000)	736.0	3744.0	520.0
Crystal size/mm^3	0.18 × 0.16 × 0.1	0.15 × 0.15 × 0.1	0.34 × 0.28 × 0.19
Radiation	CuKα (λ = 1.54184)	CuKα (λ = 1.54184)	MoKα (λ = 0.71073)
2Θ range for data collection/°	7.664 to 152.52	8.36 to 152.392	5.69 to 54.996
Index ranges	$-7 \leq h \leq 5$, $-16 \leq k \leq 17$, $-25 \leq l \leq 23$	$-45 \leq h \leq 46$, $-43 \leq k \leq 37$, $-8 \leq l \leq 6$	$-7 \leq h \leq 7$, $-13 \leq k \leq 15$, $-22 \leq l \leq 22$
Reflections collected	11976	10753	8991
Independent reflections	3290 [R_{int} = 0.0391, R_{sigma} = 0.0349]	3449 [R_{int} = 0.0364, R_{sigma} = 0.0297]	2922 [R_{int} = 0.0370, R_{sigma} = 0.0419]
Data/restraints/parameters	3290/0/192	3449/0/191	2922/0/163
Goodness-of-fit on F^2	1.091	1.066	1.040
Final R indexes [I>=2σ (I)]	R_1 = 0.0234, wR_2 = 0.0583	R_1 = 0.0363, wR_2 = 0.0881	R_1 = 0.0431, wR_2 = 0.0942
Final R indexes [all data]	R_1 = 0.0256, wR_2 = 0.0596	R_1 = 0.0384, wR_2 = 0.0894	R_1 = 0.0592, wR_2 = 0.1026
Largest diff. peak/hole / e $Å^{-3}$	0.33/-0.28	0.90/-0.71	0.24/-0.25
Flack parameter	0.092(19)	n/a	n/a
CCDC number	**1834203**	**1834205**	**1834204**

Identification code	**18**·H_2O	**19**	**20**
Empirical formula	$C_{28}H_{38}N_8O$	$C_{21}H_{22}N_4$	$C_{14}H_{18}N_2O_2$
Formula weight	502.66	330.42	246.30
Temperature/K	100(2)	100(2)	100(2)
Crystal system	orthorhombic	triclinic	monoclinic
Space group	Fdd2	P-1	I2/c
a/Å	19.3835(2)	11.2501(8)	20.2808(13)
b/Å	18.9731(2)	12.7520(10)	5.2993(4)
c/Å	14.30664(17)	13.2943(10)	24.3454(14)
α/°	90	86.090(6)	90
β/°	90	89.456(6)	98.356(6)
γ/°	90	67.095(7)	90
Volume/$Å^3$	5261.49(10)	1752.4(2)	2588.7(3)
Z	8	4	8
ρ_{calc}g/cm^3	1.269	1.252	1.264
μ/mm^{-1}	0.643	0.076	0.085
F(000)	2160.0	704.0	1056.0
Crystal size/mm^3	0.14 × 0.13 × 0.1	0.2 × 0.2 × 0.2	0.2 × 0.15 × 0.1
Radiation	CuKα (λ = 1.54184)	MoKα (λ = 0.71073)	MoKα (λ = 0.71073)
2Θ range for data collection/°	8.986 to 133.986	5.028 to 54.998	5.65 to 54.994
Index ranges	$-23 \leq h \leq 23$, $-22 \leq k \leq 22$, $-17 \leq l \leq 15$	$-14 \leq h \leq 14$, $-13 \leq k \leq 16$, $-17 \leq l \leq 16$	$-23 \leq h \leq 26$, $-6 \leq k \leq 6$, $-31 \leq l \leq 23$
Reflections collected	17184	15832	5755
Independent reflections	2222 [R_{int} = 0.0284, R_{sigma} = 0.0171]	7989 [R_{int} = 0.0352, R_{sigma} = 0.0712]	2969 [R_{int} = 0.0380, R_{sigma} = 0.0601]
Data/restraints/parameters	2222/1/171	7989/0/451	2969/0/163
Goodness-of-fit on F^2	1.096	1.023	1.021
Final R indexes [I>=2σ (I)]	R_1 = 0.0254, wR_2 = 0.0628	R_1 = 0.0557, wR_2 = 0.1057	R_1 = 0.0514, wR_2 = 0.1110
Final R indexes [all data]	R_1 = 0.0257, wR_2 = 0.0630	R_1 = 0.0931, wR_2 = 0.1217	R_1 = 0.0728, wR_2 = 0.1245
Largest diff. peak/hole / e $Å^{-3}$	0.10/-0.19	0.26/-0.24	0.29/-0.28
Flack parameter	-0.18(9)	n/a	n/a
CCDC number	**1834206**	**1834207**	**1834208**

Literature

1. (a) L. Palatinus and G. Chapuis, *J. Appl. Crystallogr.*, 2007, **40**, 786–790; (b) L. Palatinus, S. J. Prathapa and S. van Smaalen, *J. Appl. Crystallogr.*, 2012, **45**, 575–580.
2. G. M. Sheldrick, *Acta Cryst.,*, 2008, **A64**, 112–122.
3. G. M. Sheldrick, *Acta Crystallogr.*, 2015, **C71**, 3–8.
4. O. V. Dolomanov, L. J. Bourhis, R. J. Gildea, J. A. K. Howard and H. Puschmann, *J. Appl. Crystallogr.*, 2009, **42**, 339–341.
5. A. L. Spek, *A Multipurpose Crystallographic Tool*, Utrecht University, Utrecht, The Netherlands, 2005.